AN INVESTIGATION INTO THE FUNDAMENTAL UNDERSTANDING OF AN ACTIVATED SLUDGE BIOREMEDIATION PROCESS AND OPTIMISATION OF THIOCYANATE AND CYANIDE DESTRUCTION

Andries Wynand van Zyl

Thesis Presented for the Degree of **Doctor of Philosophy**

In the Department of Chemical Engineering

January 2019

Abstract

Cyanide (CN) is used in the gold mining industry to dissolve gold from free milling, complex and refractory gold containing ores. Processing sulphide containing refractory ores using biooxidation as a pre-treatment has become increasingly important due to the depletion of free milling ores. The reaction of CN with reduced sulphur species during the cyanidation process results in the formation of thiocyanate (SCN), often at relatively high concentrations (> 5 000 mg/L). The SCN and residual free CN are deported with the tailings as components of the liquid fraction. The concentration of SCN often exceeds the legislated discharge specification, necessitating on-site treatment, while water would also require treatment before on-site recycling and reuse.

Biological degradation of CN and particularly SCN in these effluents provides an alternative to the more traditional processes such as SO_2 treatment or UV destruction. The traditional destruction processes focus on breaking the chemical bonds, through physical or chemical means, thereby converting the toxic CN and SCN species to less toxic compounds. These processes generally suffer from high reagent cost, incomplete removal of CN and particularly SCN species and the generation of by-products which require further treatment. A number of microorganisms are capable of utilising CN and SCN as a source of sulphur, nitrogen and carbon, as well as generating energy from their oxidation. Additional removal of metal-CN complexes may be achieved by adsorption to the cell surface or extracellular polymeric substances secreted by the cells.

The activated sludge tailings effluent remediation (ASTER™) process was developed for the biological treatment of especially SCN, but also free CN and metal-cyanide complexes, such as CuCN and $Zn(CN)_2$. The basic ASTER™ technology consists of an aerated reactor, in which SCN and CN species are oxidised and a settler to facilitate the recovery of water and potentially biomass.

The desire to expand the commercial application of the technology necessitated a more complete, fundamental understanding of the ASTER™ process and required focused, in-depth research. This research aimed to define the viable operating window for SCN destruction, as well as optimising practical SCN and CN destruction process conditions. The ASTER™ process relies on a complex microbial community, so understanding the community structure and metabolic potential for SCN and CN destruction, further enhanced the fundamental and mechanistic understanding of this bioprocess. The research contributed to the fundamental understanding of this technology and enhanced the commercial application thereof.

The first step in defining the operating window was to investigate the effect of feed SCN concentration on the SCN destruction ability of the mixed microbial community. Experiments were conducted at feed SCN concentrations ranging from 60-1 800 mg/L. Complete SCN destruction was achieved across the range at ambient temperature. The maximum SCN destruction rate was 15.7 mg/L.h at an initial SCN concentration of 1 400 mg/L. Temperature was investigated in the range of 10-45°C with an initial SCN concentration range of 60-180 mg/L. A maximum SCN destruction rate of 17.4 mg/L.h was measured at 35°C, with an initial SCN concentration of 180 mg/L. A wide pH range (pH 5.0-10.0) was tolerated, with optimal performance recorded at pH 7.0. This evaluation identified not only the optimum operating pH, but also highlighted the negative impact of a sudden pH change on the efficiency of SCN destruction. Residual SCN concentrations below 1 mg/L were achieved in all cases, which would allow for discharge or recycling of treated water. Floc (sludge) formation was observed in experiments with high initial SCN concentrations and indicated a possible stress response during these batch experiments. Floc (sludge) formation were taken as microbial cells imbedded within extracellular polymeric substances and not only an aggregate of cells.

Evaluating the maximum potential for SCN destruction and optimising the operating conditions and system configuration was investigated using continuous reactor experiments. A maximum SCN destruction rate of 87.4 mg/L.h (2 098 mg/L.d) was achieved at a feed SCN concentration of 1 000 mg/L and eight hour hydraulic retention time (HRT) during these experiments. The formation of substantial amounts of sludge was observed, with attachment to the reactor surfaces. The maximum feed SCN concentration, where substantial destruction was measured, was at 2 500 mg/L, achieving a practical SCN destruction rate of 972 mg/L.d. Significant inhibition of microbial inactivity was observed beyond this feed SCN concentration. The microbial community was able recover performance, within six days, after an extended period (54 days) of inactivity when the feed concentration was reduced from 3 500 mg/L SCN to 1 000 mg/L. The nature of the accumulated biofilm did not appear to change during the period of limited SCN destruction activity. Calculation of specific SCN destruction rates was not possible due to the nature of the sludge and heterogeneous dispersion of microbial members.

Biomass (cells embedded in the EPS sludge) loading experiments showed SCN destruction rates increased with an increase in biomass loading, but this relationship was not proportional. A 25-fold increased biomass concentration resulted in only a 2-fold increase in destruction rate, suggesting a mass transfer limitation. The sludge most likely offers protection against unfavourable conditions, such as high residual

SCN concentrations, by presenting a mass transfer barrier, resulting in an SCN concentration gradient across the sludge matrix. This enhances the robustness of the process and would facilitate rapid recovery in the case of a system upset at commercial scale.

This research is the first to demonstrate the effective removal of SCN in the presence of suspended tailing solids, under conditions well suited for commercial application. The maximum SCN destruction rate achieved was 57 mg/L.h in the presence of 5.5% (m/v) solids. Sludge formation was not observed in the reactors containing solids, despite substantial sludge formation under similar operating conditions in the absence of solids, most likely due to shear-related effects. Fluctuations in pH, due to the nature of the solid material, were identified to negatively impact reactor performance and pH control was required. Moreover, the type of solid particle was found to influence the SCN destruction rate showing a need for adaptation not only to the presence of solids but also to various types of solids that are to be treated.

Treatment of residual CN in solution is critical to ensure safe disposal or recycling of water. Treatment of SCN and CN was successfully demonstrated at feed concentrations up to 2 000 and 50 mg/L, respectively. The presence of residual CN (0.5 mg/L) prevented complete destruction of SCN, while complete SCN destruction was measured in the absence of CN under identical conditions. A range of reactor configurations were investigated and the optimum system required biomass retention, by means of attached biomass and complete destruction of any residual CN prior to SCN destruction. Conversion of SCN-S to SO_4-S was stoichiometrically proportional in solution, while the majority of the liberated nitrogen appeared to be assimilated. Pre-colonisation of the reactor with attached biomass is beneficial and removed the need for a solid-liquid separation unit, reducing the potential footprint of the process. Additional treatment capacity could be created by operation of reactors in series.

The diversity of the microbial community responsible for destruction of especially SCN were shown to be far more extensive than initially expected. Initial molecular characterisation of the microbial community selected for 185 representatives of bacterial 16S rRNA genes, of which 106 non-identical genotypes were sequenced. In contrast, for the reactor containing solids, only 48 representatives were selected and 30 genotypes were sequenced. Bacteria implicated in SCN destruction in the reactor containing suspended solids were members from the genera *Bosea*, *Microbacterium* and *Thiobacillus*. In the absence of solids, members capable of SCN destruction were identified from genera including *Thiobacillus* and *Fusarium*. High-throughput genome sequencing, followed by sequence assembly confirmed the

dominance of *Thiobacillus spp*. Metabolic predictions indicated the autotrophs, gaining energy from the oxidation of reduced sulphur intermediates produced during SCN destruction were the dominant community members. The potential for ammonium oxidation and denitrification within the microbial community was identified during analysis of the metabolic potential, based on the metagenomic sequence data. These would be required for complete remediation of wastewater.

The data generated during the research led to the development of a conceptual model to describe the evolution of system performance. Following inoculation with planktonic culture the SCN destruction is performed by the planktonic microbial community. An increased residual SCN concentration results in floc formation and the colonisation of reactor surfaces by attached biofilm. A concomitant decrease in planktonic cell concentration was observed, while SCN destruction rates increased. The extracellular material provided a matrix for biomass retention, resulting in high cell concentrations, and provided some protection against high SCN concentrations by providing a barrier to mass transfer. The attached biofilm developed to the point where overall SCN degradation rates may become limited by reduced oxygen penetration.

The research presented in this thesis has been used to inform the design and operation of the ASTER™ process at commercial scale, specifically with respect to the benefits of attached biomass and the demonstration that the process can be used in the presence of suspended solids. The latter has been particularly important in applications where the available footprint is constrained.

Declaration

This thesis/dissertation was submitted to the Turnitin module for evaluation of similarity and originality. I acknowledge this is my own work and has not been submitted for any degree or examination at any other university.

Signed by candidate

Andries Wynand van Zyl

06 day of January 2019

I confirm that I have been granted permission by the University of Cape Town's Doctoral Degrees Board to include the following publication(s) in my PhD thesis, and where co-authorships are involved, my co-authors have agreed that I may include the publication(s):

van Zyl, A.W., Harrison, S.T.L. and van Hille, R.P. 2017. Determining an effective operating window for a thiocyanate degrading mixed microbial community. Journal of Environmental Chemical Engineering, 5:660-666.

Huddy, R., van Zyl, A.W., van Hille, R.P. and Harrison, S.T.L., 2015. Characterisation of the complex microbial community associated with the ASTER^{TM} thiocyanate biodegradation system. Minerals Engineering, 76:65-71.

van Zyl, A.W., Huddy, R., Harrison, S.T.L. and van Hille, R.P., 2015. Evaluation of the ASTER^{TM} process in the presence of suspended solids. Minerals Engineering, 76:72-80.

van Zyl, A.W., Harrison, S.T.L. and van Hille, R.P., 2011. Biodegradation of thiocyanate by a mixed microbial population. In Thomas R. Rude, Antje Freund &

Christian. Wolkersdorfer (Ed.):119-124. International Mine Water Association. Aachen, Germany.

van Zyl, A.W., Harrison, S.T.L. and van Hille, R.P., 2011. Effect of thiocyanate loading and temperature on thiocyanate degradation by a mixed microbial population. In Waste Processing and Recycling in Mineral and Metallurgical Industries – IV. Canadian Institute of Mining, Metallurgy and Petroleum. Montreal, Canada.

Signed by candidate

Andries Wynand van Zyl

24 day of January 2019

Publications and Presentations

Publications:

van Zyl, A.W., Harrison, S.T.L. and van Hille, R.P. 2017. Determining an effective operating window for a thiocyanate degrading mixed microbial community. Journal of Environmental Chemical Engineering, 5:660-666.

Applicants' contribution: Experimental conceptual development; All experimental work, data analyses and interpretation, Main author.

Rahman, S.F., Kanton, R.S., Huddy, R., Thomas, B.C., van Zyl, A.W., Harrison, S.T.L. and Banfield, J.F., 2017. Genome-resolved metagenomics of a bioremediation system for degradation of thiocyanate in mine water containing suspended solid tailings. MicrobiologyOpen. 00:1-9

Applicant's contribution: Reactor experimental and data analyses and interpretation; Provision of samples for analyses.

Huddy, R., van Zyl, A.W., van Hille, R.P. and Harrison, S.T.L., 2015. Characterisation of the complex microbial community associated with the ASTER™ thiocyanate biodegradation system. Minerals Engineering, 76:65-71.

Applicants' contribution: All experimental reactor conceptual development, data analyses and interpretation; Author contribution.

Kantor, R.S., van Zyl, A.W., van Hille, R.P., Thomas, B.C., Harrison, S.T.L. and Banfield, J.F., 2015. Bioreactor microbial ecosystems for thiocyanate and cyanide degradation unravelled with genome-resolved metagenomics. Environmental Microbiology, 17:4929-4941.

Applicants' contribution: All experimental reactor conceptual development, data analyses and results interpretation. Samples provided from experimental work conducted.

van Zyl, A.W., Huddy, R., Harrison, S.T.L. and van Hille, R.P., 2015. Evaluation of the ASTER^{TM} process in the presence of suspended solids. Minerals Engineering, 76:72-80.

Applicants' contribution: Experimental conceptual development; All experimental work, data analyses and interpretation, Main author.

van Zyl, A.W., Harrison, S.T.L. and van Hille, R.P., 2011. Biodegradation of thiocyanate by a mixed microbial population. In Thomas R. Rude, Antje Freund & Christian. Wolkersdorfer (Ed.):119-124. International Mine Water Association. Aachen, Germany.

Applicants' contribution: Experimental conceptual development; All experimental work, data analyses and interpretation, Main author.

van Zyl, A.W., Harrison, S.T.L. and van Hille, R.P., 2011. Effect of thiocyanate loading and temperature on thiocyanate degradation by a mixed microbial population. In Waste Processing and Recycling in Mineral and Metallurgical Industries – IV. Canadian Institute of Mining, Metallurgy and Petroleum. Montreal, Canada.

Applicants' contribution: Experimental conceptual development; All experimental work, data analyses and interpretation, Main author.

Presentations:

van Zyl, A.W., Harrison, S.T.L. and van Hille, R.P., 2011. Detoxification of thiocyanate laden waste water. Minerals Processing Conference, Cape Town, South Africa 2012.

van Zyl, A.W., Harrison, S.T.L. and van Hille, R.P., 2011. Effect of thiocyanate and cyanide concentration on the biodegradation ability of a mixed microbial consortium under different incubation temperatures. Minerals Processing Conference, Cape Town, South Africa 2011.

van Zyl, A.W., Harrison, S.T.L. and van Hille, R.P. Biodegradation of thiocyanate by a mixed microbial population. 11th International Mine Water Association Symposium, Aachen, Germany 2011.

van Zyl, A.W., Harrison, S.T.L. and van Hille, R.P. Effect of thiocyanate loading and temperature on thiocyanate degradation by a mixed microbial population. Conference of Metallurgists, Montreal, Canada 2011.

Acknowledgements

As a token of my appreciation, I would like to express my gratitude and acknowledge those involved in completion of this thesis as well as the support and contributions made throughout my years as a postgraduate.

I am profoundly grateful to God for walking this road with me.

My supervisors Dr Rob van Hille and Prof Sue Harrison, thank you for the opportunity to work in and contribute to this research field. I deeply appreciate your guidance and support in being my supervisors. Your dedicated hard work is truly a mark of an expert. You have always only been a message or phone call away.

To the members of CeBER, you all made for a fantastic environment to grow, question and learn in both technical and personal endeavours. All the input to presentations, experimental setup and assistance made for an excellent group to be a part of. The jokes, chats and coffee shared will be remembered for time to come.

Sincere thanks to Miranda Waldron for the hours spent on electron microscopy work. The sample preparation, advice and assistance is world class.

To Rob Huddy for the microbial and molecular input and guidance. Your knowledge and intellectual contribution is greatly appreciated.

Thanks goes to the Banfield group of UC Berkeley. The collaboration was inspiring.

I am grateful to the UCT post-graduate funding office and CeBER for funding to undertake this degree as well as for local and especially international conference opportunities.

To the group of Biomin, I am grateful for the sponsored the research, opportunities and collaboration.

My parents, Louis and Marianne van Zyl your guidance, love and persistence throughout my studies has been profound.

To my wife Alta van Zyl, I give distinct thanks for your unwavering support, love and sacrifice. Your academic input and personal advice is truly appreciated.

Table of contents

List of Figures

List of Tables

List of Abbreviations

AEV	Acute effects values
ARDRA	Amplified ribosomal DNA restriction analysis
ATP	Adenosine triphosphate
CEV	Chronic effects values
CN or CN-	Cyanide
CN-N	Nitrogen from cyanide
NH_4-N	Nitrogen from ammonium
CN_{sad}	Strong acid dissociable cyanide
CN_{wad}	Weak acid dissociable cyanide
CSTR	Continuous stirred tank reactor
DO	Dissolved oxygen
DWAF	Department of Water Affairs and Forestry
DWS	Department of Water and Sanitation
EPS	Extracellular polymeric substance
HPLC	High performance liquid chromatography
HRT	Hydraulic retention time
INCO	INCO Ltd. (now VALE)
LC_{50}	Lethal concentration to kill 50% of the population
MRL	Minimum risk level
PCR	Polymerase chain reaction
RBC	Rotating biological contactor
SCN or SCN-	Thiocyanate
SCN-S	Sulphur fraction from thiocyanate
SO_4-S	Sulphur fraction from sulphate

SEM	Scanning electron microscopy
TWQR	Target water quality range

Chapter 1: Literature review

1.1 Background

Water underpins growth of all sectors including agricultural production, energy generation and industrial manufacturing. Given the critical nature of this resource, it is up to us to ensure its protection, purity and re-use. While innovation, the likes of digital water platforms, will assist in this endeavour, it is our own entitlement and use that will determine availability in the years to come. Population growth is closely linked to food production and the current 70% use of fresh water by global agriculture is set to grow (Saccon, 2018). Water is intertwined with energy in that water offers cooling and generating power while, in turn, energy enables transport of water as well as collecting and treatment of wastewater (UN-Water, 2006). Manufacturing of goods closely accompanies a growing economy and pricing water at its true value is critical. Furthermore, mining activity requires water for various processes while contaminated water has been well documented requiring treatment for safe disposal and re-use. A breach in a tailings dam near Baia Mare released 100 000 m^3 of cyanide-laden wastewater into the river system (Dzombak *et al*., 2006). This impacted on the drinking water for 2.5 million people while destruction of fish species were caused in addition to huge socio-economic impacts for the local area. This example shows the potential for pollution of immense water resources. Economic growth coupled to increasing waste, strain on water supplies may render it unsafe and ultimately unusable. Governance of water use and treatment is critical to ensure waste thereof is prevented and access to potable water remain sustainable.

The activated sludge tailings effluent remediation (ASTER^{TM}) process has been developed to treat thiocyanate (SCN) and cyanide (CN) laden process water. The main metabolic products include sulphate, ammonia and carbon dioxide. The gold industry has relied on CN to extract gold for centuries which stems from the efficiency of CN as a lixiviant for gold and other metals, such as silver (Clennell, 1910; Zagury *et al*., 2004). Cyanidation is employed for extraction of precious metals from oxide ores, as well as pre-treated sulphide ores, either with milled ore in agitated vessels or via percolation through heaps of crushed ore. Cyanide reacts with the gold, under oxidising conditions, to form a stable gold-cyanide complex that is recovered from solution, typically by adsorption to activated carbon. The exploitation of refractory ores, where the gold is associated with sulphide minerals, is

increasing due to the depletion of free milling gold ores (Saba *et al*., 2011). This results in formation of high residual SCN concentrations as well as highly stable metal-cyanide complexes, requiring active treatment.

The most recent figures presented by the International Cyanide Management Code for the Gold Mining Industry (http://www.infomine.com/publications/docs/SummaryFactSheetCN.pdf) indicate that 18% of the 1.4 million tons of hydrogen cyanide produced each year is used for the production of NaCN for gold processing. Moreover, artisanal mining operators use mercury followed by cyanidation to recover gold while waste containing metal cyanides could be discharged to local water streams (Brüger *et al*., 2018).

Traditional approaches for processing refractory ores, such as roasting and pressure oxidation, are energy intensive and may carry an associated environmental risk, particularly from sulphur dioxide and metal emissions. Biooxidation options have emerged as a competitive alternative especially where processing of minerals containing penalty elements is concerned. The BIOX® process was developed during the 1980s as the first commercial biooxidation process for pretreatment of refractory gold-bearing concentrates and is still used among others as an alternative to conventional processes for the treatment of refractory gold ores prior to cyanide leaching (Rawlings and Johnson, 2007). BIOX® has proven economically viable and has additional environmental benefits, including the elimination of sulphur dioxide emissions. The BIOX® process makes use of a combination of iron- and sulphur-oxidising microorganisms to facilitate the degradation of the sulphide mineral matrix, exposing occluded gold and reducing the sulphur content of the concentrate. This pre-treatment is not completely effective at oxidising all reduced sulphur. SCN forms during cyanidation in such cases when sulphide and/or thiosulphate react with CN. The iron- and sulphur-oxidising organisms employed in the BIOX® process are susceptible to low levels (< 1 mg/L) of SCN^-. This has precluded the recycling of the tailings water up-stream of the bioleaching circuit (Olson *et al*., 2006). The inability to recycle this water negatively impacts the overall water balance of the operation, particularly in arid regions. Furthermore, the concentration of SCN often exceeds the legislated discharge specifications, necessitating on-site treatment. While very stringent statutory requirements govern the discharge of CN containing wastes, these are less stringent for SCN^-, often reviewed on a case by case basis.

Waste products are disposed of according to environmental regulations, often in the most economical way possible. Currently, liquid and slurry wastes are typically stored in impoundment ponds (Dzombak *et al*., 2006). These ponds require careful design and management, to ensure the anticipated flows and chemical loadings are met, as well as heavy rainfall events can be accommodated.

Chemical and physical SCN and CN treatment technologies suffer from an inability to treat hazardous by-products as well as incomplete contaminant removal. High opex and capex requirements make these technologies unfavourable in comparison to biological treatment of cyanide-laden wastewater. Microbial treatment technologies have the potential to address free cyanide, tiocyanate as well as weak and strong acid dissociable cyanide complexes in a cost-effective and reliable manner (White *et al*., 2000; du Plessis *et al*., 2001; Ebbs, 2004). During bio-treatment, microorganisms metabolise CN species to produce carbon dioxide, ammonia, sulphate and in the case of metal complexes, free metals, which are either adsorbed onto the bio-sludge or precipitated. The success of biotreatment depends on the intrinsic capability of the microbial community to degrade the targeted contaminant, the availability of required nutrients, sufficient retention time for contact of microorganisms and the contaminant as well as favourable environmental conditions for proliferation of the selected microorganisms.

1.2 Cyanide production and use in industry

Cyanide is commercially produced using a variety of processes. The primary production of hydrogen cyanide occurs via the reaction between ammonia (NH_4), methane (CH_4) and air, over a platinum catalyst, either by the Andrussow process or the Blausaure-Methan-Ammoniak process (Dzombak *et al*., 2006; Kondratenko, 2010). Commercial production of hydrogen cyanide is also done using the Shawinigan process, where ammonia is reacted with propane. The fourth process, which accounts for 30% of the global hydrogen cyanide production, is a by-product of acrylonitrile manufacture. Hydrogen cyanide may then be reacted with sodium hydroxide, or other salts, to produce products, such as sodium cyanide.

Cyanide is used extensively in a number of industries, including gold extraction, steel production, drug manufacturing, pesticide and plastics manufacturing, electroplating as well as photo development (Table 1.1).

Table 1.1: Description of various industries that use cyanide containing reagents (Taken from Dzombak *et al.*, 2006)

Industry	Component
Adhesives	Ammonium thiocyanate
Cement stabiliser	Calcium cyanide
Electroplating	Potassium or sodium cyanide
	Propionitrile
	Metal cyanides including copper, silver, zinc, nickel and mercuric cyanide
Fire retardant	Potassium ferrocyanide
Herbicides	Ammonium thiocyanate
Pesticides	Cyanogen chloride, cyanogen bromide, zinc and copper cyanide, ammonium thiocyanate, hydrogen cyanide
Mining	Sodium cyanide, malononitrile, cyanogen bromide, barium cyanide, calcium cyanide and ferrocyanide
Petroleum	Malononitrile and propionitrile
Photography	Ferricyanide bleach, mercuric cyanide and hydrogen cyanide
Pharmaceuticals	Ferricyanide, ferrocyanide, propionitrile and ammonium thiocyanate
Pigments, paints and personal care products	Ferricyanide, ferrocyanide, ferric ferrocyanide, malononitrile, mercuric and copper cyanide
Road salt	Sodium ferrocyanide, ferric ferrocyanide and potassium ferrocyanide
Rocket propellant	Ammonium thiocyanate
Synthetic fiber	Malononitrile, adiponitrile, cyanogen bromide, cyanogen chloride, hydrogen cyanide and ammonium thiocyanate
Wine	Potassium ferrocyanide

Approximately 13% of the 1.4 million tonnes of hydrogen CN produced annually is used for the production of CN reagents for gold processing (http://www.cyanidecode.org). As an example, the Ovacik Gold Mine used

approximately 240 tonnes of sodium cyanide annually (Akcil, 2002). During the processing of free-milling gold ores, the milled material is exposed to dilute CN solutions, leading to the formation of soluble gold-cyanide complexes (Gönen *et al*., 2004), from which the gold is subsequently recovered by adsorption, solvent extraction and electrowinning. Cyanide can also form complexes with other metals, including copper (Cu), zinc (Zn), iron (Fe) and nickel (Ni), which may be present in complex ores. These side reactions not only increase CN consumption, but also the complexity of the wastewater to be treated.

1.3 Thiocyanate formation

Thiocyanate is formed by the reaction of CN and reduced sulphur species (Figure 1.1). During gold extraction this occurs predominantly due to the reaction between residual CN and reduced sulphur species in an oxidising environment following cyanidation (Luthy and Bruce Jr., 1979; Stott *et al*., 2001; Akcil, 2003).

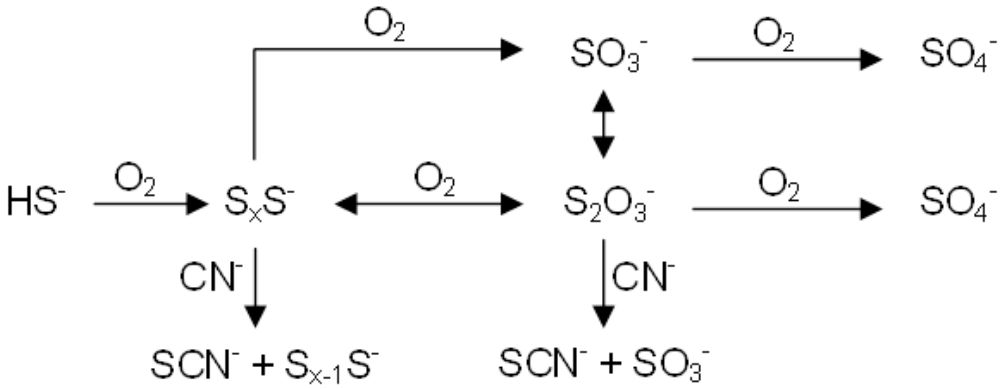

Figure 1.1: Production of thiocyanate due to possible reactions between cyanide and sulphides (Luthy and Bruce Jr., 1979)

Thiocyanate formation is particularly prevalent during the processing of refractory gold ores, where the gold is associated with sulphide minerals, typically pyrite or arsenopyrite. The ore needs to be pre-treated to remove the sulphide prior to cyanidation. Historically, this was achieved by roasting, but this has been selectively replaced by pressure oxidation or biooxidation in some operations. Microbial leaching and biooxidation operations rely on the biologically catalysed destruction of the sulphide mineral under acidic and oxidative conditions. Mineral dissolution occurs via two main pathways (Figure 1.2), depending on the type of sulphide

mineral (Schippers and Sand, 1999). Acid insoluble minerals, such as pyrite, are dissolved via the thiosulphate mechanism, while acid soluble minerals (e.g. arsenopyrite) progress via the polysulphide mechanism. In both cases ferric iron is the main oxidising agent and this is regenerated by iron oxidising bacteria and archaea. The reduced sulphur intermediates may be oxidised to sulphuric acid by sulphur oxidising species. The mineral leaching efficiencies in the bioreactors are typically high (90-97%) and some of the intermediate sulphur species pass into the cyanidation process, resulting in the formation of thiocyanate.

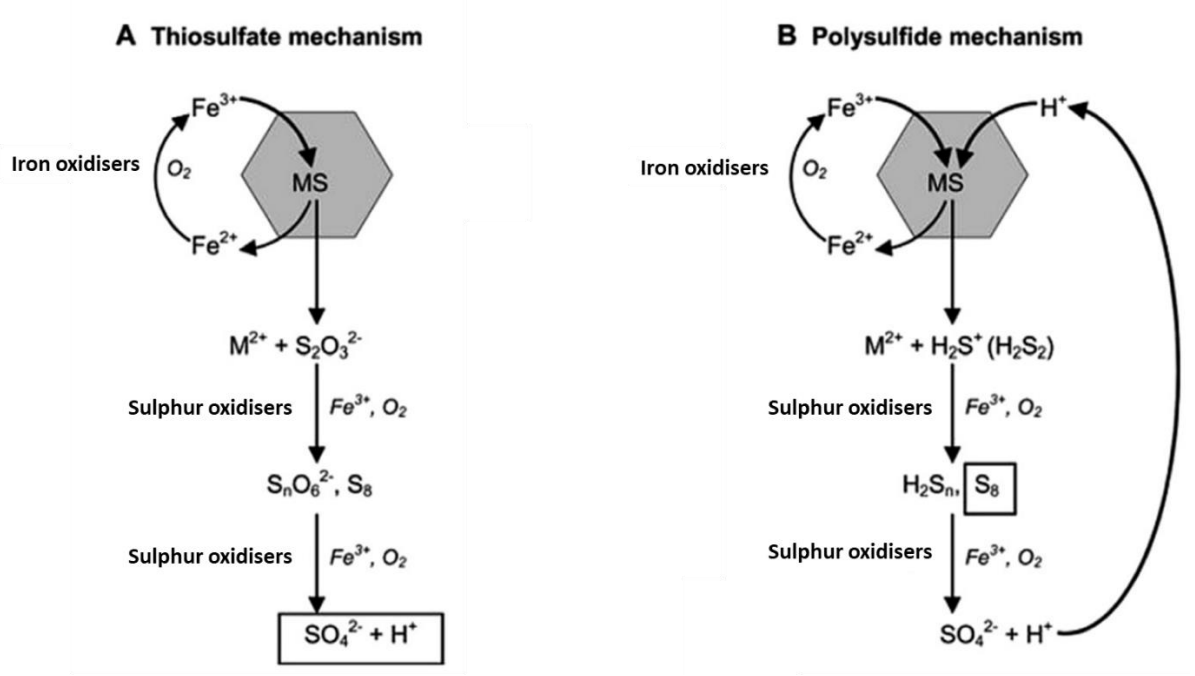

Figure 1.2: Schematic representation of bioleaching processes that result in the formation of a) thiosulphate or b) polysulphides based on the type of mineral leached (Schippers and Sand, 1999)

The rate of thiocyanate production from CN and sulphur intermediates is dependent on reactant concentrations as well as reaction conditions. The rate of reaction between polysulphide and CN was shown to be at least three orders of magnitude faster when compared to the rate of reaction between CN and thiosulphate (Schippers and Sand, 1999).

1.4 Diversity of cyanide containing compounds

The extensive use of CN in industry results in the generation of wastewater containing CN and CN complexes of variable stability and toxicity (Patil and Paknikar, 1999; Joanne Baxter and Cummings, 2006; Gupta *et al*., 2010).

CNs refer to all cyanide forms and can be grouped as follows (Dzombak *et al*., 2006):

1. free cyanide, such as hydrogen cyanide (HCN) or cyanide ions (CN^-)
2. simple CNs, such as sodium cyanide (NaCN) or potassium cyanide (KCN)
3. thiocyanate (SCN^-)
4. weak acid dissociable cyanide (CN_{wad}), including CuCN, ZnCN or NiCN and
5. strong acid dissociable cyanide (CN_{sad}), including FeCN and CoCN.

Organo-complexed cyanide can form as by-products during processing or due to deliberate product manufacturing, such as in the production of acrylonitrile (Baxter and Cummings, 2006). Toxicity decreases as one moves from group (1) to (5) mentioned above, as the metal-CN complexes become more stable and can only be dissociated under very specific conditions (Gönen *et al*., 2004; Zagury *et al*., 2004). For example, iron cyanide complexes have to be broken down using biological processes, irradiation or treatment with boiling acid, while HCN can be volatile at conditions below pH 9.24 (Meeussen *et al*., 1992).

1.5 Toxicity and environmental impact of CNs

Cyanide toxicity has been well documented, with acute as well as chronic effects on humans, aquatic organisms and wildlife recorded (Chin and Calderon, 2000; Donato *et al*., 2007). Exposure to CN may occur through ingestion, absorption or inhalation while the exposure time and concentration determines the severity of symptoms (Shifrin *et al*., 1996). The toxicity of individual CN compounds depends on how easily they release the CN anion (CN^-). The primary toxicological effect relates to the binding of CN to the metallic cofactor in metal containing enzymes, affecting enzyme and cell function. Cytochrome C oxidase, an enzyme in the mitochondrial electron transfer chain, is the most important target in terms of CN toxicity. Cyanide binds to the iron atom, thereby inhibiting the oxygen carrying capacity of red blood cells. While this affects the entire body the effect on the central nervous system is

most significant due to the high metabolic demand for oxygen of neurons and its control of the respiratory system. Respiratory failure contributes to global histotoxic hypoxia and death (ATSDR, 2006). Furthermore, the lack of pathognomonic symptoms decreases the likelihood of an immediate diagnosis.

The toxicity of CN is expressed as the dose that is lethal to 50% of the exposed population (LD_{50}) due to the different effects of CN dose-exposure between individuals. The LD_{50} and lethal dose concentrations are described in Table 1.2. The lethal dose for oral CN ingestion ranges from 0.5-3.5 mg/kg body weight, while a derived minimum risk level (MRL) of 0.05 mg/kg has been proposed (U.S. Department of Health and Human Services PHS, 2006).

Table 1.2: The minimum concentration of different cyanide compounds recorded for LD_{50} and lethal dose limits

Compound	Concentration	Exposure	Effect	Reference
HCN(g) inhalation	100-300 ppm	0-60 min	LD_{50}	CN code
HCN(g) inhalation	524 ppm	10 min	LD_{50}	ATSDR (2006)
CNCl(g) inhalation	159 ppm	10 min	Lethal	*Chamber of Mines
NaCN(s) ingestion	1.52 mg/kg	NA	LD_{50}	ATSDR (2006)
CN compounds (as HCN) ingestion	1-3 mg/kg	NA	LD_{50}	CN code
CN^- dermal absorption	100 mg/gk	NA	LD_{50}	ATSDR (2006)

*Chamber of Mines of South Africa (2008)

The health of freshwater and marine environments may be severely impacted by the use and subsequent discharge of CNs from industrial processes and sewage treatment plants. Cyanide is readily taken up by aquatic life through contact with skin and mucous membranes, with similar toxic mechanisms as found in humans, resulting in hypoxia and death.

Thiocyanate, however, is less acutely toxic compared to CN and there is less information available regarding toxic concentrations. Gould and co-workers (2012) report on a 1939 study by Garvin, which suggested a minimum lethal dose across animal species of 500 mg/kg, while a more recent study (Parachuri *et al*., 1990) suggested a concentration above 15 mg SCN per 100 mL mammalian blood represented a critical risk. Thiocyanate is particularly toxic to the iron- and sulphur-oxidising microorganisms that are used in mineral bioleaching, with on-site observations suggesting concentrations as low as 1 mg/L are acutely toxic (Olsen *et al*., 2006; van Aswegen *et al*., 2007; Adams, 2013). The mechanism of toxicity is not well understood, but is thought to involve acidification of the cytoplasm which affects the membrane potential and then inhibits the respiratory chain (Alexander *et al*., 1987). A recent study (van Hille *et al*., 2015; Edward *et al.*, 2018) has confirmed inhibition of iron and sulphur oxidation by *Leptospirillum ferriphilum* and *Acidithiobacillus caldus*, respectively and that the extent of inhibition is dose dependent. Water management is becoming increasingly critical for mining companies and if the recycling of process water following cyanidation to the biooxidation step is desired, the SCN concentration will need to be reduced to below 1 mg/L.

1.6 Examples of environmental contamination

Incidences of CN spills and uncontrolled effluent release to the environment are relatively common. The most severe case, in recent years, of CN impacting the environment occurred following the failure of a gold mine tailings dam near Baia Mare, Romania in January 2000 (Dzombak *et al*., 2006). As a result, over 100 000 m^3 of tailings water containing free and complexed cyanide, as well as heavy metals and suspended solids, was discharged into the Somes River. An estimated 100 tonnes CN were released which travelled approximately 2 000 km in the river network, decimating large sections of the Tisza River in Hungary and Serbia, before reaching the Black Sea. Cyanide concentrations were 15 to 1 500 times greater than water quality criteria for aquatic life protection even after the effects of dilution, destruction and volatilisation. Tailings dam failures and leaks have also been recorded in Nevada, Utah, Colorado and Guyana (Table 1.3). These spillages have a significant impact on not only the environment, but also on the livelihoods of nearby communities.

Table 1.3: Examples of accidental release of cyanide contaminated waters to the environment (Dzombak *et al*., 2006; van Niekerk and Viljoen, 2005)

Released waste	Waste volume	Location	Date	Cause
CN, metal cyanide, heavy metals and suspended solids	100 000 m^3	Romania	January 2000	Tailings dam failure
Heap leach effluent	927 m^3	USA, Nevada	June 1997	Heap leach pad leakage
Cyanide tailings water	4 200 000 m^3	Guyana, Omai	August 1995	Tailings dam failure
Leach solution (treated)	26 500 m^3	USA, Utah	March 1995	Storage pond failure
Tailings solution	2 500 000 m^3	South Africa	February 1994	Tailings dam failure
Cyanide solution	Sustained leaks	USA, Colorado	1986-1992	Heap leach pad, transfer pipes and tailings pond leaks

1.7 Treatment of CNs

The treatment of CN waste ranges from the slow natural destruction of simple-CN solutions to complex processes for treating slurries, which require specialist technical knowledge. Treatment can be achieved via technologies within three categories, namely: (1) chemical destruction, (2) physical treatment or (3) biological means (Akcil, 2002; Joanne Baxter and Cummings, 2006; Mekuto *et al*., 2016). Factors that need to be considered when selecting an appropriate CN treatment process include the composition of the solution or slurry, environmental regulations, volume of waste to be treated, cost implications, treatment quality and possible formation of side products that require further treatment (Mosher and Figueroa, 1996; Akcil, 2002).

In addition, multiple treatment steps or pre-treatment may have to be considered for complex waste matrices containing additional contaminants such as heavy metals or organics (Mudliar *et al*., 2009). Effluent quality is driven by regulatory requirements and, together with cost, determines the appropriate technology train required to treat CN contaminated wastes.

1.7.1 Limits for discharge of industrial wastewater

The guidelines for the quality of water discharged to the surrounding environment is described by The Chamber of Mines of South Africa (DWA, 2013) in Table 1.4. The Department of Water Affairs and Forestry (DWAF), now the Department of Water and Sanitation (DWS), published a set of water quality guidelines for discharge to the aquatic environment in 1996. The guidelines were based on three levels, the target water quality range (TWQR) below which no adverse effects on the aquatic community are expected and the chronic (CEV) and acute effect values (AEV). The latter values were determined at levels where there was a significant probability of measurable chronic or acute effects on up to 5% of the species in the environment. The limits set for discharge of wastewater containing various contaminants is very stringent and therefore necessitate efficient treatment.

Thiocyanate is not independently recognised as acutely toxic and most countries do not specify discharge limits. The Ontario Ministry of Environment has set a discharge limit of below 150 mg/L, while in Australia the New South Wales Clean Water Regulations state that SCN needs to be considered on a case-by-case basis. The Canadian Metal Mining Effluent Regulations require operations to generate effluent that is not acutely toxic to rainbow trout (LC_{50} of 243-1800 mg/L, 12-96h) and *Daphnia magna* (LC50 of 0.63-32 mg/L, 96h) (Gould *et al*., 2012).

1.7.2 Chemical treatment of cyanide and cyanide compounds

The chemical treatment of CNs is well developed, with oxidation of cyanide-laden waste the most popular route. The most common treatment options are summarised in Table 1.5 and described in more detail below. Ferrates has also been shown to oxidise CN and SCN but requires additional reagents as well as secondary treatment of by-products adding to the complexity of this process (Gonzalez-merchan *et al.*, 2017). Chemical technologies have been applied for the treatment of wastewater, slurries and sludge containing free- and simple CNs, as well as SCN, CN_{wad} and CN_{sad}. Some chemical processes are burdened by the formation of environmentally detrimental by-products, such as cyanogen-chloride, or high concentrations of ammonia. Treatment using chemical technologies has been successful for free CN, CN_{wad} and where energy intensive technologies are employed, CN_{sad}.

Table 1.4: Discharge limits for industrial wastewater as set out by the national environmental waste management act (Department of Environmental Affairs, 2013; DWA, 2013).

Substance	Limit	SA water quality guideline values (µg/L)		
		TWQR	**CEV**	**AEV**
		Target water quality range	**Chronic effect values**	**Acute effect values**
pH	5.5-9.5			
Conductivity	150 mS/m			
Aluminium		10	20	150
Ammonia	3 000	7	15	100
Arsenic	20	10	20	130
Boron	1 000			
Cadmium	5	0.25	0.5	6
Chlorine	250	0.2	0.35	5
Chromium (VI)	50	7	14	200
Copper	10	0.8	1.5	4.6
CN	20	1	4	110
Iron	300			
Lead	10	0.5	1	7
Manganese	100	180	370	1 300
Mercury	5	0.04	0.08	1.7
Nitrate/Nitrite	15 000			
Phosphorous	10 000			
Selenium	20	2	5	30
Zinc	100	2	3.6	36

*The unit of measurement for all numbers are mg/L, unless stated otherwise or in the case of pH.

1.7.2.1 INCO/Air process

The SO_2-air (INCO) process utilises sulphur dioxide and air to oxidise free cyanide as well as CN_{wad}. The INCO process was developed by The International Nickel Company during the 1980's and has been in use ever since. A catalyst, generally copper sulphate, is needed to achieve practical destruction rates (Dzombak *et al*., 2006; Joanne Baxter and Cummings, 2006). Cyanide is oxidised to cyanate, with the formation of sulphuric acid (Rxn 1). Cyanate is subsequently converted to carbon dioxide and ammonia, while the sulphuric acid product is neutralised with lime (Akcil, 2002). In practice, SO_2 requirements range from 3.5-4.5 g/g CN^- oxidised. Partial treatment of SCN (Rxn 2) is possible and ferriCN may be reduced to ferroCN. However, the process does not treat the environmentally sensitive compounds, ammonia and nitrate.

$$SO_2 + O_2 + H_2O + CN^- \rightarrow OCN^- + H_2SO_4 \qquad \text{Rxn 1}$$

$$4SO_2 + 4O_2 + 5H_2O + SCN^- \rightarrow OCN^- + 5H_2SO_4 \qquad \text{Rxn 2}$$

Full scale treatment of gold mine tailings slurries has been shown to achieve effluent CN levels below 1 mg/L. Licencing costs are associated with the proprietary INCO technology which may preclude use thereof (Mudder *et al*., 1991).

1.7.2.2 Ozone and hydrogen peroxide process

The use of ozone (O_3) or hydrogen peroxide (H_2O_2) has been employed successfully for the destruction of free cyanide and CN_{wad} (Akcil, 2002; Parga *et al*., 2003; Dzombak *et al*., 2006). Cyanate is formed in both cases under alkaline pH conditions (Reactions 3 and 4). The cyanate decomposes at a slow rate forming bicarbonate and nitrogen when treated with ozone, while ammonia and carbonate are formed during treatment with hydrogen peroxide.

$$O_3 + CN^- \rightarrow OCN^- + O_2 \qquad \text{Rxn 3}$$

$$H_2O_2 + CN^- \rightarrow OCN^- + H_2O \qquad \text{Rxn 4}$$

Cyanide oxidation using ozone is zero order with respect to CN concentration and may be enhanced by increasing the ozone addition rate, resulting in a first order reaction rate with respect to ozone addition. Oxidation of SCN using ozone results in the formation of free cyanide and sulphate, albeit at a slower rate than oxidation of CN (Parga *et al*., 2003). Treatment of CN_{wad} occurs readily, while prolonged UV light exposure is required for oxidation of CN_{sad} in the presence excess ozone.

Table 1.5: Various chemical treatment technologies used to process cyanide laden wastewater. Various levels of treatment can be achieved depending on the wastewater stream composition

Technology	Advantages	Disadvantages	By-products	CN	SCN	CN_{wad}	CN_{sad}
INCO	Inexpensive reagent cost	License fees	SO_4^{2-}, NH_3	Complete	Limited	Yes	Yes
		Precipitate formation	Precipitates				
	Wide pH range of use						
Ozone	High reaction rates possible	High reagent cost and complex equipment required	NH_3	Yes	Yes	Yes	No
Hydrogen peroxide	Simple to operate	High reagent cost	SO_4^{2-}, NH_3,	Yes	No	Yes	Limited
		Precipitate formation	Precipitates				
Alkaline chlorination	Well established technology	Potential formation of toxic cyanogen chloride	CNCl, Precipitates	Yes	Yes	Yes	No
	High reaction rate	Special handling of chloride reagents					
		Requires strict process control					
		Requires heating and retention times to treat CN_{sad}					
Photocatalytic oxidation	Can employ solar energy	Use in combination with other technologies	NH_3, Precipitates	Yes	Yes	Yes	Limited
		Require more research to achieve commercial scale treatment					

Compiled from (Rader *et al*., 1995; Akcil, 2002; Kitis *et al*., 2005; Dzombak *et al*., 2006)

The oxidation of CN in the presence of H_2O_2 is first order with respect to both H_2O_2 and copper concentration (Khodadadi *et al*., 2005; Kitis *et al*., 2005). Complete CN oxidation (60 mg/L CN_{wad}) occurred within four hours at a H_2O_2 concentration of 300 mg/L compared to 83 and 8% at 200 and 100 mg/L H_2O_2, respectively. The addition of 30 mg/L copper catalyst resulted in almost complete oxidation of 60 mg/L CN_{wad} within two hours under identical conditions.

Hydrogen peroxide and ozone treatment are preferable for CN laden solutions rather than slurries. The H_2O_2 required for successful treatment of CN species may be 200-450% higher than calculated on a stoichiometry basis due to the presence of oxidisable materials in the wastewater (Dzombak *et al*., 2006). In addition, the decomposition of H_2O_2 may add significantly to the reagent cost, but this may be reduced by employing peroxide stabilisers such as silicate or sulphuric acid. Furthermore, solutions containing organic matter (>1%), high SCN concentrations and CN_{sad} are not considered suitable for treatment with H_2O_2 or ozone. The formed CNO and NH_4 require further treatment. The treatment of CN laden wastewater using H_2O_2 or ozone provides predictable performance and a strong oxidation potential. However, the capital and operating costs are higher when compared to alkaline chlorination processes and this is compounded by the need for on-site ozone generation facilities and substantial cooling requirements.

1.7.2.3 Alkaline chlorination technology

Alkaline chlorination was widely employed in the past, but has now been replaced by alternative processes, discussed above and below, due to the highly toxic by-product cyanogen chloride (CNCl). CNO forms due to the oxidation of CN, with further oxidation producing CO_2 and N_2 (Rxn 5). A pH above 9.5 is needed to sustain the oxidation reaction rate and a solution pH greater than 10.0 to prevent the formation of highly toxic cyanogen chloride (Dzombak *et al*., 2006). The oxidation rate is high and requires a contact time of 15-30 min at a chlorine to CN ratio (mass basis) of three. Side reactions with organics result in the formation of chlorinated compounds, which adds to reagent consumption and cost.

$$2NaOH + CN \rightarrow CNO + 2Na + H_2O \qquad \text{Rxn 5}$$

Alkaline chlorination removes certain CN_{wad} complexes, low concentrations of SCN and free CN to levels below 1 mg/L, but suffers from high reagent costs and the inability to treat CN_{sad} (Young and Jordan, 1995). Furthermore, increased incubation

temperature and retention times are required in order to treat CN_{wad} complexes. Metal hydroxide precipitates are formed during treatment of CN_{wad} complexes and these may require further treatment before disposal. Special consideration is needed to ensure toxic by-products, for example sodium hypochlorite or chlorine gas, do not form or pose significant health and safety threats. This process is employed in the electroplating and gold mining industries (Barnes *et al*., 2000; Dzombak *et al*., 2006), but is becoming increasingly unpopular. Cooling costs also need to be considered since CN oxidation by chlorine treatment is exothermic thereby contributing to additional capital and operational expenditure.

1.7.2.4 Photocatalytic oxidation

Photocatalytic oxidation of CNs is usually combined with other oxidation technologies for the destruction of metal-CN complexes (Kuyucak and Akcil, 2013). Free CN is liberated and further oxidised, using ozone or H_2O_2 to ultimately form CO_2 and NH_3. Overall treatment is a one or two step process using either batch or continuous systems. Photodecomposition takes place at a UV wavelength of 350 nm, followed by oxidation of free CN in the presence of a catalyst such as titanium dioxide. Metal oxides and hydroxides, produced under alkaline conditions, are removed continuously by filtration in order to improve light penetration. Commercial scale implementation of this technology has been limited, primarily due to inadequate commercial experience and high operating costs (Rader *et al*., 1993).

1.7.3 Physical treatment technologies for treatment of cyanide and cyanide compounds

Physical treatment processes can achieve rapid detoxification rates and are used for the treatment of wastewater, sometimes at a lower cost relative to chemical treatment (Akcil and Mudder, 2003; Dash, Balomajumder, *et al*., 2009). These processes include air stripping, adsorption and precipitation technologies (Table 1.6).

Strong metal CN complexes that are not readily oxidised by chemical means are preferentially treated with physical treatment technologies. Furthermore, the reactivity of CN with certain solids, for example activated carbon, is exploited to develop adsorption technologies, while the reactivity of CN with metals is employed for precipitation purposes (Young and Jordan, 1995; Behnamfard and Salarirad, 2009).

1.7.3.1 Air stripping

Air stripping processes rely on the moderate volatility of hydrogen CN in order to remove it from water or slurries and typically operate on a counter-current principle (Gönen *et al*., 2004; Dzombak *et al*., 2006). Air stripping is generally not used to meet discharge limits but rather to reduce the concentration of dissolved free CN. This is due to stringent discharge limits of CN to the atmosphere as well as the significant energy input costs of blowing air through an air stripper. Furthermore, off-gas from the air strippers has to be treated by additional processing, such as activated carbon adsorption or biological destruction, to remove the free CN. Two process configurations have been most commonly considered. These are packed-bed towers and complete-mix reactors. The packed-bed tower configuration includes multiple mass transfer stages and offers increased mass transfer capabilities. Furthermore, the smaller footprint and higher diffusion rates achievable, relative to complete-mix reactors, makes the use of packed-bed tower technology commercially attractive. Reactor scaling may occur and is managed using anti-scaling agents.

Complete-mix reactors depend on CN stripping from the bulk liquid (Dzombak *et al.*, 2006). Consequently, multiple units and increased contact times are usually required to achieve the desired treatment levels as mass transfer at the air bubble interface is significantly slower than mass transfer through the liquid film surrounding the packing material in a tower setup.

Stripper off-gas requires secondary treatment and in the gold mining industry the CN-laden gas is passed through a sodium hydroxide (NaOH) solution, where the CN re-dissolves, before it is returned to heap leach operations (Xie and Dreisinger, 2009). Process steps include acidification, to convert ionic or CN_{wad} to hydrogen CN, followed by hydrogen CN stripping and subsequent CN recovery into NaOH, to form NaCN. The underflow is neutralised to precipitate metals, followed by transport to a tailings pond.

Table 1.6: Summary of the physical treatment technologies employed for the treatment of CN laden wastewater, depending on stream composition and concentration of contaminants

Technology	Advantages	Disadvantages	By-products	CN	SCN	CN_{wad}	CN_{sad}
Air stripping	Effective for free CN removal	Forms toxic HCN gas Coupled with other technologies for complete CN removal High operating cost	Limited	Yes	Limited	Yes	Yes
Adsorption	Effective for most CN species	High cost Low CN concentration treatment only	Acid wash water	Yes	Limited	Yes	Yes
Precipitation	Removes iron-CN complexes effectively	Potential dissolution of precipitates Precipitate disposal could be difficult	Metal precipitate	Yes	Limited	Yes	Yes

Compiled from (Young and Jordan, 1995; Gönen *et al*., 2004; Dzombak *et al*., 2006; Dash, Gaur, *et al*., 2009; Behnamfard and Salarirad, 2009; Xie and Dreisinger, 2009)

1.7.3.2 Adsorption technology

Adsorption technologies are based on the removal of specific compounds by their attachment to solid material, such as activated carbon or synthetic resins. Activated carbon is a porous, high surface area material with predominantly non-polar carbon surfaces. It is treated in various ways in order to obtain different functional surface groups and is therefore not very selective. Activated carbon has been shown to adsorb ferrocyanide, where synthetic ion exchangers are used for adsorption of free CN as well as metal-complexed CN (Young and Jordan, 1995; Dzombak *et al*., 2006; Behnamfard and Salarirad, 2009). The adsorption of CN to activated carbon has been shown to be significantly increased by the addition of metals such as zinc, iron, cobalt, nickel and copper, while the technology is specifically applied in the gold mining industry as carbon-in-column (CIC), carbon-in-leach (CIL) and carbon-in-pulp (CIP) processes, used for gold-CN adsorption. Where free CN is the primary pollutant, complexation with selected metals is preferred prior to adsorption. Synthetic exchange resins may be composed of a matrix of polystyrene, cross-linked with divinylbenzene, or made from polymeric beads containing a variety of functional groups (Dzombak *et al*., 2006). Positively- or negatively-charged groups can be employed for either anion- or cation exchange, respectively. Regeneration of the exchange material is achieved by contacting the loaded resin with a material capable of displacing the target ion, followed by treatment with sulphuric acid. The formation of hydrogen CN is a potential problem during acid regeneration. Interest in anion exchange resins for the processing of slurries from gold treatment facilities has increased due to the potential for higher recoveries and CN recycling. Synthetic adsorbents, such as the commercial polymer Vitrokele V912, have been shown to resist organic fouling, facilitate more rapid and effective desorption and regeneration, while being more cost effective than activated carbon (Young and Jordan, 1995).

Parameters that determine the adsorption efficiency include solution pH, contact time, resin-to-water ratio, resin type and loading rate (Dzombak *et al*., 2006). While there is interest in adsorption technologies, inconsistent recoveries (approximately 40% in some cases) and the loss of exchange capacity during regeneration of the anion exchange resin has meant that additional development is required before this technology will be widely adopted in industry.

1.7.3.3 Precipitation technology

The precipitation of metal CNs has been used in gold processing and also the treatment of strong metal CN complexes such as iron-, copper- and zinc CNs

(Clennell, 1910; Behnamfard and Salarirad, 2009). Precipitation is typically applied to wastewater with low CN concentrations (<50 mg/L total CN).

In relation to gold processing, zinc has been used in the Merrill-Crowe process (1990), for gold recovery (Clennell, 1910; Chi *et al*., 1997; Viramontes Gamboa *et al*., 2005). CN preferentially binds to zinc, resulting in the displacement and subsequent precipitation and recovery of gold, copper and silver. The precipitate is recovered from the solution matrix by filtration and refined to remove the copper and silver. This process is plagued by low recoveries, precipitation of impurities and cement-consuming side reactions. Additional research, aimed at better understanding the mechanisms involved, is required in order to further enhance the cementation process.

The low solubility and stable nature of iron-CN complexes has been exploited for the removal of CN species from solution (Young and Jordan, 1995; Dzombak *et al*., 2006). The most common complexes include Prussian- and Turnbull's Blue, which contain different proportions of ferric and ferrous ions. Various elements can also complex with iron-CN solids thereby facilitating their removal. For example, the removal of caesium from solution by co-precipitation with copper or zinc ferroCN has been achieved. However, challenges around pH maintenance and disposal of the resulting precipitate remain and have constrained broader industrial application of this technology (Dash *et al*., 2008).

1.7.4 Biological treatment of cyanide and cyanide compounds

The chemical and physical treatment technologies discussed above are characterised by a number of challenges, including slow metal precipitation kinetics, inefficient metal removal, inability to cope with fluctuating CN concentrations, harmful products produced as side reactions, inability to effectively remove SCN and licensing fees. This has resulted in a renewed interest in biological treatment processes.

The effective treatment of wastewaters by biological systems depends primarily on the biodegradability of the target compounds, as well as a number of critical process parameters. These include:

- The presence of suitable microorganisms at a sufficiently high concentration
- The availability of a suitable carbon source, electron donor, electron acceptor, nitrogen source and critical trace elements
- The absence of inhibitory compounds

- A suitable operating window with respect to physical and chemical parameters, including temperature, pH, salinity and ionic strength
- Sufficient contact time between the microorganisms and the pollutant

Free CN (HCN and CN^-) are biodegradable under both aerobic and anaerobic conditions and can be used as the sole nitrogen source for a range of microorganisms. In addition to free CN, metal CN complexes and SCN may also be degraded. A number of metabolic pathways have been proposed for this. CN speciation does influence the destruction of CN and current understanding of experimental data suggests that efficient destruction is limited to free CN, WAD CN complexes and SCN. Microbial treatment processes for CN containing waste produced by commercial operations are designed to accommodate large flow rates as well as elevated CN and SCN concentrations under a range of environmental conditions (Akcil and Mudder, 2003). Moreover, as regulations governing effluent discharge limits change, cleaner effluent standards are potentially achievable at lower operational and capital cost by employing biological treatment methods compared to conventional treatment technologies (Akcil, 2002). A major advantage of microbial treatment technologies is that the microbial system can be configured to fit a particular situation and waste stream. Microbial communities can thrive under changing conditions, allowing the destruction, sorption or uptake of SCN, CN, heavy metals, ammonia, sulphate and/or precipitation of selected compounds (Akcil, 2002; Akcil and Mudder, 2003; Dzombak *et al*., 2006; Baxter and Cummings, 2006).

A number of factors influence the choice of the most appropriate type of biological system for a particular application. Factors that need to be considered include the nature and composition of waste to be treated as well as the legislated environmental discharge specifications that are relevant to the site. The different CN species may be degraded via different metabolic pathways so the composition of the microbial community required to ensure effective treatment will differ. The nature of the effluent also influences the choice of reactor type and process flow sheet and this can have a significant impact on the capital and operating costs (Mosher and Figueroa, 1996).

The biological reactions involved in degradation are catalysed by enzymes, which function optimally within a relatively narrow pH and temperature range so these parameters play an important role in defining the operating window (Chaudhari and Kodam, 2010). Additional factors, such as the contaminant concentrations and loading rates, degree of aeration and/or agitation, the presence of suspended solids and the surface area available for microbial attachment select for specific microbial species and therefore influence performance (Dash, *et al*., 2009).

A significant amount of research has been conducted at laboratory scale and these studies have focussed on treating a specific CN compound, employing a specific microorganism under defined conditions. Moreover, studies have progressed to investigate real world waste streams at laboratory and pilot scale, but there have been comparatively few examples of biological systems being successfully applied at industrial scale. (Das *et al*., 1996; White and Schnabel, 1998; Ahn *et al*., 2005; Bezsudnova *et al*., 2007; Chen *et al*., 2008; Chaudhari and Kodam, 2010).

Commercial scale biological treatment processes have been used to treat wastewater generated during coal coking and gold mining. The Homestake process and the Activated Sludge Tailings Effluent Remediation (ASTER^{TM}) process are examples of commercial scale systems used in the gold industry. The Homestake process will be discussed below, while the ASTER^{TM} process, which forms the basis for this research, will be discussed in greater detail at the end of the chapter.

1.7.4.1 Homestake process

The Homestake process was developed by the Homestake Mining Company in South Dakota, USA. The facility was built in 1987 and was designed to treat 21,000 m^3 of liquid effluent per day utilising a total of 48 rotating biological contactors (RBCs) in two treatment stages. The process flowsheet is summarised in Figure 1.3.

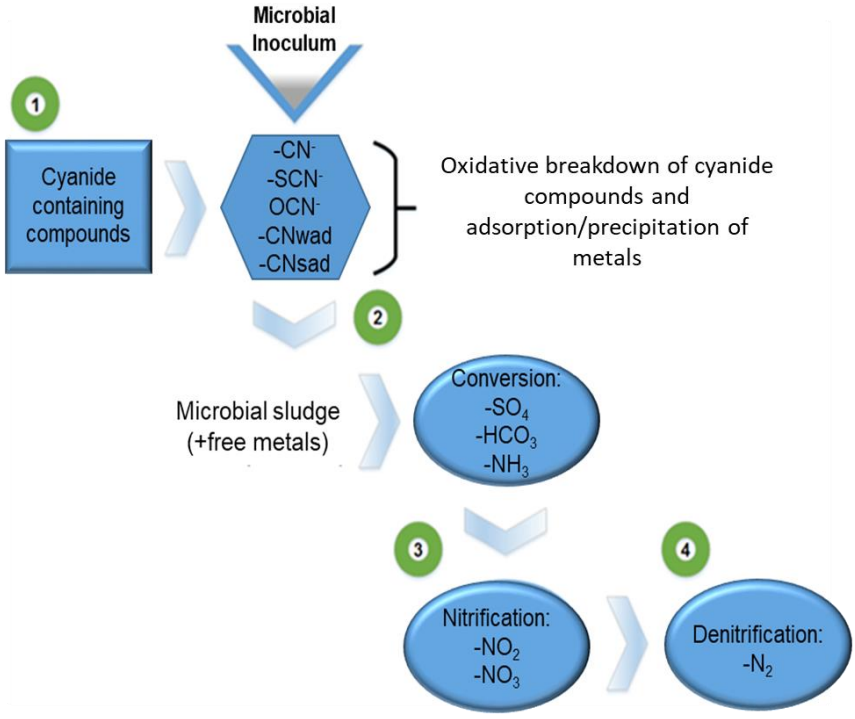

Figure 1.3: Homestake biological treatment process flow including (1) preparation of microbial inoculum and wastewater stream, (2) conversion to products due to breakdown of cyanide compounds, (3) aerobic nitrification and (4) anaerobic denitrification (Akcil and Mudder, 2003)

The process treated a blended influent stream containing SCN and CN at concentrations ranging from 35-110 mg/L and 0.5-11.5 mg/L, respectively, using RBCs (Akcil, 2003; Baxter and Cummings, 2006; Gould *et al*., 2012). The first stage, for CN and SCN treatment contained 24 RBC units (total surface area 9,290-13,935 m^2) and operated at a hydraulic retention time of one hour (Figure 1.4).

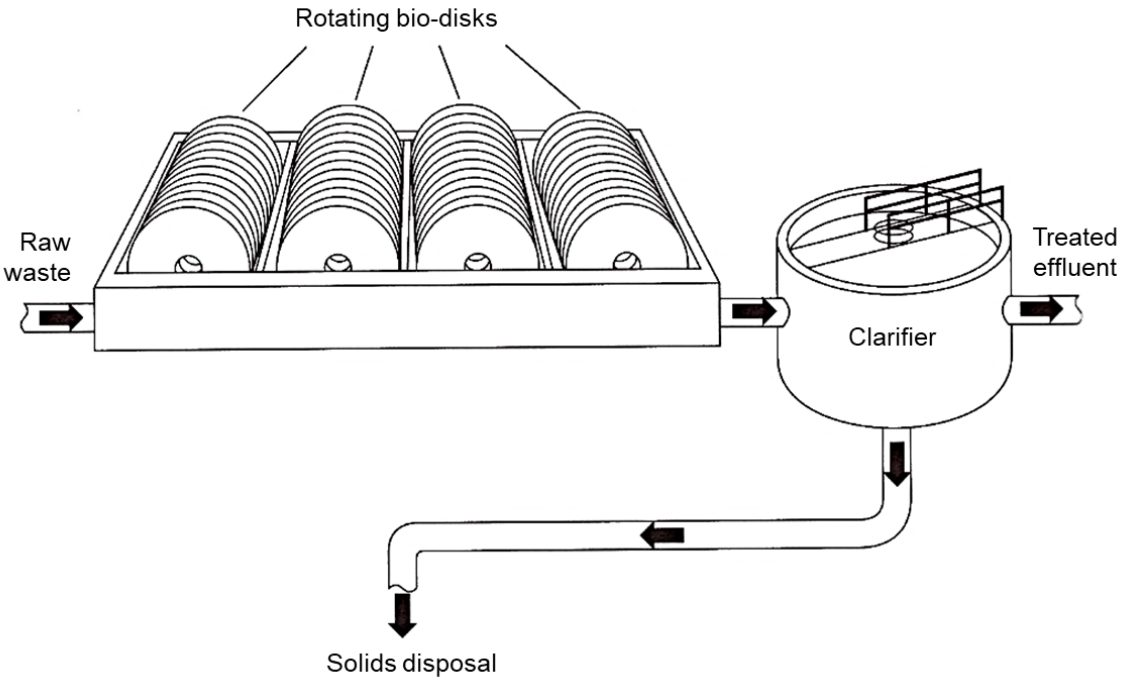

Figure 1.4: Schematic diagram of rotating biological contactor discs as an example of the reactor configuration used in the Homestake biological process (Dzombak *et al*., 2006)

The first stage includes oxidative destruction of CN and SCN (Rxn 6 and 7), with sorption and precipitation of metals to the microbial biofilm and formation of cyanate as an intermediate. Equation 6 depicts the overall SCN destruction reaction (Jeong and Chung, 2006).

$$SCN^- + 3H_2O + \ 2O_2 \rightarrow SO_4^{2-} + HCO_3^- + NH_3 + 2H^+ \qquad \text{Rxn 6}$$

$$CN^- + \tfrac{1}{2}O_2 + 2H_2O \rightarrow HCO_3^- + NH_3$$ Rxn 7

The remaining 24 reactors, with a similar surface area for bacterial growth, were employed for biological nitrification of the ammonium produced during SCN and CN degradation, but at an individual HRT of 1.5 hours (Dzombak et al., 2006). The predominant reaction chemistry is shown in Reactions 8 and 9.

$$NH_3 + \tfrac{3}{2}O_2 \rightarrow NO_2^- + H^+ + H_2O$$ Rxn 8

$$NO_2^- + \tfrac{1}{2}O \rightarrow NO_3^-$$ Rxn 9

The treated effluent contained SCN and CN at concentrations of <0.5 and 0.06 mg/L, respectively (Akcil, 2003; Baxter and Cummings, 2006; Gould *et al*., 2012). Some analysis of the microbial community was performed during the operation of the process but was limited by the techniques available at the time. *Pseudomonas paucimobilis* was identified within this process as the microorganism of interest for SCN and CN degradation. Adaptation of the microbial culture over a five year period resulted in decreased SCN and CN concentrations in the treated effluent stream while the treatment cost was lowered from \$0.20 to \$0.10 per m^3. Furthermore, CN_{wad} and CN_{sad} complexes were degraded to some extent, along with some physical adsorption to the biomass. This suggested that there may be potential for the development of a subsequent process to recover adsorbed metal species from the biomass.

1.8 CN degrading microorganisms

The efficiency of biological treatment processes depends on the presence of the correct microbial species, or consortia, and the maintenance of operational parameters within the optimal range. The following sections describe the microbial species that have been shown to degrade CN and SCN under laboratory conditions or have been identified in pilot or commercial scale reactors. This is followed by a closer look at the metabolic pathways that could be involved in the degradation of CN and SCN.

CN species (CN^- and OCN^-) represent a potential nitrogen source for microorganisms, while SCN provides an additional energy source, for chemolithotrophic species, in the form of reduced sulphur. A recent review by Watts and Moreau (2016) provides a good summary of sulphur-oxidising and nitrogen cycling consortia, as well as addressing on carbon cycling by heterotrophic SCN degrading species (Watts and Moreau, 2016). They review much of the work published to date on biological CN and SCN degradation and their findings are discussed in detail in the relevant sections of this study. Mekuto and co-workers (2018) showed simultaneous degradation of SCN and CN but did not elucidate the capability for nitrogen metabolism.

Historically, the ability to identify species involved in bioremediation systems was dependent on its isolation in pure culture. This provided very limited information, especially as not all species can be cultured in the lab in pure culture. Advances in molecular biology techniques, with the development of PCR, allowed culture independent identification of species, usually based on the 16S rRNA gene sequence.

A list of microorganisms that have been shown to degrade CN species in pure culture, along with their target substrates, is included in Table 1.7. In addition, more recent studies performed on mixed cultures from CN and SCN degrading reactors have identified a range of species that may be play a role in bioremediation. For example, the microorganisms previously identified to be active in the ASTER™ process comprise of species from the following genera: *Bosea, Sphingomonas, Pseudomonas, Ralstonia, Microbacterium* and *Pussilimonas* (du Plessis *et al.*, 2001).

These microorganisms employ different metabolic and enzymatic pathways in order to degrade or tolerate CN and SCN. A meaningful understanding of the relationship between the microbial community and the reactor systems is important in terms of optimising the treatment system. As an example, during the development of the Homestake process, initial test work employing continuous stirred-tank reactors (CSTRs) showed unfavourable results, largely due to the limited knowledge of the microbial community involved. Subsequent work using CSTRs and rotating biological contactors (RBCs), with a different microbial community, showed encouraging results for CN and SCN degradation and led to the successful development of the process (Stott *et al*., 2001). At the time, *Pseudomonas paucimobilis* was reported as the dominant organism, but the microbial characterisation was limited by the available techniques.

A relative lack of literature and the limited characterisation of the microorganisms active in biological CN and SCN degradation, specifically with respect to any synergistic relationships, have constrained the fundamental understanding of processes such as the Homestake and ASTER^{TM} systems, as well as the development of predictive operational models (Stott *et al*., 2001).

In addition to knowledge of the individual species that make up a mixed community, information on the metabolic potential of the community would make the development and optimisation of treatment systems much easier. CN containing compounds can be degraded via a number of metabolic pathways, each of which is catalysed by specific enzymes. Knowledge of the pathways and the genes that code for the specific enzymes allows important information to be extracted from metagenomic sequence data (Watts *et al.*, 2019).

Table 1.7: Microorganisms shown to be able to degrade cyanide containing compounds

Microorganism	C-Source	N-Source	Product(s)	Temp (°C)	pH	Reference
Burkholderia cepacia	Fructose	KCNO, KSCN	Formate, NH_3	30	7	(Adjei and Ohta, 1999)
Halomonas sp.	Glucose, Sucrose, Acetate, CO_2	SCN, S_2O_3	NH_4, CO_2, SO_4	20-37	6-9.3	(Stott *et al.*, 2001)
Klebsiella oxytoca	Glucose	CN, SCN	NH_4, CH_4	30	7.0	(Kao *et al*., 2003)
Klebsiella pneumoniae	Glucose	KSCN	NH_4, CO_2, H_2S	37	6.0	(Chaudhari and Kodam, 2010)
Ralstonia sp.	SCN	SCN	NH_4, SO_4	38	7.0	(Ahn *et al*., 2005)
Pseudomonas fluorescens	Glucose	$Fe(CN)_6$	NH_4, CO_2	25	5.0	(Dursun *et al.*, 1999)
Pseudomonas putida		CN	NH_4, CO_2			(Grigoreva *et al.*, 2006)
Pseudomonas sp.	Whey	CN_{wad}	NH_4, CO_2	30	9.2-11.4	(Akcil *et al*., 2003)
Pseudomonas stutzeri		CN, SCN	NH_4, CO_2			(Grigoreva *et al*., 2006)
Thiobacillus sp.	CO_2	SCN, S_2O_3	NH_4, CO_2, SO_4	20-40	6-9.3	(Stott *et al.*, 2001)
Thiobacillus sp.	SCN, CO_2	SCN	NH_4, SO_4	15-37	6.8-7.6	(Happold *et al*., 1954)
Thiobacillus thioparus	SCN	SCN	NH_4, CO_2, SO_4, COS	30	7.0	(Kim and Katayama, 2000)
Thiohalophilus thiocyanoxidans		SCN	NH_4, CO_2, SO_4	37	7.5	(Bezsudnova *et al.*, 2007)

1.9 Metabolic pathways identified for degradation of cyanide and cyanide compounds in various microorganisms

A number of metabolic pathways have been elucidated for the microbial mediated destruction of CN and CN compounds (Dumestre *et al*., 1997; Karavaiko *et al*., 2000; Baxter and Cummings, 2006; Dash, *et al*., 2009; Gupta *et al*., 2010). A wide variety of microorganisms have been implicated in the degradation of these compounds, including prokaryotes and eukaryotes such as fungi and algae (Dash *et al*., 2009).

1.9.1 Hydrolytic pathway

The hydrolytic pathway for the degradation of CN and CN compounds comprises various enzymes, including cyanidases, hydratases, hydrolases and nitrilases (Arakawa *et al*., 2007; Gupta *et al*., 2010).

thiocyanate hydrolase has been shown to catalyse SCN degradation (Rxn 10). The products include carbonyl sulphide and ammonia while further hydrolysis of carbonyl sulphide results in the formation of hydrogen sulphide and carbon dioxide (Bezsudnova *et al*., 2007).

The second pathway for SCN hydrolysis includes formation of cyanate before destruction to CO_2, NH_3 and SO_4 (Rxn 11).

$$SCN + 2H_2O \rightarrow SCO + NH_3 + OH \qquad \text{Rxn 10}$$

$$SCN + H_2O \rightarrow OCN + H_2S \qquad \text{Rxn 11}$$

Cyanidase enzymes convert CN directly to formate and ammonia (Rxn 12) without the need for additional substrate or co-factors. Cyanidase expression in *Pseudomonas stutzeri* was shown to be constitutive (Baxter and Cummings, 2006; Gupta *et al*., 2010). The *Pseudomonas stutzeri* cyanidase activity was shown to have a temperature optimum of 30°C and an optimal pH range of 6-10 which is broad compared with most enzymes. Furthermore, the formate and ammonia formed by the action of this enzyme were assimilated by *Pseudomonas stutzeri* during growth. The SCN degrading ability of *Pseudomonas stutzeri* has not been reported but this organism has been employed in a mixed culture degrading CN and SCN (Karavaiko *et al*., 2000). Other enzymes within the hydrolytic pathway category

include nitrilase enzymes which catalyse the hydrolysis of nitriles to ammonia and carboxylic acid. Nitrilases are less specific when compared to cyanidases and can catalyse a wide variety of structurally diverse nitriles, for example aliphatic nitriles.

$$R - CN + 2H_2O \rightarrow R - COOH + NH_3 \qquad \text{Rxn 12}$$

CN hydratase, nitrile hydratase and thiocyanate hydrolase catalyse direct hydrolysis of the carbon-nitrogen triple bond to form formamide (Rxn 13). CN hydratase is mainly found in fungi which produce formamide (Sexton and Howlett, 2000; Gupta *et al*., 2010). Subsequently, formamide hydratase catalyses the conversion of formamide to carbon dioxide and ammonia.

$$HCN + H_2O \rightarrow HCONH_2 \qquad \text{Rxn 13}$$

CN hydratase showed the highest substrate specificity for HCN but can also catalyse hydrolysis of tetracyanonickelate, acrylonitrile, methacrylonitrile and crotononitrile (Yanase *et al*., 2000; Dumestre *et al*., 1997). The authors concluded that CN was toxic due to the absence of growth with CN as the sole carbon and nitrogen source. Furthermore, HCN volatilisation can be minimised in industrial applications due to fungal growth under alkaline conditions (pH 9-11). Immobilised cells of *Fusarium* was found to tolerate CN levels up to 10 g/L with a drawback in that metal CN complexes could not be degraded (Gupta *et al*., 2010).

Nitrile hydratases have found industrial applications in the production of acrylamide from acrylonitrile as well as removal of nitriles from wastewater (Gupta *et al*., 2010). Nitrile hydratases contain iron or cobalt to promote structural stabilisation of the protein. Different protein domains within the enzyme contain metal ions, for example iron and cobalt, without which the domain unfolds and loses function. Nitrile hydratase activity varies from one micro-organism to the next and is located intracellularly with a broad range of substrate specificity and is inducible thus saving on metabolic energy.

1.9.2 Oxidative pathway

Utilising the oxidative pathway requires NADPH as well as an additional carbon source to degrade CN and produce carbon dioxide and ammonia, as described by Reaction 14 (Lalucat *et al*., 2006; Dash, *et al*., 2009; Gupta *et al*., 2010).

$$HCN + O_2 + 2H^+ + NADPH \rightarrow CO_2 + NH_4^+ + NADP$$ Rxn 14

Cyanide monooxygenase catalyses the conversion of one mole CN into cyanate with consumption of one mole of oxygen and NADPH to give ammonia and carbon dioxide. The consumption of CN was observed to be assimilative when oxidative enzymes were employed as bacterial growth was found to be proportional to CN degradation. Cyanide oxygenases serve well in wastewater treatment applications since specific microorganisms, such as *Pseudomonas* spp., employ these enzymes and have the ability to grow under high pH conditions (pH 11.5 in 30 mM CN) (Kunz *et al*., 1994; Baxter and Cummings, 2006). This bacterium can also employ nitroferricyanide, cyanoacetamide and other metal cyanide complexes as nitrogen sources.

1.9.3 Reductive pathway

Microorganisms, such as *Klebsiella oxytoca*, degrade CN via a reductive pathway in which CN is converted to methane and ammonia, as shown by Reaction 15 (Kao *et al*., 2003; Kao *et al*., 2004; Chen *et al*., 2008; Dash, *et al*., 2009). This pathway is considered to take place under anaerobic conditions and is catalysed by the enzyme nitrogenase. The carbon nitrogen triple bond is broken one bond at a time and replaced by hydrogen.

$$HCN + 2H^+ + 2e^- \rightarrow CH_4 + NH_3$$ Rxn 15

K. oxytoca was shown to degrade CN and SCN with methane being detected (Ebbs, 2004). Neither formate nor formamide (indicative of an organism employing an oxidative pathway) were detected following degradation of CN and SCN.

1.9.4 Transfer pathway

The transfer pathway results in the assimilative degradation of CN and is catalysed by enzymes, such as rhodanese and sulfurtransferase (Dash, *et al*., 2009). CN may be converted to the less toxic compounds cyanoalanine, aminonitrile or SCN, followed by hydrolysis. *Flavobacterium* as well as *Escherichia coli* and the fungi

Acremonium have been shown capable of the transfer pathway for the destruction of CN containing compounds.

1.10 Thiocyanate destruction kinetics

du Plessis *et al.* (2001) demonstrated successful SCN destruction using a mixed inoculum isolated from a gold mine tailings reservoir in Mpumalanga, South Africa (Table 1.8). Test work showed a maximum SCN destruction rate of 16 mg/$g_{biomass}$.h achieved at a maximum feed SCN concentration of 550 mg/L. Furthermore, it was observed that an increased biomass concentration resulted in maintaining a constant SCN effluent concentration (<1 mg/L) at shorter hydraulic retention times. Thiocyanate degrading cultures within the mixed microbial community were identified by traditional culturing techniques as *Ralstonia eutropha*, *Bosea thiooxidans* and *Sphingomonas paucimobilis*.

Similarly, a SCN destruction rate of 10 mg/L.h was achieved using an aerated reactor inoculated with sludge from a municipal wastewater treatment plant (Hung and Pavlostathis, 1997). The system was acclimatised for 150 hours, at an initial SCN concentration of 350 mg/L, before destruction of SCN was observed. Increased SCN destruction rates were observed over three consecutive SCN feeding cycles, operating as a fed-batch reactor. Rates increased from 2.76 to 7.60 mg/L.h which was lower compared to the initial acclimation experiment where a rate of 10 mg/L.h was measured. Hung and Pavlostathis (1997) concluded that a lower SCN loading ratio of 0.093 mg SCN/mg volatile suspended solids (VSS) compared to 0.7 mg SCN/mg VSS resulted in the lower rates observed. This demonstrated the importance of maintaining a high biomass concentration capable of degrading SCN to achieve maximum SCN destruction rates under maximum SCN loading (Table 1.8).

A number of investigations have shown SCN destruction under different conditions (Hung and Pavlostathis, 1997; Karavaiko *et al*., 2000; du Plessis *et al*., 2001; Ahn *et al*., 2005; Sirianuntapiboon and Chuamkaew, 2007; Lay-Son and Drakides, 2008). The published SCN destruction rates vary depending on the system used, microbial culture(s) employed, feed SCN concentration, pH and temperature. In summary, maximum SCN destruction rates do not exceed 50 mg/L.h under a broad range of conditions utilising different microorganisms and system configurations. Although a broad pH range for microbial SCN destruction was reported, the most favourable reported incubation temperature was 30°C and a dissolved oxygen concentration above 2 mg/L. Microorganisms may have specific synergistic relationships allowing

them to function in a mixed microbial population, ultimately determining system performance, and it is therefore vital to investigate system performance under different conditions. Furthermore, at an aeration rate above 0.26 vessel volume per minute (vvm), oxygen inhibition indicated by a reduced rate of ferroCN degradation as well as a reduced microbial (*Pseudomonas fluorescens*) growth rate, was observed (Dursun *et al*., 1999). Solution pH has also been shown to influence microbial activity during the degradation of CNs significantly. Reducing the pH from 10.0 to 9.5 during the growth of *Pseudomonas pseudoalcaligenes* resulted in the disappearance of the observed lag phase as well as a decreased dissolved oxygen concentration from 35-10% saturation which lasted 40-60 hours (Huertas *et al*., 2010). These factors highlight the need for microbial characterisation and acquiring growth kinetic parameters since the effects of growth conditions impacts significantly on microbial growth and performance.

Table 1.8: Microbial degradation of thiocyanate under various conditions using both batch and continuous system configurations

SCN (mg/L)	SCN degradation rate (mg/L.d)	pH	Temperature (°C)	DO (mg/L)	Inoculum	System	Reactor	Reference
500	240	<7.5	N R	>6 (2d RT)	Sludge	Fed batch	Cylindrical (4L)	Hung and Pavlostathis (1997)
250	33	7.0	38	2	*Klebsiella*	Batch	Bioreactor (1.5 L)	(Ahn *et al.*, 2005)
500	240	8.5	30	N R	Sludge	Continuous	CSTR (3 L)	(Lee *et al.*, 2008)
500	1200	7.1-7.2	29	2-4	Not reported	Continuous	CSTR (2-3 L)	(Lay-Son and Drakides, 2008)
550	275	6.2-7.8	28	2	*Ralstonia, Bosea, Spingomonas*	Continuous	Bioreactor (3.9 L)	(du Plessis *et al.*, 2001)
1000	1000	9.2-9.4	30	N R	*Pseudomonas*	Batch	Bioreactor (1-1.5 L)	(Karavaiko *et al.*, 2000)
1200	97	N R	N R	2-3	Sludge	Batch	Bioreactor (7.5 L)	(Sirianuntapiboon and Chuamkaew, 2007)

1.11 Activated sludge tailings effluent remediation process development

The microbial community employed to develop and use with the Activated Sludge Tailings Effluent Remediation (ASTER™) process technology was enriched and combined from both the Fairview BIOX® operation and the local municipal wastewater treatment process in Barberton, South Africa. The development of the ASTER™ process (Figure 1.5) was achieved first on laboratory scale (4 L) showing successful SCN destruction (van Buuren *et al*., 2011). This configuration was chosen based on previous experiments using either an activated sludge reactor or an attached microbial growth system. The reactor was aerated, using compressed air, providing not only oxygen to aerobic microorganisms, but also to ensure homogeneous mixing. Solid-liquid separation of the reactor overflow was achieved by using a settler and allowing biomass (underflow) to be recycled to the reactor or purged when required. Temperature control was achieved by using a heating coil.

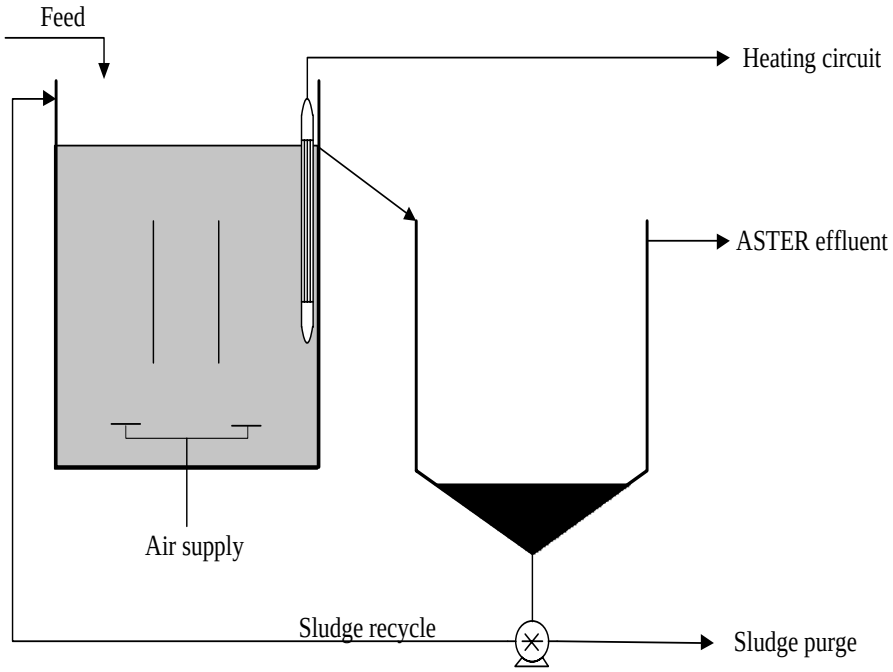

Figure 1.5: Schematic representation of the ASTER™ process consisting of an aerated bio-reactor and a clarifier. Temperature control is maintained by external heating when required while compressed air supplies both oxygen for microbial respiration and homogeneous solution mixing (van Buuren *et al*., 2011)

Initial research was performed by supplying the reactor with a feed SCN concentration of 200 mg/L which was incrementally increased to 550 mg/L while achieving >95% SCN destruction (du Plessis *et al.*, 2001). The maximum SCN

destruction rate was determined as 16 mg/g biomass.h based on dry sludge weight. It was also noted that the mass of sludge in the system increased with time but it was unclear whether it was due to an increase in SCN concentration or solely a function of sludge recycle. The SCN concentration in the clarifier was measured at 5 mg/L and remained unchanged during the experimental run.

Scale-up of the ASTER™ process to treat the solution separated from the tailings in an 80 L reactor was achieved and operated at 25°C. Destruction of SCN from various leach and CIP circuits was achieved at a degradation efficiency of >99.2% (Table 1.9). Furthermore, SCN destruction was not inhibited in the presence of anions and cations (Table 1.10). Dried sludge samples were analysed and found to contain only trace amounts of gold, copper and arsenic (van Buuren *et al*., 2011).

Table 1.9: Treatment of different solutions containing CN and thiocyanate using the ASTER™ technology. Taken from (van Buuren *et al*., 2011)

Solution	**Feed**		**Overflow**		**Sludge**		**SCN removal**
treated	SCN (mg/L)	CN- (T) (mg/L)	SCN (mg/L)	CN- (T) (mg/L)	Au (g/t)	s (g/t)	%
BIOX® CIP solution	965	n.d.	0.7	n.d.	n.d.	n.d.	99.9
BIOX® leach solution	184	2	1.4	<0.7	114	35	99.2
BIOX® tailings dam return water	405	<5	0.3	<0.02	107	465	99.9

Table 1.10: Cations and anions measured in the wastewater pre- and post-treatment by the ASTER™ process. Significant changes were not detected (Data supplied by Biomin)

Species	Concentration (mg/L)	
	Feed	Overflow
Li	<0.05	<0.05
Be	<0.05	<0.05
Mg	3040	2950
Al	<0.05	<0.05
Si	27	35
Ca	1030	1100
Ti	<0.05	<0.05
V	<0.05	<0.05
Cr	<0.05	<0.05
Mn	81	80
Fe	<0.05	3.0
Co	9.0	9.4
Ni	60	68
Cu	0.15	0.28
Zn	<0.05	<0.05
Ag	<0.05	<0.05
Cd	<0.05	<0.05
Pb	1.1	1.3

The next level of scale-up included a 2 and 6 m^3 unit, respectively. This was also employed to validate required nutrient dosages, hydraulic residence times and recycle rates obtained during operation of the 80 L reactor unit. The SCN feed concentration was controlled at 300 mg/L treating tailings solution at a hydraulic retention time as low as 2.5 hours and achieving a maximum SCN destruction rate of 43 mg/L.h. A demonstration plant was used to show continuous SCN destruction from tailings dam water using a 25 m^3 unit at solution pH conditions in the range of

7.5-11.0 (van Buuren *et al.*, 2011). Tailings solution treatment was achieved at a feed SCN and CN concentration of 110 and up to 8 mg/L, respectively, using a primary and secondary reactor fitted with a clarifier with 99.9% degradation achieved. The treatment of the tailings solution was achieved while maintaining a total CN concentration in the treated overflow of less than 2.8 mg/L, mostly reporting as free CN. The hydraulic retention time employed was 12 hours at 24°C with a sludge recycle volume of 20-30%. An interesting observation was the significant reduction in the concentration of copper, from 3 to < 0.2 mg/l, and nickel, from 7.1 to 3.7 mg/l. Furthermore, copper and nickel were detected in the sludge at concentrations of 2.3 and 1.9% by mass, respectively. This suggests either the precipitation of insoluble metal CNs or the adsorption of metal CN complexes onto the sludge particles; however, no iron data are available so it is difficult to draw definitive conclusions.

The ASTER™ plant at Consort mine South Africa was designed to treat 320 m^3/day of tailings solution containing an average SCN concentration of 120 mg/L and CN- concentration ranging between 10 and 30 mg/L (van Buuren *et al*., 2011). This ASTER™ configuration consists of four primary reactors each receiving a feed and four secondary reactors operated in series (Figure 1.6). The design hydraulic retention time was six hours across the primary reactors and expected to account for 80% of the SCN destruction. It was found that complete SCN destruction occurred during treatment in the primary reactors only which allowed additional treatment capacity should feed fluctuations occur. Overflow from the last secondary reactor was received by the clarifier from which sludge underflow was recycled to the primary reactors. The clarifier overflow delivered solution suitable for recycling to the flotation plant with a SCN concentration <0.5 mg/L.

Figure 1.6: ASTER™ pilot plant commissioned in Barberton, South Africa. Sludge, when produced, is recycled to the primary bioreactors in parallel while the secondary reactors, in series, receive primary overflow (van Buuren *et al*., 2011)

The operating conditions as well as operational performance are shown in Table 1.11. Furthermore, the operating costs were estimated to be US$ 0.42/m^3 (Feed SCN at 100 mg/L and an eight hour hydraulic retention time) and it is believed that this cost can be reduced by optimising system configuration.

ASTER™ compares favourably with not only existing biological treatment processes but also with chemical and physical treatment technologies. The ASTER™ system configuration is simple thereby lending itself to easy operation and adaptation for example treatment of slurries (Figure 1.7). Test work has shown stable operation of the ASTER™ process under defined conditions and additional research should be done to understand the controlling factors that impact on process performance under different environmental conditions.

Table 1.11: Operational design and actual parameters for the Consort pilot plant located in Barberton, South Africa (van Buuren *et al*., 2011)

Parameter	Unit	Consort design	Consort actual
Plant Design	m^3/d	320	~ 336
Feed SCN	mg/l	120	50–130
Feed free CN^-	mg/l	30	≤ 50
Retention time	hours	12	~10
Tailings solution pH			7–9
Effluent SCN	mg/l	≤ 0.5	≤ 0.2
Effluent CN^-	mg/l	≤ 0.5	≤ 0.2
Dissolved oxygen	mg/l	≥ 6	3–7
Temperature	^oC	24	≥ 20
SCN/CN^-removal	%	≥ 99	≥ 99.5
Molasses	kg/m^3	0.13	0.04
Phosphorous	kg/m^3	0.13	0.03
Reactor sludge recycle	% v/v	20-30	None

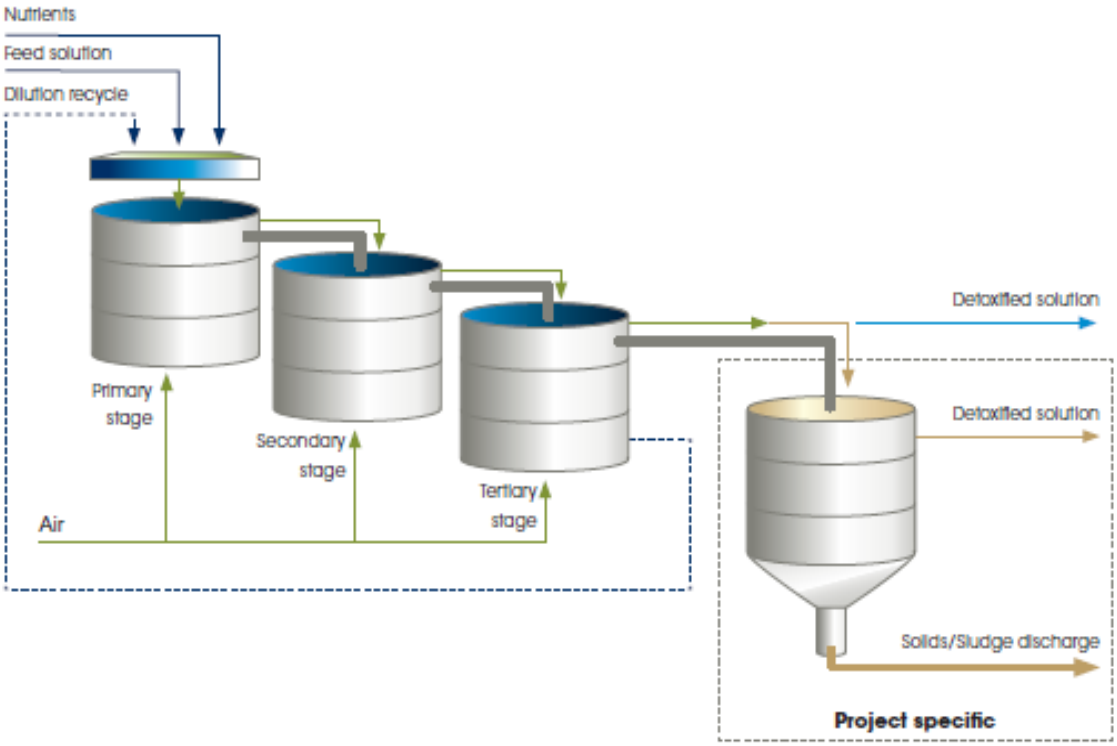

Figure 1.7: Representation of the potential system configuration of an ASTER™ process. The configuration is dependent on solution composition, treatment conditions and the volume of wastewater to be treated. (Taken from http://www.biomin.co.za/aster/technology.html)

1.12 Research motivation

The BIOX® process was developed as an alternative to conventional processes (roasting or pressure oxidation) for the treatment of refractory gold ores. The process has proven economically viable and has additional environmental benefits. The replacement of the roaster, for oxidation of the sulphidic ores, eliminated sulphur dioxide emissions as well as emissions of oxides of toxic metals such as arsenic. The BIOX® process uses a combination of iron- and sulphur-oxidising microorganisms to facilitate the degradation of the sulphide mineral matrix of ore. This results in exposure of gold for subsequent cyanidation. Sulphide mineral oxidation is not 100% efficient and cyanidation of the residual sulphur species results in the formation of a complex matrix containing relatively high concentrations of SCN (>550 mg/L) and residual CN (>30 mg/L). In addition, various metal-CN complexes are formed, which add to the complexity of the solution matrix. The SCN, residual free CN and metal-complexed CNs are deported with the tailings, as components of

the liquid fraction following treatment of any pre-treated concentrate containing sulphur.

The iron- and sulphur-oxidising microorganisms employed in the BIOX® process are susceptible to low levels (<1 mg/l) of SCN, so recycling of the tailings water up-stream of the bioleaching circuit is not feasible. The inability to recycle this water has implications for conservation and re-use, especially in arid regions. Furthermore, the concentration of SCN exceeds the legislated discharge specification, necessitating on-site treatment. The biological degradation of SCN and CN in effluents provides an alternative treatment to the more traditional processes such as hydrogen peroxide or the SO_2/air process (Akcil, 2003). CN and SCN are utilised by a number of aerobic microorganisms as a nitrogen and/or carbon and/or sulphur source (Kim and Katayama, 2000). Additional removal of metal-CN complexes is achieved by adsorption of the metal to the cell surface or extracellular polymeric substances secreted by the cells. These phenomena formed the basis for the development of a biological treatment system by researchers at Billiton Process Research , BHP-Billiton Process Research and Gold Fields Limited. The activated sludge tailings effluent remediation (ASTER™) process consists of an aerated reactor, in which the CN species are oxidised, and a settler to facilitate water recovery and recycling of the thickened sludge. The process has been successfully operated on a pilot scale under limited conditions at the Consort mine, consistently achieving effluent SCN concentrations below 1 mg/L.

Gold Fields indicated a desire to roll out the ASTER™ technology at industrial scale and export the technology to BIOX® operations outside South Africa. To support this, fundamental research to characterise the microbial operating window with respect to physicochemical conditions and loading rate as well as to unravel the microbial community and understand the role of microbial diversity in the process, is required. Destruction rates depend largely on the microbial species used as well as operating conditions. This project was therefore motivated by a need for a comprehensive investigation of the optimum operational parameters for successful wastewater treatment by the ASTER technology.

1.13 Research approach

The research approach taken followed two main pathways: investigation of operating conditions and identification of the microbial diversity. The operational research pathway first investigated the effects of SCN loading, temperature and pH on the SCN degradation ability of the microbial population, using batch studies (Chapter 4).

Subsequently, continuous studies were conducted in continuous stirred tank reactors to investigate the effect of SCN loading on the ASTER™ system under changing environmental conditions (Chapter 5). Conditions investigated included an incremental increased SCN loading rate through an increased feed SCN concentration from 100 mg/L until reactor performance was compromised (effluent SCN >1 mg/L). An assessment of the importance of biomass loading and retention was achieved by a comparison of reactor performance with different reactor geometries allowing a change in area-to-volume ratio. Reactor performance was further evaluated under different temperatures and solution pH conditions.

Based on the need to export the ASTER™ technology to different mine sites, it is feasible that the feed solution could contain solid particles due to incomplete solid-liquid separation following cyanidation. In Chapter 6, the effects of low solids loading (up to 5.5% (w/v)) on the SCN destruction ability of the mixed microbial population was investigated. Due to the potential complex nature of CN laden wastewater, the effects of CN combined with SCN in the feed on reactor performance was investigated in Chapter 7 while optimising hydraulic retention time and operating temperature to ensure complete CNs degradation.

Component species within the mixed consortium were isolated and identified using complex media. In addition, a clone library was built as part of a preliminary study to assess the microbial diversity (Chapter 3). The role played by these species, whether contributing to a mutualistic relationship or growing opportunistically on the molasses feed, was investigated through existing literature. This information can be used to infer which species will be the first to be lost from the mixed culture when reactor conditions deviate from optimal, the extent to which loss of certain species will affect performance and whether optimal performance can be recovered after the stress event without re-inoculation. Moreover, evaluation of the highly complex microbial diversity and potential symbiotic relationships within the microbial population, require a metagenomic investigation to better understand optimum inoculum requirements for ASTER™ operation. The metagenomics approach aimed to better understand the metabolic potential and ultimately the driving force behind the microbial community responsible for thiocyanate and cyanide destruction.

1.14 Hypotheses

1. The selective pressure of the feed make-up and flowrate will result in selection of a limited microbial population contributing to cyanide and thiocyanate destruction.
2. The ASTER™ mixed microbial community can tolerate a wide change of environmental conditions while maintaining practical thiocyanate destruction rates. Environmental conditions include thiocyanate and/or cyanide concentration, temperature and solution pH.
3. Sludge recycle is critical for retention of biomass in order to achieve regulatory disposal limits for effluent or allow recycle of wastewater to the BIOX® operation.
4. The ASTER™ process is capable of practical thiocyanate destruction in the presence of solids at concentrations inducing low shear.
5. Free cyanide is preferentially degraded when the feed contains both free cyanide and thiocyanate, resulting in a need for longer retention times to ensure compliant effluent concentrations are achieved.

Chapter 2: Materials and Methods

This chapter presents the materials and experimental methodologies used during the course of this study as well as the analytical techniques employed. Theoretical aspects and data analysis are also described. The detailed experimental approach and specific experimental designs will be described in the relevant chapters.

2.1 Microbial culture

The microbial culture that formed the basis of this work was obtained from the ASTER™ plant at the Consort mine in Barberton, South Africa (Figure 2.6). The ASTER™ culture was developed using mixed microbial communities was enriched from a municipal wastewater treatment works (Barberton, South Africa) and a tailings dam (Fairview BIOX® operation, South Africa). The reactor media used to maintain the stock culture and for all subsequent experiments, unless otherwise stated, contained molasses (0.15 g/L) and potassium dihydrogen phosphate (0.027 g/L PO_4^3) as well potassium SCN to the desired concentration.

2.2 Stock reactor and culture maintenance

The microbial consortium was maintained as a stock culture in a continuous stirred tank reactor (CSTR) (Figure 2.1). All experiments were initiated using culture from this reactor as the inoculum. The inoculum contained suspended flocs as well as planktonic cells.

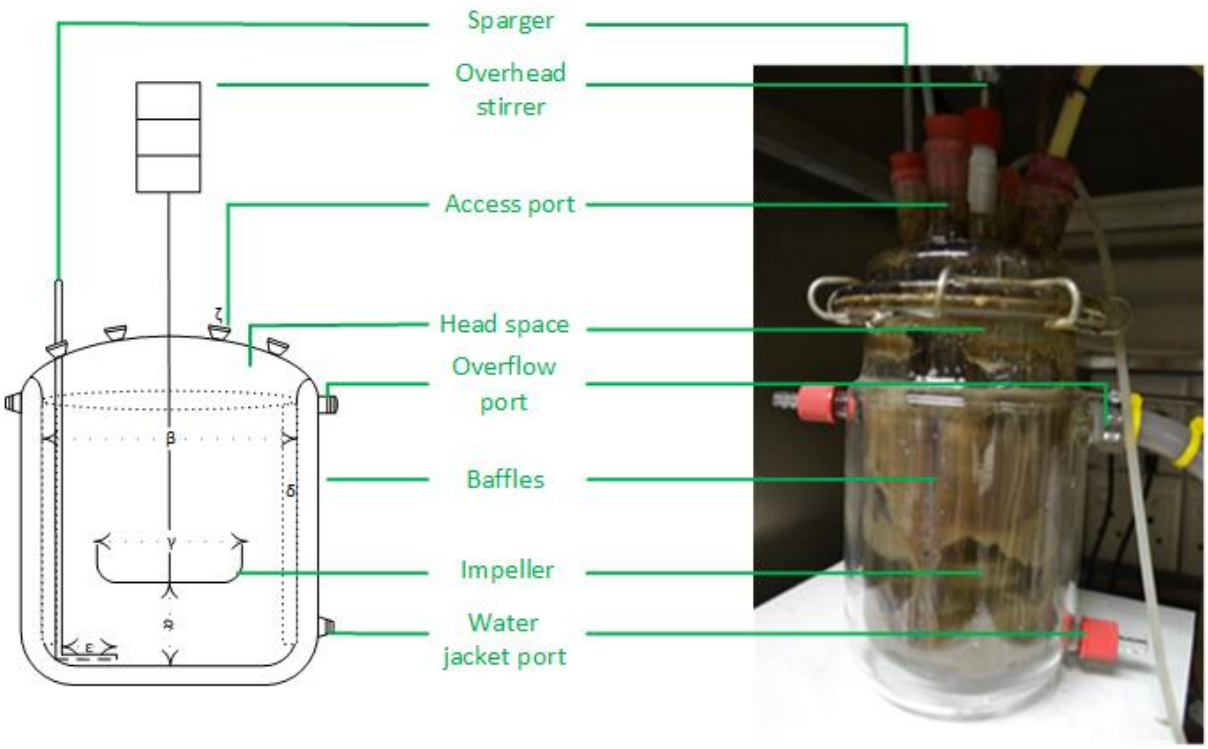

Figure 2.1: Schematic diagram and photo of the 1.3 L CSTR with cooling/heating jacket. This reactor geometry was used for both the long-term stock culture maintenance as well as for experimental work conducted under continuous operation

Table 2.1: Reactor geometry for the stock and experimental reactors.

Symbol	Description	Size
α	Impeller height from bottom of reactor	36.7 mm
β	Reactor diameter	104 mm
γ	Impeller diameter	58 mm
δ	Baffle ring/leg width	10 mm
ε	Sparger tip length	40 mm
ζ	Access port inner diameter	18 mm
Ratio of impeller diameter to reactor diameter (γ: β)		0.56
Aspect ratio		1.3
Working liquid height		118 mm
Working volume		1.00 L

The bioreactor had a height-to-diameter ratio of 1.3 and a working volume of 1.0 L. The reactor lid contained 5 ports for access, with diameters of between 10 and 20 mm. Aeration was supplied by a Peak-Scientific OAG2000DA oil-less air compressor utilising an L-shaped tube (ID of 5 mm) with four (1 mm diameter) holes. Mixing and gas dispersion was achieved using a Heidolph RZR 1 overhead stirrer with a pitched (45°) four-blade turbine impeller and vortex formation was minimised by the inclusion of four polymethyl methacrylate baffles, attached to a ring. The baffles were 150 mm long, 5 mm wide and 3 mm thick. Homogeneous mixing was attained at a speed of 270 rpm (impeller tip speed of 1.41 m/s).

A Masterflex L/S variable speed drive fitted with a standard multi-channel head and cartridges was used to supply feed (basic reactor media + 100 mg/L SCN, pH 7.0 ± 0.1) into the reactor at a defined dilution rate. Feed was supplied in through one of the ports in the reactor lid, while outflow, via an overflow port in the side wall, maintained the 1.0 L working volume. The effluent passed into a clarifier (height of 420 mm and 100 mm diameter (Figure 2.2) with an operating volume of two litres. Underflow from the clarifier was recycled back to the reactor.

The overall hydraulic retention time in the reactor was maintained at eight hours, with a recycle rate of 900 mL/h. Inlet gas was supplied as compressed air and controlled with a rotameter at a rate of 300 mL/min.

Samples for analysis were collected at regular intervals using a disposable syringe and filtered through a 0.45 µm membrane filter. Samples were stored at 4 °C when necessary and analysed for residual SCN.

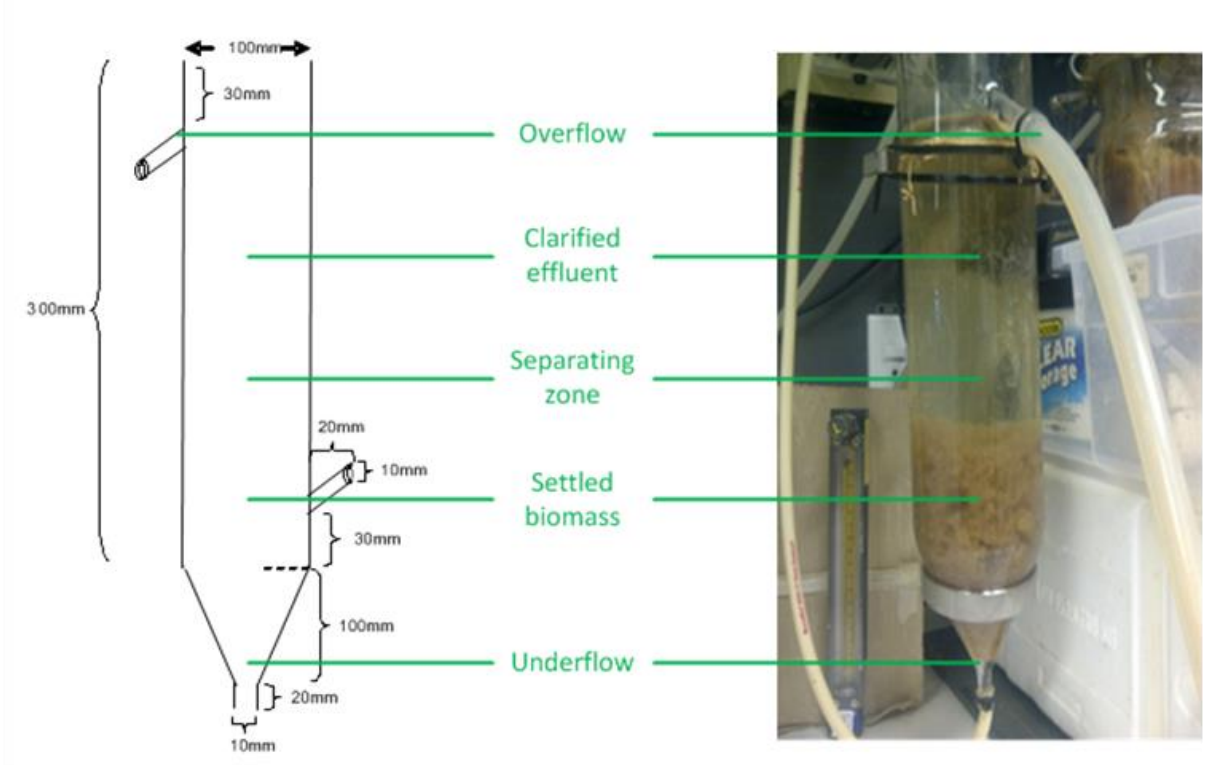

Figure 2.2: Schematic diagram and photo of the 2.0 L clarifier connected to the stock reactor.

2.3 Experimental bioreactors

Experimental studies were carried out using batch and a range of continuous stirred reactor systems. The basic reactor units are described below. Feed solutions to all reactors were prepared in bulk using graduated containers. The feed SCN and CN was analysed for each preparation before use.

2.3.1 Batch experiments

Studies were carried out using sterile conical flasks with a 40% working volume. Reactor media was used and the initial SCN concentration was varied as needed. Each flask was inoculated with a defined equal volume of suspended and particulate biomass from the stock reactor. The media pH was adjusted to pH 7.0 at sampling intervals by titration using acid or base, as required. Flasks were covered with cotton wool and aluminium foil and incubated on an orbital shaker (140 rpm) at constant temperature. Sampling was done aseptically at regular intervals and the residual SCN concentration measured.

2.3.2 Continuous reactor systems

Two types of bioreactors were employed for the experimental procedures and discussed below.

2.3.2.1 Glass 1.0 L reactors

The majority of the continuous experiments were conducted in glass bioreactors (1.0 L volume), identical to the stock reactor. The temperature of the 1.0 L borosilicate glass bioreactors was maintained by circulating water from an adjustable temperature water bath through an external glass jacket. The 1.0 L reactors were operated in an identical manner to the stock reactor, described in Section 2.2.

2.3.2.2 Sixfors reactor system

The Sixfors bioreactor system consisted of six 300 mL bioreactors, which could be independently controlled from a programmable control unit, operated in parallel (Figure 2.3). Continuous stirred tank reactors had a height-to-diameter ratio of 2.3 and a working volume of 300 mL. The stainless steel reactor lid had various ports allowing access to the reactor contents as well as for fitment of a dissolved oxygen and pH probe. Temperature was controlled by induction while mixing and gas dispersion was achieved by a magnetic stirrer and a 45 degree pitched four-blade impeller combined with stainless steel baffles. The baffles were 80 mm long, 5 mm wide and 1 mm thick.

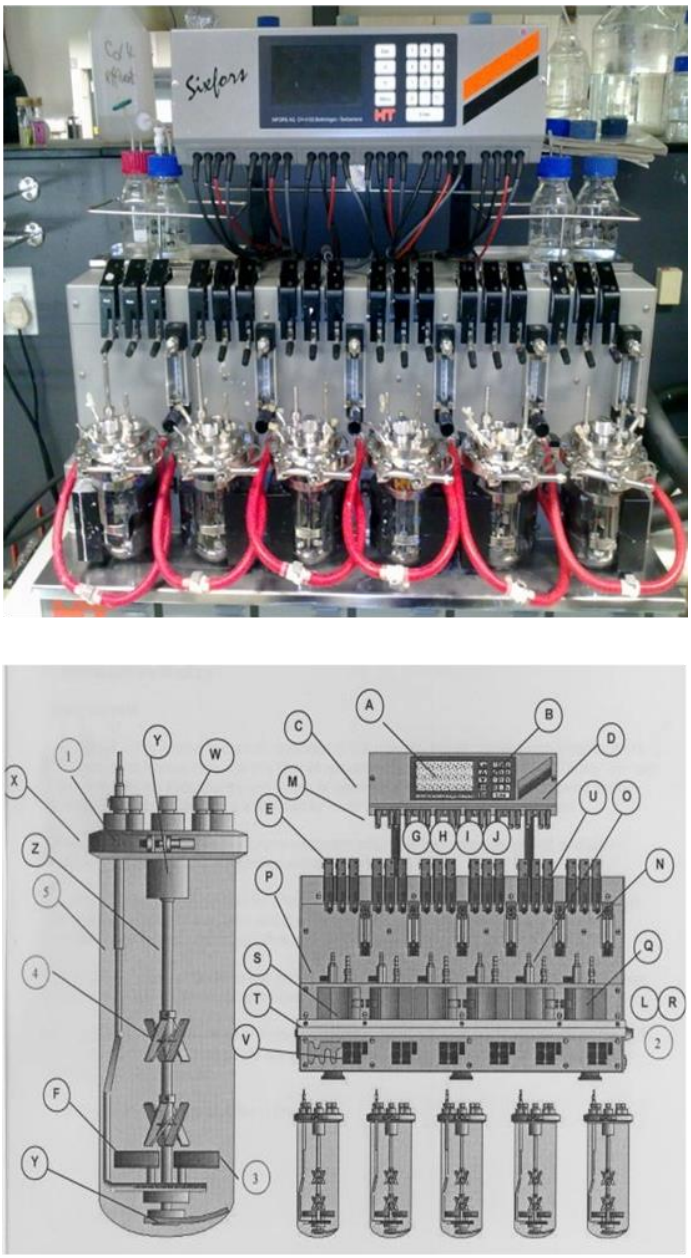

Figure 2.3: Schematic diagram of the 300 mL CSTR with cooling/heating induction clamp (**http://www.infors-ht.com**) Each part of the reactor configuration is as below from A-Z and 1-5.

A= Display, B= Keypad, C= RS232 Port, D= Memory Card Slot, E= Peristaltic Pumps, F= Magnets in vessel, G= Pt-100 Electrode Cable, H= pH ElectrodeCable, l= Oxygen Electrode Cable, J= Antifoam Probe Cable, K= Baffles (not shown, optional), L= Air Inlet, M= Operational Amplifier, N= Rotameter, 0= Water Pipe for Gas Cooler, P= Water Valve for Gas Cooler, Q= Base unit - Heater Block, R= Water Inlet, S= Spring to retain vessel, T= Vessel Support shelf, U= S. Steel Tray for Bottles, V= Magnetic Stirrer, W= Port Fittings, X= Top Plate Clamp, Y= Support for drive shaft, Z= Drive Shaft, 1= Top Plate, 2= Overflow Pipe to Drain, 3= Vessel Glass, 4= Impellers, 5= Sparger

Reactors were aerated using compressed air and the flow rate controlled using independent rotameters. Each reactor was fitted with a Mettler Toledo dissolved oxygen probe, calibrated using compressed air and certified pure nitrogen, and a gel-filled Mettler Toledo pH probe which could be calibrated using a two-point calibration (pH 4–7 or pH 7–9, as required). Feed addition was achieved using a Masterflex L/S variable speed drive fitted with a standard multi-channel head and cartridges. Dedicated software (IRIS) allowed real-time monitoring of the dissolved oxygen (DO) concentration in solution, stirrer speed, pH and temperature using a personal computer.

2.4 Analytical procedures

Filtered samples were diluted using double distilled water (ddH_2O) when necessary, followed by mixing for 30 seconds each using a vortex mixer.

2.4.1 pH measurement

Effluent pH measurements were taken using a Metrohm 704 pH meter with a combination electrode. Calibration was done using a three point calibration at pH 1.0, 4.0 and 7.0 or at pH 4.0, 7.0 and 10.0. The analytical error was found to be less than 1%.

2.4.2 Dissolved oxygen concentration measurement

The dissolved oxygen (DO) microprobe (Clark-type) OXY-10 was used to measure the DO concentration within the sludge. The OXY-meter was used to detect a change in signal strength received from the micro-probe and recorded by Unisense SensorTrace BASIC 3.0 software. The dynamic method for gassing out was used to measure the respiratory activity of the microbial population as discussed. Aeration is halted momentarily allowing oxygen consumption to be measured. Air is re-introduced under identical conditions and the increase in DO measured (Garcia-Ochoa *et al.*, 2010).

2.4.3 Thiocyanate analysis

The dissolved SCN concentration was measured as the thiocyanate-ion using HPLC (Tamosiunas *et al.*, 2006). The Thermo Scientific HPLC system was employed

using a UV-vis detector (Spectasystem UV1000) at 210 nm fitted with a deuterium lamp. The stationary phase used was a reversed phase Discovery C18-HS column (5 µm, 250 mm x 4.6 mm). The mobile phase consisted of 40% v/v acetonitrile in ddH_2O containing 2 mM tetrabutyl ammonium dihydrogen phosphate. The mobile phase was degassed in each case under vacuum while sonicated. Mobile phase was supplied at a rate of 0.5 mL/min. The SCN peak area was translated to SCN concentration using a standard curve. Thiocyanate standards between 1 – 100 mg/L were prepared fresh for each analytical run using potassium thiocyanate (Appendix A).

2.4.4 Cation analysis

Ammonium-, sodium- and potassium-ion concentration were measured using HPLC on selected samples. The Waters 717plus system with a conductivity detector (Water model 430) and a Hamilton cation exchange column (10 µm, 150 mm x 4.1 mm) was employed. The gain and range were set to 0.01 and 500 (µs x 10), respectively with a negative polarity. The mobile phase was prepared as a 30% methanol solution in ddH_2O supplied at a flow rate of 1 mL/min. The ammonium-ion standard curve was prepared fresh for each run between 1 – 100 mg/L (Appendix A).

2.4.5 Anion analysis

Selected samples were analysed for anions including phosphate (PO_4^{3-}), chloride (Cl^-), bicarbonate (HCO_3^-), nitrate (NO_3^-) and sulphate (SO_4^{2-}). The Waters 717plus system was used with a conductivity detector and a Waters IC-Pak HR anion exchange column. Gain and range were set to 0.01 and 500 (µs x 10), respectively with a positive polarity. The mobile phase used consisted of a sodium borate-gluconate solution as described in Appendix A. Standard solutions were prepared fresh with every run between 1 – 100 mg/L (Appendix A). The error analysis conducted on all measurements were performed by multiple measurements of selected samples as well as by using multiple standards in each run. The HPLC accuracy was calculated to be below 1.0 % from multiple standards included in each run. HPLC stationary phases were conditioned thoroughly before and after each run with freshly prepared and degassed (combination of vacuum and sonication) mobile phase.

2.4.6 Inductively coupled plasma atomic emission spectroscopy (ICP-OES)

ICP-OES (Varian 730-ES) was used to determine the inorganic elemental composition of the sludge fraction in CSTR's where discussed. Inorganic elemental composition analysis was also performed on the solid material (post cyanidation tailings) used.

Sludge samples (0.25 g) were digested using a MARS 5 microwave digester. A 10 mL aliquot of aqua regia was added to the samples in the control vessel. The power was set to 400 W, 100% and ramped for 25 minutes. The temperature was set to 210 °C under a pressure of 35 bar and a hold time of 15 minutes. Samples were analysed for elemental composition according to manufacturer's instructions.

2.4.7 Cynoprobe

The lab Cynoprobe (Figure 2.4) was used to measure free CN (HCN, CN^-) in solution. This electrochemical amperometric technique is based on steady state current produced in an electrolytic cell. The current produced is based on the reaction between CN and a silver electrode whereby electrons were liberated and a current established. The current produced was related to the chemical reaction rate at the silver electrode surface. The mass transfer rate at the silver electrode surface was dependent on temperature, agitation, electrode surface area and CN concentration. Temperature and agitation was maintained at 20 °C and 500 rpm (10 seconds) ensuring a homogeneous sample. The electrode surface was maintained and regular standard curves were constructed to ensure analytical accuracy. A programmable logic controller was used to convert the voltage signal into a counts value directly proportional to CN concentration.

The Cynoprobe operating cycle consisted of 3 phases including temperature control, rest for solids settling and measuring current produced by CN in solution. Standard CN solutions were prepared in the range 0.3 – 30 mg/L CN^- and a sample standard curve is included in Appendix A.

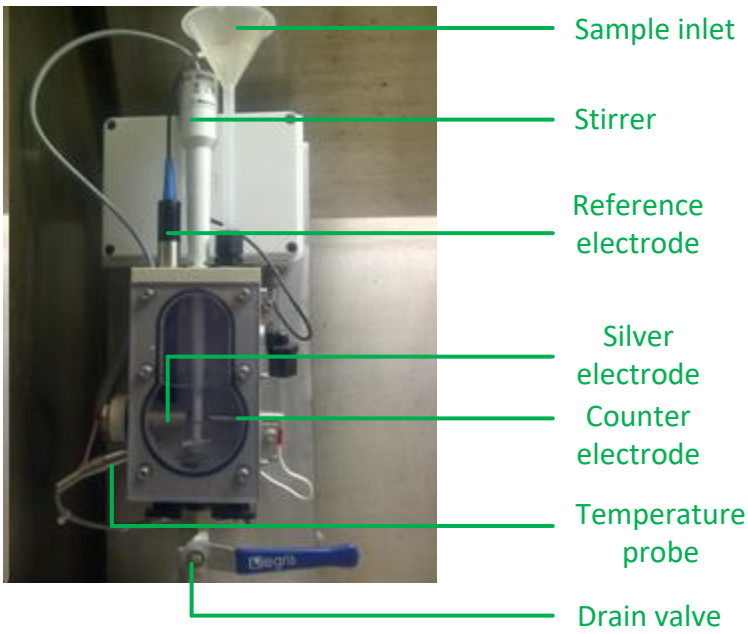

Figure 2.4: Photograph of the lab Cynoprobe used to measure feed and residual CN concentrations during experimental runs

2.4.8 Scanning electron microscopy (SEM)

Samples were collected and 20 mL was filtered onto SPI-pore poly membrane filters (0.22 µm pore size) and covered with 1% glutaraldehyde for 24 hours at 4°C. Samples were washed with 1x phosphate-buffered saline solution (pH 7.2) to clear the sample of glutaraldehyde. A dehydration series was performed following sample fixation. Ethanol of increasing concentrations was used starting at a 30% solution followed by 50, 70, 80, 90, 95 and 100%. The samples were incubated for 10 minutes in each solution before the next higher concentration was applied. The filters were cut and mounted onto aluminium stubs with carbon-containing glue and treated with hexamethyldisilazane (HMDS) to dry for three hours. The dried sample was coated with carbon using a Balzers evaporation coater and analysed using a FEI NOVA NANOSEM 230 with a field emission gun.

2.5 Molecular analysis

A three pronged approach was followed to analyse the microbial diversity in the sludge responsible for SCN destruction. Mono-cultures were isolated using traditional culturing techniques, followed by DNA extraction and identification of the 16S rRNA region used for subsequent culture identification. The second approach entailed total DNA extraction from a sludge sample and the creation of a 16S rRNA

clone library. Lastly, samples from experimental research were provided for DNA extraction and sequencing to the University of California, Berkeley, CA, USA (Kantor *et al.*, 2015). Sequence assembly was performed and the phylogenetic annotations assigned. Furthermore, potential metabolic pathways were identified from constructed genomes and was discussed accordingly in this thesis as supporting research.

2.5.1 Microbial isolation and identification

Microorganisms were isolated from the mixed microbial sludge using traditional microbial isolation techniques. Three media compositions were used to isolate individual microorganisms and in order of decreasing media richness was lysogeny broth (LB), K9 media and reactor media, all containing SCN (100 mg/L). Lysogeny broth contained yeast extract (5.0 g/L), peptone (10.0 g/L), sodium chloride (10 g/L) and bacteriological agar (15.0 g/L). K9 media consisted of ammonium chloride, sodium chloride, potassium phosphate and bacteriological agar (15.0 g/L). The reactor media contained molasses (0.15 g/L), potassium phosphate (0.027 g/L PO_4^{2-}) and bacteriological agar (15.0 g/L). Bacteriological agar was omitted for cultures grown in liquid culture. Single colonies were selected and grown as mono-cultures on solid media followed by inoculation of liquid media for nucleic acid extraction. Sample preparation for work done in Section 3.2 was performed by homogenisation of harvested sludge using a vortex and pipetting up/down for one minute each. The sludge was diluted in filtered (0.22 µm) reactor effluent as discussed and a volume of 100 µL was spread plated. Plates were incubated at ambient temperature and morphologically different single colonies were selected within one week and transferred to fresh plates. Cultures were grown for DNA extraction and amplification of the 16S rRNA gene. The 16S rRNA genes were cloned using pGEM®-T Easy vector (Promega) and sequenced for identification using the genbank culture database. Genomic DNA was extracted for construction of the clone library using the High Pure PCR Template Preparation Kit (Roche Applied Sciences). Amplification of the 16S rRNA region was followed by cloning using the pGEM®-T Easy vector (Promega). Recombinant clones were grouped into Operational Taxonomic Units (OTU), based on amplified rDNA restriction analysis (ARDRA) restriction patterns generated by single digestions using *Alu*I and *Hae*III (Fermentas).

2.5.2 Nucleic acid extraction from isolated cultures and from bio-sludge

Cell lysis buffer was added to the sample containing the liquid mono-culture as described in section 3.6.1. The sample was transferred to a sterile centrifuge tube and centrifuged at 10 000 xg for 10 minutes. The supernatant was discarded and the pellet washed with 1 x PBS solution (pH 7.0) and the centrifuge step repeated. Total DNA was extracted using the Roche High Pure PCR Template Preparation Kit according to manufacturer's instructions. The extracted DNA was quantified and qualified spectrophotometrically using the Nanodrop 2000 by analysis the wavelengths at 230, 260 and 280 nm.

Samples containing sludge were collected using sterile syringes to dislodge sludge from the reactor wall. A vortex mixer was used to disrupt the sludge using glass beads (3 mm spherical beads) to homogenise the samples in lysis buffer at maximum speed for 1 – 2 minutes. The samples were incubated overnight at -20°C and the liquid fraction was transferred to a sterile centrifuge tube and centrifuged at 10 000 xg for 10 minutes. The supernatant was discarded and the pellet washed with 1 x PBS solution (137 mM NaCl, 10 mM Na_2HPO_4, 2.7 mM KCl, 2.0 mM KH_2PO_4, pH 7.4) and the centrifuge step repeated. Total DNA was extracted as described above followed by quantification and qualified using the Nanodrop 2000.

2.5.3 Polymerase Chain Reaction (PCR) for 16S rRNA amplification of isolated mono-cultures

Bacterial 16S rRNA genes were amplified using universal forward 27f (5'-AGAGTTTGATCMTGGCTCAG-3') and reverse 1492r (5'-GGTTACCTTGTTACGACTT-3') primers (Kim *et al*., 2011). Extracted genomic DNA (gDNA) was subjected to amplification using a reaction mixture containing a final reaction volume of 25 µL that included both primers (0.25 µM), dNTP's (200 µM), magnesium chloride (1.5 mM), 1 µL FastStart Taq DNA Polymerase (Roche) and 1 µL DNA template. Amplification conditions included a denaturation step (96 °C for 6 min) followed by 35 cycles of denaturation (96 °C for 10 sec), elongation (55 °C for 15 sec) and annealing (72 °C for 25 sec). A final elongation step (72 °C for 2 min) was used to complete the process. PCR amplification was performed using a G-storm thermocycler. Agarose gel electrophoresis was used to confirm formation successful PCR products employing a 0.8% (w/v) agarose gel and ethidium bromide (0.05 µg/mL) for staining. The Syngene G:Box was used for visual confirmation of amplified products under ultra-violet illumination and Genesnap V7.12 software.

2.5.4 Polymerase Chain Reaction (PCR) for 16S rRNA amplification of selected clones for library creation

Bacterial 16S rRNA genes intended for use in construction of the clone library were amplified using the M13 forward primer (5'- AGAGTTTGATCMTGGCTCAG-3') and M13 reverse primer (5'- GGTTACCTTGTTACGACTT-3') to generate amplicons of approximately 1.2 kB long. Extracted genomic DNA was subjected to amplification using a 25 µL reaction mixture containing both primers (0.25 µM), dNTP's (200 µM), magnesium chloride (1.5 mM), 1 µL FastStart Taq DNA Polymerase (Roche) and 1 µL DNA template. Amplification conditions included a denaturation step (96 °C for 6 min) followed by 35 cycles of denaturation (96 °C for 10 s), elongation (55 °C for 15 s), and annealing (72 °C for 25 s). A final elongation step (72 °C for 2 min) was used to complete the process. PCR amplification was performed using a G-storm thermocycler. Agarose gel electrophoresis was used to confirm formation successful PCR products employing a 0.8% (w/v) agarose gel and ethidium bromide (0.05 µg/mL) for staining. The Syngene G:Box was used for visual confirmation of amplified products under ultra-violet illumination and Genesnap V7.12 software.

2.5.5 DNA gel extraction

Bands were excised from agarose gels using a sterile scalpel under long wavelength UV light under minimum exposure conditions. Excised gel fragments were placed in sterile Eppendorf tubes with 20 µL nuclease free water. The samples were incubated at 4°C overnight. The liquid fraction was used as template for the PCR reaction as described above.

2.5.6 Plasmid ligation, transformation and extraction

The pGEM®-T Easy vector system was used for cloning of the PCR products obtained to identify the isolated pure cultures as well as the clones generated in the clone library. This system allowed for replication of the highly conserved 16S rRNA sequence for subsequent species identification. Competent *E.coli* cells (DH5α) was prepared using the calcium-chloride protocol (Sambrook and Russell, 2001). Ligation was performed by mixing the DNA template with the vector reagent and incubation overnight at 4°C according to manufacturer's instructions (Promega pGEM-T Easy Vector Systems Technical Manual). These instructions were also followed for transformation. Plasmid extractions were performed on selected white colonies grown overnight in liquid Lysogeny broth at 37°C. The GenElute™HP

Plasmid miniprep kit was used for plasmid extraction. Cell were recovered by centrifugation (13 000 xg for 90 seconds) of 4 mL culture. The pellet was processed as per manufacturer's instructions.

Sequences obtained from Macrogen (automated sequencer system) were compared to a database using the basic local alignment search tool (BLAST) tool from the National Center for Biotechnology Information (NCBI) (Altschul et al., 1990).

2.5.7 Restriction fragment length polymorphism (RFLP)

Clones selected for library construction were subjected to RFLP analyses using *Alu*I and *Hae*III restriction enzymes. Samples were purified using a PCR clean-up kit (Machery-Nagel) following the manufacturer's instructions. Digestion was performed according to manufacturers instructions (Fermentas). The Syngene G:Box was used for visual confirmation of digested products under ultra-violet illumination and Genesnap V7.12 software. Digestion products ran in a single lane representing a single genotype. Clones producing unique visual patterns were selected for sequence determination.

2.5.8 Experimental approach to community structure analysis discussed in Chapter 6

To prepare culture isolates, a dilution series of a 10 ml reactor sample, harvested using a sterile syringe (Day 200), was prepared in sterile basal growth medium (pH 7.0) and spread plated onto solid reactor medium (reactor growth medium with the addition of 15 g/l bacteriological agar, 50 mg/L SCN and 50 µg/ml cyclohexamide), yeast extract malt extract agar (YEME: 4 g/l yeast extract, 10 g/l malt extract, 4 g/l glucose, 15 g/l bacteriological agar, 50 mg/L SCN and 50 µg/ml cyclohexamide, pH 7.3) and Czapek solution agar (30 g/l sucrose, 2 g/l $NaNO_3$, 1 g/l K_2HPO_4, 0.5 g/l KCl, 0.5 g/l $MgSO_4.7H_2O$, 10 mg/L $FeSO_4.7H_2O$, 15 g/l bacteriological agar, 50 mg/L SCN and 50 µg/ml cyclohexamide, pH 7.3) for the isolation of prokaryotes. Diluted samples were also plated onto Sabourand agar (10 g/l peptone, 40 g/l glucose, 15 g/l bacteriological agar, 50 mg/L SCN and 30 µg/ml chloramphenicol) for the isolation of eukaryotes. The use of cyclohexamide was to inhibit growth of eukaryotes while chloramphenicol inhibits the growth of bacteria. These aid in isolation of desired microorganisms while inhibiting possible growth of unwanted microorganisms. The plates were incubated at 22°C and individual colonies, displaying a unique phenotype, were aseptically transferred onto fresh solid growth media to confirm culture purity, before being inoculated into liquid growth media (prepared as

described above with the omission of bacteriological agar). Cultures were incubated at 22°C on a rotary shaker at 200 rpm for 48 hours or until liquid medium appeared turbid, indicating growth of the organisms.

Genomic DNA was extracted from the respective liquid cultures and used as the template for the PCR amplification of 16S rRNA and 18S rRNA genes of the individual species, using the universal bacterial, 27F (5'-GAGAGTTTGATCITGGCTCAG-3') and 1492R (5'-GTACGGITACCTTGTTACGACTT-3'), and universal 18S rRNA, Uni18S-F (5'-GAAACTGCGAATGGCTC-3') and Uni18S-R (5'-CACCTACGGAAACCTTGTTA-3'), primers, respectively. Cycling conditions for the universal bacterial primers included an initial denaturation (6 min at 96°C), followed by 35 cycles of denaturation (15 s at 96°C), annealing (15 s at 60°C), and extension (20 s at 72°C), followed by a final extension (5 min at 72°C). Cycling condition for the universal 18S rRNA primers included an initial denaturation (6 min at 96°C), followed by 30 cycles of denaturation (10 s at 96°C), annealing (15 s at 60°C), and extension (20 s at 72°C), followed by a final extension (5 min at 72°C). PCR for both primer pairs was carried out in 50 µl reaction volumes containing 2 mM $MgCl_2$, 1 U Kapa*Taq* polymerase (Fermentas), 200 µM dNTPs, 0.5 µM of each primer and approximately 20 ng of total genomic DNA.

PCR reaction products were evaluated following electrophoresis on a 0.8% (w/v) TAE agarose gel. PCR amplicons were purified using a PCR purification kit (Macher-Nagel) and cloned into pGEM®-T Easy vector (Promega), according to the manufacturer's instructions. To assess the culture-independent microbial community, total genomic DNA was extracted from a 150 ml reactor sample using the High Pure PCR Template Preparation Kit (Roche Applied Sciences), according the manufacturer's instructions. The 16S rRNA and 18S rRNA genes of the individual isolates contained within the reactor sample were amplified by PCR and cloned into the pGEM®-T Easy vector system, as described above. Recombinant clones were grouped into Operational Taxonomic Units (OTU), based on ARDRA restriction patterns generated by single digestions using *Alu*I and *Hae*III (Fermentas).

A single representative of each 16S rRNA and 18S rDNA OTU was sequenced using the universal M13F (5'-GTAAAACGACGGCCAGT-3') and M13R (5'-GCGGATAACAATTTCACACAGG-3') primers (Macrogen).

Homology and similarity searches of DNA consensus sequences were performed using the nucleotide-nucleotide basic local alignment search tool (BLASTN) program (Altschul *et al.,* 1989; Altschul *et al.,* 1997), as provided by the National Centre for Biotechnology Information (NCBI) (http://www.ncbi.nlm.nih.gov/BLAST/). For

phylogenetic analysis, reference strains selected based on lowest E-values or highest sequence similarity from BLASTN results were included. Sequences were downloaded from the GenBank database (NCBI), aligned using CLUSTAL_X, version 2.1 (Larkin *et al*., 2007) and a portion of the respective 16S rRNA and 18S rRNA sequences were manually edited to a common length. Phylogenetic and molecular evolutionary analyses were conducted using MEGA version 5 (Tamura *et al*., 2011) and a neighbour-joining (Saitou and Nei, 1987) tree constructed. Bootstrap values were based upon 1,000 re-sampled data sets (Felsenstein, 1985) and only bootstrap values greater than 40% are indicated.

Further analysis of the community structure was done by Rahman and co-workers, 2017 (Rahman *et al.*, 2017). DNA from two samples (sampled one month apart) were extracted and processed independently. Illumina sequencing was followed by gene assembly and genome prediction allowing analysis and/or identification of potential metabolic pathways of the microbial community.

Chapter 3: Microbial isolation and identification of the ASTER™ culture using traditional microbiological methods as well as molecular tools

3.1 Introduction

Various studies have shown the correlation between system performance and the presence of specifically a mixed microbial community (Baxter and Cummings, 2006; Felföldi *et al*., 2010). The group of Felföldi, (2010) showed the need for a mixed microbial community in order to degrade phenol and SCN found in coal coking effluent. Genera, for example *Pseudomonas* and *Comamonas,* was identified as key phenol degraders while *Thiobacillus* members degraded SCN and *Ottowia* related strains were responsible for floc formation. These symbiotic relationships resulted in destruction of multiple undesirable components.

The complex nature of the wastewater to be treated in the current study required culture identification using a simplified polyphasic approach. The first approach included traditional microbiological culture techniques to isolate mono-cultures from the ASTER™ sludge. This approach allowed for identification but also isolation of desirable cultures for future research and potential inoculum design. The second approach included construction of a 16S rRNA clone library that allowed for a more comprehensive analysis of the microbial diversity under reactor operation. Due to the fundamental role played by the microbial consortium it was important to identify the species involved in the ASTER™ process. It is well known that 1% or less of the microbial diversity present in environmental samples are amenable to traditional culturing methods for isolation and growth (Amann *et al*., 1992). Molecular tools were therefore employed to describe the microbial diversity of the inoculum from the stock reactor.

The research discussed in this chapter include a preliminary study into the diversity of the microbial consortium used as seed for the experiments conducted throughout the research program. It was hoped that this information could be used to further understand and optimise the operational performance of the ASTER™ process. Metabolic capability was highlighted where appropriate and discussed with potential relevance to commercial application.

The key questions addressed in this chapter are as follow:

(i) Does light or electron microscopy offer insight into the microbial diversity of a sludge sample?

(ii) What was the culturing potential of mono-cultures from the sludge using limited selective solid media?

(iii) Was there any correlation in microbial diversity between culturing and non-culturing methods?

(iv) Would a designer inoculum be favourable as an inoculum for a commercial plant?

3.2 Results and Discussion

Microbial diversity was observed visually using light microscopy as well as scanning electron microscopy (SEM). The microbial diversity was described by traditional culturing methods as well as more advanced metagenomics techniques including high through-put sequencing and sequence assembly (Kantor *et al*., 2015). Sludge from the stock and mixed SCN-CN fed reactors were sampled and spread onto plates containing selective solid media. The stock reactor setup is described in Chapter 3 while a description of the reactor setup receiving mixed feed (SCN and CN) can be found in Chapter 7. Cultures were grown for DNA extraction and amplification of the 16S rRNA gene. The 16S rRNA genes were cloned and sequenced for identification using the genbank culture database.

Homology and similarity searches of DNA sequences were performed in both approaches to diversity, using the basic local alignment search tool (BLASTN) program. Phylogenetic and molecular evolutionary analyses were conducted and a neighbour-joining tree constructed.

Light microscopy of the stock reactor sludge showed morphologically diverse bacterial species as well as fungi, algae and yeast like cells (Figure 3.1). The sludge appeared dense due to a formed network comprising extracellular polymeric

substance (EPS) and microorganisms, without specific distribution of the microorganisms. Dense microbial growth was observed from samples collected from the reactor sidewalls as well as from the reactors internal surfaces for example the impeller and baffles. In contrast, the bulk liquid contained suspended flocs, but mainly free floating cells. Furthermore, highly motile microorganisms were observed in the reactor liquid harvested without sludge addition (Huddy *et al*., 2015).

Biofilms and therefore activated sludge are believed to form in order to benefit from cooperative efforts in a community, colonisation of a nutrient rich area and protection from environmentally adverse conditions and predators (Jefferson, 2004). Biofilms are resistive to shear forces produced by high liquid velocities as well as serving to protect microorganisms against nutrient deprivation. Biofilms develop in nutrient rich areas with the aid of excreted exopolysaccharides ensuring a high likelihood for commensalism for example utilisation of sulphur and nitrogen from SCN destruction and thereby preventing build-up of potentially inhibitory compounds (Lee *et al*., 2008).

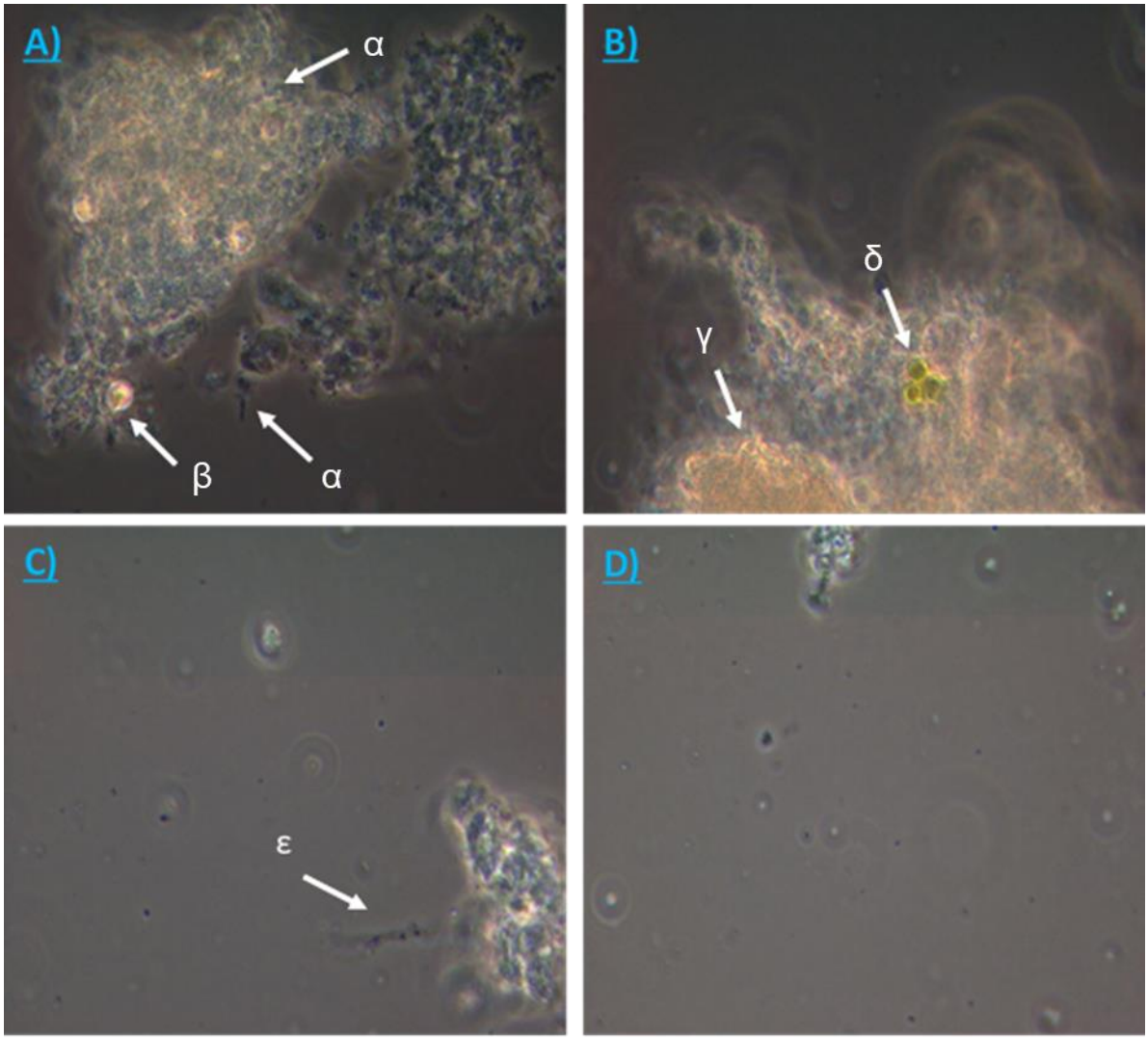

Figure 3.1: Light microscopy photographs showing the sludge structure as well as individual microbial cells from samples collected within the well matured stock reactor. Figures A and B shows sludge with visibly different bacterial morphologies (α), yeast like cells (β), fungi (γ) and algae (δ) present. Figures C and D show visibly lower concentrations of bacteria and sludge flocs in the reactor bulk liquid as well as motile microorganisms (ε).

Scanning electron micrographs (SEMs) were acquired of samples collected from the stock reactor (Figure 3.2). Samples were collected from the reactor walls and showed sludge with an irregular shape and thickness. Different cell morphologies can be seen depicting the microbial community embedded within the extracellular polymeric substance (EPS). Furthermore, EPS strands were visible indicating the structural integrity of the sludge (Figure B) while embedded with microbial cells. Figure 3.2 C and D show samples taken from the reactor impeller and compared to figures E and F, it is clear that the liquid velocity and effect of liquid shear impacted

on sludge development and structure. It is however unclear as to what effect this has on microbial diversity or distribution.

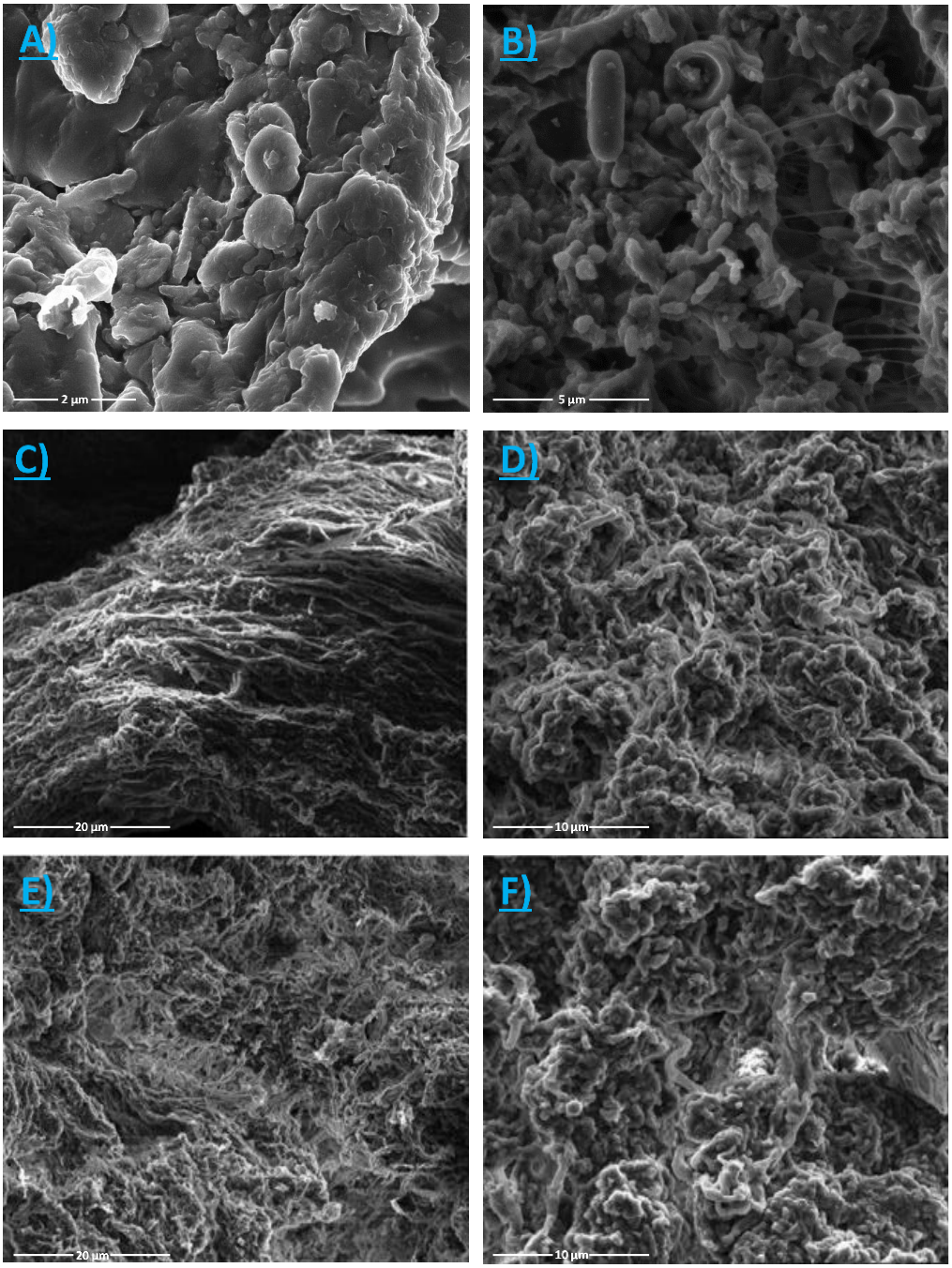

Figure 3.2: Scanning electron micrographs (SEMs) showing microbial morphology as well as sludge structure. Samples were collected from the stock reactor following 800 days of continuous operation. Figures A and B show zoomed observations of the microbial diversity and sludge structure as sampled from the reactor wall. Figures C and D show sludge sampled from the reactor impeller while Figures E and F show sludge sampled from the reactor wall. (Published in Huddy *et al.*, 2015).

3.3 Growth and isolation of mono-cultures

Sludge from two different reactors were selected for mono-culture isolation and identification. Figure 3.3 shows colonies from a sample taken from the stock reactor on spread plates at day four after incubation, showing selective growth of microorganisms within a sample taken from the stock reactor. This was also representative of the sample taken from the SCN-CN fed reactor (data not shown). Figure 3.3A shows colonies from the LB spread plate where figure 3.3B and 3.3C shows colonies from the K9 and reactor media, respectively. It was clear that the most extensive growth was observed on plates where LB media was used, followed by K9- and reactor media. Substantially reduced growth was noted on the reactor media plates regardless of the dilution used. Morphologically different colonies were observed on plates incubated at the highest dilution factor of 10^{-6} following extended incubation times of 14 days. Moreover, increased growth was observed on the plates containing the spread culture from the mixed reactor regardless of the media employed. It was also noted that the visual diversity was very low since the majority of colonies appeared round in shape and in one of three different colours. Regardless, colonies appeared as yellow, opaque or white and multiple colonies identical in colour and shape were selected for growth and used for identification.

3.3.1 Identification of selected mono-cultures

Sequence results obtained from DNA extracted from mono-cultures were used to determine the closest relatives and similarity to known microbial species (Figure 3.4). Cultures were identified to be closely related to species from genera including *Aeromonas, Pseudomonas, Alcaligenes, Thiobacillus, Delftia, Bacillus, Bacteroidales, Sphingobacterium, Flavobacterium, Microbacterium, Acinetobacter, Staphylococcus* and *Thiomonas*. This approach showed that the microbial community was complex and the diversity represented by a large number of different microorganisms, regardless of the lack in visual diversity.

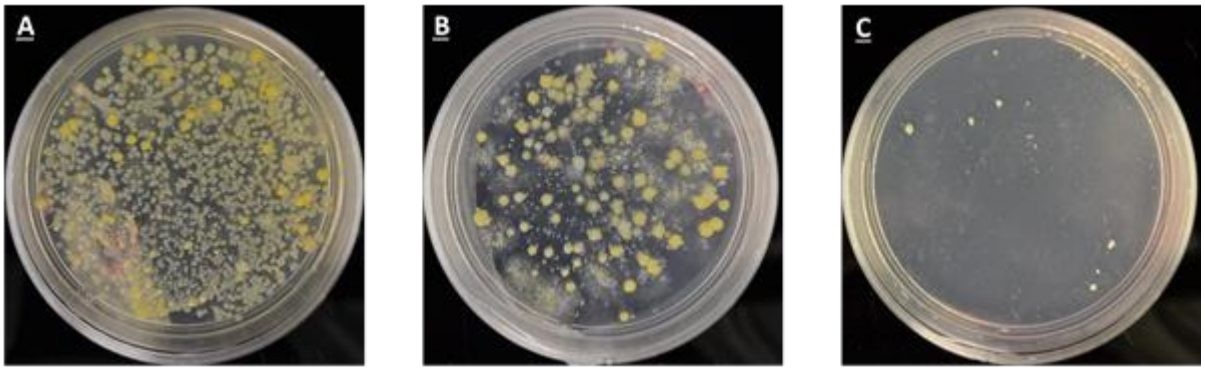

Figure 3.3: Photograph showing colony morphologies after four days incubated at ambient temperature with a SCN concentration of 100 mg/L. Figure (A) represents excessive growth on LB media, Figure (B) shows larger colonies regardless of increased zoom, grown on K9 media and Figure (C) shows significantly reduced growth on reactor media. All photos were taken four days post inoculation and represents total plate growth.

Isolates were numbered randomly and Culture 14 was found to be closely related to *Acinetobacter* sp. strain RFB1 isolated from gold mining effluent (Finnegan *et al*., 1991; Barradas, 1997). This strain has been shown as capable of degrading SCN as well as simple CN salts, cyano-metal complexes and organic nitrile complexes. This strain appeared to possess an extracellular single CN degrading enzyme complex capable of catalysing the degradation of multiple CN compounds (Finnegan *et al*., 1991; Baxter and Cummings, 2006). Growth in potassium thiocyanate was shown to be optimum at a concentration of 10 mg/L while optimum growth in potassium cyanide was shown at 100 mg/L. Limited literature is available regarding SCN and CN destruction kinetics for *Acinetobacter*.

Cultures 16, 27 and 29 showed sequence similarity to *Thiobacillus* (*Th.*) and closely related to *Th. thioparus* and *Th. denitrificans*. *Th. thioparus* was shown to grow on SCN which served as energy, carbon, nitrogen and sulphur source, as well as possess a thiocyanate hydrolase enzyme catalysing the conversion of SCN to carbonyl sulphide and ammonia (Katayama *et al*., 1992; Kim and Katayama, 2000; Chao *et al*., 2006; Arakawa *et al*., 2007; Bezsudnova *et al*., 2007).

A pure culture of *Th. thioparus* isolated from activated sludge was shown to degrade SCN at a maximum rate of 46.2 mg/L.h in a pH controlled solution at pH 6.2 with excess oxygen. *Th. denitrificans* as well as *Bacillus subtilis* and *Pseudomonas aeruginosa* related to cultures 16, 9 and 32, respectively have been reported to contain rhodanese which is responsible for conversion of CN to SCN (Ezzi and Lynch, 2002; Cipollone *et al*., 2004). This aids in detoxification by converting the more toxic CN to a less toxic SCN. Moreover, SCN has been used as electron

donor during destruction, by *Th. denitrificans*, for energy generation and CO_2 fixation (Sorokin *et al*., 2001).

Cultures 1, 8 and 9 were related to *Bacillus nealsonii, B. subtilis and B. amyloliquefaciens* which have been shown to degrade potassium CN (Perumal *et al*., 2013). Species of *Bacillus* has also been shown to produce rhodanese as well as contribute to gold biosorption in a mixed culture (Ezzi and Lynch, 2002; Gurbuz *et al*., 2004).

Flavobacterium has been shown to possess cyanase responsible for conversion of CNO to NH_4 and CO_2 (Hung and Pavlostathis, 1997; Dash, Gaur, *et al*., 2009). Cultures 11 and 15 showed sequence similarity to *Flavobacterium* which is not surprising since CNO may be present as an intermediate of SCN metabolism (Hung and Pavlostathis, 1997; Stott *et al*., 2001).

Microorganisms such as *Aeromonas* have been implicated in metal biosorption specifically of gold, chromium and cadmium (Guerrero and Olivera, 1999; Vijayaraghavan and Yun, 2008). *Aeromonas caviae* has reportedly been identified in a mixed microbial consortium responsible for metal biosorption but a specific individual role has not been elucidated. Metal biosorption has been reported to occur via binding of metals to biopolymers and cellular ligands or by intracellular accumulation and allows for subsequent metal recovery and environmental detoxification.

Cultures 13 and 23 showed sequence similarity to *Delftia* sp*.* which has been shown to possess an amidase enzyme involved in nitrile degradation (Zheng *et al*., 2007). Furthermore, amidase found in *Rhodococcus* was shown to catalyse the hydrolytic cleavage of the carbon-nitrogen triple bond in a nitrile (Kobayashi *et al*., 1998). It is likely that cultures 13 and 23, associated with *Delftia* sp., possessed carbon-nitrogen cleaving capability even though their direct role in this process is unknown.

Sulphur oxidation by *Thiomonas* has been suggested by numerous authors and similarity in sequence was shown by cultures 17 and 30 (Wentzien and Sand, 2004; Kantor *et al*., 2015). The presence of sulphate following SCN destruction would account for the oxidation of an intermediate for example tetrathionate.

Microbacterium has not been shown to be directly involved in SCN or CN metabolism although culture 12 was shown as a close relative. *Microbacterium* has been shown to form part of sludge flocculation in CN treating reactors (Quan *et al*., 2006). Isolates related to *Sphingobacterium* and *Bacteroidales* have previously been identified as either resistant to or capable of growing on SCN but their direct role in this system remains unclear.

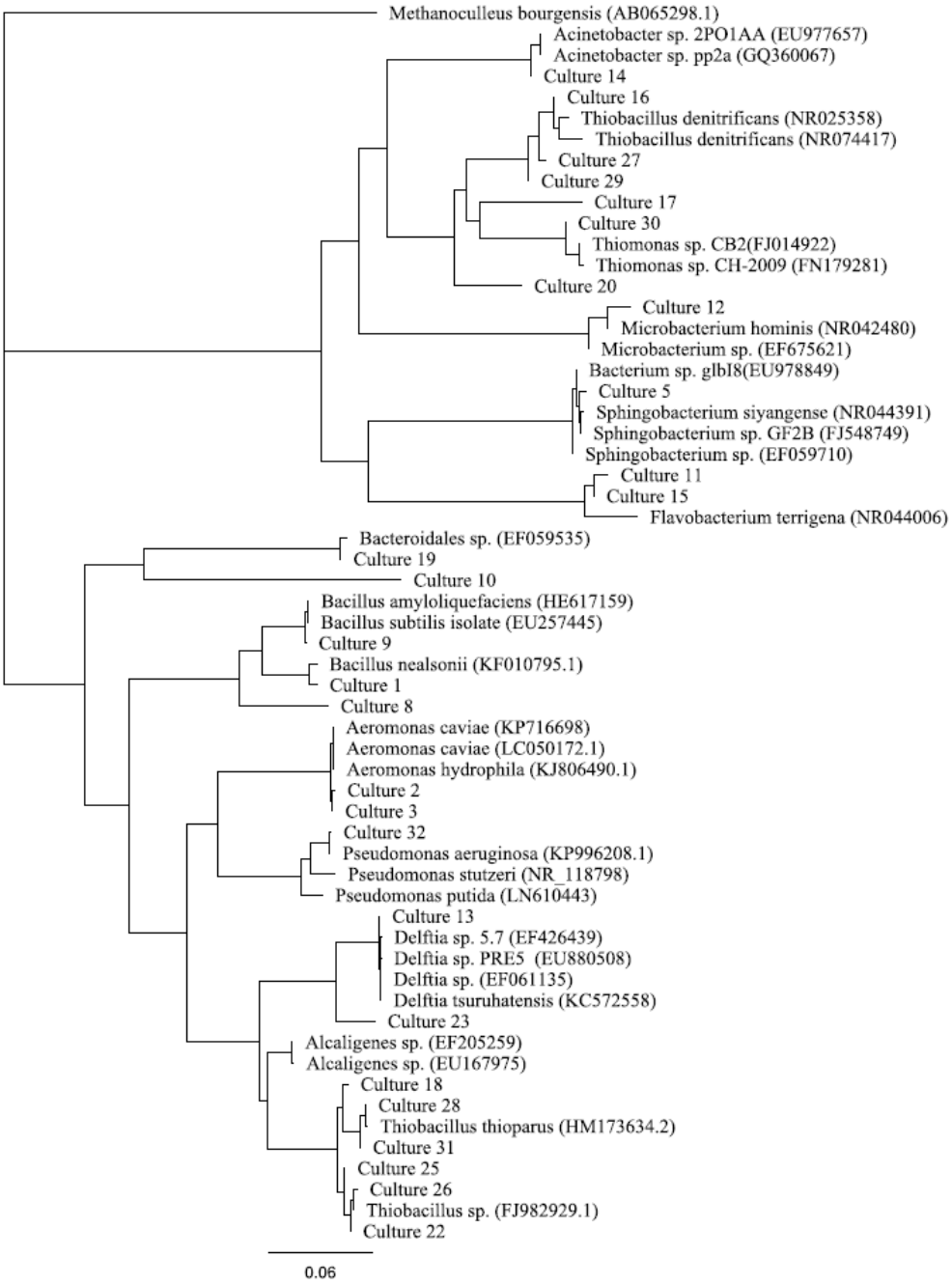

Figure 3.4: Unrooted 16S rRNA gene phylogenetic tree generated from cultured samples obtained from the stock reactor. Sequences from 32 clones were included following generation with universal bacterial primers. The tree was based on the sequence alignment of the common length nucleotide sequence constructed using the neighbour-joining method. Accession numbers (where available) are shown in brackets. The bar represents 0.06 nucleotide substitutions per nucleotide position.

3.4 Employing a 16S rRNA clone library to aid in unpacking the microbial diversity

The tools employed targeted the DNA of the various microbial members which allowed for identification of the microorganisms present within the sludge sample harvested from the stock reactor. The microbial consortium was analysed for the presence of bacteria, archaea as well as eukaryotic members by using culture independent molecular tools.

3.4.1 Selection of clones for sequence and identification

Single PCR amplicons were detected for bacterial 16S rRNA genes within the ASTER^{TM} sludge. A total of 185 bacterial representatives from the clone library were selected and analysed using ARDRA. A total of 106 patterns, including replicates, were selected for sequencing. Figure 3.5 and Figure 3.6 show photos of selected patterns that corresponded to colonies identified to contain a 16S rRNA gene and cleaved with the enzyme *HaeIII*. Figure 3.6 shows selected patterns for identical colonies as shown in Figure 3.5 but the enzyme *AluI* was used for gene cleavage. Samples were selected based on clear differences in patterns for example samples 1, 2, 5-7, 11-16, 19 and 20 were identified and selected for sequencing of the 16S rRNA genes. This procedure was followed for the 106 samples identified for sequence determination of the operational taxonomic unit used for phylogenetic analysis of the bacterial community (data not shown).

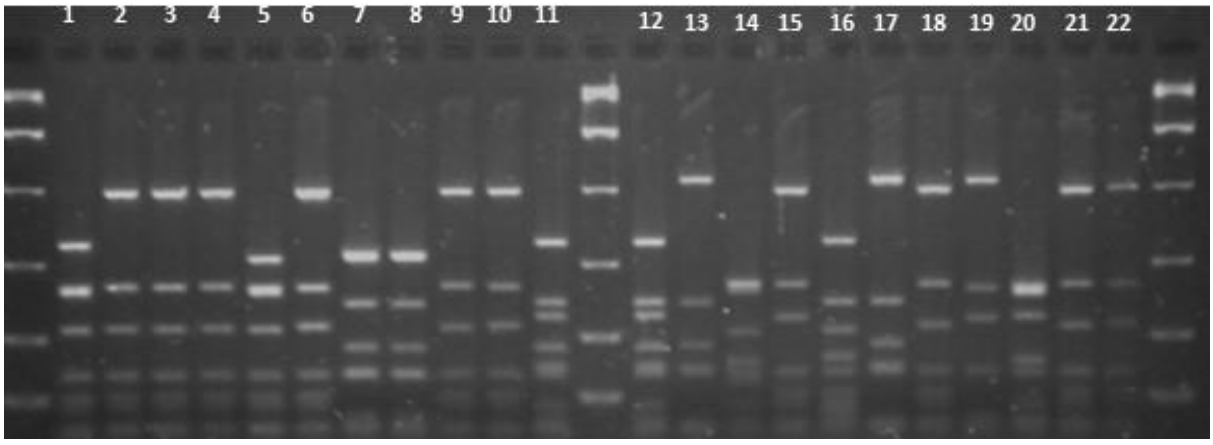

Figure 3.5: Photo of selected patterns for sequence determination. Patterns were obtained by using *HaeIII* and the gel wells numbered according to the sample

number. The molecular weight marker used included from top to bottom 8 000, 4 000, 1 600, 800, 400 and 200 base pairs.

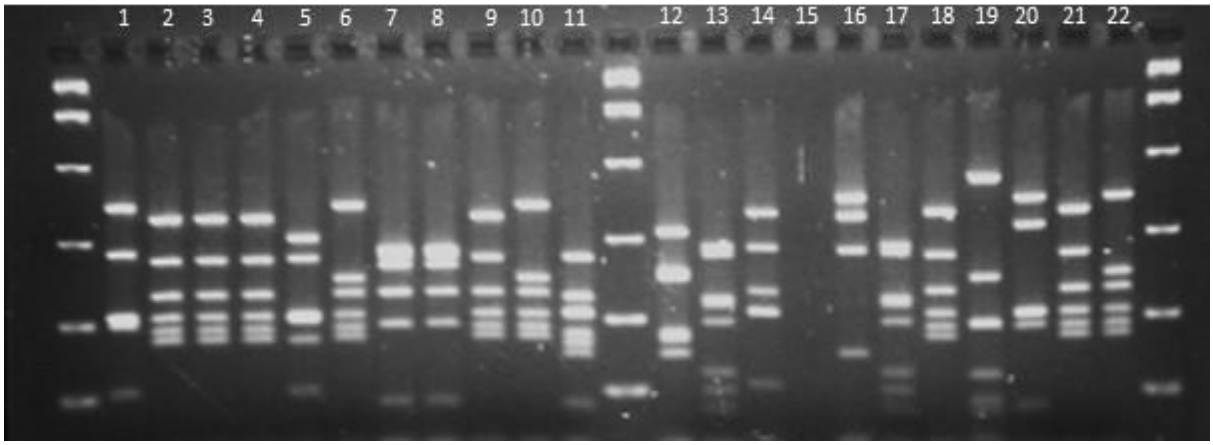

Figure 3.6: Photo of selected patterns for sequence determination. Patterns were obtained by using AluI and the gel wells numbered according to the sample number. Each sample number corresponded to a selected colony identified as positive to contain a 16S rRNA gene. The molecular weight marker used included from top to bottom 8 000, 4 000, 1 600, 800, 400 and 200 base pairs.

3.5 Bacterial phylogeny and community structure

The different bacterial genera identified using a clone library approach were captured and displayed as an unrooted phylogenetic tree shown in Figure 3.7. The microbial diversity was shown to be far more diverse than expected and discussed in Section 2.8. The bacterial genera captured and identified within the 16S rRNA clone library were composed of 21 different bacterial genera as sampled from the stock reactor. A number of *Thiobacillus* phylotypes were identified as closely related to *Th. thioparus* and Th. *denitrificans*. These phylotypes were also identified as mono-cultures isolated and discussed in section 4.2. *Thiobacillus thiophilus* has been reported to be able to oxidise thiosulphate which has been found as an intermediate in SCN destruction (Kellerman and Griebler, 2009).

Acidovorax sp. has been identified in activated sludge employed for the treatment of free CN as well as zinc and nickel complexed CN (Quan *et al*., 2006). *Acidovorax* has been shown to degrade nitriles (Quan *et al.*, 2006). *Spingopyxis*, *Agrobacterium* and *Clostridium* have also been identified in CN degrading systems while no direct role has been elucidated (Wang *et al*., 2004; Quan *et al*., 2006; Felföldi *et al*., 2010; Ryu *et al*., 2015; Villemur *et al*., 2015).

Nitrosomonas and *Nitrosospira* have been identified as key role players in nitrification (Akcil *et al*., 2003; Kim *et al*., 2011). These microorganisms are sensitive to SCN and CN where the presence of these CN compounds results in growth inhibition of especially *Nitrosomonas* (Hung and Pavlostathis, 1997; Kantor *et al*., 2015).

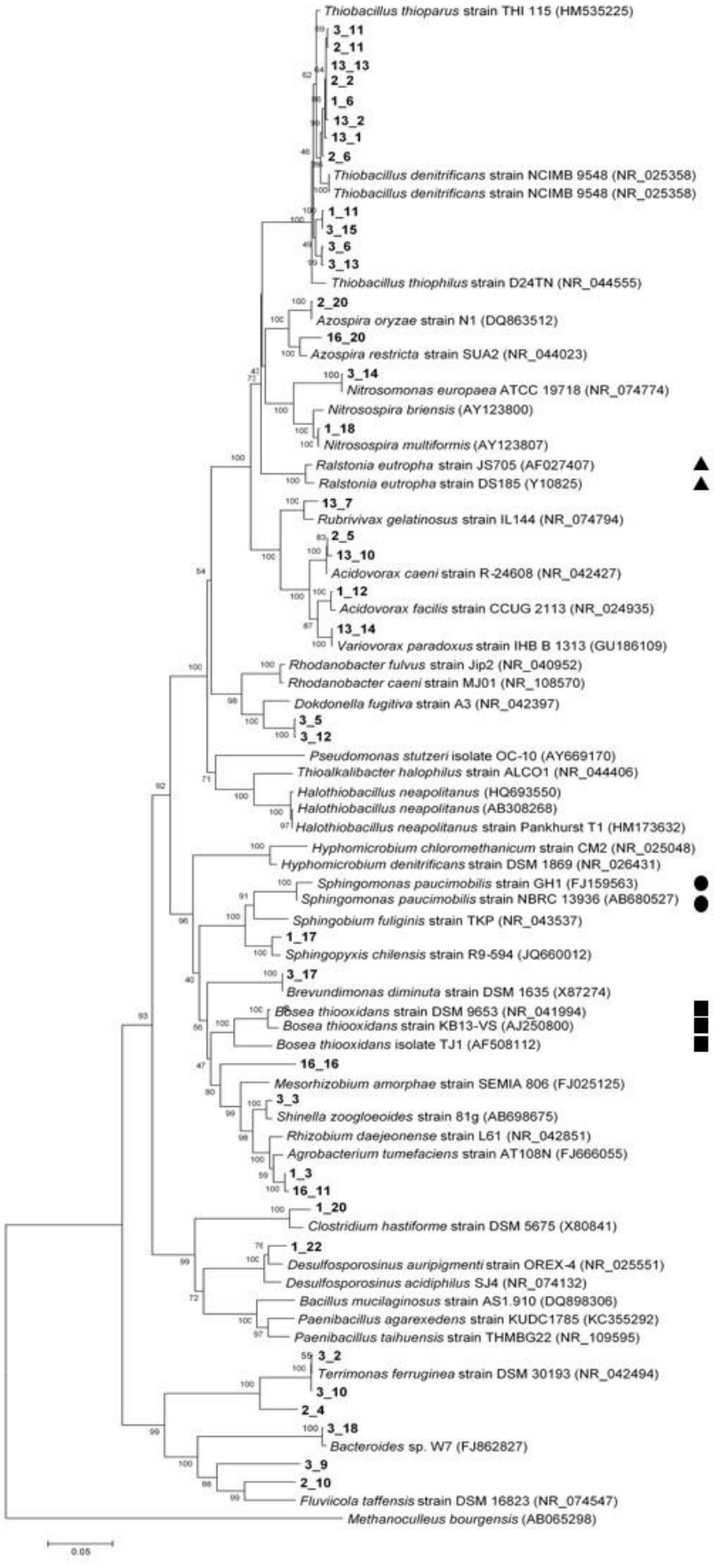
Thiobacillus thioparus strain THI 115 (HM535225)
3_11
2_11
13_13
2_2
1_6
13_2
13_1
2_6
Thiobacillus denitrificans strain NCIMB 9548 (NR_025358)
Thiobacillus denitrificans strain NCIMB 9548 (NR_025358)
1_11
3_15
3_6
3_13
Thiobacillus thiophilus strain D24TN (NR_044555)
2_20
Azospira oryzae strain N1 (DQ863512)
16_20
Azospira restricta strain SUA2 (NR_044023)
3_14
Nitrosomonas europaea ATCC 19718 (NR_074774)
Nitrosospira briensis (AY123800)
1_18
Nitrosospira multiformis (AY123807)
Ralstonia eutropha strain JS705 (AF027407)
Ralstonia eutropha strain DS185 (Y10825)
13_7
Rubrivivax gelatinosus strain IL144 (NR_074794)
2_5
13_10
Acidovorax caeni strain R-24608 (NR_042427)
1_12
Acidovorax facilis strain CCUG 2113 (NR_024935)
13_14
Variovorax paradoxus strain IHB B 1313 (GU186109)
Rhodanobacter fulvus strain Jip2 (NR_040952)
Rhodanobacter caeni strain MJ01 (NR_108570)
Dokdonella fugitiva strain A3 (NR_042397)
3_5
3_12
Pseudomonas stutzeri isolate OC-10 (AY669170)
Thioalkalibacter halophilus strain ALCO1 (NR_044406)
Halothiobacillus neapolitanus (HQ693550)
Halothiobacillus neapolitanus (AB308268)
Halothiobacillus neapolitanus strain Pankhurst T1 (HM173632)
Hyphomicrobium chloromethanicum strain CM2 (NR_025048)
Hyphomicrobium denitrificans strain DSM 1869 (NR_026431)
Sphingomonas paucimobilis strain GH1 (FJ159563)
Sphingomonas paucimobilis strain NBRC 13936 (AB680527)
Sphingobium fuliginis strain TKP (NR_043537)
1_17
Sphingopyxis chilensis strain R9-594 (JQ660012)
3_17
Brevundimonas diminuta strain DSM 1635 (X87274)
Bosea thiooxidans strain DSM 9653 (NR_041994)
Bosea thiooxidans strain KB13-VS (AJ250800)
Bosea thiooxidans isolate TJ1 (AF508112)
16_16
Mesorhizobium amorphae strain SEMIA 806 (FJ025125)
3_3
Shinella zoogloeoides strain 81g (AB698675)
Rhizobium daejeonense strain L61 (NR_042851)
Agrobacterium tumefaciens strain AT108N (FJ666055)
1_3
16_11
1_20
Clostridium hastiforme strain DSM 5675 (X80841)
1_22
Desulfosporosinus auripigmenti strain OREX-4 (NR_025551)
Desulfosporosinus acidiphilus SJ4 (NR_074132)
Bacillus mucilaginosus strain AS1.910 (DQ898306)
Paenibacillus agarexedens strain KUDC1785 (KC355292)
Paenibacillus taihuensis strain THMBG22 (NR_109595)
3_2
Terrimonas ferruginea strain DSM 30193 (NR_042494)
3_10
2_4
3_18
Bacteroides sp. W7 (FJ862827)
3_9
2_10
Fluviicola taffensis strain DSM 16823 (NR_074547)
Methanoculleus bourgensis (AB065298)
0.05

Figure 3.7: Unrooted 16S rRNA gene phylogenetic tree generated from samples obtained from the stock reactor. Sequences from 37 clones were included following generation with universal bacterial primers. The tree was based on the sequence alignment of the common length nucleotide sequence constructed using the neighbour-joining method. Bootstrap values are based upon 1,000 re-sampled data sets and only values of greater than 40% are indicated. Accession numbers (where available) are shown in brackets. The bar represents 0.05 nucleotide substitutions per nucleotide position. Taken from (Huddy, *et al.*, 2015).

The exact role for the remainder of the clones identified to close relatives has not been elucidated and, as such, it is possible that their role is secondary to SCN and CN destruction. The exact role of each individual species, however, remains unknown and metabolic analysis should be employed to further elucidate the roles of microorganisms as well as potential interactions.

Collaborative research has been done with the group of Jill Banfield at UC Berkeley (Kantor 2015), who used high-throughput sequencing of the stock reactor to determine genomes for microorganisms present in the stock reactor as well as a reactor receiving SCN and CN. *Thiobacillus, Microbacterium* as well as *Variovorax* were also identified in both reactors as discussed above. Furthermore, metabolism predictions were used to identify potential roles for specific organisms in the reactor systems. *Thiobacillus* showed genes encoding SCN hydrolase which convert SCN to carbonyl sulphide (COS) as well as cyanase that catalyse cyanate conversion to ammonium.

Genes encoding Rhodanase enzymes as well as reductases were also identified and although not tied to specific microorganisms, these indicate conversion of CN to a less toxic SCN and coding for reductases as alternative terminal reductases when oxidase cytochrome C is inhibited by CN (Kantor *et al*., 2015).

Oxidation of reduced sulphur species may be achieved by species for example *Rubrivivax* and *Thiobacillus*. Both of these were identified from the constructed clones as well as during assembly of the 16S rRNA clone library discussed before. Key genes were also identified that play a role in conversion of sulphite to sulphate as well as sulphide to sulphur (Beller *et al*., 2006).

3.6 Metagenomic Approach

This project has enabled a collaboration with the group of Prof Jill Banfield at UC Berkeley. DNA extracted from the samples referred to in Section 3.5 were provided

by me to Rose Kantor, a PhD candidate at UCB. They performed high-throughput metagenomic sequencing and used the data analysis techniques they developed to reconstruct microbial genomes from communities sampled from the stock reactor and solid reactor. The results have been published collaboratively with UCT, with the collaborating team as lead authors (Kantor *et al.,* 2015).

The thiocyanate hydrolase enzyme encoding genes were identified in three *Thiobacillus* species genomes in the SCN only fed reactor. This enzyme together with cyanase responsible for conversion of SCN and cyanate (CNO) to COS and ammonium was detected, however carbonyl sulphide hydrolase was not detected.

Pathways for oxidation of sulphur compounds were identified and postulated to be involved in key energy generating processes by oxidation of sulphur intermediates, resulting in accumulating sulphate in the reactor system. Furthermore, pathways for APS reductase and ATP sulfurylase were identified and involved in oxidation of sulphite to sulphate. The complex microbial system further showed the presence of heterotrophs that may utilise the organic carbon from the reactor feed (molasses) as well as nitrogen directly from SCN.

3.7 Conclusions

The capacity for nitrogen removal, carbon utilisation and sulphur oxidation showed an ideal system for wastewater decontamination, given reactor conditions that promote desirable reactions at a practical rate. The use of metagenomics, in addition to culturing and non-culturing techniques, aid in a holistic understanding of a complex microbial system to promote commercial wastewater bioremediation.

Light microscopy as well as electron microscopy of the sludge showed morphologically diverse bacterial species as well as fungi, algae and yeast like cells. Furthermore, the nature of sludge was shown to range from having an amorphous structure to dense ribbon like structures, although the impact of this on diversity remain unclear.

The culturing potential of the microbial community showed a large diversity and offered potential isolation of microorganisms of interest, but when coupled to culture independent techniques, it was shown that the majority of microorganisms was not cultured using the selected media and techniques. Furthermore, cultured isolated were also detected using culture independent methods for example building of a clone library.

Due to the selective pressure exerted by the cyanides destruction process, ultimately a designer inoculum would be naturally selected. However, a specifically designed inoculum could prove useful to eliminate heterothrophs not contributing to SCN destruction and therefore eliminate the addition of organic carbon in the feed solution.

Chapter 4: Describing the practical operating window for thiocyanate destruction

4.1 Introduction

Successful biological destruction of SCN requires favourable conditions for microbial growth and activity. These critical operating parameters include optimum substrate loading, temperature and solution pH. Describing the operating window for microbial SCN destruction is thus highly desirable.

Destruction of SCN occurs at different rates according to the specific type and number of microorganisms present, their specific activity as well as the available SCN concentration. Thiocyanate destruction has been well studied and rates vary from 1.4 - 9.4 mg/L.h at initial SCN concentrations ranging from 10 – 600 mg/L employing different bacterial species (Karavaiko *et al*., 2000; Ahn *et al*., 2005). These studies have also shown that the time required to achieve SCN destruction increased with increasing initial SCN concentration in a non-linear fashion.

It is well known that an increase in microbial metabolic reaction rate occurs at an increased temperature within the optimum bacterial activity range (Madigan *et al*., 2003). The cardinal temperatures described as the minimum, optimum and maximum temperatures differ from species to species and determining of the optimum operational temperature for the inoculum is vital. The optimum temperature for most microorganisms is traditionally closer to the maximum than the minimum implying a sharp drop-off in activity at temperatures higher than the maximum temperature. Patil and Paknikar, (2000) showed bacterial CN degradation to be optimal at 35°C when compared to degradation rates at 20°C and 30°C using a mixed culture (Patil and Paknikar, 2000). Complete inhibition at only a 5°C increment was shown at 45°C. Other authors have shown optimum temperatures for SCN destruction at 30-40°C using different cultures, while operating outside this temperature window resulted in significantly decreased SCN destruction activity (Akcil *et al*., 2003; Chaudhari and Kodam, 2010).

The pH has been shown to be significantly influential on SCN destruction (Akcil, 2002; Chaudhari and Kodam, 2010). Chaudhari and Kodam, (2010) showed significant destruction of SCN at ranging pH 5.0 – 7.0 while substantially reduced SCN destruction was attained at pH 8.0 and 9.0. Insignificant SCN destruction was

also shown at pH 4.0. The change in SCN destruction rate occurred rapidly with a change in pH when operating outside the optimum pH window for this specific co-culture.

The key questions discussed in this chapter are as follows:

(i) What was the effect of different initial SCN concentrations (60-1 800 mg/L) on the SCN destruction ability of the mixed microbial population?

(ii) What was the effect of different incubation temperatures (10-45 °C) on the SCN destruction ability of the mixed microbial population inoculated with different start SCN concentrations?

(iii) How did solution pH (6.5-10.0) affect the SCN destruction ability of the mixed microbial population?

(iv) Can a broad operating window be determined that is relevant to industrial processes for destruction of SCN?

4.2 Experimental Programme

A series of batch experiments were conducted to investigate the effects of inoculation SCN concentration, temperature and pH on the SCN destruction rates of a mixed microbial community. Experiments were performed as discussed in Section 2.3.1.

The first set of experiments investigated the effect of SCN concentration (60, 120 and 180 mg/L) at inoculation on the SCN destruction ability of the mixed microbial community at ambient temperature (24±1°C). The SCN concentration at inoculation was based on operational data during plant start-up as well as exposure to SCN spikes. Selected flasks were challenged with five times the inoculated SCN concentration following complete destruction of the first SCN load. Moreover, the mixed microbial community was also challenged with a high SCN concentration of up

to 1 800 mg/L following an identical operating protocol as described above. This allowed the assessment of the capability of the mixed microbial community to acclimate to as well as degrade high SCN concentrations in solution.

The effect of temperature was evaluated across a temperature range of 10-45°C in 5°C intervals. The starting SCN concentration was 60, 120 and 180 mg/L. Flasks were removed for sampling individually to minimise temperature fluctuations while operated as described in Section 2.3.1.

The effect of pH was tested across a range of pH 5.0-10.0 under a constant ambient temperature of 24±1°C. The starting SCN concentration was selected at 100 or 150 mg/L and is discussed accordingly. The solution pH was adjusted as required during sampling intervals using either sulphuric acid or sodium hydroxide.

4.3 Results and Discussion

Batch experiments were conducted to determine the operating window wherein SCN destruction was possible. These experiments were also used to infer more specific conditions to assess SCN destruction rates using continuous stirred tank reactors (CSTR's).

4.3.1 Tolerance of the mixed microbial sludge to different thiocyanate concentrations

Tolerance of the mixed culture to SCN was initially investigated by exposing the consortium supported on a feed of 100 mg/L SCN to SCN concentrations of 60-180 mg/L at a constant temperature of 24°C. In all cases, apparent inactivity was observed during which insignificant (< 10% of inoculated) SCN destruction was measured. An initial acclimation period of approximately 4 hours was observed for an inoculation SCN concentration of 60 mg/L and, 8 hours for 120 and 180 mg/L (Figure 4.1). This phase was likely a result of the bacterial cells being exposed to a significantly higher SCN concentration compared to the residual SCN concentration present (< 1 mg/L steady state SCN concentration) in the continuous stock reactor.

Hung and Pavlostathis (1997) demonstrated acclimatisation of sludge obtained from a municipal wastewater plant to SCN after exposing cultures to SCN in consecutive feeding cycles. Significant SCN destruction occurred following 150 hours exposure to SCN with the observed lag phase attributed to unacclimated sludge. Initial acclimatisation, following exposure of microbial cultures to SCN, was also shown by

authors employing mixed and pure cultures (Kim and Katayama, 2000; Lee *et al*., 2003, Grigoreva *et al*., 2006). Moreover, acclimatisation of microorganisms to an environmental contaminant can be attributed to an increase in biomass concentration as a result of growth or due to the induction of metabolic regulatory genes responsible for the expression of gene(s) required for the desired activity or both (Stafford and Callely, 1969; Dictor *et al*., 1997; Hung and Pavlostathis, 1997; Lee *et al*., 2003; Felföldi *et al*., 2010).

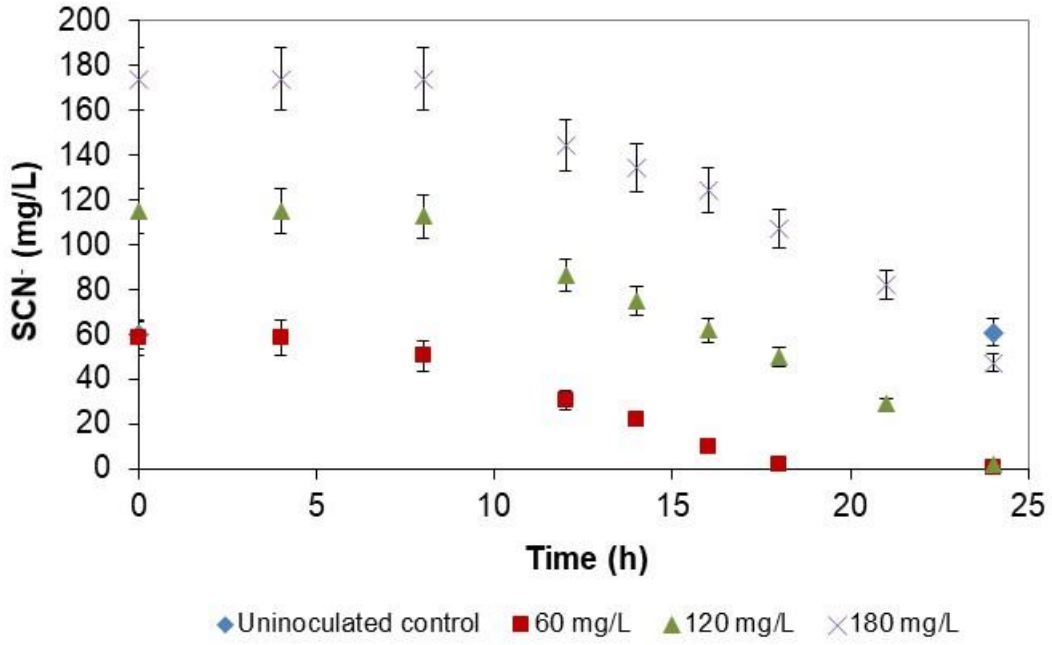

Figure 4.1: Effect of inoculation thiocyanate concentration on the thiocyanate destruction ability of the mixed microbial sludge. The starting thiocyanate concentration, 60-180 mg/L, is indicated by the legend. Data points represent mean values (± S.E.) of triplicate experiments over time. The uninoculated control did not show significant SCN destruction.

The volumetric SCN destruction rate increased following acclimation to a maximum level where it remained constant, following a linear pattern with an average rate of 4.9, 6.4 and 7.0 mg/L.h for the inoculation concentrations of 60, 120 and 180 mg/L, respectively. The increased volumetric SCN destruction rate was contributed to by the increased initial SCN concentration able to support an increasing biomass concentration. Complete SCN destruction was achieved with a measured residual SCN concentration in solution of less than 1 mg/L in all cases, following 18, 24 and by extrapolation, 33 h incubation, respectively. No measurable decrease in residual

SCN concentration occurred in the uninoculated controls for the duration of the study.

Cultures exposed to SCN during the first phase of batch experiments were subsequently challenged with a SCN concentration five times the previous starting concentration (Figure 4.2).

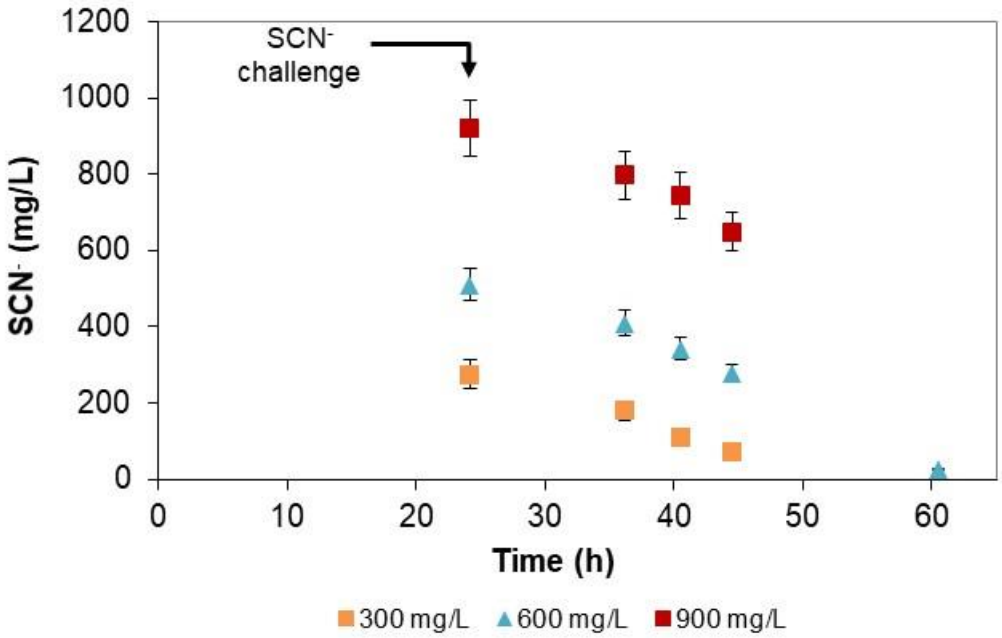

Figure 4.2: Effects of a five times increased thiocyanate concentration on cultures pre-exposed to thiocyanate. The challenge thiocyanate concentration is indicated by the graph legend and was in the range of 300-900 mg/L. Data points represent mean values (± S.E.) of duplicate experiments over time.

The effect of pre-exposure to SCN was significant and resulted in immediate SCN destruction following addition of the challenging SCN dose. No lag phase was detected for SCN destruction in the initial SCN concentration range of 300-900 mg/L.

The exposure of the mixed microbial consortium to SCN, even at a concentration as low as 60 mg/L, was shown to have a beneficial effect on the SCN destruction rate, further supporting the idea of a positive metabolic response. A maximum SCN destruction rate of 12.7 mg/L.h was achieved at a dose of 900 mg/L SCN. Experiments dosed with 300 and 600 mg/L SCN showed similar average SCN destruction rates of 9.8 and 11.1 mg/L.h, respectively, calculated from the linear portion of the degradation profiles. The increased SCN destruction rates followed the increased SCN dose between 60 and 900 mg/L although this increase was not

proportional. This suggests that the maximum SCN destruction rate is not a direct function of SCN concentration. The increase could be attributed to an increase in biomass, which would be greater where more SCN was degraded as the sole nitrogen source. Verifying biomass by cell counting was particularly challenging as the biomass aggregated into flocs upon exposure to the higher concentrations, making accurate counting impossible. Visual assessment of the flocs by light microscopy suggested they consisted of microbial cells, inorganic material (crystals) and extracellular polymeric substances (EPS). The presence of significant non-cellular material made the determination of cellular dry mass difficult, so specific SCN degradation rates could not be determined.

Exposure of the mixed microbial consortium to significantly higher SCN concentrations between 900 and 1 800 mg/L, resulted in a substantially longer acclimatisation phase (Figure 4.3). The acclimatisation phase lasted for a minimum of 84 hours at a start SCN concentration of 900 and 1 400 mg/L, increasing to 97 hours at 1 800 mg/L. The consortium was, however, able to tolerate significantly higher SCN concentrations without prior acclimatisation compared to previous studies (Karavaiko *et al*., 2000; Sirianuntapiboon *et al*., 2007). Furthermore, slightly higher rates were observed at increasing SCN concentrations between 900 and 1 800 mg/L.

The highest rate, calculated as 15.7 mg/L.h (R^2 = 0.96), was obtained at an initial concentration of 1400 mg/L, while rates of 12.5 and 11.1 mg/L.h (R^2 = 0.96 and 0.99 respectively) were calculated for initial concentrations of 900 and 1 800 mg/L, respectively. Complete SCN degradation, to below 1 mg/L occurred at all three concentrations. The group of Karavaiko (2000) showed lower bacterial SCN destruction rates ranging between 8.0-9.4 mg/L.h at initial SCN concentrations of 170-600 mg/L employing a mixed *Pseudomonas* culture (Karavaiko *et al*., 2000). In addition, Ahn *et al.* (2005) demonstrated a SCN destruction rate of 2.1 mg/L.h at an inoculation SCN concentration of 250 mg/L over six days employing a pure *Klebsiella* culture. Kim and Katayama (2000), using a substrate adapted culture isolated from wastewater containing 1 000-2 000 mg/L SCN, observed a maximum SCN destruction rate of 26.8 mg/L.h under controlled conditions at optimum pH and excess oxygen supply. This rate decreased by 25% under oxygen limited conditions and a lower than optimum solution pH. The experiments confirmed the robustness of the microbial community to degrade SCN and provided some insights into the degradation rates achievable, which were used to inform the selection of initial hydraulic residence time selections for subsequent studies using continuous reactor systems.

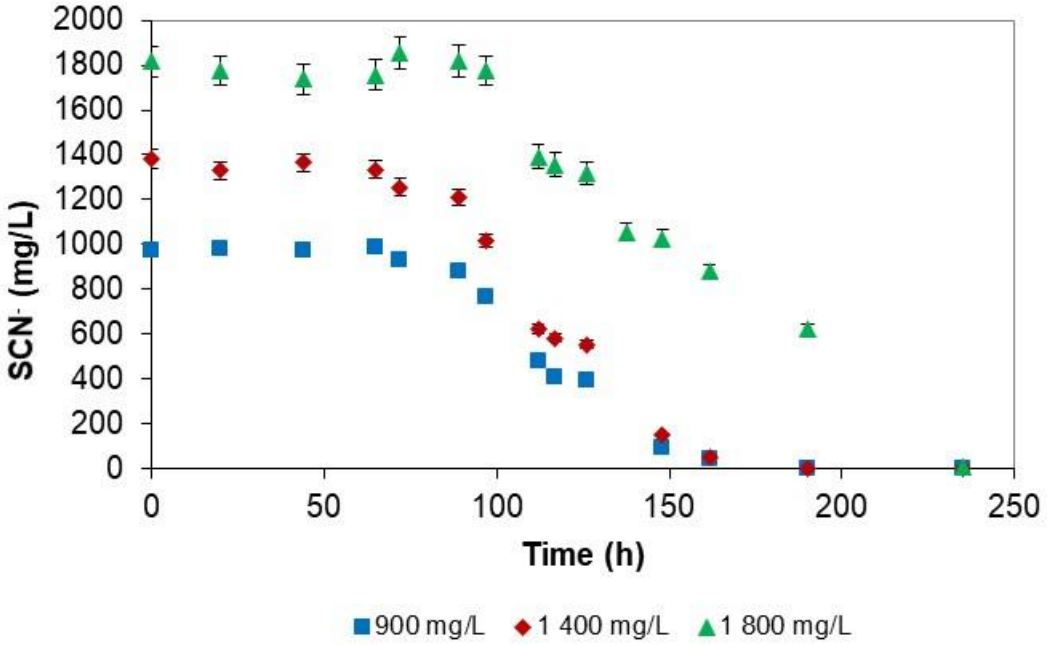

Figure 4.3: Effects of high initial thiocyanate concentration on the thiocyanate destruction ability of a mixed microbial population. Data points represent mean values (± S.E.) of duplicate experiments over time.

4.4 Effect of temperature on the thiocyanate destruction ability of the mixed microbial culture

Temperature has been identified as a critical parameter associated with environmental biological treatment technologies (Akcil, 2003). Seasonal changes result in increased contaminant concentrations due to curtailed reactions over winter periods, especially at temperatures below 10°C. The necessity to heat reaction vessels in commercial processes represents a significant economic input. Therefore, it is desirable to characterise SCN destruction across a temperature range above 10°C.

Batch studies were performed at temperatures ranging from 10-45°C and starting SCN concentrations of 60-180 mg/L in batch culture. The SCN degradation profiles for data collected at 60 mg SCN/L are presented in Figure 4.4. Across all data, acclimatisation times were calculated as the time required to degrade 10% of the start SCN concentration and are presented in Table 4.1. Acclimatisation was more pronounced at 10°C and 15°C (35.5 and 46.4 hours, respectively) compared to the acclimatisation at 20°C (8 hours). Furthermore, increased incubation temperatures

of 5°C increments to 40°C resulted in decreased acclimatisation times. Acclimatisation to SCN at 20°C decreased by 70-88% compared to acclimatisation at 10 and 15°C incubated with start SCN concentrations between 60 and 180 mg/L. Acclimatisation reduced by between 81-98% at incubation temperatures between 25-40°C with a start SCN concentration between 60 and 180 mg/L. The SCN degradation rates at incubation temperatures between 20°C and 40°C were relatively stable over the experimental period, with a slight increase in the latter stages. However, the degradation rate at 10°C and 15°C increased more significantly over time, suggesting a progressive adaptation to the lower temperature (Chattopadhyay, 2006), or possibly the effect on an increase in biomass concentration. The latter is less likely, as cell growth is slower at lower temperature and this phenomenon was not observed at higher temperatures.

The SCN destruction rates increased with increasing temperatures in the range 10-40°C and increasing SCN concentrations in the range 60-180 mg/L (Table 5.1). Insignificant SCN destruction activity was measured at 45°C regardless of the initial SCN concentration, suggesting that the cultures were metabolically inactive at this temperature.

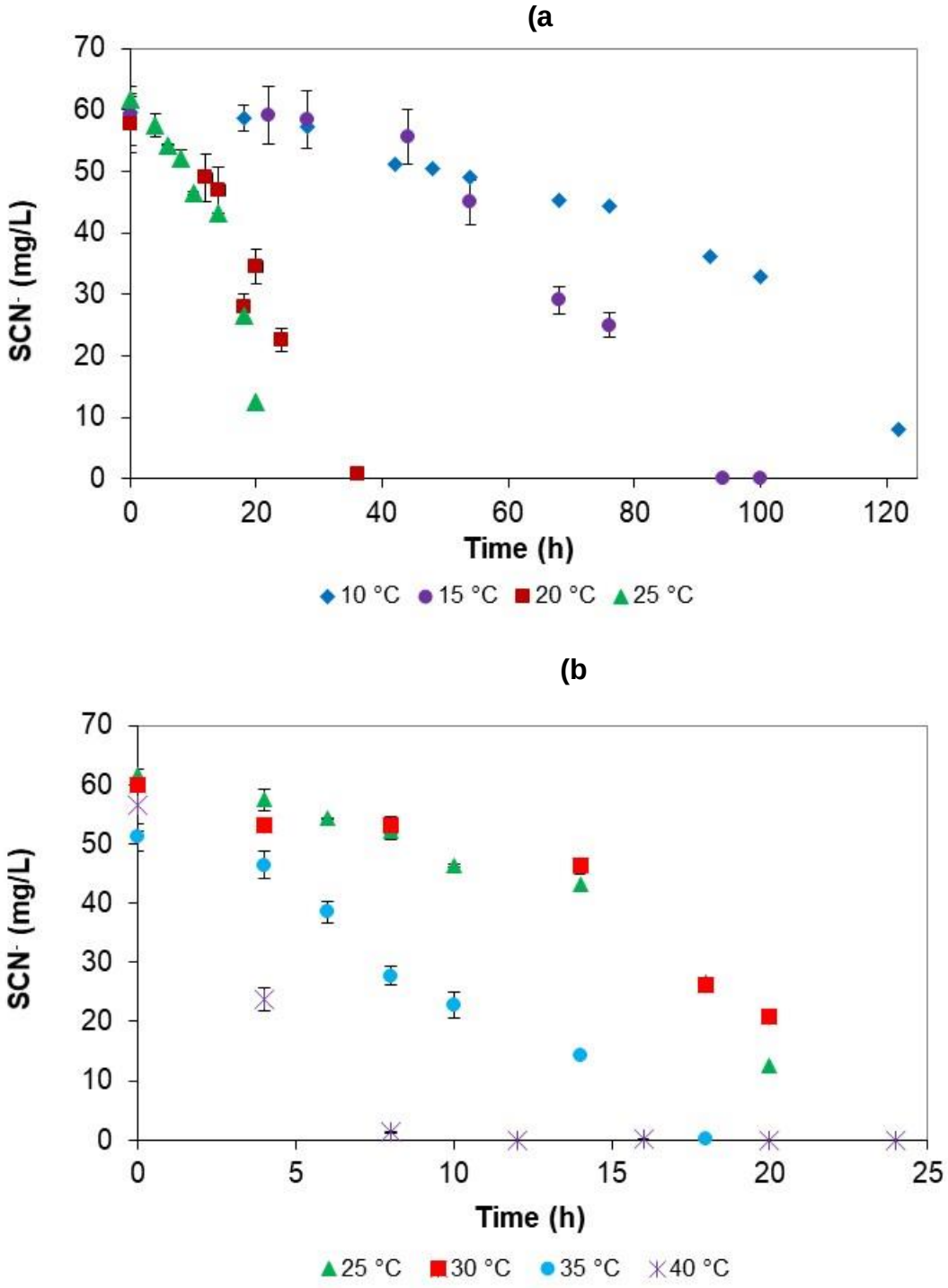

Figure 4.4: Effect of temperature on thiocyanate destruction with an initial thiocyanate concentration of 60 mg/L at (a) low operating temperature and (b) moderately high operating temperature. The temperature profile at 25°C in (a) and (b) represent identical data. Data points represent mean values (± S.E.) of duplicate experiments over time.

Table 4.1: : a) Duration (h) of the acclimatisation required to degrade 10% of the start thiocyanate concentration, b) the maximum thiocyanate destruction rate calculated over the experimental run time and c) the time required to achieve the maximum thiocyanate destruction rate.

Temperature	**[a)]Acclimatisation period (h)**			**[b)]Maximum SCN destruction rates (mg/L.h)**			**[c)]Time to reach maximum SCN destruction rate (h)**		
	60mg/L	120mg/L	180mg/L	60mg/L	120mg/L	180mg/L	60mg/L	120mg/L	180mg/L
10	35.54		73.40	0.31		1.56	18.00		166.0
15	46.35	45.45	39.15	0.99	0.84	1.28	28.00	28.00	104.0
20	7.98	13.68	9.00	2.04	2.80	6.39	12.00	18.00	20.0
25	5.28	8.47	7.90	2.48***	2.50	6.80	10.00	14.00	6.00
30	2.64	6.68	6.79	3.52	5.49	7.85	8.00	6.00	8.00
35	3.00	3.78	2.48	4.08	11.84	17.36**	4.00	8.00	8.00
40	0.69	1.34	2.45	6.91	14.03	17.34	0.69	1.34	4.00

Coefficient of determination (R^2) was calculated over the linear of maximum thiocyanate destruction range and calculated to be in the range 0.985-1.00 except those marked ** 0.91 and *** 0.87.

The SCN destruction rates increased with increasing incubation temperatures following an Arrhenius projection (Figure 4.5). Furthermore, significantly higher, maximum SCN destruction rates were observed at a start SCN concentration of 120 and 180 mg/L, compared to the rate at 60 mg/L. It is likely that a combination of higher specific metabolic activity at higher residual SCN concentration and higher temperature and higher bacterial growth and hence concentration at the higher initial SCN concentrations contributed to higher volumetric SCN destruction rates.

Several studies employing microorganisms previously identified to be active in the ASTER^{TM} process, for example *Pseudomonas* sp., have shown optimum microbial growth temperatures of 30-35°C (Patil and Paknikar, 2000; Gokulakrishnan and Gummadi, 2006). The improved acclimatisation time combined with increased rates at higher temperatures, supports a practical operating temperature above 20°C, and where practically and economically feasible, in the optimal range of 35-40°C.

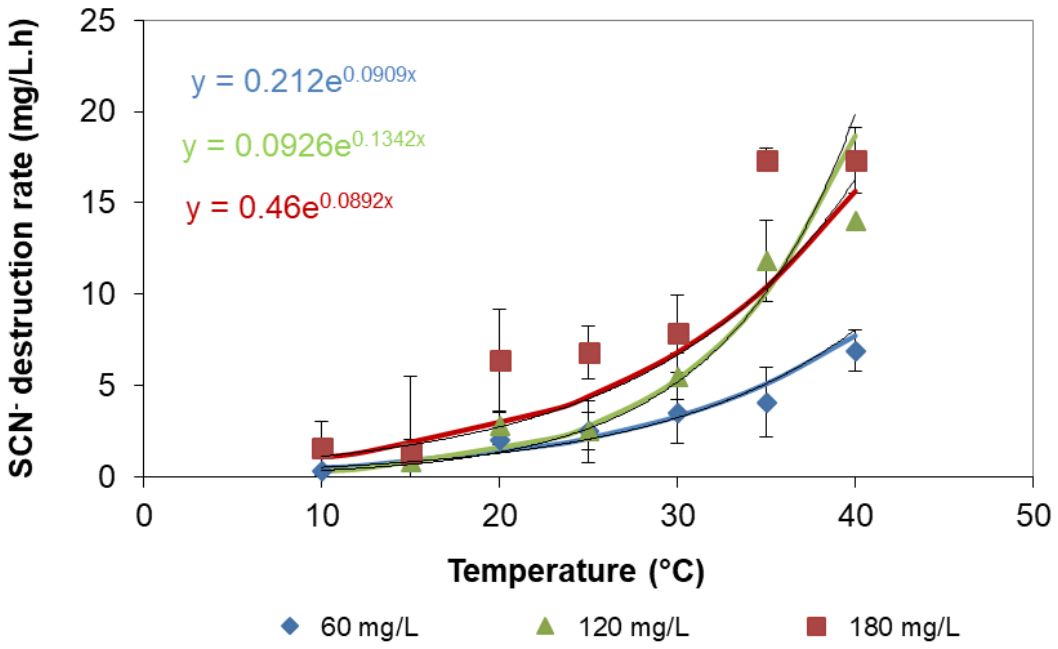

Figure 4.5: Effect of temperature on thiocyanate destruction rates at different inoculation thiocyanate concentrations. Solid lines represent an Arrhenius function with the projection shown on the graph and data points are representative of experimental results.

The time required to achieve complete SCN destruction decreased substantially with increasing incubation temperatures (Figure 4.6). This was consistent with the increasing SCN degradation rate, even when the acclimatisation was not considered, in that increased performance was observed at temperatures above 20°C. A

substantial decrease in the duration of the active SCN destruction phase was observed following an increase in temperature from 15 to 20°C, regardless of the initial SCN concentration. The active SCN destruction time period further decreased at temperatures above 25°C, albeit more moderately. This shows the effect of sub-optimal incubation temperatures on the SCN destruction rate of the mixed microbial population even after extended acclimatisation. This was not surprising since metabolic activity and subsequent SCN destruction rates decreased with decreasing temperatures (Akcil, 2003).

The activation energy was calculated from Figure 4.5 as 66.80, 69.60 and 65.51 KJ/mol, for experiments inoculated with SCN concentrations at 60, 120 and 180 mg/L, respectively. Activation energy for chemically controlled reactions is typically greater than 40 KJ/mol, while for diffusion or mass controlled reactions values ranging between 5-20 KJ/mol are typical (Zhang, 2004). The high values calculated for the flask experiments is indicative of reaction rates controlled by available reactants, in this case biomass and SCN concentrations. A practical operating temperature range was found to be above 20°C where the need for acclimatisation was substantially reduced and a higher SCN destruction rate can be maintained.

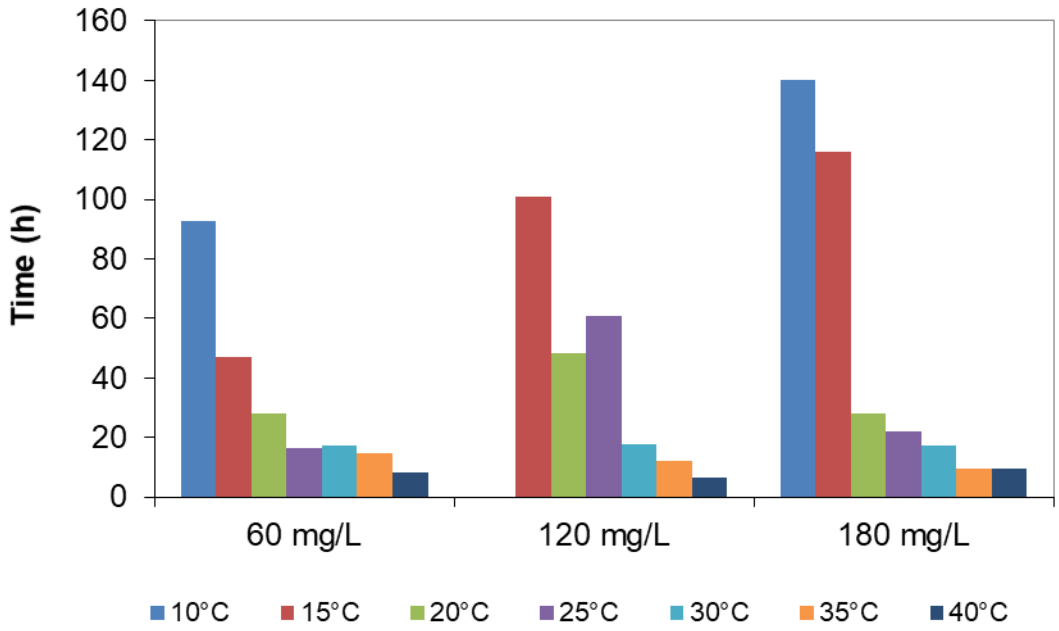

Figure 4.6: Duration of active thiocyanate destruction (duration of acclimation excluded).

Temperature has been identified as a critical factor for treatment of SCN and CN (Patil and Paknikar, 2000; Baxter and Cummings, 2006; Dash, *et al*., 2009; Kim *et al*., 2013). A culture consisting of *Pseudomonas* and *Citrobacter* was isolated from soil and used to degrade copper and zinc CNs (Patil and Paknikar, 2000). The optimum temperature while achieving complete SCN destruction was identified as 35°C while over 20% reduced efficiency was noted at 20°C and 30°C, respectively. Protein denaturation occurs at temperatures higher than the maximum growth temperature resulting in rapid and irreversible cell death (Madigan *et al*., 2003). Temperature control for industrial processes, like ASTER™, is usually circumvented if possible, due to the significant cost associated with heating and cooling of bulk liquids. Since temperature in this case was shown to contribute significantly to the potential achievable SCN destruction rate, it is necessary to consider any trade-off between the cost of heating and processing time required to treat SCN laden effluent at significantly lower environmental temperatures.

4.5 Effective pH range for thiocyanate destruction

The effect of maintained pH on SCN destruction was investigated in the range of pH 5.0-10.0 (Figure 4.7) by assessing the extent of degradation achieved under like conditions, over an 18 hour period. Maximum SCN destruction of 95.53 and 93.26% was achieved at pH 7.0 for SCN starting concentrations of 100 and 150 mg/L, respectively. SCN destruction at pH 6.5 was only 41.2% of the total available SCN in solution. The degree of SCN destruction further decreased with decreasing pH achieving only 17.0% at pH 5.0.

A similar effect was observed at solution pH values above 7.0 although more pronounced. A solution pH of 8.0 resulted in only 70.9% of available SCN being degraded, while 9.6% of SCN was degraded at pH 9.0 and less than 2.0% at pH 10.0. Therefore, solution pH has a significant impact on the observed SCN destruction. The inoculum was maintained at pH 7.0 prior to inoculation thus precluding the need for acclimatisation. This allowed the microbial consortium to degrade SCN at a maximum rate for the duration of substrate availability. Acclimatisation of the mixed microbial consortium to sub-optimum pH conditions was observed and increased as conditions moved further from the inoculum's original pH.

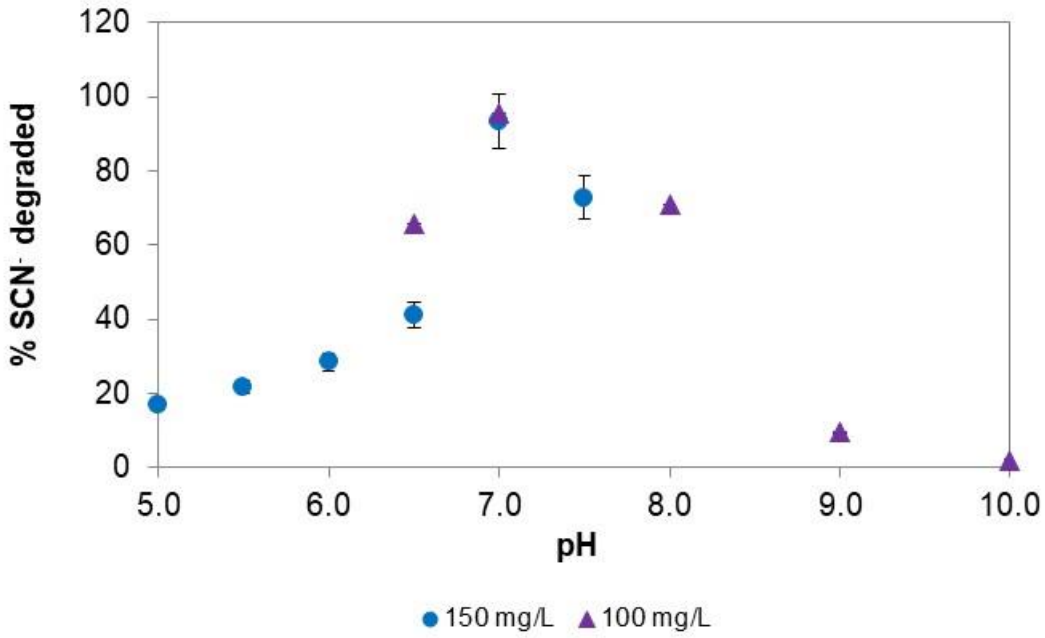

Figure 4.7: The effect of pH on the extent of thiocyanate destruction 18 hours post inoculation as a percentage destruction of the inoculated thiocyanate concentration. The start thiocyanate concentration was either 100 or 500 mg/L as indicated by the graph legend. The inoculation temperature was maintained at 30°C.

Previous studies have shown destruction of SCN across a relatively narrow pH range for microbial consortia and individual species (Kim and Katayama, 2000; Vázquez *et al*., 2006). Chaudhari and Kodam, (2010) achieved optimal SCN degradation at pH 6.0 using a *Klebsiella* and *Ralstonia* co-culture while significant impact was measured at pH conditions above and below pH 6.0, while Kim and Katayama, (2000) found an optimal pH of 6.2 using a pure culture of *Thiobacillus thioparus*. (Kim and Katayama, 2000; Chaudhari and Kodam, 2010). In the study conducted by Kim and Katayama (2000), it was found that a slight drop in pH from 6.2 to 6.1 resulted in strong inhibition of SCN destruction activity as well as cell growth. Furthermore, the maximum rate decreased from 26.8 mg/L.h to 5.8 mg/L.h while significant increases in activity was not observed at an increased pH of 8.0.

Vazquez and co-workers showed a maximum SCN destruction rate using a mixed consortium at a solution pH of pH 6.0, obtaining a SCN destruction rate of 3.94 mg/L.h. This rate decreased to 0.41 mg/L.h at a solution pH of pH 7.0 with complete inhibition at a solution pH of 8.0 over the 63 hour duration of the experiment. The different pH optima between the current study and other published work relates to the nature of the microbial community and the dominant species.

From the available literature it is clear that a narrow pH range exists for optimum SCN degradation, regardless of the microbial community structure. The data from the current study is consistent with published work. There appears to have been little research to investigate the potential of adaptation to a wider pH range and this should be investigated ahead of widespread industrial application.

4.6 Conclusions

This study showed initial acclimatisation of the mixed microbial population to SCN concentrations not previously experienced. The culture was able to tolerate and degrade SCN at concentrations up to 1800 mg/L once acclimatised. Initial SCN concentrations below 1 800 mg/L were not observed to result in significant substrate inhibition. Acclimatisation to SCN was shown to be a function of the SCN concentration in solution and the time required for acclimatisation increased with increasing SCN concentration, especially without prior exposure to SCN at significant levels. Acclimatisation to higher SCN concentrations was rapid following pre-exposure to residual SCN in solution. SCN concentrations investigated did not adversely affect the SCN destruction ability of the mixed microbial population.

The optimum temperature for SCN destruction was in the range of 35-40°C. Moreover, it was shown that an increased temperature resulted in a shorter lag phase. The Arrhenius function showed an exponential dependence of the SCN destruction rate on temperature between 10-40°C. Activation energy values calculated are consistent with a rapid increase in reaction rate as incubation temperature increased (Gokulakrishnan and Gummadi, 2006). Ultimately, higher SCN destruction rates were attained at higher temperatures in the range investigated.

An optimum solution pH was shown as pH 7.0 while substantially decreased SCN destruction was measured below and above pH 7.0. This result speaks to a sudden change in solution pH and not incremental changes allowing for adaption.

The critical conditions identified for efficient SCN destruction include SCN concentrations below 1500 mg/L, temperatures above 30 but at or below 40°C at a solution pH of 7.0. These conditions were shown as most suitable for SCN destruction using the ASTER^{TM} culture. Fluctuations in pH are likely to be detrimental since acclimation was shown to be beneficial for the culture used in this study.

Fluctuations in the SCN levels in industrial feeds could be well tolerated due to the reduced need for acclimatisation as a result of prior exposure to SCN. Moreover, exposure of the culture to elevated SCN concentrations induced the formation of flocs and this increased with increasing SCN concentration. Extensive floc formation may result in a mass transfer limitation, but at the same time could reduce the inhibitory effect of high solution concentrations and warrants further investigation.

Temperature control for industrial processes, like ASTER™, is usually not considered, due to the significant cost associated with heating and cooling of bulk liquids. The current research confirmed that the maximum SCN degradation rate was significantly affected by temperature, so it may be necessary for commercial operations to consider the trade-off between the costs associated with maintaining the temperature of reaction vessels and the time required to treat SCN laden effluent at lower ambient temperatures. This is likely to be considered on a case-by-case basis and the potential for heat integration may exist for certain applications, such as the coupling of ASTER™ with the BIOX® technology, where the bioleaching reactors often generate excess heat.

Using batch studies does not provide a maximum possible rate under specific conditions and predicted performance is usually underestimated (Doran, 1995). Although acclimatisation was investigated, adaptation was not considered. Continuous reactor experiments provide more insight into volumetric performance. This batch information was used to inform ongoing management of an industrial ASTER™ plant as well as provide insight into design of continuous reactor experiments.

Chapter 5: Continuous reactor studies using a mixed microbial sludge

5.1 Introduction

SCN destruction has been well described in literature employing various microorganisms under different environmental conditions (Section 1.8). The operating window for SCN destruction was determined and discussed in Chapter 0. This chapter is presented as a series of unique data sets produced from continuously operated reactors as well as batch experiments. The primary focus of this chapter is to discuss the effect of high SCN feed concentration and the impact of environmental conditions on SCN destruction. Furthermore, this chapter aims to evaluate any constraints to enhanced SCN destruction and elucidate the driving forces behind SCN destruction by the microbial population.

The following key questions are addressed in Chapter 5:

i) What was the maximum feed SCN concentration utilised at an eight hour hydraulic retention time by the mixed microbial population, while maintaining a residual SCN concentration below 1 mg/L?

ii) What was the maximum residual SCN concentration tolerated by the mixed microbial population?

iii) What was the effect of reactor pH on the SCN destruction rate?

iv) To what extent could the culture be adapted to different environmental conditions?

v) Did the SCN destruction rate recover following selected conditions outside of the operating window identified in Chapter 0?

5.2 Experimental Programme

This study focussed on SCN destruction under continuous conditions and the reactors were started under batch conditions with 100 mg/L SCN in the basal medium and 10% (w/v) inoculum from the stock reactor containing planktonic cells as well as suspended flocs. The 1L CSTR was operated in continuous mode following complete SCN destruction during batch operation. The feed SCN was incrementally increased to a maximum of 3 500 mg/L and the HRT hydraulic retention times are discussed accordingly. Significant sludge formation prompted an evaluation of potential mass transfer limitations starting with reduced volume-to-area reactors. Five 300 mL reactors were operated identically to the 1.0 L reactors and received feed SCN concentrations in the range 250-2 000 mg/L and operated in parallel. Biomass was homogenised from two of these reactors at the end of the experimental run and used as inoculation for batch experiments to further investigate the relationship between SCN destruction and biomass accumulation. The reactors sampled for inoculum received 500 and 1 500 mg/L feed SCN concentrations. The inoculum for the batch experiments was increased five-fold as well as twenty five-fold to evaluate the effect of biomass loading on SCN destruction rates.

Dissolved oxygen (DO) was measured using a micro DO probe at various positions in a 1.0 L CSTR. The reactor lid was removed and while the DO measured in the bulk solution remained unchanged, the probe was inserted into the sludge at a predetermined position. The starting point for measuring was at first probe wetting and measurements continued with sludge depth penetration. Finally, the effect of pH was investigated on SCN destruction and especially recovery of the SCN destruction ability of the reactor following prolonged pH induced stress since commercial operations may suffer from changing conditions.

5.3 Results and Discussion

The effect of SCN loading on the destruction ability of the microbial community was investigated using CSTRs. Homogenised sludge from the Sixfors reactors were used to inoculate batch experiments for investigating the effect of biomass retention on SCN destruction. A fresh inoculation of the Sixfors was done to investigate the effect of pH change on SCN destruction under low SCN loading conditions and

operated as discussed. This information has allowed development of a conceptual model of the reactor phases to reach maturation and SCN destruction performance.

5.3.1 Effect of thiocyanate concentration on the thiocyanate destruction ability of the mixed microbial sludge in 1 L continuous stirred tank reactor

The reactor was operated in batch mode allowing degradation of the initial 100 mg/L SCN added in solution prior to continuous operation. Complete SCN destruction was measured during the batch phase while an increased residual SCN concentration was measured directly after starting the continuous feed at 100 mg/L SCN (eight hour HRT). Thiocyanate destruction at the theoretical maximum was achieved at an initial feed SCN concentration of 100 mg/L. The spike in residual SCN concentration was again observed following each increment in SCN feed concentration up to a feed SCN concentration of 1 000 mg/L. Results are summarised in Table 5.1 followed by a detailed discussion of the data generated from individual reactors. Maximum SCN destruction rate was detected as a feed SCN concentration of 1 000 mg/L.

Table 5.1: Results of thiocyanate destruction and maximum rates at different feed thiocyanate concentrations. The reactor volume was maintained at 1.0 L and operated at a constant temperature of 22°C at a hydraulic retention time of eight hours. The converted thiocyanate was calculated based on the maximum thiocyanate destruction rate.

Run time (days)	Feed SCN concentration (mg/L)	Max. % SCN converted	Maximum SCN destruction rate (mg/L.h)
0.0 – 4.2 *(4.2 days)	100	99.99	12.50
4.2 – 25.6 (21.4 days)	250	99.74	31.17
25.6 – 46.5 (20.9 days)	500	77.06	48.16
46.5 – 84.8 (38.3 days)	1 000	69.95	87.44
84.8 – 118.5 (33.7 days)	1 500	26.93	50.49

* - The duration of each feed cycle is indicated in brackets

Continuous feed to the reactor was started with 100 mg/L SCN and lasted 4.2 days (Figure 5.1). The residual SCN concentration in the reactor increased to a maximum of 24.62 mg/L within the first 15 hours of continuous feeding and thereafter complete SCN destruction was measured within a further 21 hours. Complete SCN destruction was measured for the majority of the feed cycle containing 100 mg/L SCN except for a residual SCN concentration of 6.5 mg/L at day 2.9 which decreased to 2.1 mg/L at day 4.2.

The feed SCN concentration was increased to 250 mg/L thereby increasing the SCN loading by a factor of 2.5. Residual SCN in solution reached 41.40 mg/L during the first 7.2 hours and was also the highest measured residual SCN concentration at a feed SCN concentration of 250 mg/L. The residual SCN in solution decreased over the next 26.4 hours and reached a concentration of 1.4 mg/L by the fourth HRT achieving >99% SCN destruction efficiency. The residual SCN concentration remained consistent for 60.0 HRTs.

A subsequent feed SCN concentration of 500 mg/L resulted in accumulation of SCN in solution reaching 465.1 mg/L within 7 hours. The residual SCN concentration decreased to 259.6 mg/L over the following 12 hours and further decreased to below 180 mg/L following another 12.5 hours. The residual SCN concentration consistently measured below 200 mg/L over 18.5 days.

The feed SCN concentration was doubled to 1 000 mg/L which resulted in accumulation of SCN reaching a concentration of 667.6 mg/L within 16.8 hours. The residual SCN concentration further decreased and remained consistently below 310 mg/L. The residual SCN concentration increased to 1 087 mg/L within 1.2 days of a feed SCN concentration increase to 1 500 mg/L and remained above 1 100 mg/L during 33 days of continuous operation.

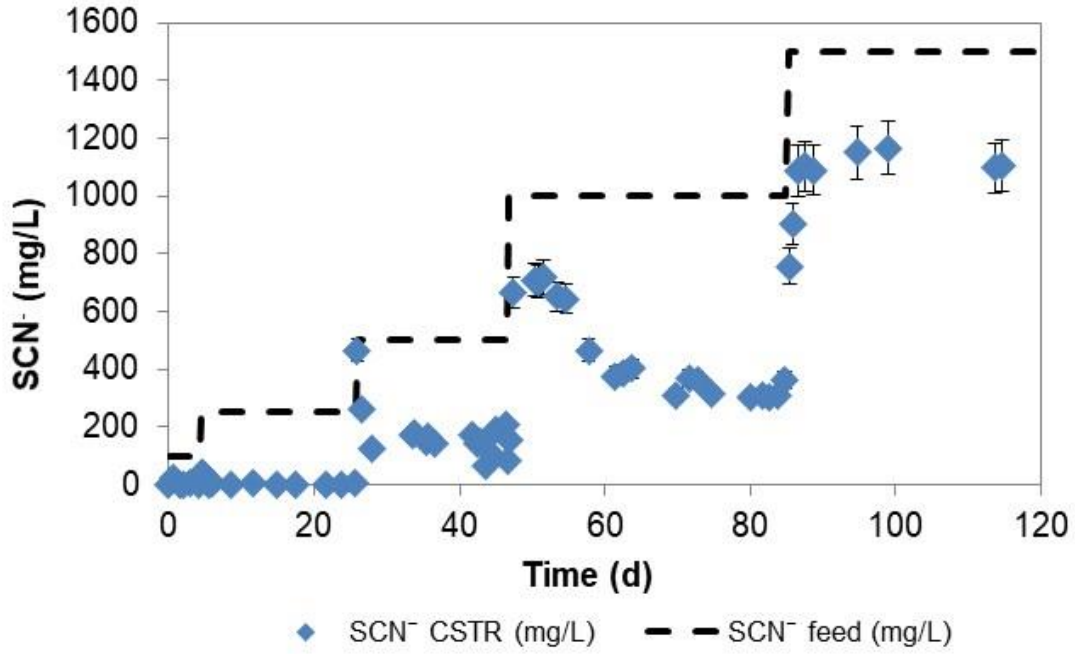

Figure 5.1: Residual thiocyanate was measured for the primary CSTR while the dashed line represent the feed thiocyanate concentration indicating the incremental increases over time at a constant HRT of eight hours.

Figure 5.2 shows the volumetric SCN destruction rates obtained under increasing feed SCN concentrations. The maximum possible rate of 12.5 mg/L.h was reached within three HRTs and a 2.5 fold increased feed SCN concentration resulted in a rate increase to 31.3 mg/L.h within four HRTs.

The rate further increased to a maximum of 48.2 mg/L.h at a feed SCN concentration of 500 mg/L. This rate increased by 54% even though the feed SCN load doubled.

Following this was an initial decreased SCN destruction rate (35.3 mg/L.h) directly after a feed SCN increase to 1 000 mg/L. The rate increased over 16.4 days to a maximum of 87.4 mg/L.h and remained in a pseudo-steady state for the remainder of this feed cycle. The SCN destruction rate increased by 81.6% following a doubling of the feed SCN concentration from 500 to 1 000 mg/L.

At a feed SCN concentration of 1 500 mg/L the rate decreased directly after the feed increased, observed before, but did not increase even after an extended time period of 32.4 days (259.2 HRTs). Furthermore, not only did the rate not recover, but was lower than the rate at a feed SCN concentration of 1 000 mg/L. The rate at a feed SCN concentration of 1 500 mg/L fluctuated and decreased by between 29.3-52.1%.

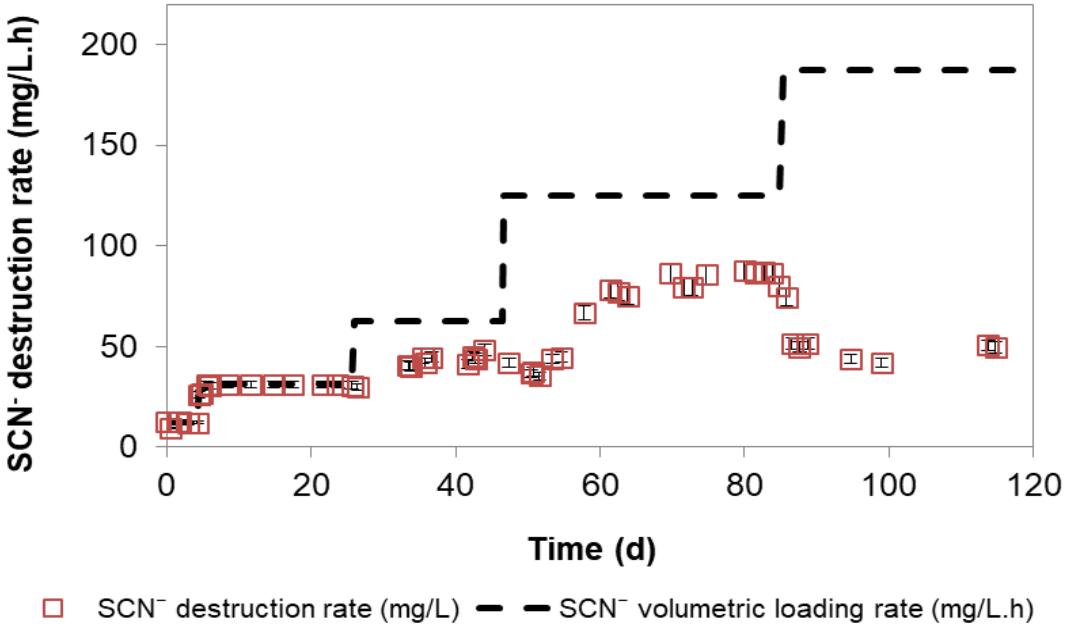

Figure 5.2: Thiocyanate destruction rate at different thiocyanate volumetric loading rates. All data described by reactor operation at a hydraulic retention time of eight hours.

The SCN destruction rate achieved at a feed SCN concentration of 100 mg/L (12.5 mg/L.h) was not unexpected since a rate of 16.8 mg/L.h was reached using flask experiments discussed in Chapter 4. An increased degradation rate of 31.25 mg.L.h was detected at a feed SCN concentration of 250 mg/L whereby all SCN was degraded using a continuous reactor system. The increase in the feed SCN concentration from 250 mg/L to 500 mg/L did not increase the SCN destruction rate to the same extent nor was all the SCN degraded.

Furthermore, it was expected that an increased SCN feed concentration of 1 000 mg/L would result in an increased residual SCN concentration by a minimum of 500 mg/L, in a steady-state system. This decreased residual SCN concentration, at a feed of 1 000 mg/L SCN, was reflected by an increased SCN destruction rate reaching a maximum of 87.44 mg/L.h. Visual inspection of the reactor (Figure 5.3) showed significant biomass accumulation. The increased biomass was likely in response to the residual SCN concentration over an extended time period, resulting in the rapid growth of biomass either as a stress response or due to excess substrate. Rapid biomass accumulation within the reactor increased with increasing SCN destruction rates up to a feed SCN concentration of 1 000 mg/L at an 8 h HRT.

At a feed SCN concentration of 1 500 mg/L a higher than expected residual SCN concentration measured above 1 000 mg/L. This was indicative of either substrate and/or product inhibition since the SCN destruction rate was substantially lower than before. It is also possible that the microbial community changed significantly eliminating a symbiotic relationship.

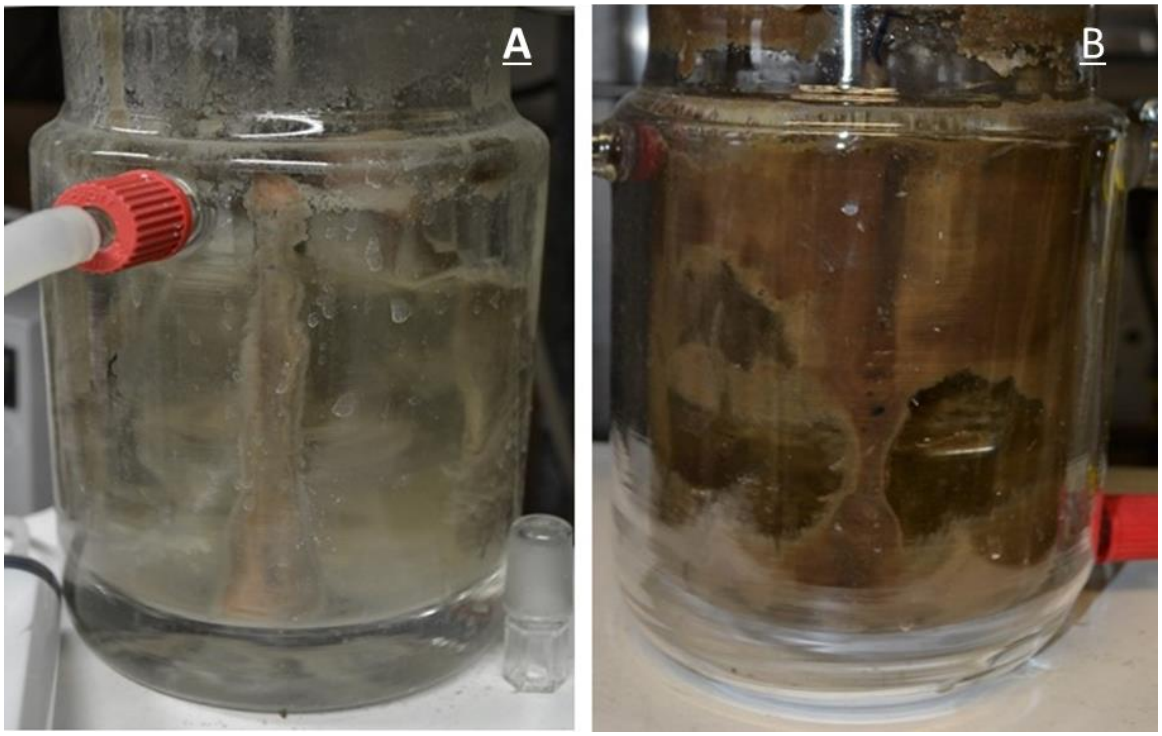

Figure 5.3: Visual inspection of reactor containing A) sludge at a feed thiocyanate concentration of 500 mg/L and B) increased sludge at a feed thiocyanate concentration of 1 000 mg/L. Figure B was taken at the end of the feed cycle containing a 1 000 mg/L thiocyanate.

The HRT was increased due to a high residual SCN concentration at a feed SCN concentraton of 1 500 mg/L. The HRT was first increased to 16 hours followed by 24 hours (Table 5.2). The HRT was chosen for practical plant considerations. The remainder of the experiment was conducted at an HRT of 24 hours while the feed SCN concentration was increased.

Table 5.2: Results of thiocyanate destruction at different feed thiocyanate concentrations. The reactor volume was maintained at 1.0 L and operated at a constant temperature of 22°C.

Run time (days)	Feed SCN concentration (mg/L)	% SCN degraded	SCN destruction rate$_{max}$ (mg/L.h)
[D]118.5 – 127.4 (8.9 days)	1 000	61.89-78.43	49.0
*127.4 – 137.7 (10.3 days)	1 000	96.02-99.31	41.4
137.7 – 144.6 (6.9 days)	1 500	70.85-79.18	49.5
144.6 – 151.7 (7.1 days)	2 000	29.42-48.92	40.8
151.7 – 158.7 (7.0 days)	2 500	25.62-38.89	40.5
158.7 – 178.8 (20.1 days)	3 000	1.97-34.54	43.2
178.8 – 232.6 (53.8 days)	3 500	0.03-0.72	1.1
[Z]232.6 – 238.8 (6.2 days)	1 000	20.98-44.37	55.5

[D] - HRT at 16 hours for days 118.5-127.4.

[Z] - HRT at 8 hours for days 232.6-238.8.

* - HRT set at 24 hours for feed SCN concentrations at 1 000-3 500 mg/L.

Figure 5.4 shows the SCN destruction rates achieved at different feed SCN concentrations following on from day 118.5. The HRT was increased from 8 to 16 hours while the feed SCN concentration was decreased from 1 500 to 1 000 mg/L. The residual SCN concentration was 215.7 mg/L at the lowest point, reflecting a maximum SCN destruction rate of 49.0 mg/L.h. The HRT was further increased to 24 hours to eliminate any possible substrate inhibition that may have occurred as well as aid in decreasing the residual SCN concentration. The degree of SCN destruction increased to above 98.7% within 6.3 days and remained high for the remainder of the feed cycle at 1 000 mg/L SCN.

The feed SCN concentration was increased to 1 500 mg/L at day 138. The residual SCN concentration increased to 426.4 mg/L within 21 hours reflected by a SCN destruction rate of 44.8 mg/L.h. The residual SCN concentration decreased to a minimum of 313.1 mg/L within 6.9 days following the increased feed SCN concentration. The maximum SCN destruction rate calculated was 49.5 mg/L.h. This rate was substantially lower when compared to the rate obtained at a feed SCN

of 1000 mg/L at an 8 hour HRT. The residual SCN concentration increased substantially at 2 000, 2 500 and 3 000 mg/L SCN feed concentrations over 7.1, 7.0 and 6.9 days, respectively. The residual SCN concentration equalised with a feed SCN concentration of 3 000 mg/L and above even after an extended period of 20.1 days. The residual SCN concentration was also reflected by the feed SCN concentration at 3 500 mg/L for a further duration of 53.8 days. Furthermore, visual observation did not indicate a significant change in biomass build-up from day 180 onwards. Interestingly, a SCN destruction rate of 55.46 mg/L.h was reached within only 6.2 days of changing the feed to contain 1 000 mg/L SCN, measuring a residual SCN concentration of 556.3 mg/L. However, this rate was lower when compared to the previous maximum rate of 87.44 mg/L.h indicative of a change in microbial population.

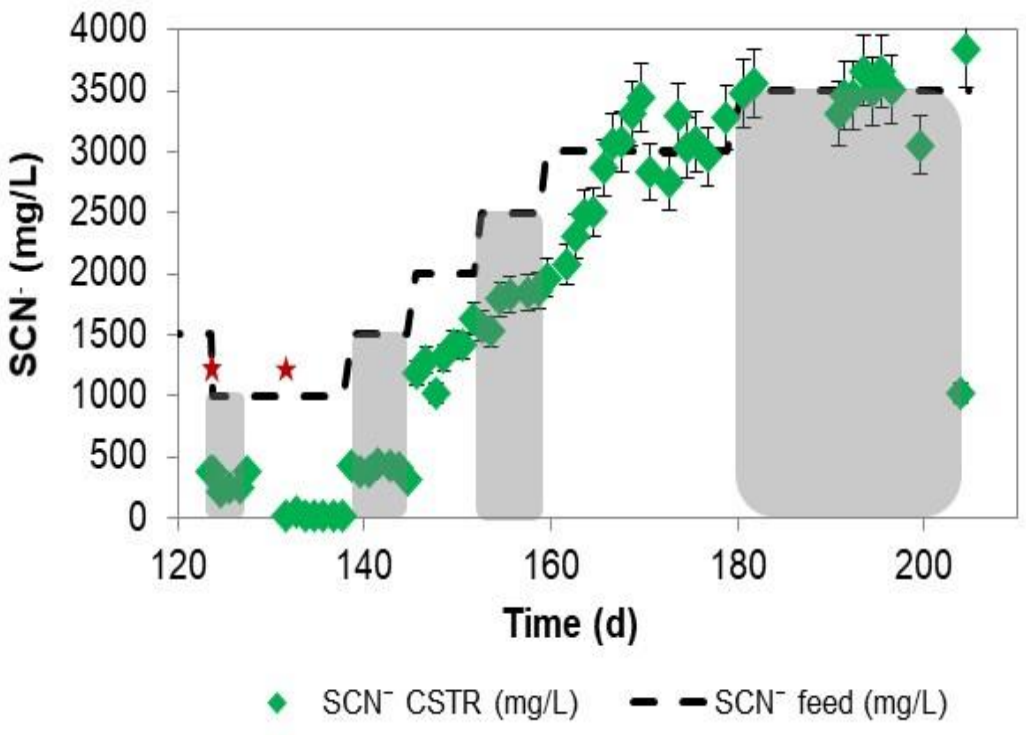

Figure 5.4: Residual thiocyanate concentration in solution was measured for the CSTR over time. The change in feed thiocyanate concentration is shown while the grey blocks aid visualisation of the changes made. The first ✶ (at 123 days) indicates a change from 8 to 16 hours hydraulic retention time and the second ✶ indicates (at 131.5 days) a change from 16 to a 24 hour hydraulic retention time.

5.3.2 Effects of thiocyanate on the thiocyanate destruction ability of the mixed microbial community in a 0.3 L reactor.

Reactors were supplied with reactor media containing SCN at concentrations of 250, 500, 1 000, 1 500 or 2 000 mg/L (Table 5.3) and the results are discussed in this order unless otherwise stated. Five reactors were operated in parallel and initially received a feed SCN concentration of 100 mg/L for a period of 24 hours (3 HRTs). The majority of SCN (> 75%) was degraded during this time by each individual reactor and was followed by an increased SCN feed concentration in the range of 250-2 000 mg/L. SCN was detected within 30.4 hours (3.8 HRTs) at residual levels ranging from 56% to 91% of the feed concentration supplied. Reactors were subsequently operated in batch mode for 7.5 days to allow for SCN destruction and acclimation of the biomass to the higher residual SCN concentrations. Biomass accumulation was visually observed as free floating floc formation and attached biomass noted especially for the reactors receiving a feed of 1 000 mg/L SCN and above.

Table 5.3: Degree of maximum thiocyanate destruction as well as the maximum thiocyanate destruction rate reached during a minimum of three HRTs.

Feed SCN concentration (mg/L)	**Theoretical maximum SCN destruction rate (mg/L)**	**Max SCN degraded (%) $_{0.3\ L}$**	**SCN destruction rate$_{max}$ (mg/L.h)$_{0.3\ L}$**
250	31.25	100	31.25
500	62.50	100	62.5
1000	125.0	61.3	76.69
1500	187.5	29.4	55.07
2000	250.0	20.8	51.89

Figure 5.5 shows residual SCN concentrations for reactors receiving feed SCN concentrations of 250, 500, 1000, 1 500 or 2 000 mg/L. Residual SCN was substantial during the first 2.22 days of continuous operation measuring 140.0 and 1 819.9 mg/L for CSTR 250 and 2 000, respectively. Due to the high residual SCN

concentration the reactors were operated in batch mode for 6.21 days. The reduction in residual SCN was 99.5, 59.1, 37.3, 30.4, 27.3% for each of the reactors in order of increased SCN feed concentration. The SCN destruction rate calculated for each reactor, in order, was 22.4, 35.9, 42.4, 65.4 and 80.0 mg/L.day during the batch phase. It is likely that the planktonic cell population increased at a more rapid rate in the reactors with higher initial SCN concentrations compared to the reactors containing a lower residual SCN concentration which resulted in the higher destruction efficiencies. The higher observed sludge formation likely offered protection against the higher SCN concentration by mass transfer limitation. It was evident that an increased residual SCN concentration resulted in an increased SCN destruction rate and a concomitant biomass increase. This showed a critical residual SCN concentration above 500 mg/L required for activation of substantial biomass production indicative of a protective function against detrimentally high SCN levels.

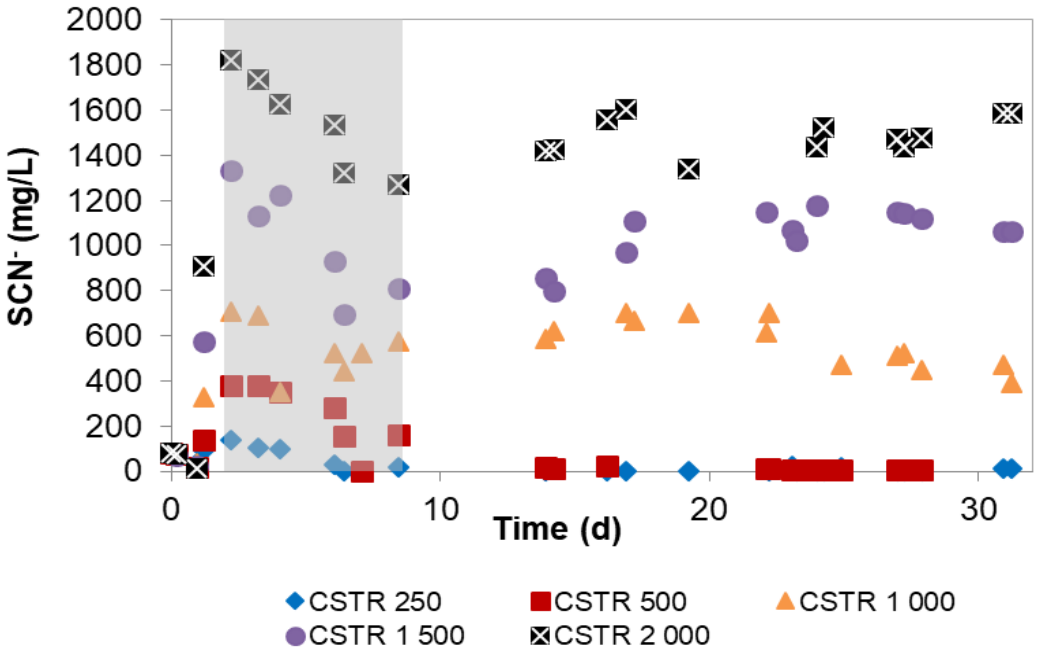

Figure 5.5: Residual thiocyanate concentrations for each reactor over time. The area in grey represent the duration of the batch operational phase following start-up in continuous operating mode (eight hour HRT). Continuous operation again was followed for the rest of the experimental run shown after day 8.43. The feed thiocyanate concentration is indicated by the numbers in the graph legend.

Due to significant SCN destruction, it was decided to start continuous operation of each reactor receiving an independent feed. The maximum theoretical SCN destruction rate of 31.25 mg/L.h was reached within 5.48 days for the reactor

receiving 250 mg/L feed SCN which was maintained for the duration of the experimental run (Figure 5.6). The residual SCN concentration for CSTR 500 decreased to 0.19 mg/L within 26.49 days during continuous feeding. The theoretical maximum SCN destruction rate of 62.5 mg/L.h was achieved and maintained for the balance of the experimental run. The maximum destruction rate achieved for CSTR 1 000 was 76.69 mg/L.h. However, the maximum rate calculated for CSTR 1 500 was 55.07 mg/L.h showing again a decreased rate at an increased residual SCN concentration above 1 000 mg/L. Furthermore, the average rate calculated for CSTR 2 000 was 54.53 mg/L.h over the last 3.48 days of the experiment with a maximum of 59.35 mg/L.h. Thiocyanate and converted NH_4 were available as nutrients for biomass growth the need for protection against increasing residual SCN concentrations in CSTR 1 000-2 000 likely resulted in formation of EPS rather than active SCN degrading biomass. It is proposed that this increased EPS fraction would also likely have caused mass transfer limitations for substrate access in deeper parts, while limiting gas mass transfer.

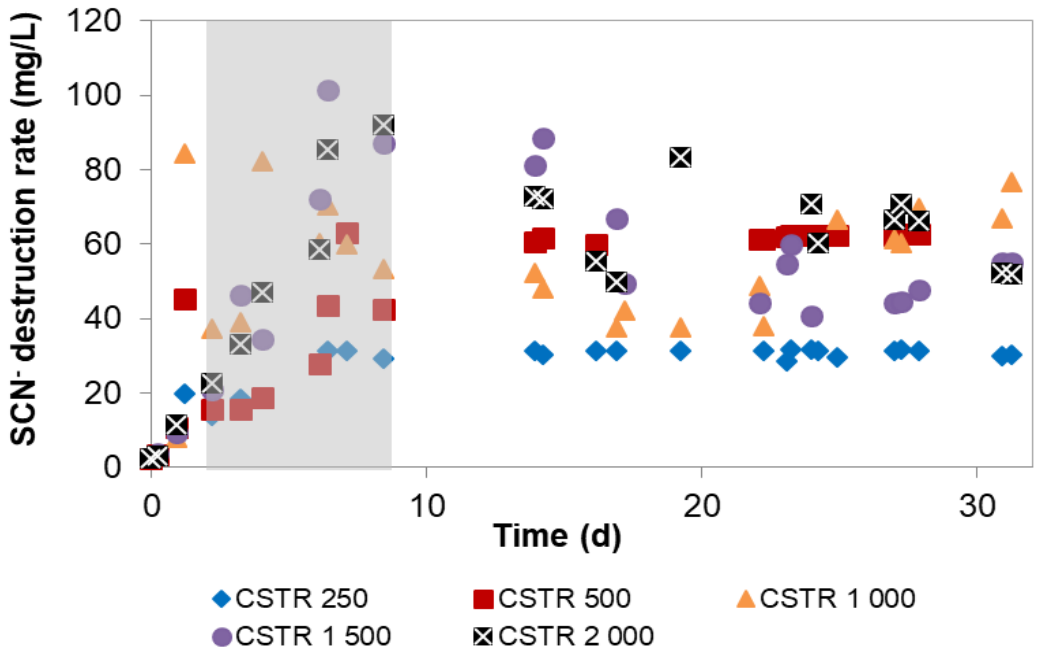

Figure 5.6: The area in grey represent the duration of the batch operational phase following start-up in continuous operating mode (eight hour HRT). The calculated thiocyanate destruction rates for each reactor is shown. Continuous operation again followed for the rest of the experimental run shown in white after day 8.43. The feed thiocyanate concentration is indicated by the numbers in the graph legend from 250-2 000 mg/L.

The SCN destruction rate did not increase to the same extent as the feed SCN concentration. This was also observed for the 1.0 L CSTR experiment discussed in Section 5.3.1. The significantly higher residual SCN measured during the batch phase in CSTR 2 000 for example showed the highest SCN destruction rate over the batch operated time period followed by CSTR 1 500, 1 000, 500 and 250 in order. If residual SCN was inhibitory, the overall rate would likely have been lower and the reverse rates observed. It is therefore likely that the higher residual SCN concentration resulted in increased sludge growth and a subsequent mass transfer limitation or the maximum metabolic rate was reached.

5.3.3 Effect of biomass concentration on thiocyanate destruction

Work done in Chapter 0 showed a decreased acclimation period for cultures pre-exposed to SCN concentrations above 60 mg/L. In addition, SCN destruction rates were not significantly different when comparing 1.0 L and 0.3 L CSTRs as discussed above although differences in reactor dimensions were noted. It was clear that the volumetric SCN destruction rates increased with increasing feed SCN concentration up to a maximum before significant decrease in rate was noted with further increase in the feed concentration. It was postulated that the increase in rate with increasing SCN feed concentration and thereby loading was due to increased biomass concentration being supported. In this case, where the specific SCN degradation rate was unchanged, one would expect an increased volumetric SCN degradation rate. This prompted an investigation of the potential impact of sludge loading on the SCN destruction rate and the effect of sludge pre-exposure to SCN.

Sludge was harvested from the reactors discussed in Section 5.3.2 receiving either 500 mg/L (CSTR 500) or 1 500 mg/L (CSTR 1 500) SCN in the feed. The sludge was homogenised by manual blending of the total harvested sludge from each reactor. This sludge was used to inoculate flasks with a starting SCN concentration of 1 000 mg/L at different biomass loadings.

Figure 5.7 shows the residual SCN concentration for flasks inoculated with 0.2, 1.0 and 5.0 g/L homogenised sludge. An acclimation period was noted and the duration thereof decreased as the inoculated biomass loading increased. The acclimation was described by the time required to destruct 10% of the starting SCN concentration. This trend was observed regardless of the inoculums' pre-exposure to SCN. The duration of acclimation was recorded as 41, 20 and 6 hours and 41, 23 and 5.5 hours, respectively for the sludge harvested from CSTR 500 and 1 500. The culture harvested from CSTR 500 showed a reduced acclimatisation time of 51%

while the culture harvested from CSTR 1 500 showed a reduction of 44%. A twenty five times increased biomass concentration of 5.0 g/L resulted in an additional decrease in acclimatisation time of 14 hours (70%) and 17.5 hours (76%) for the cultures from CSTR 500 and 1 500. The substantially increased sludge loading did not result in a decreased acclimatisation time to the same extent to which the biomass was increased nor was the trend found to be linear.

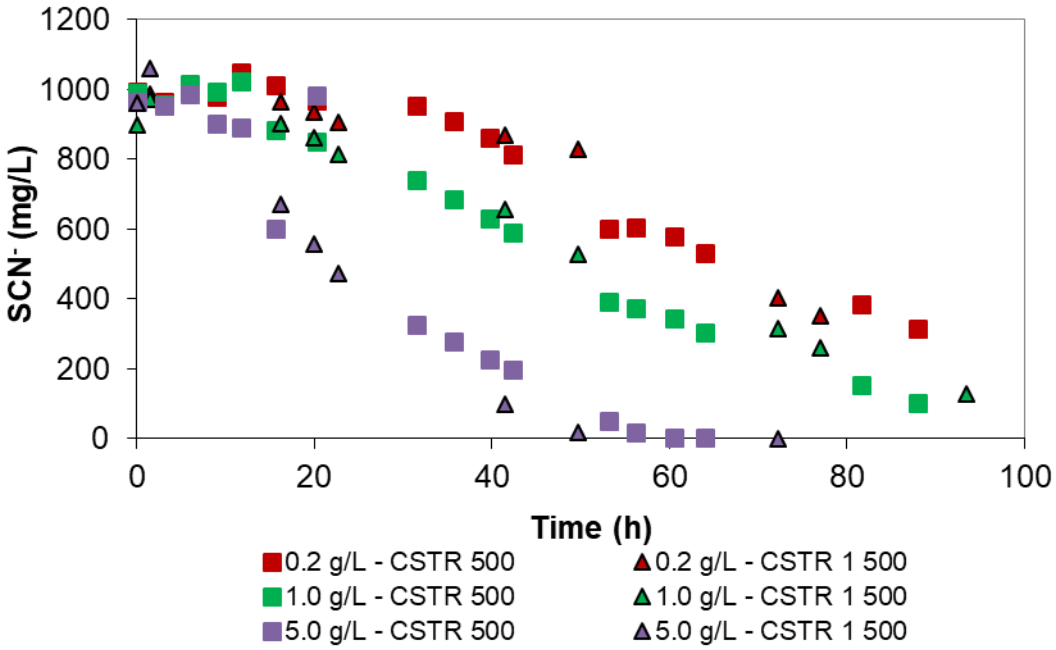

Figure 5.7: Residual thiocyanate in solution was measured for each flask inoculated with either 0.2, 1.0 or 5.0 g/L biomass from either CSTR 500 or CSTR 1 500. CSTR 500 was operated as discussed in section 5.3.2 and fed with 500 mg/L SCN while CSTR 1 500 received 1 500 mg/L SCN in the feed.

Figure 5.8 shows the maximum SCN destruction rates calculated for flasks inoculated from CSTR 500 and 1 500 with 0.2, 1.0 and 5.0 g/L sludge. The maximum rates calculated were 10.39 and 11.34 mg/L.h for the 0.2 g/L inoculum load. An inoculum size of 1.0 g/L resulted in maximum rates of 9.96 and 10.33 mg/L.h which was surprising since the inoculum size increased five-fold. A maximum inoculum load of 5.0 g/L from CSTR 500 and 1 500 resulted in significantly increased rates of 21.0 and 19.53 mg/L.h, respectively. Although this increased rate was almost double when compared to the lower inoculum loads, the rate did not correlate to the twenty-five fold increase in biomass. Moreover, substantial differences in the maximum SCN destruction rates were not observed for cultures pre-exposed to different feed and especially residual SCN concentrations. This was

also the case during acclimatisation where it was shown that similar acclimatisation time periods were required regardless of the pre-exposure to significantly different residual SCN concentrations. The volumetric SCN destruction rate was not proportional to the increased biomass loading and reasons that the specific microbial activity decreased with an increased SCN concentration. It is therefore plausible that the specific SCN destruction activity decreased due to a mass transfer limitation, nutrient limitation and exchange or substrate inhibition.

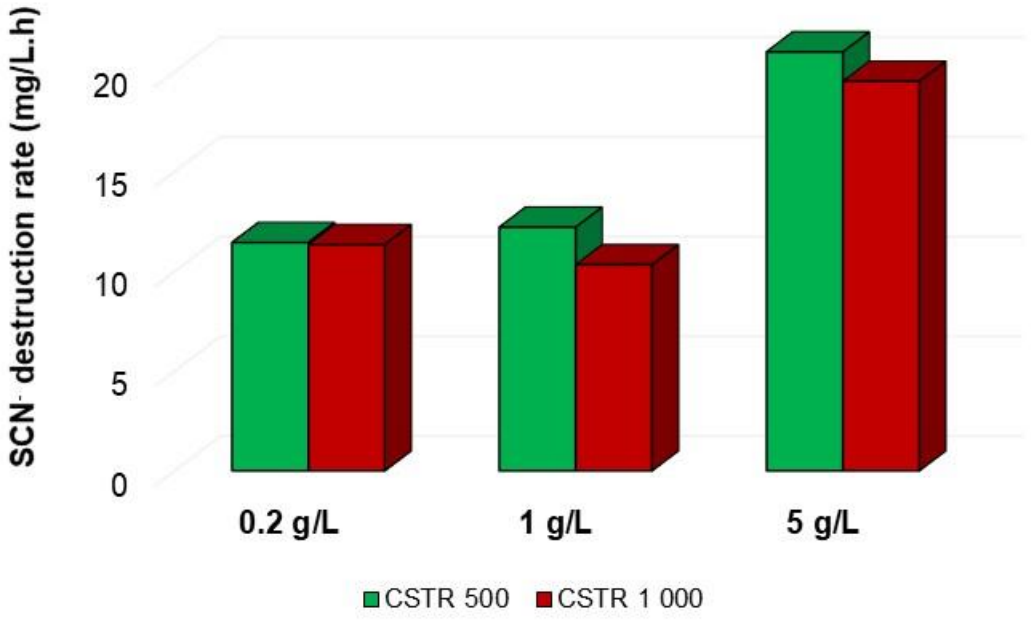

Figure 5.8: Effect of biomass concentration on volumetric thiocyanate destruction rate. Inoculum (0.2, 1.0 and 5.0 g/L) harvested from the reactor that received 500 and 1 500 mg/L feed thiocyanate concentration. The thiocyanate destruction rates were calculated as maximum rates from triplicate data.

5.3.4 Dissolved oxygen concentration in a continuous stirred tank reactor

In the previous section it was proposed that a likely contributor to limited SCN destruction could be a mass transfer limitation. Dissolved oxygen (DO) was measured to determine the sludge thickness at which transport could be impeded as well as whether anoxic regions within the sludge may exist. The DO concentration within the sludge in a CSTR was measured as a function of sludge depth. Oxygen is consumed by aerobic degradation of SCN, shown by Reaction 6.1 and used to calculate the stoichiometric oxygen consumption required for SCN destruction.

$$SCN^- + 2H_2O + \tfrac{5}{2}O_2 \rightarrow SO_4^{2-} + HCO_3^- + NH_3$$ Rxn 6.1

Measurement of DO was repeated at different positions within the reactor using a micro DO probe with fine adjustment allowing sludge penetration at 1 µm intervals. Position zero (X, Y and Z-axis) was taken at the point of first probe wetting. The DO probe penetrated the sludge at equal distance between the reactor wall and baffle ring. This allowed measurement of DO in the sludge which diffused into the sludge by means of bulk media contact and diffusion from the headspace gas. Sludge growth was observed to increase over time and accumulate on the submerged reactor parts including the inside reactor walls, baffles and impeller. In this case, oxygen diffusion into the sludge was used as an indicator of sludge permeability. DO was measured (M1) between the reactor wall and baffle ring (top of reactor) and the M2 measurement was done at an angle in sludge (bottom of reator) while air supply continued. DO measurement in the bulk liquid was consistently measured at a maximum of 9.20 mg/L.

The maximum DO concentration measured (readings taken at equilibrium) in the interface liquid of the sludge in the reactor during measurement 1 (M1) was 9.13 mg/L (Figure 5.9). The DO concentration rapidly decreased within 16 µm depth by 54.3% to a concentration of 4.17 mg/L. A further 36.7% net decrease in DO was measured 80 µm into the sludge reaching a DO concentration of 2.64 mg/L. Variability in DO concentration was measured as sludge depth increased, suggesting differing sludge and EPS composition and integrity. The DO concentration plateaued at 2.5-3.0 mg/L within 0-40 µm sludge depth while little change in DO concentration (above 3.0 mg/L) was measured at a sludge depth of 60-120 µm.

Extra polymeric substances (EPS) are produced by microorganisms composing of the mainly studies polysaccharides and proteins (Yang *et al.*, 2019). The formation of EPS has been linked to offer protection to microorganisms against unfavourable and stress inducing environments as well as enhance attachment of microorganisms to solid surfaces and promote aggregation between biomass and suspended solids (Nouha *et al.*, 2018). The changes in DO with sludge depth showed areas with low oxygen penetration while spikes in DO showed the extent of the amorphous nature of the sludge (Figure 5.9). The dense and viscous nature of the sludge likely impeded oxygen transfer with increasing sludge depth and is dependent on the degree of mono- and polysaccharide branching (Zhou *et al.*, 2019). Currently, research on EPS still has to fully clarify the mechanism of production and link function to components of EPS composition.

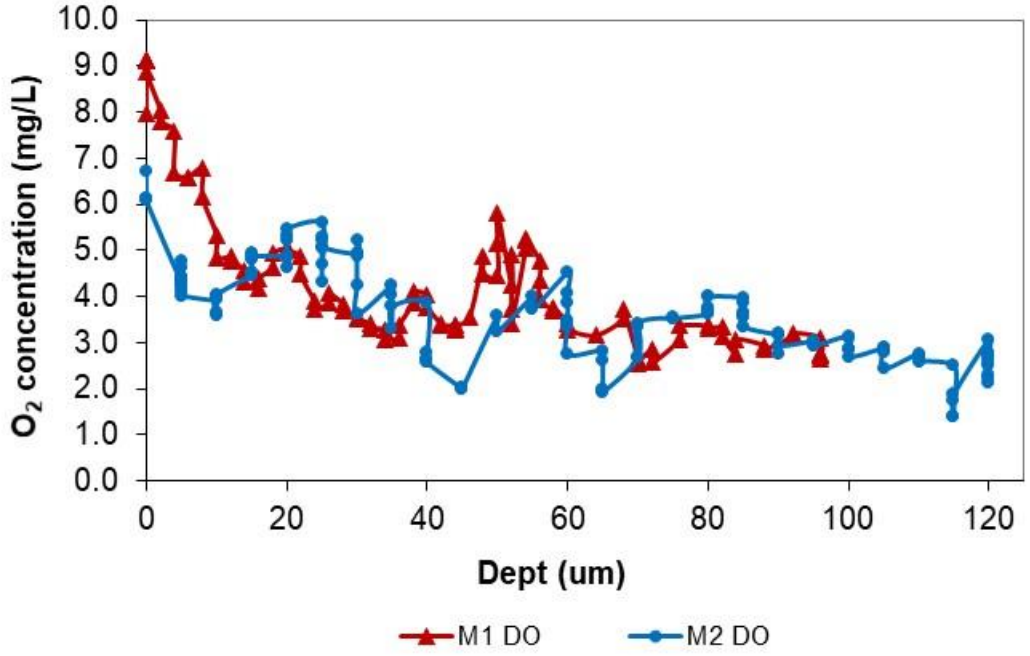

Figure 5.9: Dissolved oxygen concentration measured as a function of vertical sludge depth in the sludge located between the reactor wall and baffle ring. Measurement 1 (M1) and Measurement 2 (M2) show profiles measured at different positions. Measurements were taken at the end of the experimental time (day 239) for the reactor discussed in Section 5.3.1. Mixing was achieved by aeration only while feed to the reactor was ceased during measurements since residual SCN concentration provided substrate for oxygen utilisation. This was done practically to enable measurements.

The net stoichiometric demand for oxygen to convert SCN was based on a molar ratio of 7:1 (Rxn 6.1) and calculated as 1.93 g oxygen required to degrade 1.00 g SCN. Thus, an oxygen consumption rate of 166.1 mg/L.h would have been required to maintain a purely aerobic steady-state SCN degradation rate of 87.4 mg/L.h at a feed SCN concentration of 1 000 mg/L and an 8 h HRT. The oxygen transfer rate (OTR) calculated for the reactors used in Section 5.3.2 using the dynamic method was in the range 205.8 mg/L.h (data not shown). The OTR was 1.3 times higher at the maximum SCN destruction rate when compared to the oxygen uptake rate for each reactor offering a high concentration gradient between the bulk liquid and the sludge. The limited diffusion of oxygen into the sludge was clear despite the high OTR into the reactor bulk liquid. This data further supports the theory of a mass transfer limitation that becomes progressively worse as sludge growth increases.

Previous research showed the potential of floc variation with regards to pH, nutrients and dissolved oxygen which impact on the microbial community (Fan *et al.*, 2017). In particular, a low dissolved oxygen concentration may result in inhibited growth of nitrifiers where adapted ammonia oxidising bacteria are absent. Moreover, a low dissolved oxygen concentration has been linked to EPS formation impacting on floc properties including gas mass transfer and nutrient availability ultimately dictating microbial population structure (Fan *et al.*, 2017).

5.3.5 Stages of reactor colonisation and thiocyanate destruction

Reactor colonisation was described by various levels of development and SCN destruction capacities as conceptualised in Figure 5.11. Thiocyanate destruction was initially driven by a majority planktonic community (Stage 1) during reactor start-up with a low feed SCN concentration (<12.5 mg/L.h). Microscopic observation of the planktonic community included motile and non-motile organisms as well as fungi, yeast-like and algal-type cells. The residual concentration of SCN during this stage was measured as < 1 mg/L.

Increased feed SCN concentrations resulting in an increased SCN loading rate (31.3 mg/L.h) and residual SCN concentration resulted in the formation of sludge flocs during Stage 2 that settled in the clarifier underflow. As the residual SCN concentration increased, a biofilm formed on the exposed reactor surfaces.

Although the SCN destruction rate significantly increased during Stage 3 development, residual SCN remained high due to the high volumetric SCN loading (62.5 mg/L.h). The biofilm community continued to grow and mature through EPS production in response to the high residual SCN concentration in the reactor. The increased rates were measured while the increased biomass was visually confirmed.

The mature attached biofilm observed in Stage 4 offered increased SCN destruction at a significantly higher volumetric SCN loading rate (125 mg/L.h) compared to the previous stages. The biofilm has sufficiently formed to offer micro environments for optimum SCN destruction while maintaining sufficient gas and nutrient exchange with the bulk liquid. The EPS also offers protection against high residual SCN concentrations that could be inhibitory to growth while promoting advantageous symbiotic relationships.

The densely packed matured biofilm (Stage 5) precludes microorganisms deeply embedded in the biofilm from access to SCN and required gas, especially oxygen,

exchange with the bulk liquid. It is likely that sufficient nutrient exchange in the deeper layers of the biofilm was not possible. The SCN destruction rates decreased during this stage at an even higher volumetric SCN loading. The rate was likely impacted by a combination of SCN inhibition and mass transfer limitations as a result of the thickened biofilm formed.

The proposition of this conceptual model offers insight into an operational strategy whereby the first in line reactor(s) in the treatment plant should be operated under conditions of high SCN loading and potentially high residual SCN. This allows formation of a biofilm on exposed surfaces capable of maximum SCN destruction, offering a robust system capable of quick recovery following any upset due to unfavourable conditions or variation in SCN loading. A polishing reactor downstream of this would be required to reduce the residual SCN concentration from the biofilm reactors to maintain a low final residual SCN concentration (< 1 mg/L), making use of multiple-reactor configurations as required.

The thick nature of the sludge developed during Stage 4-5, showed a complex structure of EPS and embedded microbial cells (Figure 5.10). The packed nature of the embedded cells offers high biomass concentrations responsible for SCN destruction even at lower HRTs. Furthermore, the sludge offers protection against stress conditions while ensuring recovery is rapid when favourable conditions return. This further supports the conceptual model where biofilm development was in response to high residual SCN concentrations.

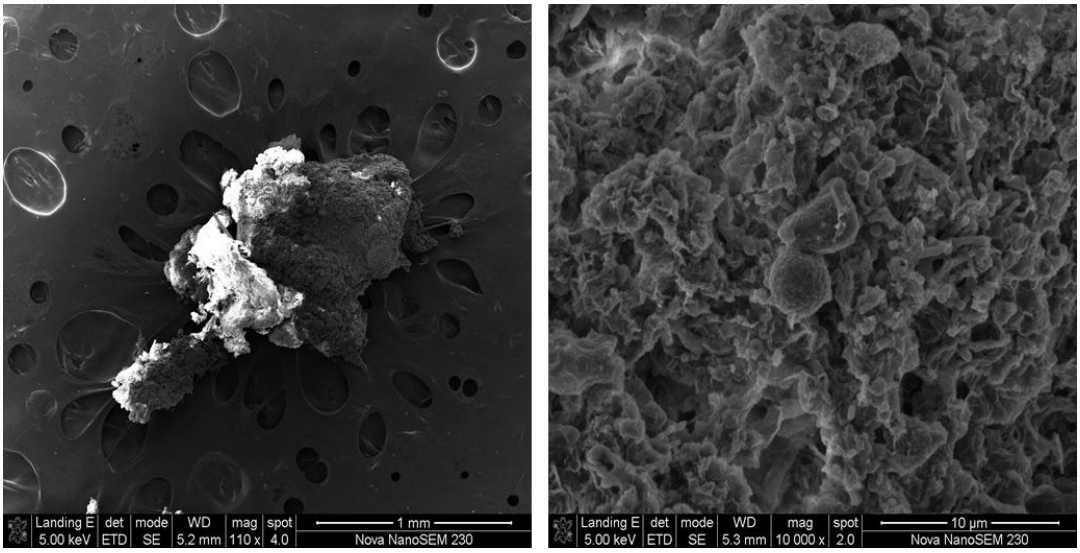

Figure 5.10: Scanning electron micrograph of whole sludge flocs (left) and the structure with embedded microbial cells (right).

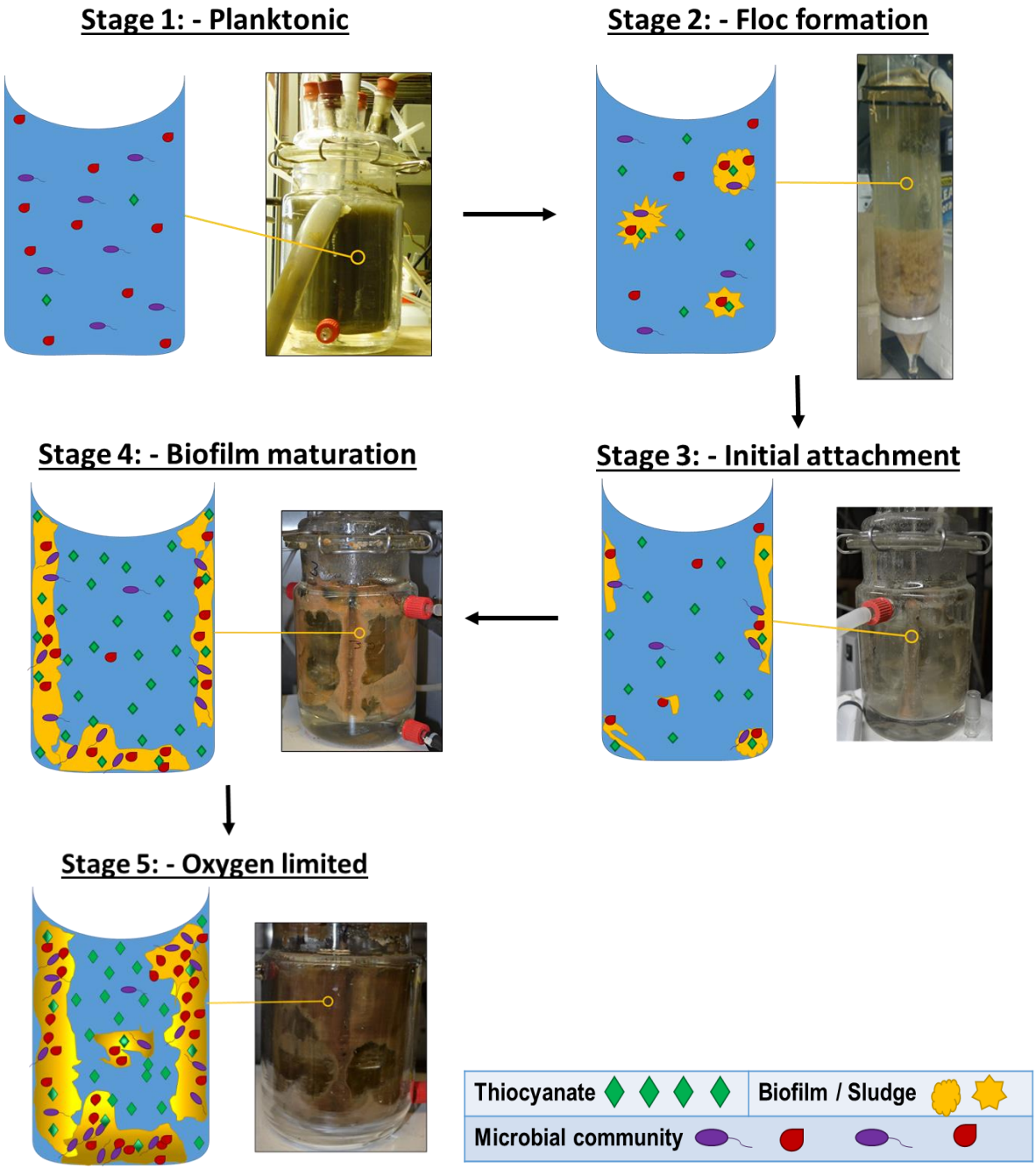

Figure 5.11: Illustration depicting the different stages of sludge growth and biofilm formation as a function of residual thiocyanate concentration. **Stage 1** shows the majority planktonic community responsible for thiocyanate destruction at low thiocyanate feeds. **Stages 2-4** show an increased residual thiocyanate concentration and while sludge floc formation is prominent in **Stage 2**, biofilm formation and attachment occur in **Stage 3** at a critical residual thiocyanate concentration in the range 450-700 mg/L. **Stage 4** was dominated by attached sludge offering a high thiocyanate destruction rate in the presence of a high residual thiocyanate concentration. **Stage 5** showed matured, thick biofilm development described by gas mass transfer limitations.

5.3.6 Effect of a change in solution pH on the thiocyanate destruction rate at a low feed thiocyanate concentration

The initial pH window identified for maximum SCN destruction (>93%) was very narrow at a solution pH of 7.0 (Section 4.5). A change to pH 6.5 or 7.5 showed a significant impact on SCN destruction resulting in destruction at only 41.2 and 72.66%. This study enhanced the understanding of system performance by monitoring pH continuously while evaluating the SCN destruction capability of the mixed microbial population. A series of reactors were operated continuously at a HRT of eight hours receiving a feed SCN concentration of 100 mg/L.

The Sixfors reactor system was operated in continuous culture across the pH range of pH 2.85-10.3. The feed SCN concentration and HRT was constant at 100 mg/L and 8 hours, respectively while pH was adjusted by increasing or decreasing the feed pH. Three reactors were inoculated and immediately operated on a continuous feed cycle with a feed pH of 7.0 ±0.5. Inconsistent pH measurements as well as residual SCN concentrations were measured during the initial 15 days which stabilised over the next 10 days achieving a steady state with complete SCN destruction.

The feed pH for CSTR 3 was increased incrementally over 32 days to give an increased reactor pH from 7.41 to 10.45. The calculated SCN destruction rate decreased rapidly at a reactor pH above 9.77. Insignificant SCN destruction was measured at a reactor pH of 10.13. The feed pH was adjusted back to a reactor pH of 7.02-7.09 following 7.29 days of insignificant SCN destruction. Recovery of SCN destruction following adjustment of the feed pH to reach a reactor pH in the range 7.02-7.11 was rapid and complete SCN destruction measured within 1.74 days (5.22 hydraulic residence times).

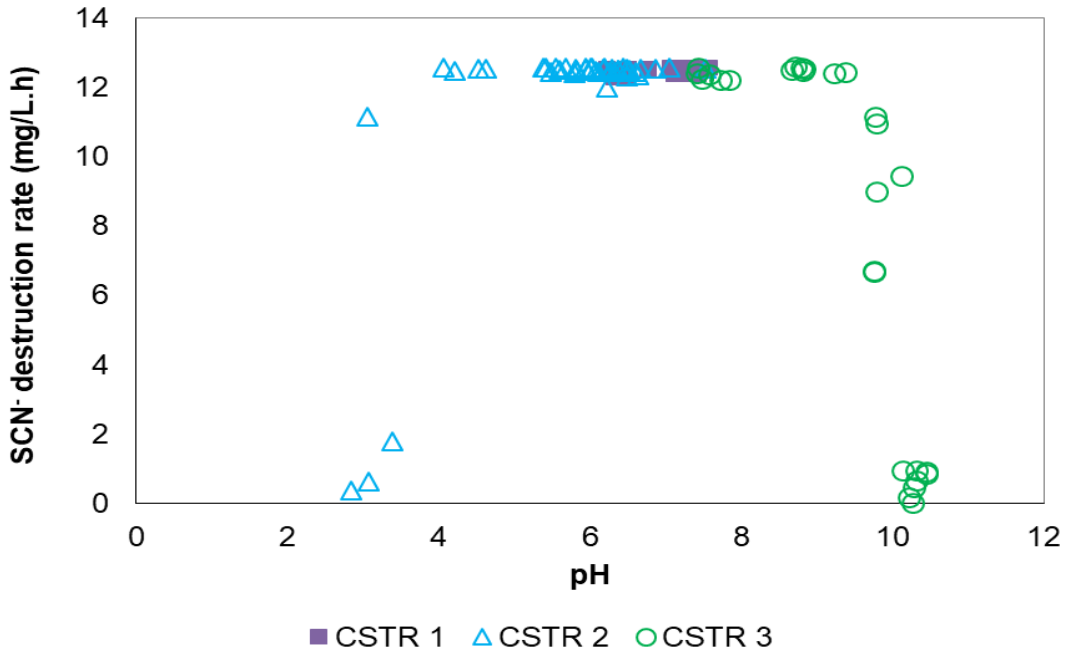

Figure 5.12: Effect of reactor pH on thiocyanate destruction at a loading rate of 12 mg/L.h. Three continuous stirred tank reactors received pH adjusted feed to control the pH of the reactor media. All CSTR's received 100 mg/L thiocyanate in the feed over the experimental run time.

CSTR 2 was operated in parallel while the feed pH was decreased to a measured reactor pH from 7.05 to 2.85 over 36 days. The SCN destruction rate decreased rapidly at a reactor pH below 4.21 while insignificant SCN destruction was measured at a reactor pH <3.38. CSTR 1 was operated in a narrow pH band (pH 6.22-7.57) compared to CSTR 2 (pH 2.85-7.53) CSTR 3 (pH 7.41-10.45). The maximum SCN destruction rate was obtained in CSTR 1 following 25 days post inoculation and maintained while the pH was consistent over the experimental run time. Although the pH range for SCN destruction is wide following acclimation, intermittent pH fluctuations result in inconsistent SCN destruction and a desire to achieve predictable SCN destruction performance would require pH control.

5.4 Conclusions

The maximum SCN destruction rate of 87.44 mg/L.h (2 099 mg/L.d) was achieved at a feed SCN concentration of 1 000 mg/L and an eight hour hydraulic retention time. Significant accumulated sludge was noticed primarily as attached biomass which

contributed to SCN conversion. This is the highest reported volumetric SCN destruction rate to date in the literature under these conditions.

The highest feed SCN concentration at which SCN destruction was still active was 2 500 mg/L, corresponding to a volumetric SCN loading rate of 125 mg/L.h. This was the highest reported feed concentration and loading rate achieving a practical SCN destruction rate of 972.2 mg/L.d. Rapid inactivity was found at a feed SCN concentration of 3 500 mg/L and subsequently the residual concentration which remained unchanged over 53.8 days. Recovery of SCN destruction was remarkable with a feed SCN concentration change to 1 000 mg/L reaching a SCN destruction rate of 55.46 mg/L.h within 6.2 days. The sludge offered robustness to the system during unfavourable conditions for SCN destruction which allowed continued operation when conditions returned to a favourable state.

This was also shown during extreme pH changes and a wide operating window was identified which included a pH range of pH 3.5-9.5. The importance of acclimation was shown and was in agreement with the batch experimental data. Moreover, fluctuations in solution pH resulted in unstable SCN destruction.

Sludge harvested from continuous reactors showed an increased volumetric SCN destruction rate as sludge loading increased. However the increase in biomass was not directly proportional to the SCN loading rate. Further the increase in volumetric SCN destruction rate was not directly proportional to the increase in biomass, suggesting a lower specific SCN destruction rate at higher biomass concentration. Culture adaption was shown to have a high potential offering robustness of the culture to be used under different environmental and process conditions.

The sludge was likely composed of a disproportionate amount of EPS compared to the microbial cells and therefore did not translate into increased SCN destruction rates to the expected extent. Differences in performance of the 1.0 and 0.3 L reactors were likely due to the nature of the sludge since a purely planktonic population would offer similar SCN destruction rates. Dissolved oxygen measured in the sludge showed a steep gradient of rapidly decreasing oxygen with sludge depth over 0 to 40 µm. The OTRs calculated in the planktonic region showed significantly higher supply compared to the consumption rates and coupled with the sludge loading data, it is postulated that the sludge acted a mass transfer barrier to SCN access. The reactor performance with respect to SCN destruction was dictated by exchange of nutrients and gasses between the attached biofilm and bulk liquid.

Chapter 6: Thiocyanate destruction in the presence of solids

6.1 Introduction

The work described in this Chapter investigated the potential to operate continuous stirred tank reactors in the presence of suspended solids. To date, complete removal of the tailings from the liquid effluent stream has been achieved prior to application of the ASTER™ process; however, a number of advantages result from processing in the presence of tailings, including the remediation of the tailings stream. This study was motivated by the proposed exploitation of a refractory gold deposit in the Philippines, using the BIOX® technology. The topography of the proposed site constrained the overall footprint of the plant, such that complete removal of the tailings from the cyanidation effluent is not possible. It is estimated that the feed to the ASTER™ plant contains between 4 and 5.5% (m/v) suspended solids. The aim of the research was to determine the impact of these residual solids on the ASTER™ community and its associated performance in terms of SCN degradation.

The following key questions are discussed in this Chapter:

i) Can the mixed microbial culture adapt to and survive in the presence of solids?

ii) Does the presence of solids in the range of 1.0-5.5% (m/v) affect the SCN destruction ability of the microbial population?

iii) What is the effect of solids on the microbial population structure and, in turn, on the system integrity?

iv) Does the SCN destruction rate recover following operating conditions during negligible SCN destruction?

6.2 Experimental programme

The reactor system setup included three reactors receiving individual continuous feed solution with a combined overflow into a single secondary reactor. Therefore, the HRT of the secondary reactor was one third of that of any one of the primary reactors. The reactor feed contained the desired solids load achieving solids suspension by continuous stirring (270 rpm; 45° pitched four bladed turbine impeller). Each of the primary reactors was inoculated with 200 ml of the adapted culture and 800 ml of basal medium. The initial SCN concentration was controlled at 100 mg/L. The reactors were initially operated in the presence of 5.5% solids, with a residence time in the primary reactors of eight hours. The impeller speed in all reactors was set to 270 rpm. Temperature was not specifically controlled, but the reactor system resided in an air-conditioned laboratory (22 ± 2°C). However, performance under these conditions was poor, with only limited SCN degradation. From day 7, the solids were removed from the feed. Once complete degradation of the SCN was achieved in the primary reactors (day 26), solids were gradually re-introduced over a 23 day period, at increments equivalent to 1-1.5% total loading, until the desired loading of 5.5% was reached (day 49).

The system was operated under the desired specifications (5.5% solids, 8 h residence time in primary reactors, residual SCN below 1 mg/L in effluent from the secondary reactor) between day 49 and day 77 (84 residence times). Some accumulation of solids at the bottom of the reactors was observed. This was confirmed experimentally by increasing the stirrer speed (to 500 and 700 rpm) for short periods and measuring solids suspension. The impeller speed was increased to 400 rpm on day 75 and further to 500 rpm on day 77. The latter coincided with an increase in feed SCN concentration to 125 mg/L. On day 81, following a period of poor performance, the operating conditions were restored to previous levels (100 mg/L, 270 rpm), but performance remained erratic. From day 102, the pH of the feed was increased from pH 7 to pH 9 and the residence time in the primary reactors increased from 8 to 12 hours on day 105. The feed SCN concentration was incrementally increased from 100 to 300 mg/L (increments of 50 mg/L) between day 107 and 157. On day 170 the residence time in the primary reactors was decreased to 10 hours and further to 8 hours on day 177. Finally, on day 180, the feed SCN

concentration was increased to 450 mg/L and the reactors were operated under these conditions until the end of the experiment (day 198).

6.3 Results and Discussion

The effect of solids on the destruction ability of a mixed microbial consortium was explored in shake flasks, and further investigated using continuous stirred tank reactors. The effect of SCN concentration as well as solution pH was investigated as was the subsequent influence on microbial community structure.

6.3.1 System Performance

The initial attempt to operate the system under conditions similar to those anticipated for plant operation at 5.5% solids was unsuccessful, despite prior adaptation of the culture to the presence of 5.5% solids in shake flasks (data not shown). The residual SCN concentrations in all reactors, including the secondary reactor, increased rapidly following the onset of the 100 mg/L SCN feed (Figure 6.1) with SCN degradation efficiency remaining below 20%. It is well recognised that the solids suspension achieved in shake flask and well-mixed stirred tank reactor is not the same. In the shake flask, the expanded solids bed provides substantial attrition between particles, whereas in a well-mixed stirred tank, particulates are fully suspended from the floor of the vessel, carry higher momentum impacting particle-particle collision events and may result in increased shear stress associated with the impeller (Scholtz *et al.*, 1997). The removal of solids from the feed resulted in a rapid improvement in performance, with the residual SCN concentration in the secondary reactor falling below the desired threshold (1 mg/L) by day 16. This confirmed the negative impact of suspended solids on process performance in the reactor system in which adaptation has not been achieved.

The re-introduction of solids, from day 24, was performed gradually. Effective SCN degradation, to less than 1 mg/L, was observed in the primary reactors at 2% (day 28) and 3% (day 30) solids loading. A further increase to 4% (day 38) solids resulted in some inconsistency in primary reactor performance, particularly in primary reactor 1, where SCN concentrations of up to 20 mg/L were observed. During this period the SCN concentration in the effluent from the secondary reactor was also above 1 mg/L (Figure 6.1), indicating that very little SCN degradation had occurred in the secondary reactor. However, by day 46 the system had stabilised, with residual

SCN concentrations across all three primary reactors at below 1 mg/L, so the solids loading in the feed vessel was increased to 5.5% (day 48). This represented the anticipated operating conditions at the Metals Exploration PLC Runruno plant in the Philippines. The laboratory scale system performed well under these conditions, with almost complete SCN degradation observed across the primary reactors and on the occasions when some residual SCN was detected in the primary reactors, the SCN was completely degraded in the secondary reactor.

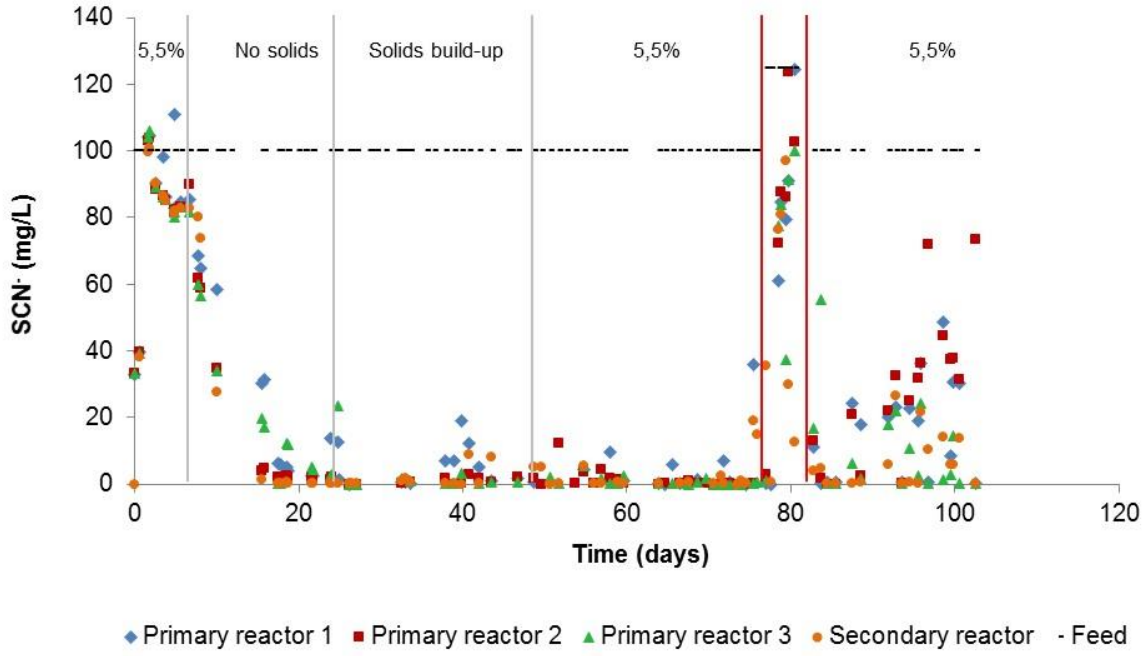

Figure 6.1: Summary of performance data across the three primary and one secondary reactor. Data represent residual thiocyanate concentrations. Solids build-up began on day 24 at 1% loading followed by 2, 3, 4 and 5.5% at days 28, 30, 38 and 48 respectively. Impeller speed was increased from 270 to 500 rpm between day 77 and 81. The pH of the feed was adjusted to pH 7 across the time span 0 to 102 days. The dotted line indicates the feed SCN concentration.

Visual observation of the primary reactors indicated some accumulation of solids at the bottom of the reactors. Prior to setting up the reactors, a mixing study was conducted to empirically determine the critical impeller speed (N_{js}) required to ensure just off-bottom suspension of all particles. Triplicate samples (2 ml) were taken from three different levels (top, middle and just off bottom) and suspended solids mass calculated. This method validated off-bottom suspension and samples were stored for potential analyses of particle size distribution. The preliminary study indicated that 270 rpm was sufficient to achieve complete suspension, within the error

associated with the gravimetric assay. However, during extended operation (84 residence times at 5.5% solids loading), there was some accumulation of the coarser material. The volume in the reactor was maintained by a level control overflow port near the top of the reactor, so only particles that were suspended to that level would exit the reactor. The increase in impeller speed to 500 rpm (between day 77 and 81) resulted in a measured solids concentration of 7.45 ± 0.25% across the three primary reactors within 15 minutes of the change. The increased solids suspension was expected and clearly showed a reduced SCN destruction in all four reactors (Harrison *et al.*, 2012).

The solids used in this study were generated during small scale metallurgical testing to assess gold recovery so a limited mass was provided at the start. As a consequence, the solids had to be recycled by centrifuging the accumulated effluent from the secondary reactor and drying the recovered material (70°C for 48 hours). This was a time consuming and labour intensive process. Midway through the experiment a second batch of tailings (5 kg) was provided, following further metallurgical testing. The particle size distribution and density were similar to the first batch and these solids were introduced into the reactor system from day 77. As a result, no solids recycling was required for approximately 20 days.

The combined effect of the increased agitation rate, increased feed SCN concentration and use of fresh solids was a rapid and substantial decrease in performance across the system (Figure 6.2), with residual SCN concentrations increasing to 100 mg/L. Reducing the feed SCN concentration back to 100 mg/L and the impeller speed to 270 rpm resulted in some improvement, but overall performance remained inconsistent, with the SCN concentration in the effluent from the secondary reactor remaining between 10 and 20 mg/L. This period coincided with a decrease in the measured pH in the reactors, which will be discussed in greater detail later (Section 6.4.2).

The pH of the feed suspension was increased from pH 7 to pH 9 on day 102 and the feed rate was reduced on day 105, resulting in an increase in residence time from 8 to 12 hours in the primary reactors. These interventions resulted in a rapid improvement in performance, with SCN concentrations falling below 1 mg/L in all reactors (Figure 6.2). With stable performance achieved, the system was challenged with increasing SCN concentrations. While each incremental increase resulted in a short term increase in residual SCN in the primary reactors, the residual SCN passing into the secondary reactor was efficiently degraded resulting in an effluent SCN concentration below 1 mg/L for the duration of the experimental run.

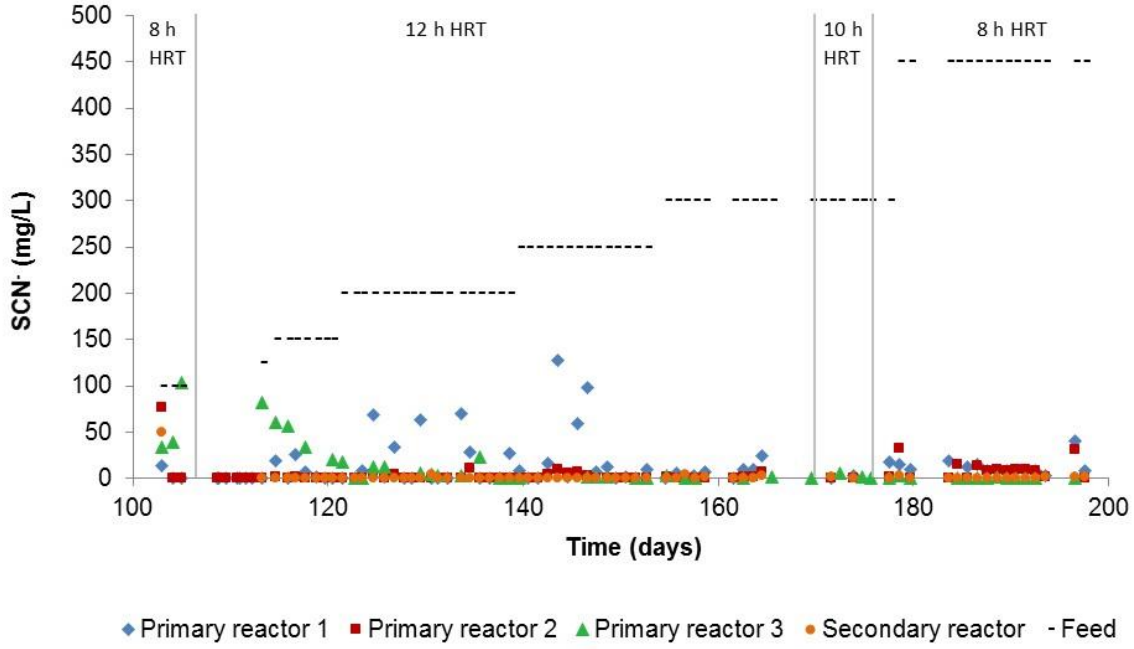

Figure 6.2: Summary of performance data across the three primary and one secondary reactor from day 102. Data represents residual thiocyanate concentrations. Increases in feed concentration and changes in residence time (HRT) of the primary reactors are indicated. The feed pH was increased to pH 9 for the period of day 102 to 198.

Following stable performance (20 residence times) at a feed SCN concentration of 300 mg/L, the residence time in the primary reactors was reduced to 10 hours (day 170). This had no impact on performance, so the residence time was further reduced, back to the original design specification of 8 hours. This resulted in a transient increase in the SCN concentration in the primary reactors, but again complete degradation was achieved in the secondary reactor. Finally, on day 180 the feed SCN concentration was increased from 300 to 450 mg/L, again with no effect on the overall performance of the system.

The SCN degradation rate data is represented in Figure 6.3. The periods of unstable performance are clearly visible, particularly over the first ten days and between day 77 and 102. During periods of efficient performance, the SCN degradation rate in the secondary reactor is low, due to the low residual SCN concentrations in the primary reactors. The two points around day 80 where the volumetric degradation rate in the secondary reactor were high were due to the failure of the primary reactors, resulting in a very high loading to the secondary

reactor. During the period between day 81 and 102, the degradation rate in the secondary reactor was consistently lower than that of the primary reactors. This was not a consequence of limited loading, as SCN was detected in the effluent from the secondary reactor, which suggests inhibition of the microbial culture. This was most likely related to fluctuating pH condition in the range pH 4 to 8.

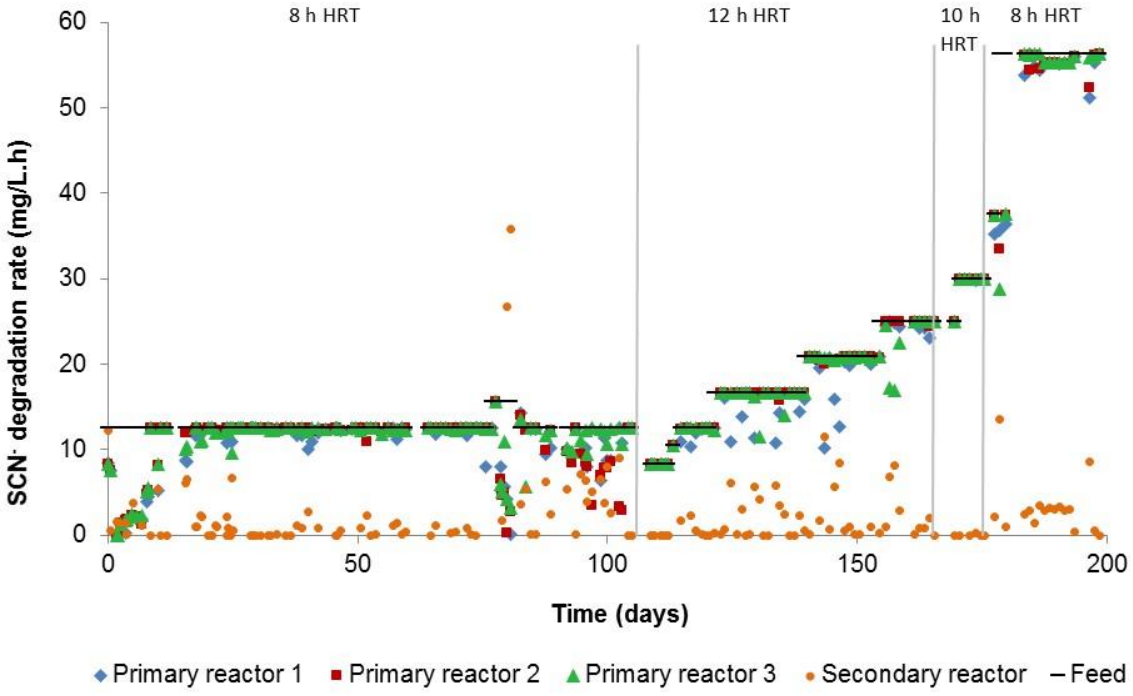

Figure 6.3: Calculated thiocyanate degradation rates for each of the reactors. The loading rate to the primary reactors is represented by the feed (-), while the loading to the secondary was calculated based on thiocyanate concentrations in the primary reactors.

6.3.2 Effect of pH on system performance

The pH during the first days of the study was between pH 5.3 and pH 6.1 (Figure 6.4), despite the feed having been adjusted to pH 7. On operating the system without solids, the pH in the reactors was stable between pH 6.5 and 7. This continued during the solids build-up phase, with the occasional exception. The decreased pH around day 40 was associated with the increase in solids loading from 3 to 4%, while the decrease around day 55 coincided with the increase from 4 to 5.5%. The most substantial decrease in pH occurred after day 75, when the new batch of solids was introduced to the reactor, with the pH dropping below pH 5 in many cases. This suggested that the solids released acidity or consumed alkalinity,

resulting in a decrease in the measured pH. This phenomenon was confirmed in offline tests. In addition to the pH change, agitation of the solids resulted in the leaching of both calcium and sulphate from the solids. The effect became progressively less significant when recycled solids were used, explaining relatively stable pH up to day 77 and the significant decrease thereafter. This highlights the need to establish the physicochemical impact of the fresh solids prior to their use in the operating plant.

The apparent relationship between pH and performance of the system prompted a parallel investigation to determine the effective operating window, with respect to pH. The study identified an optimum between pH 7 and pH 7.5, with a decrease in degradation rate of over 50% below pH 6.5 and above pH 8.5 (van Zyl *et al*., 2017). This is consistent with the performance data discussed before (Section 4.5 & Section 5.3.6).

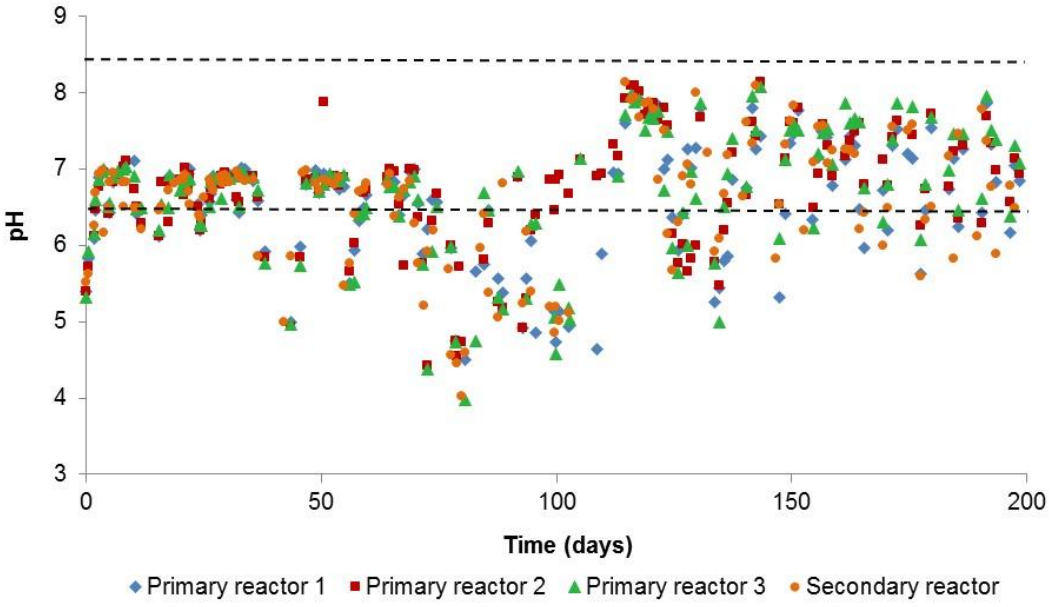

Figure 6.4: Summary of pH data for the duration of the experiment. From day 0 to day 102 the pH of the feed solution was initially adjusted to pH 7 after which it was adjusted to pH 9. The dashed lines represent the optimal pH window, previously determined.

6.4 Microbial community structure

The stock reactor, in the absence of solids, became colonised with a thick, gelatinous biofilm. The biofilm was densely packed with microbial cells, with several distinct morphologies visible (Huddy *et al.*, 2015). As the biofilm developed, the planktonic cell concentration decreased to around 2 x 10^6 cells/ml, suggesting the majority of the biomass was confined to the biofilm. The absence of attached biofilm and the relatively higher planktonic cell concentration (1-3 x 10^7 cells/ml) in the solids-containing reactor prompted a more detailed investigation of the microbial community in the reactors with solids.

The microbial community was characterised by a combination of culture-dependent and –independent methods. Single PCR amplicons were observed for both 16S rRNA and 18S rRNA genes (data not shown), from total DNA extracted from the reactor, indicating the presence of bacteria and eukaryotes, respectively. A total of 16 bacterial and three eukaryotic isolates were cultured. In addition, 48 clones of the bacterial 16S rRNA gene clone library were analysed by ARDRA and 30 patterns were selected for sequencing. A total of 24 18S rRNA gene library clones were analysed by ARDRA and four were sequenced. The sequenced operational taxonomic units (OTUs) formed the basis for the 16S rRNA and 18S rRNA phylogenetic analyses of the bacterial and eukaryotic populations within the reactor system.

The analyses indicated approximately 21 different bacterial genera within the 16S rRNA clone library (Figure 6.5). Of particular interest are the 16S rRNA phylotypes found to be closely related to *Bosea, Microbacterium* and *Thiobacillus* species. van Buuren and co-workers (2011) implicated *Bosea thiooxidans* and *Microbacterium schleiferi* as dominant ASTER^{TM} consortium members involved in the destruction of SCN.

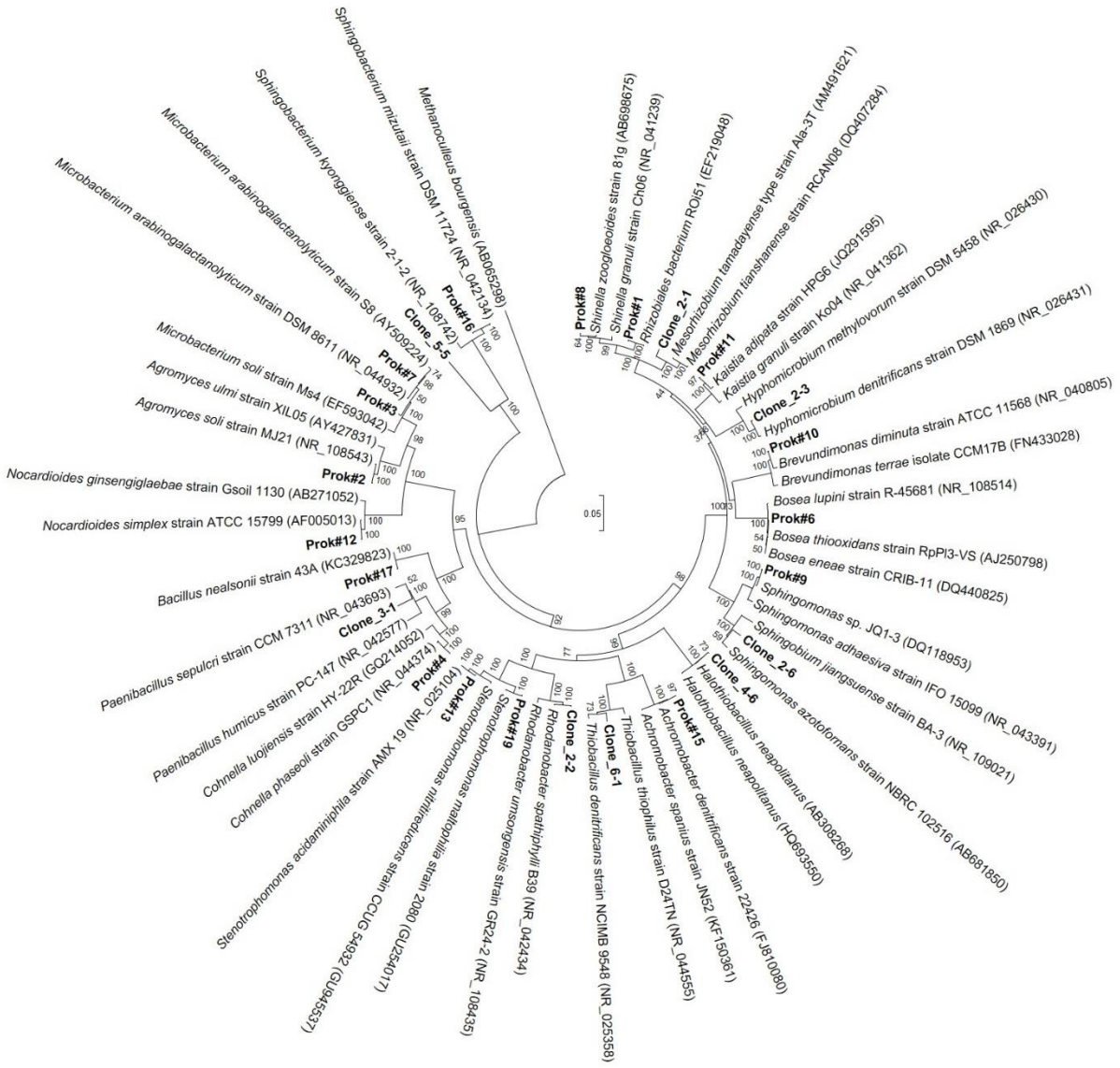

Figure 6.5: Unrooted 16S rRNA gene phylogenetic tree of 16S rRNA library clones, generated with universal bacterial primers, and prokaryotic isolates from the ASTER™ stock reactor and related sequences. The tree was based on the sequence alignment of a common length portion (1,420 nucleotides) and was obtained using the neighbor-joining method. Bootstrap values are based upon 1,000 resampled data sets and only values of greater than 40% are indicated. Accession numbers (where available) are shown in brackets. The bar represents 0.05 nucleotide substitutions per nucleotide position. *Methanoculleus bourgensis* was included as an outlier.

The 18S rRNA gene clone library revealed the presence of four eukaryotes within the solids reactor system (Figure 6.6). All four are fungi, with two identified as filamentous fungi, namely Euk#2 and Euk#3, and two yeasts, namely Euk#1 and 18S_1-4. The cultivated yeast isolate, Euk#1, is related to a *Candida* species. *Candida humulis* has previously been shown to be present in the ASTER™ microbial

consortium (du Plessis *et al.,* 2001). To date we have not identified a fungal species closely related to *Fusarium oxysporium*, within the solids reactor system. *F. oxysporium* has been previously shown to be capable of CN degradation as well as being present in the ASTER™ microbial consortium (du Plessis *et al.,* 2001).

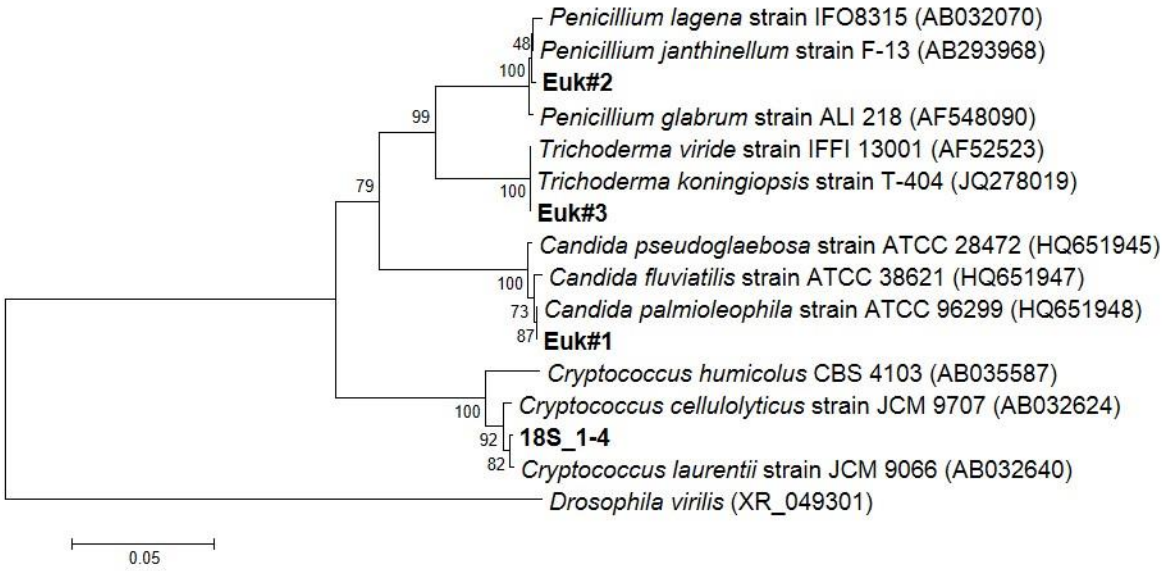

Figure 6.6: Unrooted 18S rRNA gene phylogenetic tree of 4 clones, generated with universal 18S rRNA primers from the ASTER™ stock reactor and related sequences. The tree was based on the sequence alignment of a common length portion (1,140 nucleotides) and was obtained using the neighbor-joining method. Bootstrap values are based upon 1,000 resampled data sets. Accession numbers (where available) are shown in brackets. The bar represents 0.05 nucleotide substitutions per nucleotide position. *Drosphila virilis* was included as an outlier.

Genome prediction done by Rahman and co-workers, showed that *Sphingobacteriales* was the dominant taxon in the reactor containing solids while *Thiobacillus* spp. was identified as the dominant genus in the solids-free reactor *(*Kantor *et al.*, 2015; Rahman *et al.*, 2017). The difference in diversity between the solids containing and solids-free reactor was further shown in that heterotrophs dominated the solids containing reactor while the majority of the abundant organisms in the solids-free reactor was composed of autotrophs. This has implication for nutrient supply since reactors containing solids likely need a supply of additional organic carbon for example molasses. Microorganisms able to degrade SCN was in lower abundance in the solids reactor compared to the reactor with an absence of solids. This likely contributed to the increased sensitivity to process changes compared to the solids-free reactor.

6.5 Conclusions

The data presented in this chapter show that efficient SCN degradation is possible in the presence of suspended solids, at solids concentrations of up to 5.5%. Adaption was required during several steps of increasing the solids loading. The presence of suspended solids had a significant impact on the habitat of the microbial community but did not prevent microbial proliferation or successful SCN destruction. A period of adaptation was required prior to stable performance being acquired. Thiocyanate degradation rates of up to 57 mg/L.h were achieved in the primary reactors during the current study. These correlated to complete SCN degradation, i.e. they were limited by the SCN loading rate, so are not necessarily the highest rates attainable.

The primary constraint on performance of the system was found to be pH, with the efficiency of SCN degradation falling sharply when the pH in the reactors fell below pH 6. The optimal pH window for the community was determined to be between pH 6.5 and pH 8.5 in a parallel study. The tailings provided for this study resulted in the acidification of the medium when well-agitated, coupled with the release of calcium and sulphate. The reaction chemistry involved is still being determined. This may be an artefact of the conditions used during the metallurgical testing. If not, pH control will be a critical element of the process operation at Runruno.

The presence of suspended solids had a profound effect on the composition of the microbial community as shown by the clone library work done, with a significant reduction in diversity relative to reactors operated in the absence of solids. This appears to be related to the absence of biofilm and the anaerobic and microaerobic microenvironments associated with the biofilm. Despite the lower diversity and the lack of biomass retention through formation of biofilm, high rates of SCN degradation were achieved and recovery following detrimental conditions described by the temporary absence of SCN destruction was shown. The research results showed that the ASTER^{TM} process is viable in the presence of suspended solids and that the SCN degradation rates required to treat the anticipated effluent from the Runruno operation should be comfortably achieved.

6.6 Contribution to and commercial application of findings

Commercialisation of the ASTER^{TM} technology with solids present was initiated by an inoculum build up over two weeks using two 98 L pilot plant primary reactors. The pilot plant primary reactors were inoculated using 40 L inoculum from the UCT lab scale reactors under fed-batch mode. The pilot plant reactors were operated under continuous mode with a feed SCN concentration of 50 mg/L only, due to raw material constraints and a HRT of 10.7 h. Only one primary reactor was operated with a solid loading of 5.0% while the second reactor received no solids and both degraded SCN successfully to below 1 mg/L continuously. Overflow from the two 98 L pilot reactors were used to inoculate a 14 m^3 stock tank. Fed-batch operation of the stock tank was followed by solution withdrawals of 2 m^3 and replacement of an equal volume substrate upon successful SCN degradation. A total volume of 25 m^3 reactor solution was collected from the fed-batch tank and inoculated with 90 m^3 fresh feed in a 600 m^3 primary reactor. In addition, 2 m^3 of reactor volume from the stock reactor was added to the 600 m^3 primary reactor every 3rd day and monitored for SCN degradation activity.

Chapter 7: Simultaneous thiocyanate and cyanide destruction under different operating conditions and system configurations

7.1 Introduction

The reaction between CN and reduced sulphur species results in formation of high concentrations of SCN, while the presence of residual, unreacted CN adds complexity to the solution. Chemical or physical treatment of CN is possible, but typically results in a limited reduction in SCN concentration and by-product formation. Additional treatment may be required to manage the by-products, reducing the economic viability of the technology. Simultaneous degradation of both SCN and CN was shown for the Homestake plant in the USA, employing microorganisms to degrade SCN and CN at concentrations of up to 100 and 12 mg/L, respectively (Akcil and Mudder, 2003; Grigoreva *et al.*, 2006). Literature describing the simultaneous destruction of both SCN and CN in a biological system is relatively limited. Work done by the group of Grigoreva (2006) showed preferential CN degradation in the presence of SCN and was attributed to either the higher availability of CN as the nitrogen source, or the inhibition of SCN degradation. Furthermore, Lay-son and Drakides (2008) observed partial inhibition of SCN destruction under conditions where residual NH_4 concentrations reached 2 mg/L and higher.

The ASTER^{TM} process had proven successful at demonstration scale at the Consort site, removing up to 120 mg/L SCN and 30 mg/L CN. This, coupled with the encouraging data generated during the early stages of this research suggested that the technology could be more widely applied at operations using the BIOX® technology. A survey of potential operations highlighted the requirement for simultaneous treatment of SCN and CN at concentrations up to 800 and 50 mg/L, respectively (van Buuren, pers. comm.). These included operations in locations where prevailing temperatures were as low as 15˚C and where traditional CN destruction technologies (eg the INCO process) were being used.

The work describes in the previous chapters indicated that the colonisation of the reactor with attached biofilm could enhance process performance. This represents a departure from the traditional ASTER^{TM} configuration, with the settling and recycle of

suspended flocs. A series of experiments were performed to assess the ability of the microbial consortium to simultaneously remove CN and SCN and evaluate the effect of reduced temperature and changes in reactor configuration and operating parameters.

The following key questions are discussed in this chapter:

i. Was simultaneous degradation of SCN and CN, at concentrations up to 800 mg/L and 50 mg/L respectively, possible at a hydraulic retention time of eight hours?

ii. What was the effect of reducing operating temperature from 25°C to 15˚C on the SCN and CN degradation ability of the microbial consortium?

iii. Do pseudo steady state conditions change following removal of a recycle loop?

iv. Which key factors influence the destruction of simultaneous SCN and CN?

v. Will system performance and stability be affected if simulated INCO-treated process water is used as the feed?

7.2 Experimental programme

This study consisted of three experimental phases consisting of experimental setups summarised in Table 7.1. The reactor configuration selected for each Phase of the experimental setup was to investigate specific commercial applications. The system configuration used during Phase one (day 1-160) of this study was set up to investigate the pseudo steady state conditions for simultaneous destruction of a feed containing SCN and CN up to concentrations of 800 mg/L and 50 mg/L, respectively (Figure 7.1). Thiocyanate was supplied during start-up at 100 mg/L while CN was supplied at a starting concentration of 18.62 mg/L. The feed CN concentration was increased incrementally to 50 mg/L over an 88 day period, followed by an incremental increase in feed SCN concentration over 62 days to reach 800 mg/L. The specific reactor and clarifier retention times for Phase One was 2.42 and 5.84 hours, respectively. Steady state conditions were maintained for 6.90 HRTs.

Table 7.1: Summary of the reactor configuration and conditions discussed in this study.

Experimental Setup:	HRT (h):	Feed rate (mL/h):				HRT (h):			
		Primary CSTR:	Secondary CSTR:	Clarifier overflow:	Clarifier underflow:	Primary CSTR:	Secondary CSTR:	Clarifier overflow:	Clarifier underflow:
Phase 1	42.00	413.0		71.43	342.0	2.42		28.00	5.85
Phase 2	14.00	71.43				14.00			
Phase 3									
Configuration A	35.93	55.67	55.67			17.96	17.96		
Configuration B	34.88	446.7	71.67	71.67	375	2.24	13.95	6.98	1.33
Configuration C	34.88	446.7	446.7	71.67	375	2.24	2.24	6.98	1.33
Configuration D	34.88	125.7	125.7	71.67	54	7.96	7.96	6.98	9.26

- The HRT indicated is the overall hydraulic retention time.
- The working volume for each CSTR in each experimental Phase was 1.0 L.
- The working volume for the clarifier in Phase 1 was 2.0 L while for Phase 3, the working volume was 0.5 L.
- Phase 1 was started with a fresh inoculation and continued through Phase 2 and Phase 3, Configuration A.
- Phase 3, Configuration B was started with a fresh inoculation and continued to Configurations C and D.

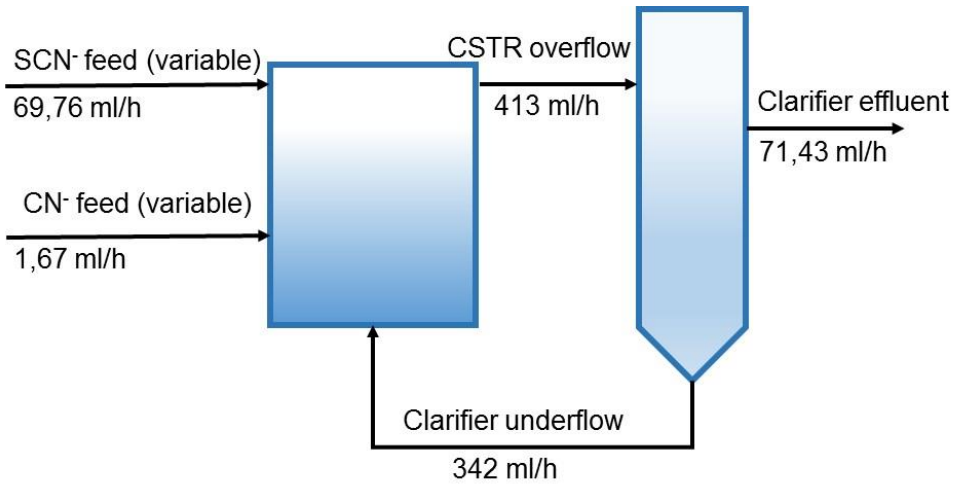

Figure 7.1: Continuous stirred tank reactor setup for Phase 1 with a clarifier coupled in series to activate a recycle loop for biomass. The working volume for the reactor and clarifier used was 1.0 L and 2.0 L respectively showing flow rates over each unit.

Phase two (day 160-290) consisted as a continuation from the Phase one (day 1-160) setup bar the clarifier, receiving SCN and CN in the feed at concentrations of 800 and 50 mg/L, respectively (Figure 7.2). The reactor was operated under steady state conditions for 130 days at a HRT of 14 hours. The reactor temperature was controlled at 25, 20, 18 and 15°C to evaluate steady state residual SCN concentration.

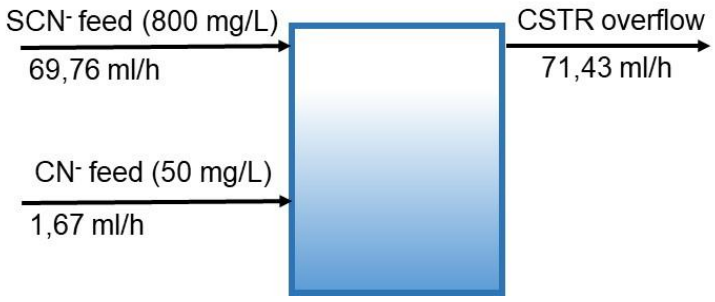

Figure 7.2: Primary reactor operated at a 14 hour hydraulic retention time. Reactor temperature was controlled at 25, 20, 18 and 15°C as discussed. The working volume of the reactor was 1.0 L.

Phase three of the study consisted of four different reactor configurations (A-D) to optimise the system configuration for SCN and CN degradation efficiency specifically under higher SCN loading conditions (Figure 7.3 and Figure 7.4).

Configuration A:

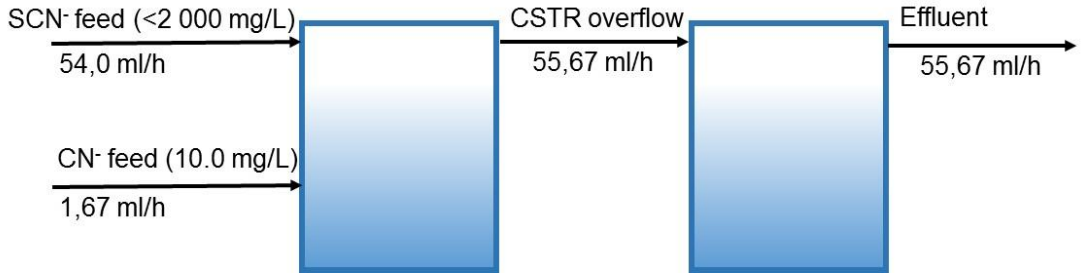

Figure 7.3: Phase three, Configuration A consisting of a primary and secondary reactor in series operated at an HRT of 18h respectively. The final feed thiocyanate concentration was 2 000 mg/L while the CN feed concentration was 20.0 mg/L. The operating temperature was constant at 25°C.

Configuration B of (Figure 7.4; Configuration B) allowed for operation of a primary reactor and a clarifier with a recycle ratio of 5.23 (underflow) followed by a secondary reactor, all in series. The combined HRT for the primary reactor and clarifier was 20.93 hours while the secondary reactor was operated at an HRT of 13.95 hours. Configuration C was operated with the primary and secondary reactors at an HRT of 2.24 hours, respectively and the clarifier at 1.12 hours, all connected in series. The recycle ratio from the clarifier was 5.23 (underflow) to the primary reactor. Configuration D was operated in an identical fashion to Configuration C but the primary and secondary reactors were each operated at an HRT of 7.96 hours with the clarifier at 3.98 hours. The recycle ratio to the primary reactor was 0.75 (underflow).

Configuration B:

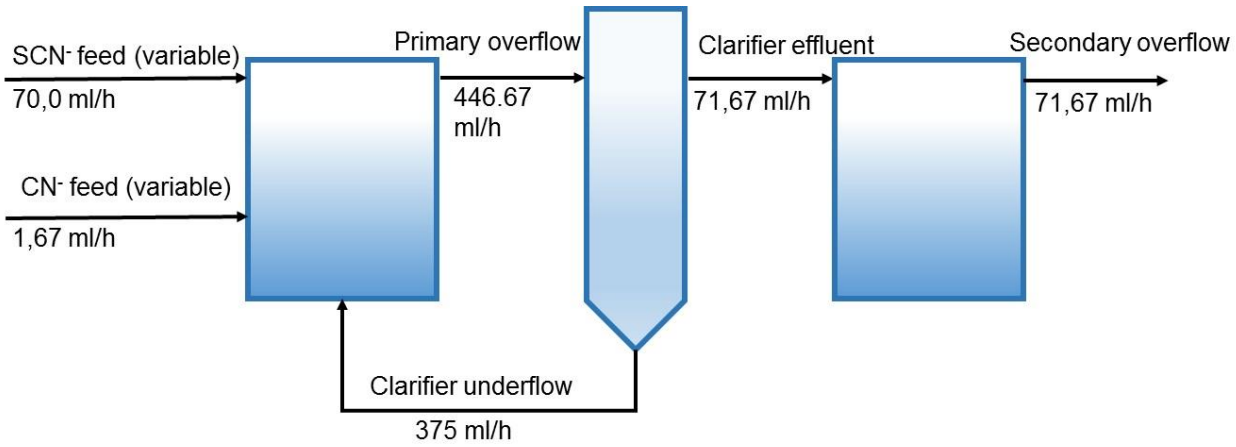

Configuration C:

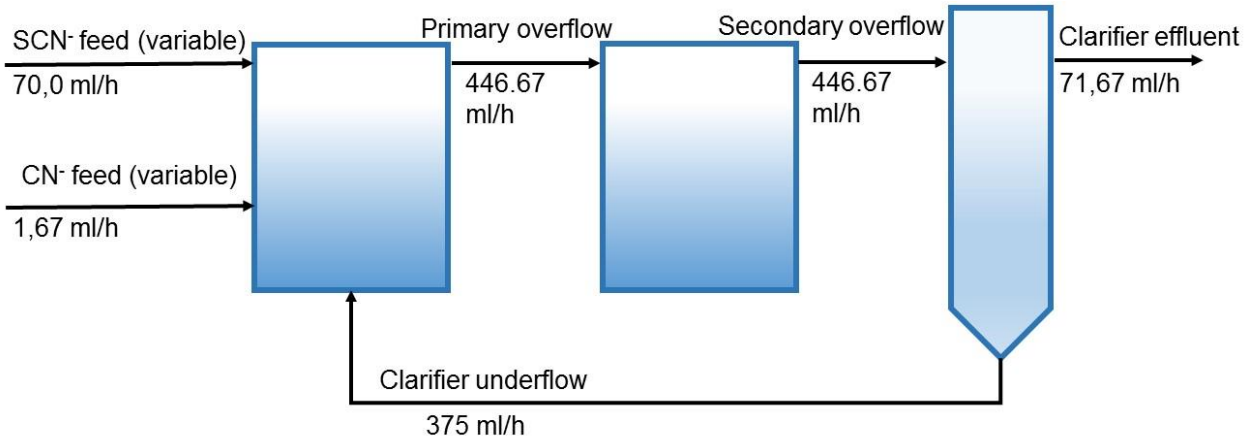

Configuration D:

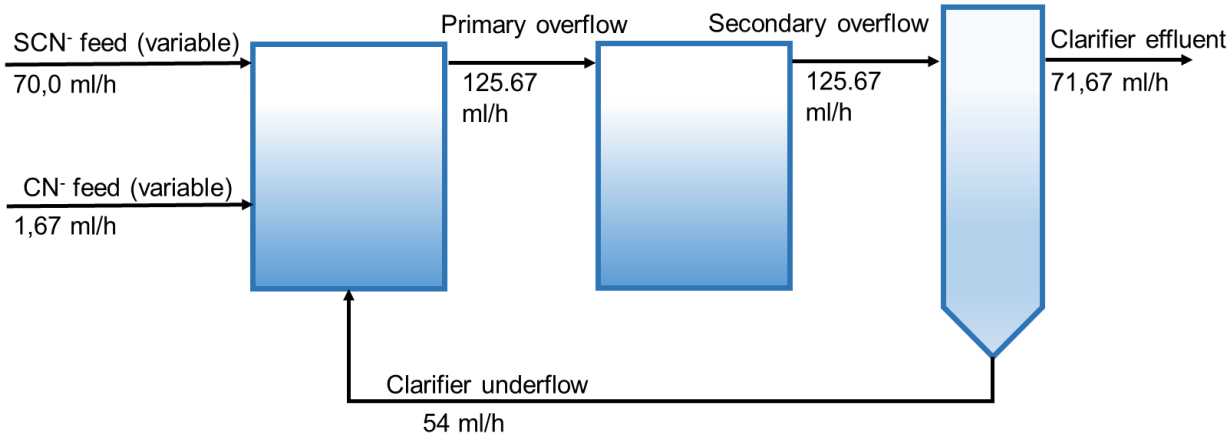

Figure 7.4: Configuration B) Primary-clarifier-secondary in series with the clarifier underflow recycled to the primary. The clarifier overflowed into the secondary; Configuration C) primary-secondary-clarifier in series with the clarifier underflow fed

to the primary and received feed from the secondary; Configuration D) identical setup to configuration B but at a reduced primary overflow (125.7 mL/h) and subsequent reduced recycle flow rate (54 mL/h) while the inlet and outlet flow rates remained unchanged.

7.3 Results and discussion

Continuous reactor systems were employed to investigate SCN destruction in the presence of CN under different loading conditions as well as temperatures. Furthermore, SCN destruction was investigated as a function of process configuration for critical process units and conditions.

7.3.1 Simultaneous destruction of thiocyanate and cyanide (Phase 1)

Phase 1 of the experimental plan started with the reactor feed containing 100 mg/L SCN only. A clarifier was connected in series receiving reactor overflow with a recycle of any settled biomass back to the reactor. Thiocyanate destruction was measured following inoculation (Figure 7.5). Cyanide was introduced into the feed at day six at 18.62 mg/L (Primary CSTR HRT of 2.42h). Almost complete destruction of SCN and CN was observed. An upset of the SCN destruction capacity was measured upon doubling of the CN feed load to 37.2 mg/L, while CN was periodically detected in the reactor at a concentration below 1.68 mg/L. Decrease of the SCN and CN feed concentrations to 50.0 and 26.0 mg/L, respectively resulted in complete destruction of SCN andCN. The feed SCN concentration was increased again to 100 mg/L following complete SCN and CN destruction. Residual SCN was detected initially, followed by complete destruction when steady state was reached. The feed CN concentration was then increased to 40.0 mg/L for 11.38 overall residence times followed by 50 mg/L in a step fashion without any disruption to the residual SCN or CN concentrations. This operational pseudo steady state was maintained for 34.32 HRTs before increasing the SCN feed concentrations incrementally.

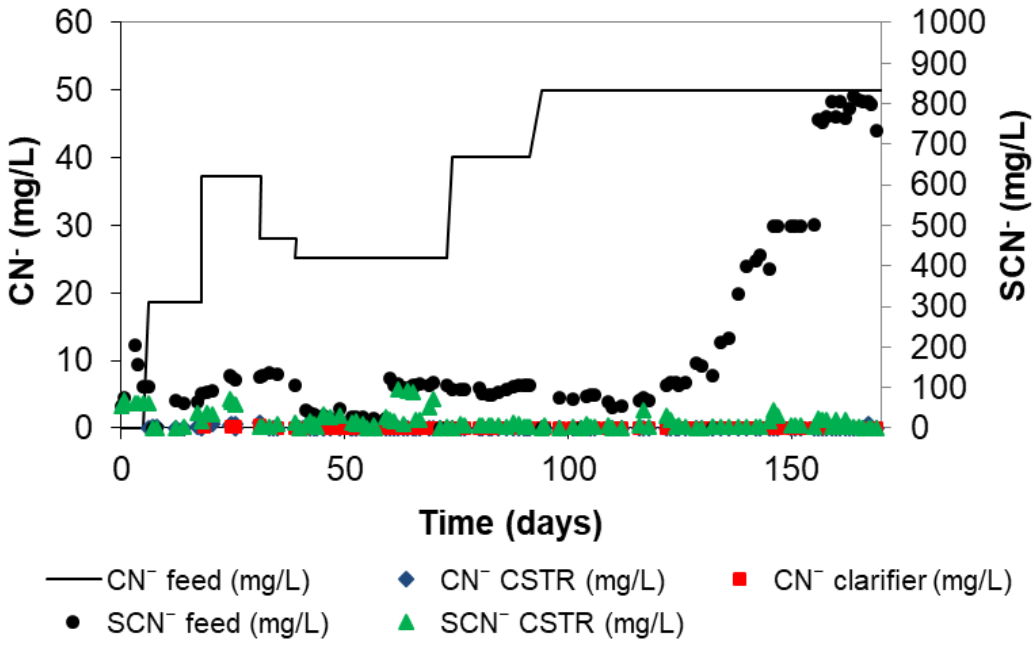

Figure 7.5: Simultaneous destruction of SCN and CN in a single reactor fitted with a clarifier and biomass recycle at a retention time of 5.85 h. The single reactor HRT was operated at 2.42 h with an overall HRT of 42.0 h. Data represent feed and residual thiocyanate and cyanide concentrations.

Residual SCN was measured from samples taken from the primary reactor and clarifier with each step increase of the feed SCN concentration (Phase 1). The highest residual SCN concentration was 45.81 mg/L which was reduced by 30% within 0.5 HRT. Residual SCN concentration in the reactor was consistently measured to lie below 1.68 mg/L at a feed SCN concentration of 800 mg/L for 2.3 HRTs. The relatively short lived residual SCN spikes measured in the reactor was indicative of rapid microbial response to each step increase of the feed SCN. Significant biomass floc formation was noticed with attached biomass also increasing during this period. Metabolic pathways identified for sulphur oxidation and energy generation were identified to exist in the microbial community (Kantor *et al.*, 2015). This further shows sulphur metabolism as a key metabolic driving force.

7.3.2 Effect of reduced operating temperature on simultaneous thiocyanate and cyanide destruction (Phase 2)

Phase 2 of the experimental programme followed on from Phase 1 where complete destruction of the feed SCN and CN was achieved. The CSTR was operated as a single unit with a HRT of 14 hours. This allowed an investigation of the effect of reduced biomass retention as well as the effect of reduced operating temperatures

on the SCN and CN destruction. The single reactor was operated for four HRTs before the operating temperature was reduced from 25 to 15°C (Figure 7.6). The complete destruction of SCN and CN showed that a single populated reactor could be operated to degrade SCN and CN simultaneously at a load of 56.50 and 3.57 mg/L.h, respectively. The planktonic population was initially responsible for SCN and CN destruction since any attached biomass required time to develop and was also noted to develop more rapidly under conditions of high (> 800 mg/L) residual SCN concentration.

Significant residual SCN and CN was not initially measured at 20 or 18°C achieving consistent destruction efficiencies of >96% and >99%, respectively. However, at 15°C CN was measured as high as 3.2 mg/L while the residual SCN concentration increased to 746.48 mg/L. Residual CN was detected prior to residual SCN indicating a higher resilience to temperature decreases by the SCN destruction microorganisms but not to residual CN in solution. The reactor temperature was again increased to 18°C and recovery of the SCN and CN destruction capacity was observed. A second attempt at operating the CSTR at 15°C following 22 days of operation at 18°C was met with significant residual SCN and CN concentrations. Complete SCN and CN destruction was not achieved at this operating temperature even after 53 days. Fluctuations in residual SCN levels were measured and observed to increase dramatically where residual CN levels were detected at 1.0 mg/L or higher. Recovery was again shown with a rapid decreased residual SCN and CN concentration at an operating temperature of 18°C. The effects of lower temperature on SCN and CN destruction were not surprising since cell membrane and metabolic enzymes would need to adapt to thrive (Chattopadhyay, 2006; Kim *et al.*, 2013). Rapid recovery of SCN and CN destruction was observed by a rapid reduction of the residual SCN and CN concentrations during both instances where the operating temperature was increased to 18°C.

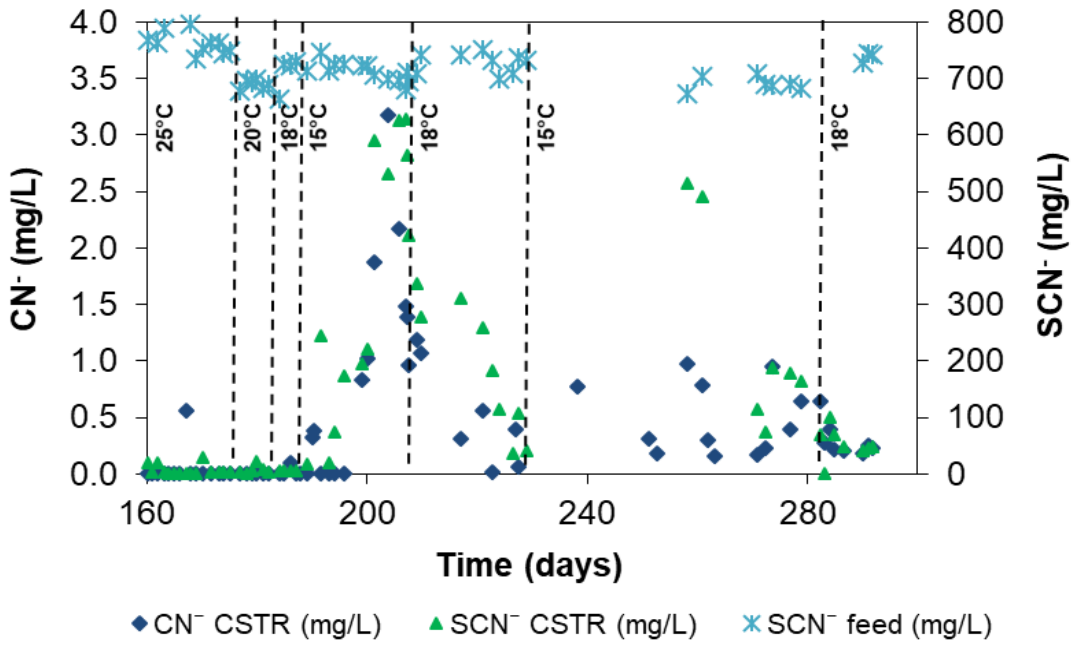

Figure 7.6: Simultaneous destruction of SCN and CN under changing reactor temperatures using a single reactor. The dashed lines indicate the point of temperature change. The single reactor HRT was operated at 2.42 h with an overall HRT of 42.0 h. CN was supplied at 3.57 mg/L.h.

7.3.3 Simultaneous destruction of thiocyanate and cyanide at increased concentrations (Phase three; Configuration A)

Phase three, Configuration A of the experimental programme consisted of a primary reactor connected to a secondary reactor in series. The primary reactor used was a continuation from Phase 2 following a temperature change to 25°C with an identical feed while a secondary reactor in series received overflow from the primary each operated at an HRT of 18 hours.

The feed SCN concentration was increased to 2 000 mg/L in addition to 10 mg/L CN (Figure 7.7). The residual SCN concentration measured was in the range 1140-1495 mg/L with the residual CN measured below 0.51 mg/L. The feed SCN was subsequently reduced to 1 000 mg/L due to the high residual SCN concentration. The feed CN was eliminated to achieve complete SCN destruction whereupon CN was reintroduced at 10 mg/L in the feed, following 11.9 HRT turnovers of near complete (>99.0%) SCN destruction. The feed CN concentration was doubled while the feed SCN was incrementally increased to 800 mg/L over 12.8 HRT turnovers. Residual SCN was detected at a feed SCN concentration of 1460.4 mg/L. The residual SCN concentration increased to a maximum of 1 277.2 mg/L at a feed SCN

of 1 972.0 mg/L. The residual SCN concentration decreased over time and was measured in the range 627.7-952.5 mg/L.

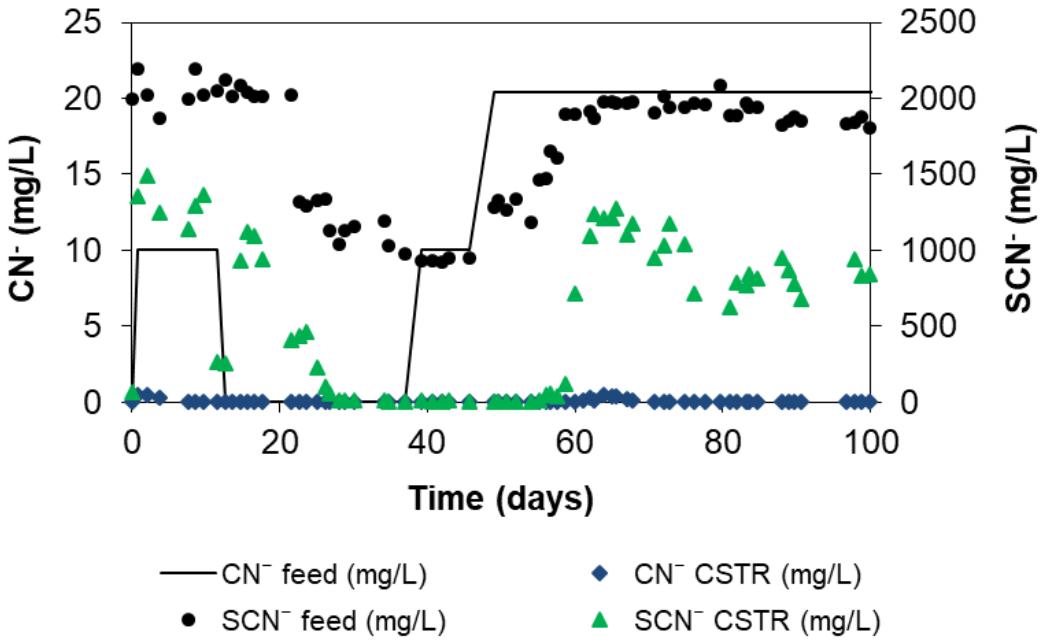

Figure 7.7: Simultaneous destruction of SCN and CN for two reactors operated in series (Phase3, Configuration A). Data shows feed and residual cyanide and thiocyanate concentrations at a constant temperature of 25°C. The solid line shows the feed cyanide concentration.

The residual SCN concentration measured in the secondary reactor fluctuated initially with the feed fluctuations from the primary reactor achieving destruction efficiencies between 14.5-84.0% during the first 23.7 days (Figure 7.8). The feed SCN decreased to insignificant levels as received from the primary reactor during days 25.15-55.10. Increased feed SCN to the secondary reactor was measured up to 1 277 mg/L which coincided with the increased feed SCN concentration of 2 000 mg/L to the primary reactor. The average SCN destruction rate was calculated to be 58.1 mg/L.h while the maximum was 98.7 mg/L.h over 4.8 HRTs. The highest measured residual SCN concentration in the secondary reactor was 452.3 mg/L at day 62. The remainder of the experimental time was described by fluctuating residual SCN levels in the secondary reactor which coincided with similar fluctuations in feed SCN levels with SCN destruction efficiencies above 90%.

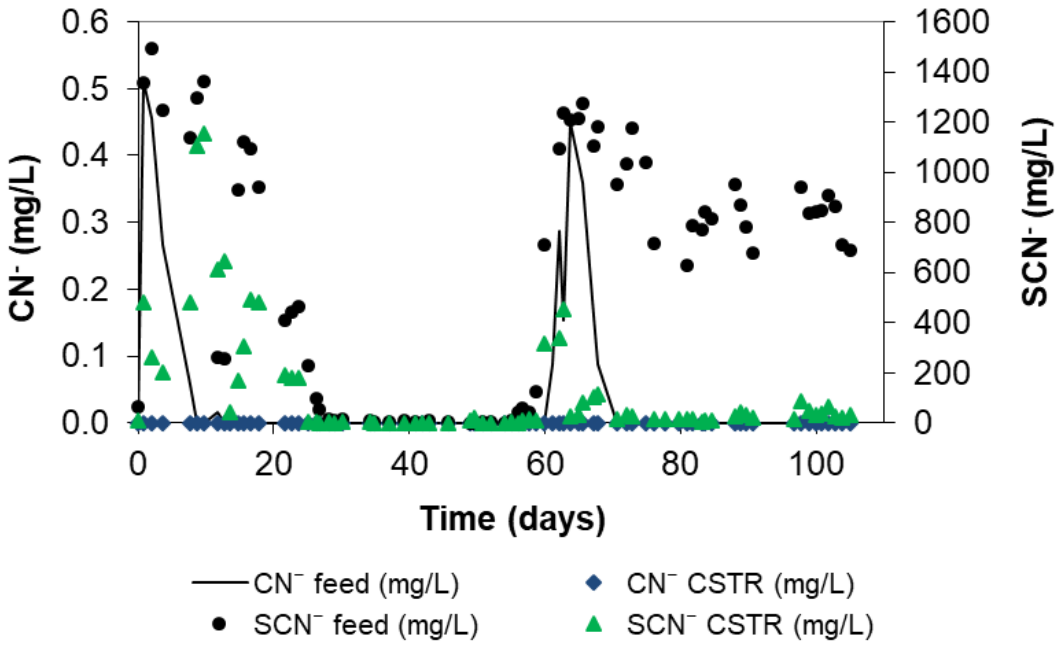

Figure 7.8: Performance data for the secondary CSTR in a configuration consisting of a primary and secondary CSTR in series. Data shows feed and residual CN and thiocyanate concentrations at a constant temperature of 25°C. The solid line shows the feed CN concentration overflowing from the primary CSTR.

Low levels of CN (<0.5 mg/L) were measured in the feed to the secondary reactor during two periods, between days 0-12 and 61-68. Increasing residual SCN concentration coincided with the measured residual CN. It is likely that the fluctuating feed SCN concentration resulted from a reactive microbial population responding to changing conditions since a mature, attached sludge population developed at a notably slower rate compared to the primary reactor population and the effect of CN entering the system resulted in a transient negative impact on SCN destruction. Furthermore, the reduced SCN in solution provided a limited source of sulphur for oxidation as a driving force for microbial growth.

7.3.4 Sulphur and Nitrogen metabolism from thiocyanate and cyanide destruction (Phase 3, Configuration A)

Sulphate was measured as the dominant sulphur metabolite due to conversion of SCN. The theoretical SO_4 values (Figure 7.9) were calculated for 100% sulphur conversion from SCN-S to SO_4-S. The measured residual SO_4 concentration did not deviate notably from the values calculated stoichiometrically. This sulphur balance showed no notable insoluble or precipitated sulphur in the system with limited assimilation into microbial biomass.

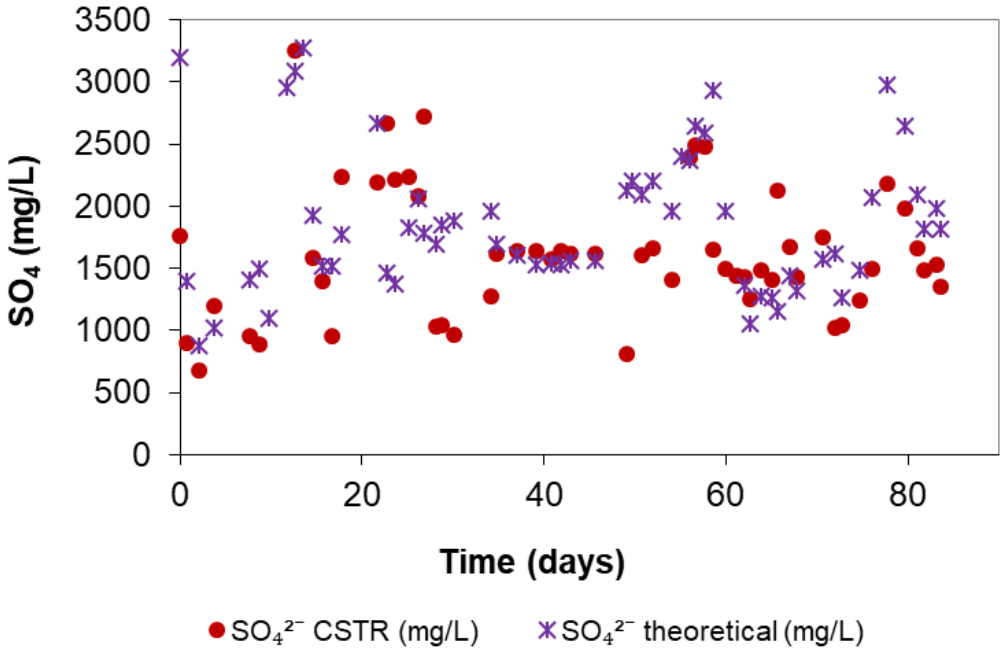

Figure 7.9: Sulphate concentration measured as residual levels in the primary reactor as well as the calculated concentration values from stoichiometric conversion of the SCN-S to SO_4-S. This data represent Phase 3, Configuration A of the experimental setup.

The residual SO_4 concentration in the secondary reactor coincided with stoichiometrically-expected concentrations due to SCN and CN destruction. From day 26.23 to 54.10, no notable SCN entered the reactor and SO_4 measurements mimicked the residual concentration received from the primary reactor. This indicated the absence of notable assimilation or precipitation SO_4. The maximum measured residual SO_4 concentration was 3 373 mg/L and was accounted for by the SO_4 influx from the primary reactor in combination to destruction of SCN. SO_4 was not shown to be inhibitory to SCN or CN destruction rates.

The main nitrogen source for use by the microbial population was SCN and CN; these yield NH_4 during destruction. Low levels of residual NO_3 (<45 mg/L) were detected initially during the introduction of CN to the system while the residual NH_4 concentrations mimicked stoichiometric values calculated from measured SCN and CN destruction (Figure 7.10). This was indicative of a pseudo steady state whereby nitrogen was assimilated and followed cycles of nitrification and denitrification. Metagenomic analysis done by Kantor *et al.* (2015) of samples taken from this reactor showed the absence of anaerobic ammonium oxidation. Any nitrification was reliant upon oxygen accessible biomass whereby the bulk biomass had limited

oxygen exposure (Section 5.3.4) adding to the incomplete removal of residual NH_4. Furthermore, SCN destruction rates were high in comparison to literature reported values suggesting NH_4 formation occurred at a notable rate compared to assimilatory or nitrification rates.

The residual NH_4 concentration in the secondary reactor showed expected levels coinciding with SCN and CN destruction in addition to the overflow received from the primary reactor (Figure 7.11). Furthermore, measured residual NH_4 concentrations in the secondary reactor mimicked NH_4 concentrations measured in the primary reactor during days 28-54 due to complete SCN and CN destruction achieved in the primary reactor. Increased NH_4 concentrations were measured during SCN influx as expected. Residual SCN was detected in the secondary reactor during days 60-70.7 and coincided with CN in the feed from the primary reactor and a subsequent delayed increased residual NH_4 concentration in the secondary reactor. Nitrogen fixation was likely the result of the lower than stoichiometrically calculated concentrations and coincided with SCN and CN destruction. Insignificant concentrations of NO_3 were measured for the duration of the experimental run up to day 85.

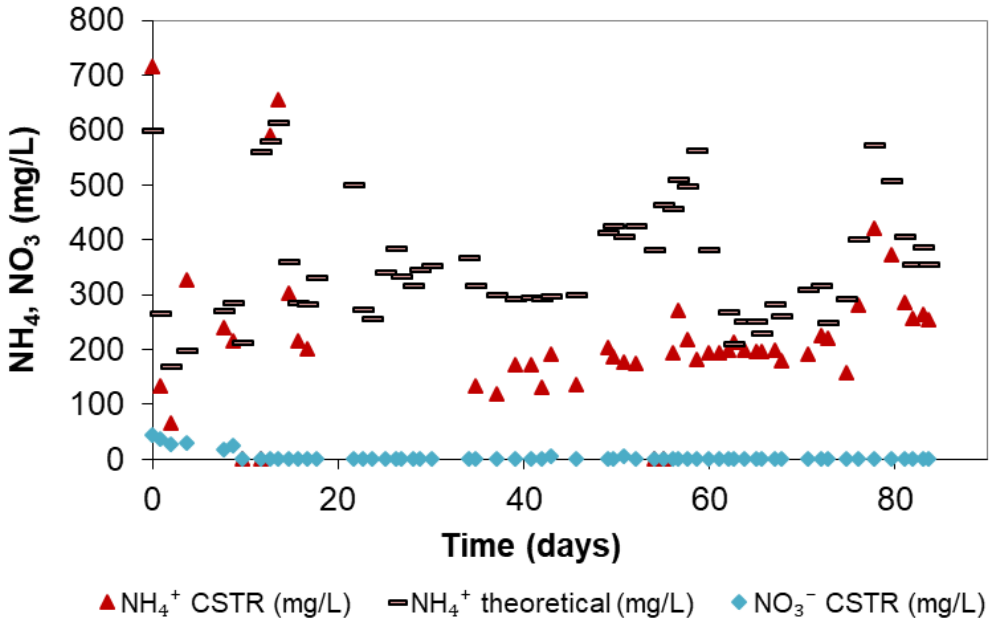

Figure 7.10: Residual NH_4 and NO_3 concentrations measured in the primary reactor receiving feed free from NH_4. The calculated NH_4 concentration was based on 100% stoichiometric conversion of the reacted SCN and CN. This data represent Phase 3, Configuration A of the experimental setup.

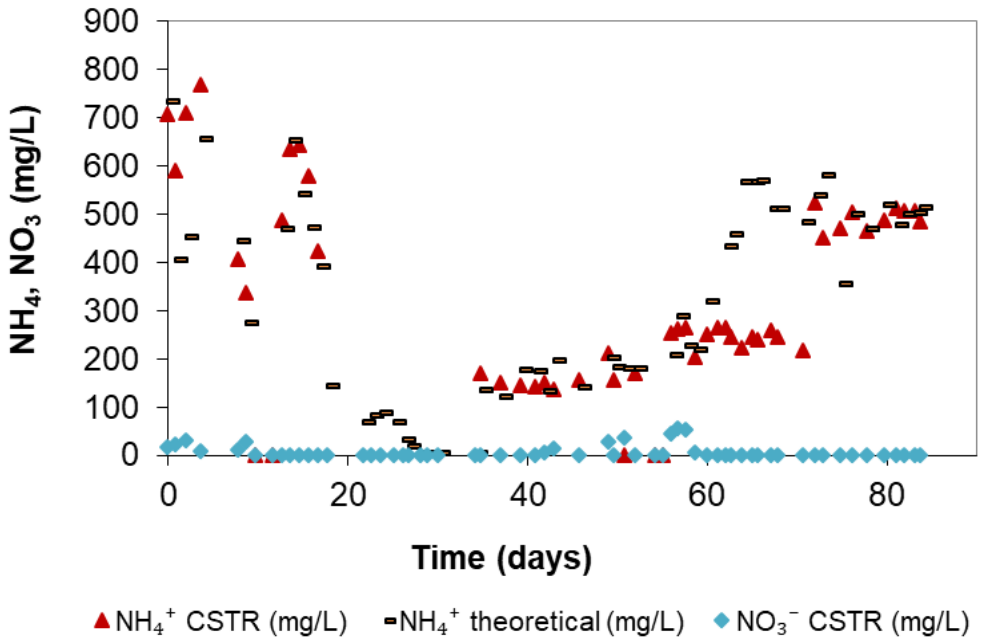

Figure 7.11: Residual NH_4 and NO_3 concentrations measured in the secondary reactor receiving feed from the primary reactor coupled in series. The calculated NH_4 concentration was based on 100% stoichiometric conversion of the reacted thiocyanate and CN-N to NH_4-N. This data represent Phase 3, Configuration A of the experimental setup.

7.3.5 Effects of system configuration and biomass recycle on thiocyanate and cyanide destruction (Phase three; Configurations B-D).

Phase three of the experimental setup consisted of Configuration B (day 1-80), Configuration C (day 80-105) and Configuration D (day 105-193). The HRT for the primary reactor-clarifier was calculated as 20.9 hours and showed residual SCN concentrations in the range 1 177-2 168 mg/L (Figure 7.12). Residual CN was measured in the range 0.31-0.62 mg/L during the first 21.7 days of operation. The feed CN to the primary reactor was first stopped followed by a reduced feed SCN concentration to 1 000 mg/L in order to reduce the residual SCN concentration. Almost complete SCN destruction (residual concentration of 17.2 mg/L) was achieved with the feed SCN concentration at 1 000 mg/L and CN in the feed at 20 mg/L by day 42.98. An incremental increased SCN feed concentration to 2 000 mg/L resulted in residual SCN concentrations consistently above 750 mg/L with

measured residual CN at day 62 and 63 with respective concentrations of 0.895 and 0.448 mg/L. Residual SCN concentrations in the secondary reactor mimicked that of the overflow from the clarifier unit indicating insignificant SCN destruction while achieving between 15.00-51.92% CN destruction of the feed in the range 0.12-0.34 mg/L. Thiocyanate destruction was measured in the secondary reactor following day 34.15 at low feed SCN concentrations measured below 92.24 mg/L over 16.6 days. The feed SCN concentration as overflow from the clarifier increased to within the range 823.9-1 145 mg/L while the residual SCN concentration measured consistently below 186.9 mg/L. In one instance residual SCN in the secondary reactor spiked and was likely due to CN in the feed while during a second instance residual SCN increased gradually to 253.2 mg/L over six days. The second increase was likely due to an external system disruption while the system quickly recovered showing a residual SCN concentration of only 31.7 mg/L by day 77.7.

At day 80, a system configuration change was made to a primary CSTR followed by a secondary CSTR and clarifier in series (Phase three; Configuration C) while the clarifier recycled to the primary CSTR (Figure 7.4 - Configuration C). This resulted in an overall HRT to be identical to that of configuration A at 34.9 hours but the HRT of the primary CSTR and clarifier remained unchanged at 2.2 and 1.12 hours, respectively. The secondary CSTR's HRT changed from 13.95 to 2.24 hours. The feed to the primary remained identical and during the 25 days of operation SCN destruction rates remained largely unchanged. The secondary reactor showed continued SCN destruction but not at an increased rate while the presence of CN at one instance (day 88.9) resulted in a transient increased residual SCN concentration. The HRT for the primary and secondary reactors was increased to 7.96 hours each while the clarifiers increased to 3.98 hours and coincided with improved SCN destruction rates. Residual SCN concentrations decreased substantially from 1 047.3 mg/L during days 80-105 to an average of 368.54 mg/L during days 106-177.8 (Phase three; Configuration D). The maximum SCN destruction rate for the primary combined clarifier was in the range 80.21-84.78 mg/L.h from day 111.8-119.1 while the average SCN destruction rate calculated over the experimental time was 58.77 mg/L.h. Almost complete SCN destruction was measured in the secondary reactor by day 177.8 at 4.20 mg/L residual. The improved SCN destruction rates in comparison with the work done in Section 7.3.3 was likely due to the retention of biomass by employing a clarifier even though the system could function without a clarifier but at a reduced destruction efficiency.

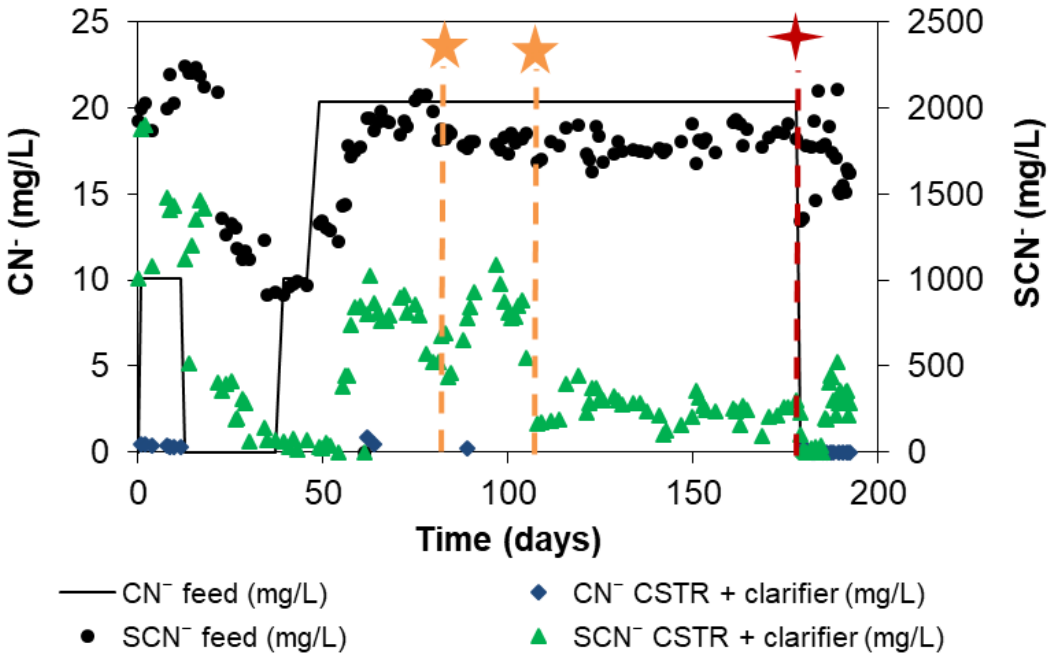

Figure 7.12: Simultaneous destruction of SCN and CN measured for a primary reactor connected to a clarifier that overflowed into a secondary CSTR (Phase 3, Configuration B). The configuration was changed (★) whereby the primary reactor overflowed into a secondary reactor connected to a clarifier with a recycle to the primary (Phase 3, Configuration C). The second ★ indicates a change of recycle flow rate from 375 to 54 mL/h (Phase 3, Configuration D). Treated effluent from the INCO process was supplied (✦) from day 179.

The residual SO_4 concentration measured in the primary reactor showed a steady increase up to day 137.7 followed by an almost consistent SO_4 concentration (Figure 7.13). This coincided with a net decreased residual SCN concentration. The high residual SO_4 concentrations mimicking the stoichiometric converted SCN showed the primary energy source as sulphur in both primary and secondary reactors. A transient increased residual SO_4 concentration was measured during days 56-67 and coincided with an increased SCN feed while maintaining a residual SCN concentration below 84.52 mg/L. Neither reactor showed any signs of sulphur precipitation or significant assimilation.

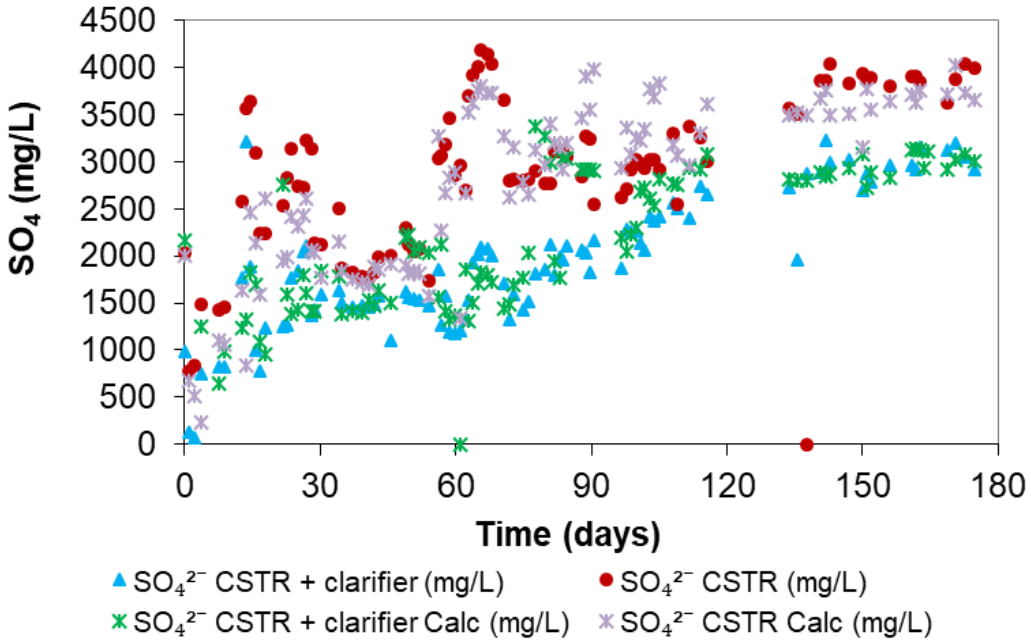

Figure 7.13: SO_4 concentration measured in the combined primary-clarifier units. The calculated values were determined from stoichiometric conversion of SCN-S to SO_4-S in all three units.

The stoichiometric calculated values for NH_4 in the combined primary CSTR-clarifier was consistently higher compared to the measured residual NH_4 concentration (Figure 7.14). The difference was likely due to nitrogen assimilation. Biomass was visually observed to increase primarily as attached biomass but floc formation was also present. An increased residual NH_4 concentration measured from day 70.69 mimicked an increased SCN feed concentration to the primary CSTR after a short delay. Interestingly was the insignificant change in residual NH_4 concentration following day 108 where a significant drop in residual SCN was measured. The high residual SCN concentration coincided with a lower than expected residual NH_4 concentration, indicative of nitrogen assimilation. Similarly, lower residual NH_4 concentrations measured in the secondary CSTR was indicative of nitrogen assimilation. Significant residual nitrate was not measured for the primary or secondary CSTR which was indicative of insignificant nitrification and subsequent denitrification.

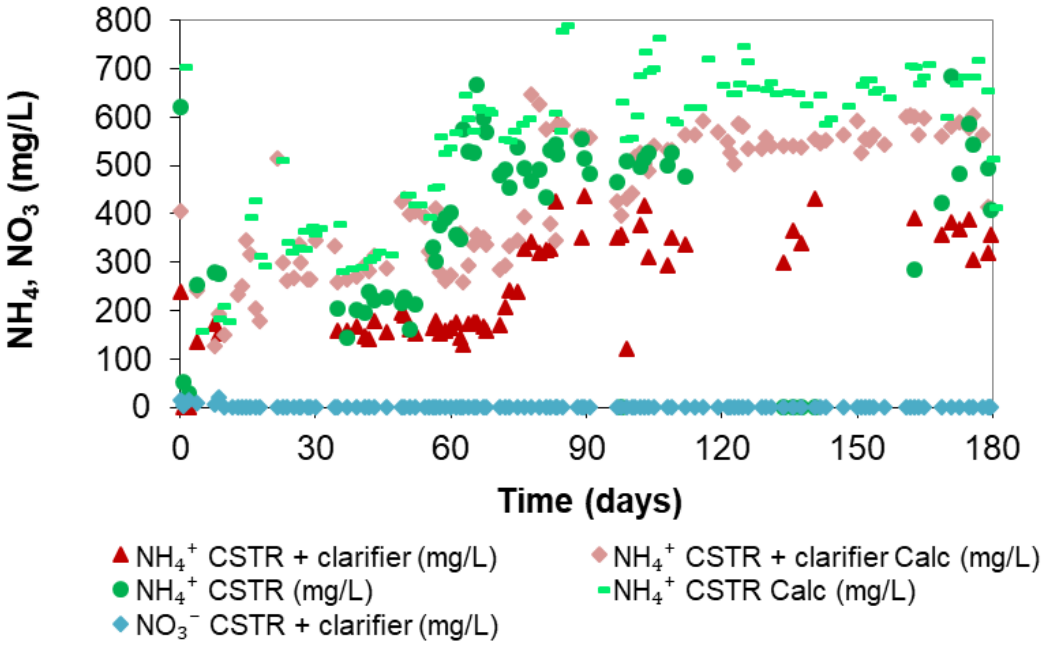

Figure 7.14: Residual and stoichiometric ammonium concentrations for the combined primary CSTR-clarifier units (labelled as CSTR + clarifier). The residual and stoichiometric calculated (calc) [theoretical] concentrations are also shown for the secondary CSTR (labelled as CSTR) and residual nitrate concentration for the primary CSTR-clarifier combination.

INCO treated effluent was used as feed to the primary reactor (Figure 7.15). Incremental increased volumes were blended with the standard feed up to a feed of 100% INCO treated effluent. The weak acid dissociated CN was primarily treated in the primary reactor up to 36.5 mg/L. Residual CN_{wad} was measured at a feed of 51.1 mg/L and while the secondary reactor showed destruction capacity, residual CN_{wad} was also detected. This indicates the capacity for treatment of CN_{wad} in the presence of 2 000 mg/L SCN. CN was not included in the feed during the supplementation with INCO treated effluent. Residual SCN was reduced completely from day 179.69-185.06 while significant concentrations in the range 196.8-522.8 mg/L was measured during the increased feed CN_{wad} from 51.1-73.0 mg/L. This showed a robust system capable of treating multiple CN compounds even when exposure changes rapidly. SO_4 from the INCO treated effluent resulted in residual concentrations as high at 7 280 mg/L which may have contributed to the increased residual SCN concentration up to 522.8 mg/L.

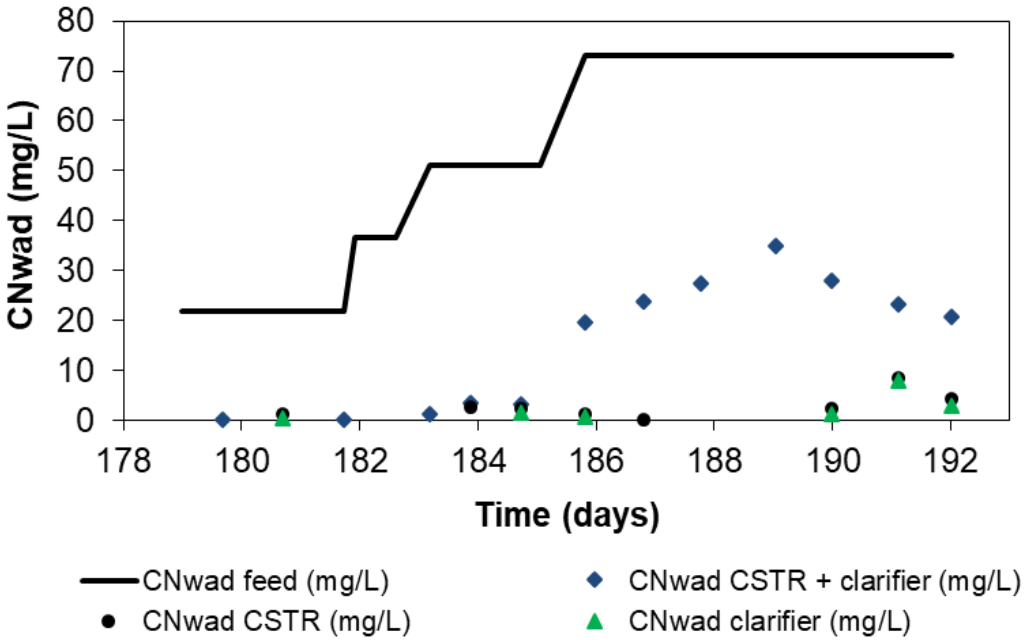

Figure 7.15: INCO treated effluent was used as feed to the primary reactor from day 179.98. Residual weak acid dissociated CN was measured for the combined primary CSTR-clarifier and secondary CSTR.

7.4 Conclusions

During start-up it is beneficial to have biomass retention to ensure a practical operating HRT without the loss of significant biomass. The planktonic population is responsible for SCN and CN destruction in the absence of significant attached biomass. If biomass retention by ways of solid-liquid separation is not possible due to economic or physical constraints, a batch start-up with a high residual SCN concentration could be employed to advance the formation of the attached biomass population prior to continuous operation. Destruction of a consistently high concentration of SCN and CN at 800 and 50 mg/L was showed between 18-25°C. At 15°C however, residual SCN and CN concentration were measured above disposal limits. Recovery of SCN and CN destruction was rapid following an increased temperature to 18°C even after a prolonged period at 15°C. The microbial population showed resilience to changing conditions and multiple combined stress factors in this case of lower operating temperature with residual SCN and CN in solution. Residual CN in solution resulted in transient inhibition of SCN destruction followed by rapid recovery when the residual CN was degraded. Furthermore, a high feed SCN concentration above 1 800 mg/L resulted in a residual SCN concentration below 1 000 mg/L which was tolerated by the microbial population in

the primary CSTR and degraded in the secondary CSTR. The residual SCN concentration further decreased in the absence of CN in the feed while the presence of CN_{wad} at concentrations up to 36.5 mg/L was degraded. The microbial population showed adaptation to rapidly changing conditions and fast recovery from unfavourable conditions.

The recycle loop used was shown to be non-essential following colonisation of a reactor and formation of a mature biofilm. During the start-up phase of a reactor it would be beneficial to recycle biomass as a method of biomass retention.

Residual SO_4 concentrations as high as 4 000 mg/L did not result in any observed inhibition of SCN or CN destruction. The residual SO_4 concentration could be used as a proxy to measure the degree of SCN destruction under steady state operation. Residual concentrations of NH4 in each experimental run was lower compared to stoichiometric values where SCN destruction was shown to occur. In the absence of SCN destruction, no significant differences in residual NH_4 and stoichiometric NH_4 concentrations were observed. This indicated substantial nitrogen assimilation while energy generation from sulphur oxidation acted as a driving force. Substantial nitrification and denitrification was not measured due to the lack of residual NO_3 in the presence of substantial residual NH_4. The INCO treated effluent did not negatively impact on the SCN and CN destruction rates initially. However, residual SCN was measured in the presence of residual CN_{wad} when the CN_{wad} in the feed exceeded the maximum destruction capacity at a feed concentration of 36.5 mg/L.

Chapter 8: Conclusions and Recommendations

The primary aims of this investigation were to develop the fundamental understanding of the ASTER^{TM} process under different operating and environmental conditions. Furthermore, the aims included an undertaking of a qualitative characterisation of the microbial community responsible for SCN destruction, in order to evaluate the potential for wider commercial application of the process and optimise performance at existing treatment operations. Prior to this research, process development was guided by an empirical model for SCN destruction, developed across a narrow range of process conditions and feed SCN concentrations by the group of du Plessis.

8.1 Microbial characterisation

The characterisation of the microbial community clearly illustrated the value of culture-independent techniques, particularly the utilisation of clone library technology as well as next generation sequencing and advanced data analysis tools. This section further addresses the key questions relating to the microbial identification and characterisation work done in this thesis. Traditional isolation techniques, using a range of general and selective media, resulted in identification of at least 12 genera using 16S rRNA sequence analysis. These included members of the genera *Thiobacillus* and *Thiomonas*, which had not been isolated from the ASTER^{TM} community previously and pointed to the potential role of sulphur oxidisers. As the media became more selective the number of isolates decreased, showing that synergistic relationships may be critical for SCN and CN destruction.

The clone library approach indicated that the community was substantially more complex than previously imagined. A total of 106 clones, selected on the basis of ARDRA, were sequenced leading to the identification of representatives from 21 different genera. In particular phylotypes were found closely related to *Thiobacillus denitrificans,* as well as *T. thioparus,* that have been shown to possess the metabolic capability to degrade SCN as an energy source. The presence of eukaryotes showed members related to *Fusarium oxysporium,* which has been shown to be capable of CN degradation.

The project enabled the development of a close collaboration with the Banfield group at UC Berkeley and samples obtained from both the SCN only and mixed CN-SCN reactors were subjected to high-throughput metagenomic sequencing to reconstruct microbial draft and curated genomes from these two communities. This was the first time this approach had been used on SCN degrading communities and provided information on community structure and diversity, relative abundance and metabolic potential. Community analysis revealed even greater microbial diversity, particularly in the mixed CN-SCN reactor. Data from both systems showed the dominance of members of the *Thiobacillus* genus, whose genomes contained a previously unreported operon for SCN degradation. The operon showed genes coding for SCN hydrolase, known to convert SCN to carbonyl sulphide and ammonium. These genes were located in a conserved operon co-located with thiocyanase genes responsible for conversion of cyanate to ammonium.

Genome-based metabolic predictions suggested that SCN degradation in both reactors was driven by chemoautolithotrophy, with reduced sulphur compounds providing the bulk of the energy. Genes involved in the Calvin-Benson_Bassham cycle were identified and in conjunction with the sulphur oxidation pathway identified indicated that inorganic carbon fixation dominated. This is a significant departure from the prevailing theory during the development of the ASTER^{TM} process, which supposed that SCN was degraded primarily as a carbon and nitrogen source. Heterotrophs comprised a smaller proportion of the community and are believed to utilise molasses from the feed, ammonium from SCN destruction and extracellular compounds produced by autotrophs. This revelation suggested that the concentration of molasses in the feed could be substantially reduced, with cost savings for commercial operations.

Genes responsible for nitrification and denitrification were identified for *Nitrosomonas* spp*.* which likely resulted in bioconversion of a portion of the ammonium produced from the destruction of SCN. Complete denitrification pathways were identified for the *Thiobacillus* spp*.* present in the stock reactor containing only SCN in feed. Furthermore, the potential for anaerobic nitrite reduction was identified for the *Rhizaria* eukaryote. The fact that genes were identified for both nitrification and denitrification indicate the potential for nitrogen removal from the system, although this was not observed during the current study.

Microorganisms can detoxify CN by conversion to SCN, using *rhodanese* enzymes, or by conversion to nitriles and subsequent degradation by *nitrilases*. Both *rhodaneses* and *nitrilases* were identified and are likely involved in CN bioconversion and ultimate destruction.

An initial investigation of the reactor sludge using microscopy techniques showed the presence of morphologically diverse bacterial species as well as fungi, algae and yeast like cells. Floc formation of sludge suggested the presence of EPS allowing the formation of a favourable micro-environment for advanced SCN destruction. Furthermore, it was observed that highly motile microorganisms were present in the bulk liquid surrounding the sludge particles. This suggested the presence of distinct microbial communities. Visualisation of the sludge from different parts within the reactor, for example samples from the reactor wall and impeller, were compared visually and a distinct difference was observed whereas the sludge from the impeller was noted as having a ribbon, filamentous appearance. The sludge from the reactor wall appeared physically different and as having a fibrous sponge-like appearance. This suggests that the liquid velocity and fluid flow across the reactor solid surface impacted significantly on the structural characteristics of the ASTER™ sludge. The distribution of microorganisms within the sludge was noted as highly random regardless of the sludge origin.

8.2 Operating window for SCN destruction using the ASTER™ culture

Batch experiments used to evaluate the effective operating window for the ASTER™ process illustrated the need for an acclimation period when culture was initially exposed to elevated SCN concentrations. The duration of the acclimation period was affected by SCN concentration, but the relationship was not proportional. Pre-exposure of the mixed culture to SCN resulted in immediate destruction of SCN, at an increased rate, upon introduction of a challenging SCN dose. Pre-exposed culture was able to degrade SCN at an initial concentration of 1 800 mg/L, at rates favourably comparable to published values. Exposure of planktonic culture to concentrations above 300 mg/L induced floc formation. Light microscopy on the flocs revealed concentrated biomass, extracellular polymeric substance and crystalline precipitates, while the concentration of motile, planktonic cells decreased substantially.

Temperature has been considered an important parameter for industrial processes due to the cost associated with temperature control. The acclimatisation time period was reduced by at least 80% at 25°C and higher compared to temperatures as low as 10°C, at the investigated SCN concentrations and supports a practical operating temperature of at least 25-40°C. It is well known that higher metabolic activity and growth rates are supported by higher temperatures and this has to be balanced with

the potential cost of temperature control. The optimum solution pH was identified as pH 7.0 while a significant reduction in SCN degradation was measured at a solution pH below and above pH 7.0. This suggests the requirement of acclimatisation for practical operations under changing conditions prior to treatment of SCN. Furthermore, inoculation of flask experiments showed a need for acclimation when the culture was exposed to pH conditions different to the historical pH exposure in the stock reactor. The operating window for the ASTER^{TM} culture was shown to be broad with regards to a SCN concentration up to 1 800 mg/L, a temperature range of 10-40°C and solution pH of 5.0-9.0.

8.3 Characterisation of reactor performance under different conditions including feed SCN and CN concentrations, solids loading, sludge loading and pH

Continuous reactor operated systems were employed to further elucidate the volumetric reaction kinetics under changing conditions of feed SCN and -CN concentration and solution pH. Although the desire was to operate the reactors under conditions where the effluent SCN concentration remained below 1 mg/L, it is noted that in some instances this was intentionally changed to allow observation of sludge reaction to dynamic conditions in order to evaluate system robustness. The maximum SCN destruction rate obtained during this study was 87.44 mg/L.h at an eight hour hydraulic retention time with a feed SCN concentration of 1 000 mg/L. This rate was obtained following incremental increases in the feed SCN concentration over 84.8 days. Notably was the build-up of sludge in the reactor especially during the time period when the feed SCN concentration was set to 1 000 mg/L. Carbon fixation was actively promoted during this time period whereby sludge growth was visually noted to be rapidly increasing in the presence of conditions high in excess to nutrients. This was also in agreement with the genes identified to be involved in the Calvin-Benson Bassham cycle. The result of carbon fixation and sludge promotion resulted in additional complexity whereby a favourable environment for growth was created but also areas of mass transfer limitation.

Sludge loading experiments showed an increased sludge loading resulted in a decreased acclimatisation phase as well as an increased overall volumetric SCN destruction rate. The improved acclimatisation and the increased overall volumetric SCN destruction rate, did not show improvement to the same extent as the increased biomass loading nor was there a linear correlation between these parameters. The first five-fold increment in biomass loading resulted in an insignificant rate improvement with an average rate of 10.49 mg/L.h, where a twenty-

five fold biomass increment resulted in an almost doubling of the average degradation rate to a maximum of 19.53 mg/L.h. Elemental analysis of the sludge (data not shown) suggested an excess of fixed carbon while dissolved oxygen measurements showed a heterogeneous sludge make-up with respect to oxygen permeability. Areas were identified at both higher and lower permeability indicative of both a higher microbial load having a higher oxygen demand as well as lower oxygen permeability due to a denser EPS medium. This is in agreement with the structures observed during scanning electron microscopy whereby a porous matrix was observed and inhabited by microorganisms. The mass transfer rates of nutrients likely decreased with an increased carbon fixation rate and therefore created a limited SCN destruction capacity over time. For commercial application it is important to promote sludge formation and growth to ensure critical mass is reached for optimum SCN destruction. The proposed model for reactor colonisation (Section 5.3.5) summarised the steps involved in progressing from a purely planktonic community to an attached biofilm community. This proposed that an attached biofilm community developed under selective conditions offer sufficient active biomass for SCN destruction without the need for biomass recovery and recycle.

The effect of a feed SCN at 1 500 mg/L was immediate and a decreased destruction rate of 52.1% was measured. The increased residual SCN concentration would have likely impacted on the microbial population structure, thereby directly or indirectly affecting the overall volumetric SCN destruction performance. Systematic increase of the feed SCN concentration at a 24 h HRT resulted in a maximum destruction rate of 49.49 mg/L.h while the reactor fell over at a feed SCN concentration of 3 000 mg/L. Following an extended time period of insignificant SCN destruction, the feed concentration was decreased to 1 000 mg/L whereby SCN destruction resumed albeit at a lower maximum rate of 55.46 mg/L.h. This further indicated that the microbial population changed significantly thereby affecting reactor performance.

This research was the first known study to show SCN destruction in the presence of suspended solids. Adaptation of the microbial population to 5.5% suspended solids required 20 days of gradual solids build-up while maintaining a residual SCN concentration of 1 mg/L. The maximum SCN degradation rate of at least 56.0 mg/L.h was measured at a feed SCN concentration of 450 mg/L while maintaining a residual SCN concentration below 2 mg/L in the secondary reactor. Periods where a system upset was observed coincided with an increased suspended solids concentration of 7.45% or as a result of decreased reactor pH. This highlighted the

combined effect of multiple stress factors on the microbial population as well as the effect of a single parameter for example solution pH. Furthermore, the microbial diversity was shown to be greatly reduced compared to a reactor system not containing solids while preliminary data showed unsuccessful SCN destruction in the presence of tailings solids. In addition, the solids containing reactor showed dominance of heterotrophs compared to dominating autotrophs in the solids-free reactor. This likely contributed to the increased fluctuation in reactor performance with respect to SCN destruction. *Thiobacillus* sp. was present in both reactors although the specific species identified were not the same. In a more detailed study it was found that the tolerance of the microbial population to extreme pH conditions showed SCN destruction at a low feed concentration of 100 mg/L. Complete SCN destruction was shown in the pH range of pH 4.07-8.83. The optimum operating pH was shown to be in the range of pH 7.0-7.5. Cessation of destruction occurred outside this pH range although recovery was rapid when conditions returned to within this range. The work done in this study paved the way for full scale commercial application.

Simultaneous destruction of SCN and CN was shown to be practically feasible at commercially useful rates. The presence of CN resulted in reduced SCN destruction while operating temperatures below 18°C were shown to impact negatively on the SCN and CN destruction rates. The presence of CN in the feed make-up poses a rate limiting step since CN destruction not only precedes SCN destruction but rates were significantly lower compared to SCN destruction rates. Conversion of CN to SCN could potentially circumvent this rate limitation imposed by the presence of CN while optimisation of the microbial community to increase CN destruction rates could offer an alternative.

Based on the outcomes of the present study, the following areas are recommended for further investigation to improve the operating performance of the ASTER^{TM} process:

1) Full characterisation of the individual species within the microbial community responsible for SCN and CN destruction so as to design an inoculum specific to the conditions under which the process is to be operated.
2) Metabolic elucidation to fully treat any sulphur and nitrogen by-products for re-use as well as optimise any nutrient requirements.
3) Reactor design to promote area for microbial growth in a thin layer while maximising the area to volume ratio.

4) Investigate the effect of different solid types on SCN and CN destruction rates.
5) Investigate the need for addition of organic carbon in the feed solution especially in combination with elucidating the microbial diversity.
6) Research would be required to investigate the recovery of valuable metals due to adsorption to the sludge.
7) Fully characterise the extent of treatment for CN_{wad} and CN_{sad} species.
8) Quantification of the microbial concentration will be valuable in offering specific kinetic rates and contributions to SCN and CN destruction to allow the design of a predictive performance model.
9) Treatment of CN to convert CN to SCN could result in treatment of a simpler matrix containing SCN only.

Appendix A: Analytical methods

A.1 Thiocyanate assay standard curve

The following curve was generated for each run of samples prepared. Standards were prepared by using a known dilution series analysed by HPLC as described in the Materials and Methods section of this thesis. This was also done for all analytical methods described in Chapter 2. Potassium thiocyanate was diluted in the range 0-100 mg/L using reactor media.

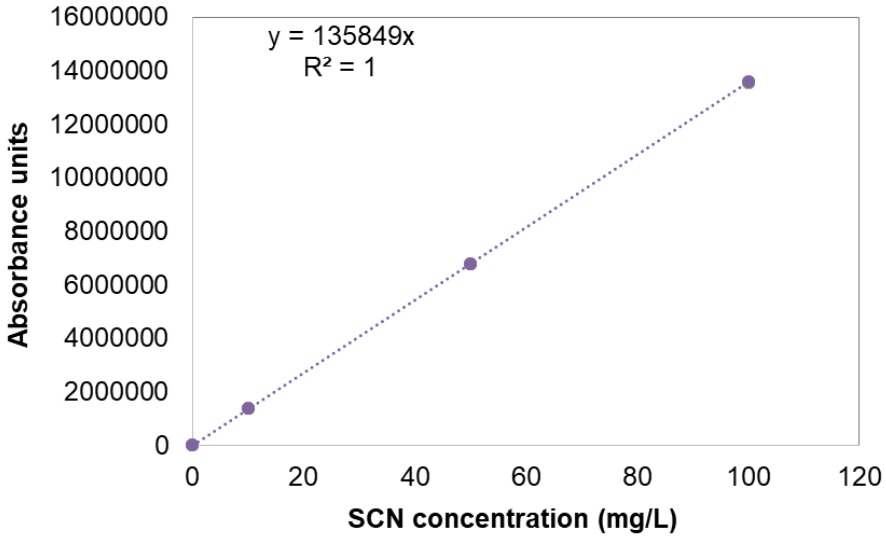

Figure A.1: Thiocyanate standard curve for the concentration 0-100 mg/L. Absorbance units were used to calculate the peak area relating to concentration.

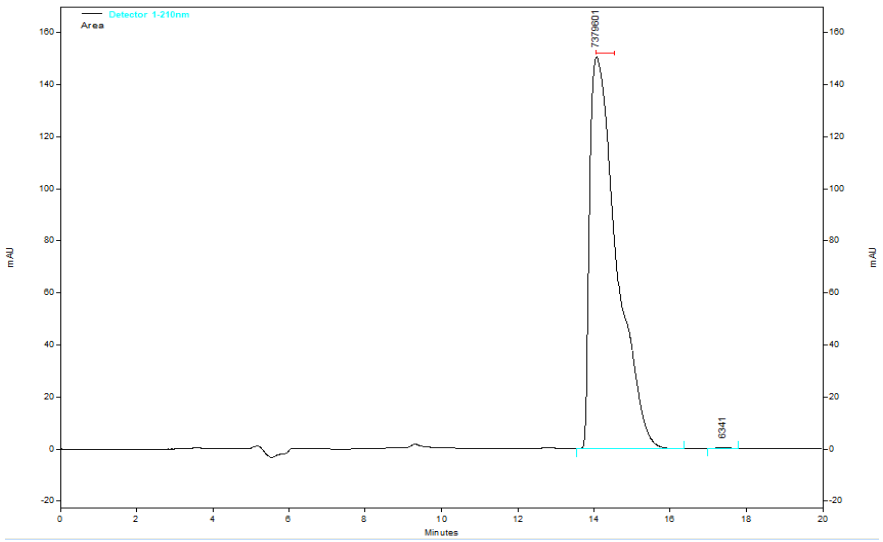

Figure A.2: Sample of a HPLC analysis chromatogram representing a standard solution. The peak between 14-16 min was integrated to determine the area and subsequently the SCN concentration. Absorbance units were used to calculate the peak area relating to concentration.

A.2 Ammonium assay standard curve

The following curve was generated for each run of samples prepared. Ammonium sulphate was diluted in the range 0-100 mg/L using reactor media.

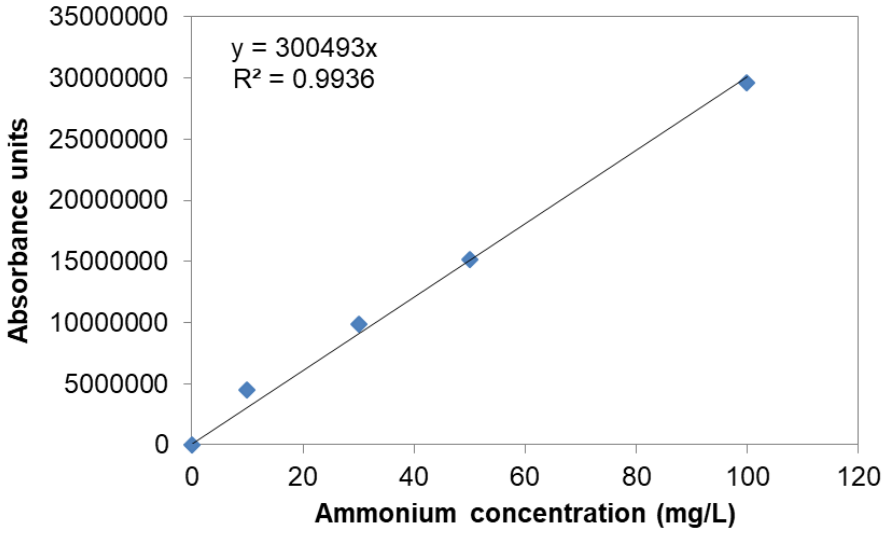

Figure A.3: Standard curve for ammonium in the range 0-100 mg/L. Absorbance units were used to calculate the peak area relating to concentration.

A.3 Nitrate and sulphate assay standard curve

Nitrate and sulphate was analysed for each run with included internal standard solutions prepared fresh. The mobile phase degassed and used is described below.

A.3.1 Mobile phase preparation

A.3.1.1 Sodium Borate-Gluconate stock solution (1L)

1. 16g Sodium gluconate
2. 18g Boric acid
3. 25g sodium tetraborate decahydrate
4. Add 750 mL dH2O and mix until the above salts dissolve
5. Add 250 mL glycerol and mix throughly
6. Thereafter filter solution and autoclave in order to prevent the growth of fungus

A.3.1.2 Moblie phase solution (1L)

1. 500 mL of dH2O to a schott bottle
2. 20 mL Sodium borate-gluconate stock solution (prepared as in Section A.3.1.1)
3. 20 mL 1-Butanol (HPLC grade)
4. 120 mL Acetonitrile (HPLC grade)
5. 340 mL dH2O

The following curve was generated for each run of samples prepared. Nitrate and sulphate was diluted in the range 0-300 mg/L using reactor media and analysed together.

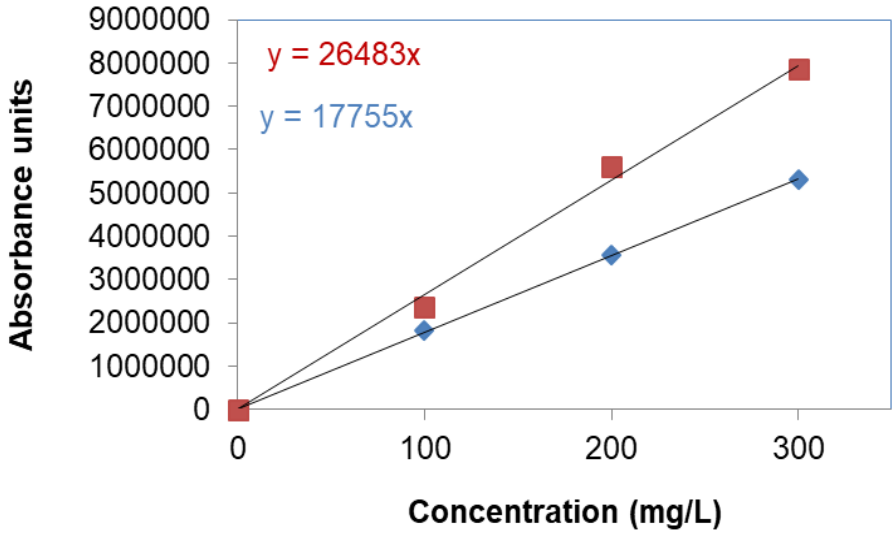

Figure A.4: Standard curve for nitrate and sulphate in the range 0-300 mg/L. Sulphate is represented by ■ and nitrate by ◆.

A.4 Free cyanide and weak acid dissociated cyanide assay standard curve

The cynoprobe is based on amperometric measurement of the cyanide concentration in solution. Standard solution were prepared and measured in the presence and absence of reactor sludge, media and water to ensure the absence of any interferences.

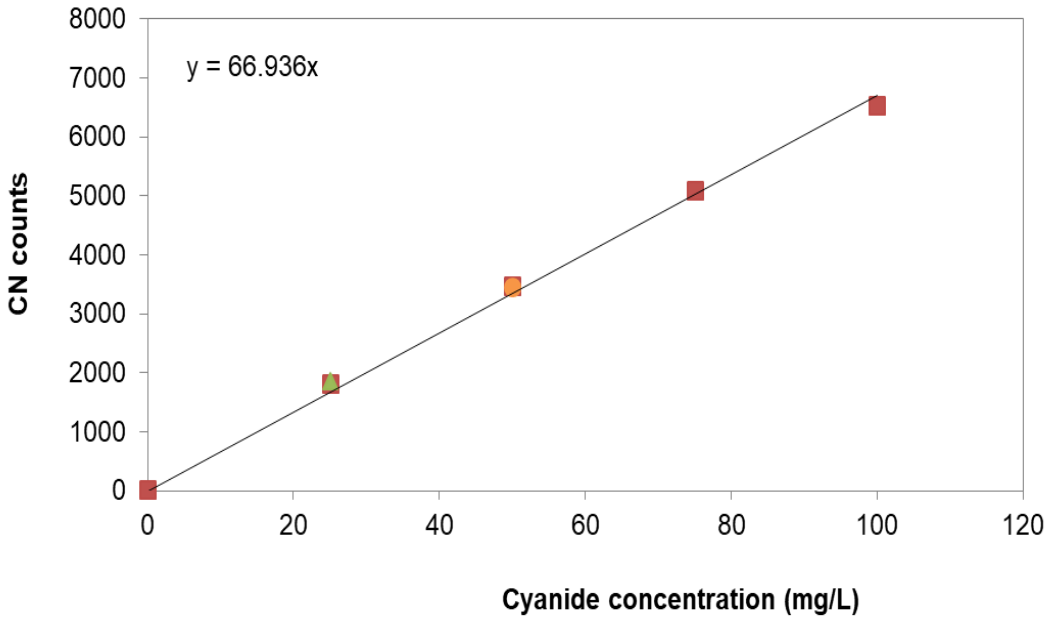

Figure A.5: Standard curve for cyanide in the range 0-100 mg/L. The symbols in the graph used represent three replicate measurements.

Bibliography

Adjei, M. and Ohta, Y. 1999. Isolation and characterization of a cyanide-utilizing Burkholderia cepacia strain. *World Journal of Microbiology and Biotechnology*, 15(6): 699–704.

Ahn, J.H., Lee, S. and Hwang, S. 2005. Growth kinetic parameter estimation of Klebsiella sp. utilizing thiocyanate. *Process Biochemistry*, 40(3–4): 1363–1366.

Akcil, a. 2002. First application of cyanidation process in Turkish gold mining and its environmental impacts. *Minerals Engineering*, 15(9): 695–699.

Akcil, A. 2003. Destruction of cyanide in gold mill effluents: Biological versus chemical treatments. *Biotechnology Advances*, 21(6): 501–511. 31 January 2014.

Akcil, A., Karahan, A.G., Ciftci, H. and Sagdic, O. 2003. Biological treatment of cyanide by natural isolated bacteria (Pseudomonas sp.). *Minerals Engineering*, 16(7): 643–649. 9 March 2014.

Akcil, A. and Mudder, T. 2003. Microbial destruction of cyanide wastes in gold mining: process review. *Biotechnology letters*, 25(6): 445–450.

Altschul, S., Gish, W., Miller, W., Myers, E. and Lipman, D. 1990. Basic local alignment search tool.pdf. : 403–410.

Amann, R.I., Stromley, J., Devereux, R., Key, R. and Stahl, D. a. 1992. Molecular and microscopic identification of sulfate-reducing bacteria in multispecies biofilms. *Applied and Environmental Microbiology*, 58(2): 614–623.

Arakawa, T., Kawano, Y., Kataoka, S., Katayama, Y., Kamiya, N., Yohda, M. and Odaka, M. 2007. Structure of Thiocyanate Hydrolase: A New Nitrile Hydratase Family Protein with a Novel Five-coordinate Cobalt(III) Center. *Journal of Molecular Biology*, 366(5): 1497–1509.

Barnes, D.E., Wright, P.J., Graham, S.M. and Jones-Watson, E. a. 2000. Techniques for the determination of cyanide in a process environment; a review V. N. ;Gregoir. C. ;Barne. D. E. . Potts P.;Mitkin, ed. *Geostandards Newsletter*, 24(2): 183–195.

Barradas, S. 1997. *CO2 activation and functionalization*.

Baxter, J. and Cummings, S.P. 2006. The current and future applications of microorganism in the bioremediation of cyanide contamination. *Antonie van Leeuwenhoek, International Journal of General and Molecular Microbiology*, 90(1): 1–17. 9 March 2014.

Baxter, J. and Cummings, S.P. 2006. The impact of bioaugmentation on metal cyanide degradation and soil bacteria community structure. *Biodegradation*, 17(3): 207–217. 19 February 2014.

Behnamfard, A. and Salarirad, M.M. 2009. Equilibrium and kinetic studies on free cyanide adsorption from aqueous solution by activated carbon. *Journal of Hazardous Materials*, 170(1): 127–133. 9 March 2014.

Beller, H.R., Chain, P.S.G., Letain, T.E., Chakicherla, A., Larimer, F.W., Richardson, P.M., Coleman, M. a., Wood, A.P. and Kelly, D.P. 2006. The genome sequence of the obligately chemolithoautotrophic, facultatively anaerobic bacterium Thiobacillus denitrificans. *Journal of Bacteriology*, 188(4): 1473–1488.

Bezsudnova, E.Y., Sorokin, D.Y., Tikhonova, T. V. and Popov, V.O. 2007. Thiocyanate hydrolase, the primary enzyme initiating thiocyanate degradation in the novel obligately chemolithoautotrophic halophilic sulfur-oxidizing bacterium Thiohalophilus thiocyanoxidans. *Biochimica et Biophysica Acta - Proteins and Proteomics*, 1774(12): 1563–1570. 4 February 2014.

Brüger, A., Fafilek, G., Restrepo B., O.J. and Rojas-Mendoza, L. 2018. On the volatilisation and decomposition of cyanide contaminations from gold mining. *Science of the Total Environment*, 627: 1167–1173.

van Buuren, C., Makhotla, N. and Olivier, J.W. 2011. The Aster Process: Technology Development through to Piloting, Demonstration and Commercialisation. In *ALTA 2011 Nickel-Cobalt-Copper, Uranium and Gold Conference*.

Chao, Y.M., Tseng, I.C. and Chang, J.S. 2006. Mechanism for sludge acidification in aerobic treatment of coking wastewater. *Journal of Hazardous Materials*, 137(3): 1781–1787. 27 February 2014.

Chattopadhyay, M.K. 2006. Mechanism of bacterial adaptation to low temperature. *Journal of Biosciences*, 31(1): 157–165.

Chaudhari, A.U. and Kodam, K.M. 2010. Biodegradation of thiocyanate using co-culture of Klebsiella pneumoniae and Ralstonia sp. *Applied microbiology and biotechnology*, 85(4): 1167–1174. 9 March 2014.

Chen, C.Y., Kao, C.M. and Chen, S.C. 2008. Application of Klebsiella oxytoca immobilized cells on the treatment of cyanide wastewater. *Chemosphere*, 71(1): 133–139. 9 March 2014.

Chi, G., Fuerstenau, M.C. and Marsden, J.O. 1997. Study of Merrill-Crowe processing. Part I: Solubility of zinc in alkaline cyanide solution. *International Journal of Mineral Processing*, 49(3–4): 171–183.

Chin, R.G. and Calderon, Y. 2000. Acute cyanide poisoning: A case report. *Journal of Emergency Medicine*, 18(4): 441–445.

Cipollone, R., Bigotti, M.G., Frangipani, E., Ascenzi, P. and Visca, P. 2004. Characterization of a rhodanese from the cyanogenic bacterium Pseudomonas aeruginosa. *Biochemical and Biophysical Research Communications*, 325(1): 85–90.

Clennell, J.E. 1910. *The cyanide handbook*. McGraw-hille book company.

Das, S.K., Mishra, a K., Tindall, B.J., Rainey, F. a and Stackebrandt, E. 1996. Oxidation of thiosulfate by a new bacterium, Bosea thiooxidans (strain BI-42) gen. nov., sp. nov.: analysis of phylogeny based on chemotaxonomy and 16S ribosomal DNA sequencing. *International journal of systematic bacteriology*, 46(4): 981–987.

Dash, R.R., Balomajumder, C. and Kumar, A. 2009. Treatment of cyanide bearing water / wastewater by plain and biological activated carbon. : 3619–3627.

Dash, R.R., Balomajumder, C. and Kumar, A. 2008. Treatment of metal cyanide bearing wastewater by simultaneous adsorption and biodegradation (SAB). *Journal of Hazardous Materials*, 152(1): 387–396. 9 March 2014.

Dash, R.R., Gaur, A. and Balomajumder, C. 2009. Cyanide in industrial wastewaters and its removal: A review on biotreatment. *Journal of Hazardous Materials*, 163(1): 1–11. 21 February 2014.

Department of Environmental Affairs. 2013. National Environmental Management: Waste Act, 2008 (Act No . 59 of 2008): National norms and standards for the assessment of waste for landfill disposal. *Government Gazette*, 7(10505): 34–45.

Dictor, M., Battaglia-Brunet, F., Morin, D., Bories, A. and Clarens, M. 1997. Biological treatment of gold ore cyanidation wastewater in fixed bed reactors. *Environmental Pollution*, 97(3): 287–294.

Donato, D.B., Nichols, O., Possingham, H., Moore, M., Ricci, P.F. and Noller, B.N. 2007. A critical review of the effects of gold cyanide-bearing tailings solutions on wildlife. *Environment International*, 33(7): 974–984. 10 February 2014.

Doran, P.M. 1995. *Bioprocess Engineering Principles*. Elsevier.

Dumestre, a, Chone, T., Portal, J., Gerard, M. and Berthelin, J. 1997. Cyanide Degradation under Alkaline Conditions by a Strain of Fusarium solani Isolated from Contaminated Soils. *Applied and environmental microbiology*, 63(7): 2729–2734.

Dursun, a. Y., Çalik, a. and Aksu, Z. 1999. Degradation of ferrous(II) cyanide complex ions by Pseudomonas fluorescens. *Process Biochemistry*, 34(9): 901–908.

DWA. 2013. Revision of General Authorisations in Terms of Section 39 of the National Water Act, 1998 (Act No. 36 of 1998) (the Act). *Gazette*, 19182(19182): 42.

Dzombak, D.A., Ghosh, R.S. and Wong-Chong, G.M. 2006. *Cyanide in water and soil*. Taylor & Francis Group.

Ebbs, S. 2004. Biological degradation of cyanide compounds. *Current Opinion in Biotechnology*, 15(3): 231–236. 5 February 2014.

Edward, C.J., Kotsiopoulos, A. and Harrison, S.T.L. 2018. Low-level thiocyanate concentrations impact on iron oxidation activity and growth of Leptospirillum ferriphilum through inhibition and adaptation. *Research in Microbiology*, 169(10): 576–581.

Ezzi, M.I. and Lynch, J.M. 2002. Cyanide catabolizing enzymes in Trichoderma spp. *Enzyme and Microbial Technology*, 31(7): 1042–1047.

Fan, H., Liu, X., Wang, H., Han, Y., Qi, L. and Wang, H. 2017. Oxygen transfer dynamics and activated sludge floc structure under different sludge retention times at low dissolved oxygen concentrations. *Chemosphere*, 169: 586–595.

Felföldi, T., Székely, A.J., Gorál, R., Barkács, K., Scheirich, G., András, J., Rácz, A. and Márialigeti, K. 2010. Polyphasic bacterial community analysis of an aerobic activated sludge removing phenols and thiocyanate from coke plant effluent. *Bioresource Technology*, 101(10): 3406–3414. 26 February 2014.

Felsenstein, J. 1985. Confidence Limits on Phylogenies: an Approach Using the Bootstrap. *Society for the Study of Evolution*, 39(1): 1–15.

Finnegan, I., Toerien, S., Abbot, L., Smit, F. and Raubenheimer, H.G. 1991. Identification and characterisation of an Acinetobacter sp. capable of assimilation of a range of cyano-metal complexes, free cyanide ions and simple organic nitriles. *Applied Microbiology and Biotechnology*, 36(1): 142–144.

Garcia-Ochoa, F., Gomez, E., Santos, V.E. and Merchuk, J.C. 2010. Oxygen uptake rate in microbial processes: An overview. *Biochemical Engineering Journal*, 49(3): 289–307.

Gokulakrishnan, S. and Gummadi, S.N. 2006. Kinetics of cell growth and caffeine utilization by Pseudomonas sp. GSC 1182. *Process Biochemistry*, 41(6): 1417–1421. 1 March 2014.

Gönen, N., Kabasakal, O.S. and Özdil, G. 2004. Recovery of cyanide in gold leach waste solution by volatilization and absorption. *Journal of Hazardous Materials*, 113(1–3): 231–236. 9 March 2014.

Gonzalez-merchan, C., Tanabene, R., Genty, T., Bus-, B., Potvin, R., Allaire, M. and Neculita, C.M. 2017. Simultaneous Treatment of Thiocyanates and Ammonia Nitrogen in Gold Mine Effluents Using Advanced Oxidation and Nitrification-Denitrification Processes. *Mine water and Circular Economy*, (3): 1039–1047.

Gould, W.D., King, M., Mohapatra, B.R., Cameron, R. a., Kapoor, A. and Koren, D.W. 2012. A critical review on destruction of thiocyanate in mining effluents. *Minerals Engineering*, 34: 38–47. 9 March 2014.

Grigor'eva, N.V., Kondrat'eva, T.F., Krasil'nikova, E.N. and Karavaiko, G.I. 2006. mechanism of cyanide and thiocyanate decomposition by an association of Pseudomonas putida and Pseudomonas stutzeri strains. *Microbiology (New York, NY, United States)*, 75(3): 259–265. 9 March 2014.

Guerrero, J.J. and Olivera, S.C. 1999. ENVIRONMENTAL BIOTECHNOLOGY FOR MINING AND METALLURGY ‡ José J. Guerrero * (1) & Sonia C. Olivera (1) (1) * : , (1): 1–8.

Gupta, N., Balomajumder, C. and Agarwal, V.K. 2010. Enzymatic mechanism and biochemistry for cyanide degradation: A review. *Journal of Hazardous Materials*, 176(1–3): 1–13. 22 February 2014.

Gurbuz, F., Ciftci, H., Akcil, A. and Karahan, A.G. 2004. Microbial detoxification of cyanide solutions: A new biotechnological approach using algae. *Hydrometallurgy*, 72(1–2): 167–176. 9 March 2014.

Harrison, S.T.L., Stevenson, R. and Cilliers, J.J. 2012. Assessing solids concentration homogeneity in Rushton-agitated slurry reactors using electrical resistance tomography (ERT). *Chemical Engineering Science*, 71: 392–399.

Huddy, R.J., van Zyl, a. W., van Hille, R.P. and Harrison, S.T.L. 2015. Characterisation of the complex microbial community associated with the ASTER™ thiocyanate biodegradation system. *Minerals Engineering*, 76: 65–71.

Huddy, R.J., Van Zyl, A.W., Van Hille, R.P. and Harrison, S.T.L. 2015. Characterisation of the complex microbial community associated with the ASTER??? thiocyanate biodegradation system. *Minerals Engineering*, 76: 65–71.

Huertas, M.J., Sáez, L.P., Roldán, M.D., Luque-Almagro, V.M., Martínez-Luque, M., Blasco, R., Castillo, F., Moreno-Vivián, C. and García-García, I. 2010. Alkaline cyanide degradation by Pseudomonas pseudoalcaligenes CECT5344 in a batch reactor. Influence of pH. *Journal of Hazardous Materials*, 179(1–3): 72–78. 9 March 2014.

Hung, C.H. and Pavlostathis, S.G. 1997. Aerobic biodegradation of thiocyanate. *Water Research*, 31(11): 2761–2770.

Jefferson, K.K. 2004. What drives bacteria to produce a biofilm? *FEMS Microbiology Letters*, 236(2): 163–173.

Jeong, Y.S. and Chung, J.S. 2006. Biodegradation of thiocyanate in biofilm reactor using fluidized-carriers. *Process Biochemistry*, 41(3): 701–707. 9 March 2014.

Kantor, R.S., van Zyl, a. W., van Hille, R.P., Thomas, B.C., Harrison, S.T.L. and Banfield, J.F. 2015. Bioreactor microbial ecosystems for thiocyanate and cyanide degradation unraveled with genome-resolved metagenomics. *Environmental Microbiology*, 17(12): 4929–4941.

Kao, C.M., Lin, C.C., Liu, J.K., Chen, Y.L., Wu, L.T. and Chen, S.C. 2004. Biodegradation of the metal-cyano complex tetracyanonickelate (II) by Klebsiella oxytoca. *Enzyme and Microbial Technology*, 35(5): 405–410. 9 March 2014.

Kao, C.M., Liu, J.K., Lou, H.R., Lin, C.S. and Chen, S.C. 2003. Biotransformation of cyanide to methane and ammonia by Klebsiella oxytoca. *Chemosphere*, 50(8):

1055–1061.

Karavaiko, G.I., Kondrat, T.F., Savari, E.E., Grigor, N. V and Avakyan, Z.A. 2000. Microbial Degradation of Cyanide and Thiocyanate. , 69(2): 167–173.

Katayama, Y., Narahara, Y., Inoue, Y., Amano, F., Kanagawa, T. and Kuraishi, H. 1992. A thiocyanate hydrolase of thiobacillus thioparus: A novel enzyme catalyzing the formation of carbonyl sulfide from thiocyanate. *Journal of Biological Chemistry*, 267(13): 9170–9175.

Kellerman, C. and Griebler, C. 2009. Thiobacillus thiophilus sp. nov., a chemolithoautotrophic, thiosulfate-oxidizing bacterium isolated from contaminated aquifer sediments. *International Journal of Systematic and Evolutionary Microbiology*, 59(3): 583–588.

Khodadadi, A., Abdolahi, M. and Teimoury, P. 2005. Detoxification of cyanide in gold processing wastewater by hydrogen peroxide * 1. , 2(3): 177–182.

Kim, J., Cho, K.J., Han, G., Lee, C. and Hwang, S. 2013. Effects of temperature and pH on the biokinetic properties of thiocyanate biodegradation under autotrophic conditions. *Water Research*, 47(1): 251–258. 9 March 2014.

Kim, S.J. and Katayama, Y. 2000. Effect of growth conditions on thiocyanate degradation and emission of carbonyl sulfide by Thiobacillus thioparus THI115. *Water Research*, 34(11): 2887–2894.

Kim, Y.M., Cho, H.U., Lee, D.S., Park, C., Park, D. and Park, J.M. 2011. Response of nitrifying bacterial communities to the increased thiocyanate concentration in pre-denitrification process. *Bioresource Technology*, 102(2): 913–922. 27 February 2014.

Kitis, M., Akcil, a., Karakaya, E. and Yigit, N.O. 2005. Destruction of cyanide by hydrogen peroxide in tailings slurries from low bearing sulphidic gold ores. *Minerals Engineering*, 18(3): 353–362. 9 March 2014.

Kobayashi, M., Goda, M. and Shimizu, S. 1998. The catalytic mechanism of amidase also involves nitrile hydrolysis. *FEBS Letters*, 439(3): 325–328.

Kondratenko, V.A. 2010. Mechanistic aspects of the Andrussow process over Pt-Rh gauzes. Pathways of formation and consumption of HCN. *Applied Catalysis A: General*, 381(1–2): 74–82. 9 March 2014.

Kunz, D. a, Wang, C.S. and Chen, J.L. 1994. Alternative routes of enzymic cyanide metabolism in Pseudomonas fluorescens NCIMB 11764. *Microbiology*, 140 (Pt 7: 1705–1712.

Kuyucak, N. and Akcil, A. 2013. Cyanide and removal options from effluents in gold mining and metallurgical processes. *Minerals Engineering*, 50–51: 13–29. 16 August 2014.

Lalucat, J., Bennasar, A., Bosch, R., García-Valdés, E. and Palleroni, N.J. 2006.

Biology of Pseudomonas stutzeri. *Microbiology and molecular biology reviews : MMBR*, 70(2): 510–47. 27 January 2014.

Larkin, M.A., Blackshields, G., Brown, N.P., Chenna, R., Mcgettigan, P.A., McWilliam, H., Valentin, F., Wallace, I.M., Wilm, A., Lopez, R., Thompson, J.D., Gibson, T.J. and Higgins, D.G. 2007. Clustal W and Clustal X version 2.0. *Bioinformatics*, 23(21): 2947–2948.

Lay-Son, M. and Drakides, C. 2008. New approach to optimize operational conditions for the biological treatment of a high-strength thiocyanate and ammonium waste: pH as key factor. *Water Research*, 42(3): 774–780. 9 March 2014.

Lee, C., Kim, J., Chang, J. and Hwang, S. 2003. Isolation and identification of thiocyanate utilizing chemolithotrophs from gold mine soils. *Biodegradation*, 14(3): 183–188.

Lee, C., Kim, J., Do, H. and Hwang, S. 2008. Monitoring thiocyanate-degrading microbial community in relation to changes in process performance in mixed culture systems near washout. *Water Research*, 42(4–5): 1254–1262. 22 February 2014.

Luthy, R.G. and Bruce Jr., S.G. 1979. Kinetics of reaction of cyanide and reduced sulfur species in aqueous solution. *Environmental Science and Technology*, 13(12): 1481–1487.

Madigan, M., Martinko, J. and Parker, J. 2003. *Brock biology of microorganisms*.

Meeussen, J.C.L., Keizer, M.G., Frans, A. and Haan, D. 1992. Soil Solutions. , 26(3): 511–516.

Mekuto, L., Ntwampe, S.K.O. and Akcil, A. 2016. An integrated biological approach for treatment of cyanidation wastewater. *Science of the Total Environment*, 571: 711–720.

Mosher, J.B. and Figueroa, L. 1996. Biological oxidation of cyanide: A viable treatment option for the minerals processing industry? *Minerals*, 9(5): 573–581.

Mudder, T., Botz, M.M. and Smith, A. 1991. The Chemistry and Treatment of Cyanidation Wastes. : 373.

Mudliar, R., Umare, S.S., Ramteke, D.S. and Wate, S.R. 2009. Energy efficient-Advanced oxidation process for treatment of cyanide containing automobile industry wastewater. *Journal of Hazardous Materials*, 164(2–3): 1474–1479. 9 March 2014.

Nouha, K., Kumar, R.S., Balasubramanian, S. and Tyagi, R.D. 2018. Critical review of EPS production, synthesis and composition for sludge flocculation. *Journal of Environmental Sciences (China)*, 66: 225–245.

Olson, G.J., Brierley, C.L., Briggs, A.P. and Calmet, E. 2006. Biooxidation of

thiocyanate-containing refractory gold tailings from Minacalpa, Peru. *Hydrometallurgy*, 81(3–4): 159–166. 24 January 2014.

Parga, J.R., Shukla, S.S. and Carrillo-pedroza, F.R. 2003. Destruction of cyanide waste solutions using chlorine dioxide , ozone and titania sol. , 23: 183–191.

Patil, Y.B. and Paknikar, K.M. 2000. Biodetoxification of silver-cyanide from electroplating industry wastewater. *Letters in applied microbiology*, 30(1): 33–37.

Patil, Y.B. and Paknikar, K.M. 2000. Development of a process for biodetoxification of metal cyanides from waste waters. *Process Biochemistry*, 35(10): 1139–1151.

Patil, Y.B. and Paknikar, K.M. 1999. Removal and recovery of metal cyanides using a combination of biosorption and biodegradation processes. *Biotechnology Letters*, 21(10): 913–919.

Perumal, M., J, J.P. and Kamaraj, M. 2013. Isolation and Characterization of Potential Cyanide Degrading Bacillus nealsonii from Different Industrial Effluents. , 5(5): 2357–2364.

du Plessis, C.A., Barnard, P., Muhlbauer, R.M. and Naldrett, K. 2001. Empirical model for the autotrophic biodegradation of thiocyanate in an activated sludge reactor.pdf. *Letters in applied microbiology*, 32: 103–107.

Quan, Z., Rhee, S. and Bae, J. 2006. Bacterial community structure in activated sludge reactors treating free or metal-complexed cyanides. *Journal of Microbiology and Biotechnology*, 16(2): 232–239.

Rader, W.S., Soiuji, L., Miiosavijevl, E., Hendrlx, J.L. and Nelson, J.H. 1993. Sunlight-Induced Photochemistry of Aqueous Solutions of I I) Ions Hexacyanoferrate (I I) and - (I. , 27(9): 1875–1879.

Rader, W.S., Solujic, L., Milosavljevic, E.B., Hendrix, J.L. and Nelson, H. 1995. PHOTOCATALYTIC DETOXIFICATION OF C Y A N I D E A N D METAL CYANO-SPECIES FROM PRECIOUS-METAL MILL EFFLUENTS. , 90(3): 331–334.

Rahman, S.F., Kantor, R.S., Huddy, R., Thomas, B.C., van Zyl, A.W., Harrison, S.T.L. and Banfield, J.F. 2017. Genome-resolved metagenomics of a bioremediation system for degradation of thiocyanate in mine water containing suspended solid tailings. *MicrobiologyOpen*, (December 2016): 1–9.

Rawlings, D.E. and Johnson, D.B. 2007. *Biomining*. Berlin, Heidelberg: Springer-Verlag.

Ryu, B., Kim, W., Nam, K., Kim, S., Lee, B., Park, M.S. and Yang, J. 2015. Bioresource Technology A comprehensive study on algal – bacterial communities shift during thiocyanate degradation in a microalga-mediated process. *Bioresource Technology*, 191: 496–504.

Saba, M., Mohammadyousefi, A., Rashchi, F. and Moghaddam, J. 2011. Diagnostic pre-treatment procedure for simultaneous cyanide leaching of gold and silver from a refractory gold/silver ore. *Minerals Engineering*, 24(15): 1703–1709. 28 February 2014.

Saccon, P. 2018. Water for agriculture, irrigation management. *Applied Soil Ecology*, 123(November 2017): 793–796.

Saitou, N. and Nei, M. 1987. The neighboring-joining method: a new method for reconstructing phylogenetic trees. *Mol.Biol.Evol.*, 4(4): 406–425.

Sambrook, J. and Russell, D. 2001. *Molecular Cloning - A laboratory manual*.

Schippers, A. and Sand, W. 1999. Bacterial Leaching of Metal Sulfides Proceeds by Two Indirect Mechanisms via Thiosulfate or via Polysulfides and Sulfur Bacterial Leaching of Metal Sulfides Proceeds by Two Indirect Mechanisms via Thiosulfate or via Polysulfides and Sulfur. , 65(1): 1–4.

Scholtz, N.J., Pandit, A.B. and Harrison, S.T.L. 1997. Effect of solids suspension on microbial cell disruption. *Bioreactor & Bioprocess Fluid Dynamics. Wiley.*

Sexton, a C. and Howlett, B.J. 2000. Characterisation of a cyanide hydratase gene in the phytopathogenic fungus Leptosphaeria maculans. *Molecular & general genetics : MGG*, 263(3): 463–470.

Shifrin, N.S., Beck, B.D., Gauthier, T.D., Chapnick, S.D. and Goodman, G. 1996. Chemistry, toxicology, and human health risk of cyanide compounds in soils at former manufactured gas plant sites. *Regulatory toxicology and pharmacology : RTP*, 23(2): 106–116.

Sirianuntapiboon, S., Chairattanawan, K. and Surasinanant, P. 2007. Some properties of a sequencing batch reactor for treatment of wastewater containing thiocyanate compounds. *Journal of Environmental Management*, 85(2): 330–337. 9 March 2014.

Sirianuntapiboon, S. and Chuamkaew, C. 2007. Packed cage rotating biological contactor system for treatment of cyanide wastewater. *Bioresource Technology*, 98(2): 266–272. 9 March 2014.

Sorokin, D.Y., Tourova, T.P., Lysenko, a M. and Kuenen, J.G. 2001. Microbial thiocyanate utilization under highly alkaline conditions. *Applied and environmental microbiology*, 67(2): 528–538.

Stafford, D. and Callely, A. 1969. The Utilization of Thiocyanate by a Heterotrophic Bacterium. *Journal of general microbiology*, 55: 285–289.

Stott, M.B., Franzmann, P.D., Zappia, L.R., Watling, H.R., Quan, L.P., Clark, B.J., Houchin, M.R., Miller, P.C. and Williams, T.L. 2001. Thiocyanate removal from saline CIP process water by a rotating biological contactor, with reuse of the water for bioleaching. *Hydrometallurgy*, 62(2): 93–105.

Tamosiunas, V., Padarauskas, A. and Pranaityte, B. 2006. Thiocyanate determination by ion pair chromatography. , 17(2): 21–24.

Tamura, K., Peterson, D., Peterson, N., Stecher, G., Nei, M. and Kumar, S. 2011. MEGA5: Molecular evolutionary genetics analysis using maximum likelihood, evolutionary distance, and maximum parsimony methods. *Molecular Biology and Evolution*, 28(10): 2731–2739.

U.S. Department of Health and Human Services PHS. 2006. Toxicological Profile for Cyanide. *US Department of Health and Human Services*, (July): 298.

UN-Water. 2006. *Water: A Shared Responsibility The United Nations World Water Development Report*.

Vázquez, I., Rodríguez, J., Marañón, E., Castrillón, L. and Fernández, Y. 2006. Simultaneous removal of phenol, ammonium and thiocyanate from coke wastewater by aerobic biodegradation. *Journal of Hazardous Materials*, 137(3): 1773–1780. 26 February 2014.

Vijayaraghavan, K. and Yun, Y.S. 2008. Bacterial biosorbents and biosorption. *Biotechnology Advances*, 26(3): 266–291.

Villemur, R., Juteau, P., Bougie, V., Ménard, J. and Déziel, E. 2015. Development of four-stage moving bed biofilm reactor train with a pre-denitrification configuration for the removal of thiocyanate and cyanate. *Bioresource Technology*, 181: 254–262.

Viramontes Gamboa, G., Medina Noyola, M. and López Valdivieso, a. 2005. Fundamental considerations on the mechanisms of silver cementation onto zinc particles in the Merril-Crowe process. *Journal of Colloid and Interface Science*, 282(2): 408–414. 9 March 2014.

Wang, C.-C., Lee, C.-M. and Chen, L.-J. 2004. Removal of nitriles from synthetic wastewater by acrylonitrile utilizing bacteria. *Journal of environmental science and health. Part A, Toxic/hazardous substances & environmental engineering*, 39(7): 1767–1779.

Watts, M.P. and Moreau, J.W. 2016. New insights into the genetic and metabolic diversity of thiocyanate-degrading microbial consortia. *Applied Microbiology and Biotechnology*, 100(3): 1101–1108.

Watts, M.P., Spurr, L.P., Lê Cao, K.A., Wick, R., Banfield, J.F. and Moreau, J.W. 2019. Genome-resolved metagenomics of an autotrophic thiocyanate-remediating microbial bioreactor consortium. *Water Research*, 158: 106–117.

Wentzien, S.W. and Sand, W. 2004. Tetrathionate disproportionation by Thiomonas intermedia K12. *Engineering in Life Sciences*, 4(1): 25–30.

White, D.M., Pilon, T. a. and Woolard, C. 2000. Biological treatment of cyanide containing wastewater. *Water Research*, 34(7): 2105–2109.

White, D.M. and Schnabel, W. 1998. Treatment of cyanide waste in a sequencing batch biofilm reactor.pdf. : 254–257.

Xie, F. and Dreisinger, D. 2009. Studies on solvent extraction of copper and cyanide from waste cyanide solution. *Journal of Hazardous Materials*, 169(1–3): 333–338. 9 March 2014.

Yanase, H., Sakamoto, a, Okamoto, K., Kita, K. and Sato, Y. 2000. Degradation of the metal-cyano complex tetracyanonickelate (II) by Fusarium oxysporum N-10. *Applied microbiology and biotechnology*, 53(3): 328–334.

Yang, P., Li, D., Zhang, W., Wang, N., Yang, Z., Wang, D. and Ma, T. 2019. Flocculation-dewatering behavior of waste activated sludge particles under chemical conditioning with inorganic polymer flocculant: Effects of typical sludge properties. *Chemosphere*, 218: 930–940.

Young, C.A. and Jordan, T.S. 1995. Cyanide remeciation: Current and past technologies. In *10th Annual conference on Hazardous Waste Research*. 104–129.

Zagury, G.J., Oudjehani, K. and Deschênes, L. 2004. Characterization and availability of cyanide in solid mine tailings from gold extraction plants. *Science of the Total Environment*, 320(2–3): 211–224. 23 January 2014.

Zhang, S. 2004. *Oxidation of refractory gold concentrates and simultaneous dissolution of gold in aerated alkaline solutions*. Murdoch University.

Zheng, R.-C., Wang, Y.-S., Liu, Z.-Q., Xing, L.-Y., Zheng, Y.-G. and Shen, Y.-C. 2007. Isolation and characterization of Delftia tsuruhatensis ZJB-05174, capable of R-enantioselective degradation of 2,2-dimethylcyclopropanecarboxamide. *Research in microbiology*, 158(3): 258–64. 23 March 2014.

Zhou, Y., Cui, Y. and Qu, X. 2019. Exopolysaccharides of lactic acid bacteria: structure, bioactivity and associations: A review. *Carbohydrate Polymers*, 207: 317–332.

van Zyl, A.W., Harrison, S.T.L. and van Hille, R.P. 2017. Determining an effective operating window for a thiocyanate-degrading mixed microbial community. *Journal of Environmental Chemical Engineering*, 5(1): 660–666.

Web References:

http://www.cynidecode.org Last accessed: 11/2017

http://www.biomin.co.za/aster/technology.html Last accessed: 10/2018

http://www.infors-ht.com Last accessed: 10/2018